eman ta zabal zazu

Universidad del País Vasco
Euskal Herriko Unibertsitatea
The University of the Basque Country

GLIA- RETINAL GANGLION CELL INTERACTIONS IN THE MAMMALIAN RETINA: A NEUROPROTECTIVE APROACH

Noelia Ruzafa Andrés

Leioa, 2017

Thesis Director:

Elena Vecino Cordero

A mis padres

AGRADECIMIENTOS

Al llegar al final de estos más de cuatro años en los que he estado trabajando con el objetivo de realizar mi tesis doctoral, quiero dar las gracias a todas las personas que me han acompañado en este proceso.

En primer lugar, quiero dar las gracias a mi directora de tesis, la Doctora Elena Vecino, por darme la oportunidad de trabajar en su laboratorio para desarrollar la tesis, por descubrirme la verdadera vocación investigadora, por enseñarme este bonito mundo que es la ciencia, y por enseñarme y demostrarme qué es ser una buena científica.

I would like to express my sincere gratitude to Doctor Tatjana Jakobs, from Schepens Eye Research Institute, Harvard Medical School, in Boston, for giving me the opportunity to work with her wonderful group for three months.

I would like also to thank to Doctor Sansar Sharma for his help and for his time to read and correct my work.

Me gustaría también agradecer especialmente la ayuda de todas las personas que han pasado por el laboratorio, entre ellos quiero destacar la ayuda de Xandra, que me ha apoyado tanto dentro como fuera del laboratorio en todo lo que he necesitado.

Quiero dar las gracias a todos los miembros del departamento: profesores, personal administrativo, servicios generales, y sobre todo, becarios, por su ayuda, su apoyo, y su ánimo, ya que han hecho que sea un camino más fácil de recorrer.

Quisiera agradecer también esta tesis doctoral a la UPV/EHU, por otorgarme una beca predoctoral que ha hecho posible que pueda dedicarme a lo que más quería. Asimismo quiero dar las gracias a la educación pública por sus becas y ayudas, y por sus profesores y maestros, tanto a los de la Universidad del País Vasco como a los de la Universidad de Granada, además de los de mi instituto y colegio, porque gracias a lo que me enseñaron he llegado hasta aquí.

Por supuesto quiero dar las gracias a mis amigos de siempre y a los nuevos, entre los que se encuentran muchos compañeros que he conocido estos años.

Por último, y con un especial énfasis quiero agradecer el haber podido realizar esta tesis doctoral a toda mi familia, en especial a mis padres y a mi hermano. Por su apoyo incondicional en la distancia, por escucharme, animarme, motivarme, por quererme… porque sin ellos nada de esto habría sido posible, porque esta tesis es tanto mía como suya. Y a Alex, el que ha vivido más de cerca todo el proceso, las palabras no pueden describir todo lo que me ha ayudado, simplemente quiero agradecerle que me haga tan feliz, porque se que a su lado puedo conseguir todo lo que me proponga.

Con todo mi cariño, muchas gracias a todos!

ÍNDICE

RESUMEN

Las células ganglionares de la retina (RGCs) son las neuronas responsables de la comunicación entre el ojo y el cerebro, y su muerte puede causar una ceguera irreversible, como ocurre en el glaucoma, tras la degeneración axonal, o tras isquemia, entre otros daños.

Las RGCs se encuentran en estrecho contacto con las células de la glía. En la retina de mamíferos hay tres tipos de células gliales, cuya función es mantener la homeostasis de la retina, estos tipos son: astrocitos, células Müller y microglía. Cuando se induce un daño o lesión en la retina, la glía puede percibir este daño y responder a él, pudiendo actuar como sensores de daño además de poder neuroproteger a las RGCs (*ANEXO 0*).

A fin de estudiar la relación entre la glía y las RGCs, en la presente Tesis hemos utilizado un modelo de hipoxia neonatal en cerdos, y hemos estudiado que proceso tiene lugar en los momentos iniciales tras el daño. Hemos encontrado que el cerebro percibe el daño antes que la retina, así los astrocitos y las neuronas en colículo superior se ven dañadas antes que los astrocitos y las RGCs en la retina. Este hecho podría explicarse debido la presencia de células Müller en la retina, ya que estas células de soporte no están presentes en el cerebro (ANEXO 1).

Para estudiar la neuroprotección de las RGCs por las células de Müller y la relación entre estos dos tipos celulares hemos utilizado cultivos primarios. Estudios previos del grupo habían comprobado que las células Müller pueden neuroproteger a las RGCs por contacto célula-célula, además de secretar moléculas con efecto neuroprotectoras. En la presente Tesis hemos analizando el secretoma de las células de Müller mediante proteómica, combinado con una estrategia funcional en la que se analiza la supervivencia y neuritogénesis de RGCs. De entre las moléculas candidatas hemos seleccionado varias proteínas con posible función neuroprotectora. Hemos comprobado que la osteopontina y la basigina son proteínas candidatas noveles que aumentan la supervivencia de las RGCs, sin embargo no descartamos la intervención de otras moléculas (ANEXO 2, 3).

Además, en cultivos primarios y explantes de retina, hemos comprobado que el plasma rico en factores de crecimiento (PRGF), al contrario que en otros tipos celulares,

disminuye drásticamente la supervivencia de las RGCs, aumenta la proliferación de las células de Müller y activa la respuesta inflamatoria en la retina. Dicho efecto lo hemos comprobado mediante la observación del aumento de la migración de microglía. Este hecho podría ser debido a la presencia de citoquinas inflamatorias en el PRGF (ANEXO 4).

Sabiendo que la osteopontina tiene propiedades neuroprotectoras, estudiamos el efecto de su ausencia *in vivo*. La falta de osteopontina en ratones *knock-out* produce la muerte de las células ganglionares de la retina, así como desaparición o disminución de astrocitos en ciertas partes de la retina. Estos resultados confirman que la osteopontina tiene un papel importante en el normal funcionamiento de la retina y podría ser un buen candidato para tratar la neurodegeneración retiniana (ANEXO 5).

Finalmente, la osteopontina también puede usarse como biomarcador de daño, debido a su sobreexpresión tras una lesión como es el pinzamiento del nervio óptico, donde los niveles de RNA de osteopontina aumentan más de 9 veces en la cabeza del nervio óptico. Con el fin de establecer un buen biomarcador molecular de daño de las células ganglionares, nos propusimos cuantificar la sobreexpresión de la osteopontina, además de la lipocalina 2, a nivel proteico tanto en la cabeza del nervio óptico como en el humor acuoso. Dichos estudios aun se encuentran en progreso (ANEXO 6).

En conclusión, la glía retiniana puede ayudarnos a detectar signos de daño mediante cambios morfológicos o mediante la secreción de marcadores moleculares. Además, podemos usar sus propiedades neuroprotectoras para desarrollar posibles tratamientos contra enfermedades neurodegenerativas en las que se afectan las células ganglionares de la retina.

ABSTRACT

Retinal ganglion cells (RGCs) are the neurons that connect the eye to the brain and their death can provoke irreversible blindness, as occurs in glaucoma, after axonal degeneration or as a result of ischemia. RGCs are in close contact with glial cells, of which there are three main types in the mammalian retina that serve to maintain retinal homeostasis: astrocytes, Müller cells and resident microglia. Following injury to the retina, the glia can "sense" the damage and respond to it, offering protection to RGCs (ANNEX 0).

In order to study the relationship between glia and RGCs, in this Doctoral Thesis we have used a model of neonatal hypoxia in pigs and we have studied the events that take place in the initial moments after this damage. We found that the brain perceives the damage before the retina, such that astrocytes and neurons in the superior colliculus are damaged before astrocytes and RGCs in the retina. This could be due to the presence of Müller cells in the retina, since these support cells are not present in the brain (ANNEX 1).

We have used primary cell cultures to study the neuroprotection of RGCs afforded by Müller cells and the relationship between these two cell types. It was shown previously that Müller cells offer neuroprotection to RGCs through cell-cell contact, as well as by secreting molecules with neuroprotective effects. In the present Thesis, the secretome of Müller cells was analyzed by combining a proteomic approach with a functional strategy in which the survival and neuritogenesis of RGCs was assessed. We selected proteins with possible neuroprotective activity from among the candidate molecules identified. Thus, osteopontin and basigin were considered to be novel candidate proteins that enhance the survival of RGCs, although we do not rule out the involvement of other molecules (ANNEX 2, 3).

In addition, in primary cultures and retinal explants we found that plasma rich in growth factor (PRGF) drastically reduces the survival of RGCs relative to other cell types, increasing the proliferation of Müller cells and activating an inflammatory response in the retina (evident as an increase in microglia migration). This response could reflect the presence of inflammatory cytokines in PRGF (ANNEX 4).

Given the neuroprotective properties of osteopontin, we studied the effect of its depletion *in vivo*. The absence of osteopontin in *knock-out* mice results in the death of RGCs, as well as a decrease in the area occupied by or the disappearance of retinal astrocytes in certain parts of the retina. These results confirm that osteopontin plays an important role in the normal functioning of the retina and that it may be a good candidate protein to treat the retinal neurodegeneration (ANNEX 5).

Finally, osteopontin may also serve as a biomarker of retinal damage as its RNA expression is upregulated more than 9-fold in the optic nerve head after injury (e.g. optic nerve crush). In order to establish a good molecular biomarker for RGC damage, we attempted to quantify the overexpression of osteopontin and that of the lipocalin 2 protein, both at the optic nerve head and in the aqueous humor. These studies are still ongoing (ANNEX 6).

In conclusion, retinal glia can help identify signs of damage through the changes in their morphology or through their secretion of specific molecular markers. Moreover, we can use the neuroprotective properties of these secreted proteins to develop possible treatments against neurodegenerative diseases in which RGCs are affected.

1. INTRODUCCIÓN

1.1. Retina: estructura y función

La retina es la parte sensorial del ojo y proporciona una excelente oportunidad para el estudio de las interacciones entre la glía y las neuronas. Forma la capa interna que se dispone en la parte posterior del globo ocular, y podemos diferenciarla de la parte más externa formada por la esclera y la cornea, y de la parte intermedia en la que se incluyen el iris y el cuerpo ciliar en la zona anterior, y la coroides en la zona posterior (Fig. 1).

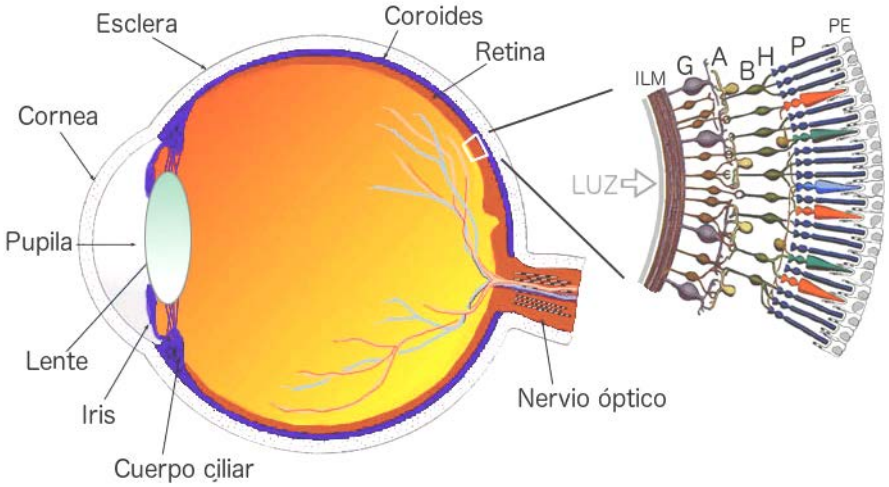

Fig. 1. Dibujo esquemático de los componentes del ojo y esquema aumentado de la retina en el que se observa su disposición en el ojo y las distintas capas de neuronas que la forman. Se representan: membrana limitante interna (ILM), células ganglionares (G), células amacrinas (A), células bipolares (B), células horizontales (H), fotorreceptores (P) y epitelio pigmentario (PE).

La retina forma parte del sistema nervioso central (CNS). Se forma durante el desarrollo embrionario a partir de dos vesículas ópticas que nacen directamente del tubo neural (Mann, 1964).

Las retinas de vertebrados están formadas por tres capas de cuerpos celulares y entre ellas, dos capas plexiformes caracterizadas por ser el lugar de las interacciones sinápticas. La capa nuclear externa (outer nuclear layer, ONL), es la capa formada por los cuerpos celulares de los fotorreceptores, es decir, de los conos y bastones. Más hacia el exterior, se encuentran los segmentos externos de los fotorreceptores, que están en contacto con el epitelio pigmentario, que a su vez está en contacto con la coroides. Hacia el interior, se encuentra la capa nuclear interna (inner nuclear layer, INL), formada por los cuerpos de las células horizontales, bipolares y amacrinas además de

los cuerpos celulares de las células de Müller astrocitos y algunas células de la microglía. Por último se encuentra la capa de las células ganglionares (ganglion cell layer, GCL), en la que se encuentran las células ganglionares de la retina (retinal ganglion cell, RGC) además de astrocitos, algunas células de la microglía y los vasos y arteriolas con las células endoteliales correspondientes que además transcurren verticalmente hasta ramificarse de nuevo en el límite externo de la capa ONL. La capa plexiforme externa (outer plexiform layer, OPL) se encuentra entre la ONL y la INL, y es la parte de la retina en la que contactan los fotorreceptores con las células bipolares y horizontales. Y la capa plexiforme interna (inner plexiform layer, IPL) se encuentra entre la INL y la GCL, y es la parte en la que contactan las RGCs con las células amacrinas y las células bipolares. Es importante mencionar que en la estructura de la retina, integradas entre las neuronas previamente mencionadas, se encuentran también las células de la glía (Fig. 2) (Polyak, 1941; Rodieck, 1973; Vecino et al., 2016).

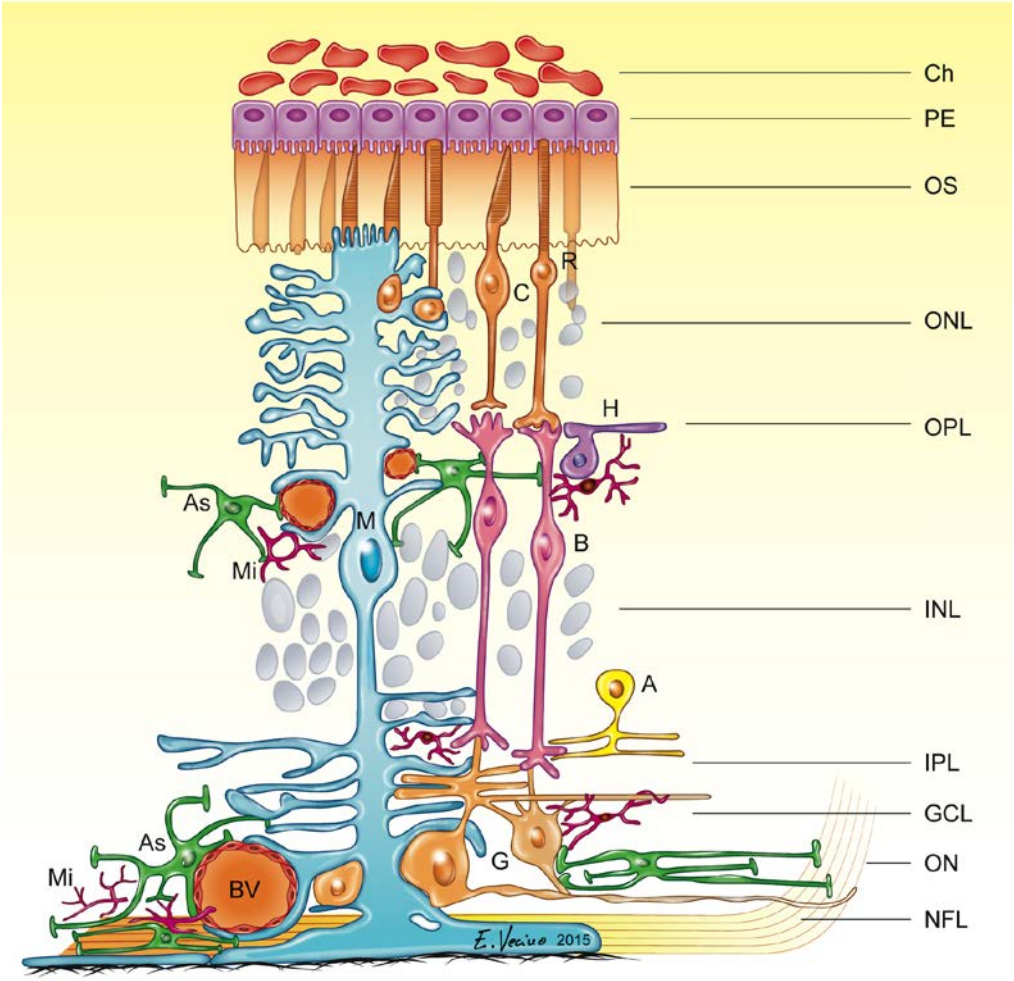

Fig. 2. Dibujo esquemático de los componentes celulares de la retina: glía y neuronas. Disposición de los distintos tipos celulares en una retina de mamífero estándar. Nótese la localización de las distintas capas de la retina, desde la parte más externa a la más interna: coroides (Ch), epitelio pigmentario (PE), capa de segmentos externos (OS), capa nuclear externa (ONL), capa plexiforme externa (OPL), capa nuclear interna (INL), capa plexiforme interna (IPL), capa de células ganglionares (GCL), capa de fibras nerviosas (NFL), nervio óptico (ON). Nótese además la interacción entre las distintas células y con los vasos sanguíneos (BV). Células amacrinas (A), astrocitos (As), células bipolares (B), conos (C), células ganglionares (G), células horizontales (H), células de Müller (M), microglía (Mi), bastones (R) (Vecino et al., 2016).

Las terminaciones sinápticas de los fotorreceptores, transmiten la información a las células bipolares, y estas transmiten la señal hacia las células ganglionares. Los fotorreceptores liberan un solo neurotransmisor, el glutamato, pero las células bipolares pueden reaccionar al estímulo de dos maneras diferentes. En algunas células bipolares se activa la vía ON y en otras la vía OFF, asociadas a una hiperpolarización y despolarización del potencial de membrana respectivamente. Esta repuesta está asociada a la expresión de distintos receptores para el glutamato, metabotrópico para las células ON e ionotrópico para las OFF. Las células bipolares transmiten la información a las células ganglionares, las conexiones entre estas células ocurren en la capa plexiforme interna. Las células ganglionares, son las encargadas de transmitir la información al cerebro, a través de sus axones, que forman el nervio óptico (Nelson and Connaughton, 1995).

El perfeccionamiento de la imagen se obtiene a través de las asociaciones laterales. Las células horizontales son células de asociación lateral entre los fotorreceptores, y las células amacrinas de asociación lateral entre células bipolares, ganglionares y otras amacrinas. Estas células, envían señales usando varios aminoácidos excitadores e inhibidores, como GABA (ácido gamma-aminobutírico), glicina, dopamina, serotonina y acetilcolina entre otros. Las células horizontales modulan la señal de los fotorreceptores bajo diferentes condiciones de iluminación, además, pueden hacer que la respuesta de células bipolares sea codificada por colores a través de circuitos de retroalimentación con los conos. Por otro lado, las células amacrinas participan en la modulación del procesamiento de las señales luminosas (Kolb, 2003; Rodieck, 1973).

Para la realización de esta Tesis Doctoral han sido utilizados distintos modelos animales, como son el cerdo, la rata y el ratón. La retina porcina tiene un gran parecido

a la retina humana, se asemejan en tamaño forma y función, número y distribución de conos y bastones (Beauchemin, 1974; De Schaepdrijver et al., 1990; Prince and Ruskell, 1960; Ruiz-Ederra et al., 2004; Ruiz-Ederra et al., 2003; Veiga-Crespo et al., 2013), lo que hace que sea un modelo atractivo para el estudio del sistema visual, especialmente si el interés recae en la patologías humanas (Komaromy et al., 2003; Li et al., 1998). La retina porcina es más similar a la retina humana que a los de otros grandes mamíferos, como perros, cabras y vacas (Prince and Ruskell, 1960). Además, su vasculatura es similar a la de los seres humanos (Galdos et al., 2012). Aunque los primates no-humanos se consideran el mejor sustituto de la retina humana debido a su gran parecido y a que son los únicos en poseer macula (Polyak, 1941; Volland et al., 2015), su gasto y disponibilidad limitan su uso. En la retina porcina, se han identificado diferentes regiones tras analizar la distribución de RGCs según la densidad celular y el tamaño de soma. En el centro de la retina se encuentra una banda horizontal de alta densidad de RGC, donde hay una alta proporción de RCGs con tamaño de soma pequeño. De la retina central a la más periférica, se observa una disminución de la densidad RGC, junto con una mayor presencia de RGCs con somas más grandes (Garca et al., 2005). Sin embargo, también han sido utilizadas otras especies como el ratón y la rata, ya tienen otras ventajas debido a su fácil manejo y estabulación, a que tienen menos restricciones éticas, son más económicos, y pueden ser modificados genéticamente. En la retina de roedores la población de RGCs se distribuye también en gradiente de centro a periferia y algunos autores han sugieren una región con mayor densidad de RGC en la región temporal superior de la retina (Drager and Olsen, 1981; Dreher et al., 1985; Fukuda, 1977; Jeon et al., 1998; Reese and Cowey, 1986; Salinas-Navarro et al., 2009).

1.2. Células Ganglionares de la Retina

Las células ganglionares de la retina o RGCs son las encargadas de decodificar y transmitir la información visual desde la retina a los centros visuales del cerebro. La información visual es detectada por receptores de membrana de las RGCs en forma de mensajes químicos enviados por células bipolares y amacrinas. Los receptores transmembrana de las RGCs transforman este mensaje en señales eléctricas para transmitir la información largas distancias a través de sus axones, que están contenidos en un haz formando el nervio óptico. Estos axones terminan en los centros visuales del

cerebro, principalmente en el núcleo geniculado lateral y en el colículo superior (Wassle and Boycott, 1991).

Las RGCs constituyen una población diversa respecto a su morfología y fisiología, por lo que ha sido importante estudiar su clasificación con el fin de entender sus posibles distintos roles en diferentes patologías que impliquen la degeneración de las mismas y que conducen a una ceguera irreversible. Sin embargo, la sensibilidad de los distintos subtipos de RGCs a la muerte celular que ocurre en enfermedades o daños neurodegenerativos como el glaucoma, la retinopatía diabética o la isquemia retiniana, es aún un tema controvertido. La subdivisión más significativa surge dependiendo del lugar de la proyección de sus axones, por ejemplo, si transmiten señales a las capa magnocelular del núcleo geniculado lateral serían RGCs tipo M, y si por el contrario, proyectan a la capa parvocelular serían tipo P (Polyak, 1941; Veiga-Crespo et al., 2013). A su vez, se pueden clasificar basándose en el tamaño del cuerpo celular, la morfología y la ramificación dendrítica, o los niveles de estratificación en la capa plexiforme interna (Peichl and Wassle, 1983; Veiga-Crespo et al., 2013). Cabe destacar, que un pequeño porcentaje de RGCs son fotosensibles y contribuyen a la determinación del ritmo circadiano y el reflejo pupilar, pudiendo incluso detectar características sutiles de la escena visual (Amthor et al., 1984; Boycott and Wassle, 1974; Masland, 2001; Polyak, 1941). Además, en diferentes especies hay diferentes clasificaciones de RGCs debido a las diferentes morfologías encontradas, por ejemplo en ratón se han encontrado 22 tipos diferentes de RGCs, y en cerdo las RGCs se pueden clasificar en 9 tipos (Veiga-Crespo et al., 2013; Volgyi et al., 2009).

El estudio de la neurodegeneración de las RGCs en humanos es complejo, ya que normalmente, cuando se diagnostica el trastorno, el daño ya ha comenzado. Además es complicado debido a la dificultad de obtención de muestras en el mismo estadio de neurodegeneración. Por este motivo se han desarrollado modelos animales de glaucoma, una neuropatía óptica caracterizada por la perdida progresiva de las RGCs con la consecuente pérdida de visión gradual e irreversible. Estos modelos ayudan a estudiar el inicio y la progresión de la enfermedad, y además facilitan el desarrollo de tratamientos (Urcola et al., 2006; Vecino, 2008; Vecino and Sharma, 2011). También han sido desarrollados modelos de isquemia retiniana, de retinopatía diabética o de degeneración

macular asociada a la edad (Grigsby et al., 2014; Pinar-Sueiro et al., 2013; Tuo et al., 2007).

Por otro lado, con el objetivo de simplificar el modelo animal, se han establecido distintos modelos *in vitro* para el estudio de estas células. Un método de cultivo de las células de la retina particularmente útil es el explante o cultivo organotípico de retina. En este modelo, aunque se realiza la axotomía de las células ganglionares, que pierden la conectividad con el cerebro, se preserva la arquitectura tisular de la retina. Conservándose así las distintas características histológicas y bioquímicas de las células que la componen, pudiendo mantenerse durante varios días o incluso semanas (Seigel, 1999). Los explantes de retina han sido ideales para estudios de organización sináptica (Sassoe-Pognetto et al., 1996), interacciones célula-célula (Feigenspan et al., 1993), o de diferenciación de la retina (Veroman, 1981), ya que conservan el mayor grado de preservación de tejido de todos los sistemas de cultivo de células retinianas. Sin embargo, para otros estudios puede resultar más útil la realización de cultivos primarios de células retinianas disociadas, como pueden ser los cultivos de RGCs (Fig. 3), que aunque carecen de la organización célula-célula de los explantes, pueden ser más recomendables en algunos estudios de transfección, patch-clamp, videomicroscopia o para la realización de análisis cuantitativos (Seigel, 1999).

Los modelos de cultivo de las células de la retina son una poderosa herramienta en la investigación oftalmológica, porque aunque ningún cultivo celular descrito puede reemplazar al ojo intacto, estos cultivos proporcionan sistemas experimentales controlables para el examen de procesos fundamentales de retina, así como de la simulación de determinadas patologías y de la búsqueda de posibles tratamientos. En estos estudios, ha sido demostrado que tras axotomía, las RGCs tienen una capacidad de regeneración limitada *in vitro* y que no todas ellas mueren a la vez, ya que debido a su heterogeneidad, hay células más sensibles que otras (Luo et al., 2001; Mey and Thanos, 1993; Morgan, 1994; Ruiz-Ederra et al., 2005).

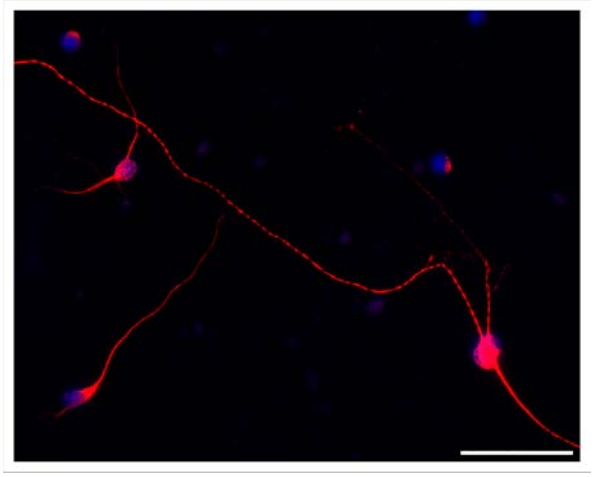

Fig. 3. Células Ganglionares de la Retina (RGCs) *in vitro*. Cultivo primario de RGCs de rata. Las RGCs han sido marcadas con anticuerpo frente a βIII-Tubulina en rojo, y los núcleos celulares han sido teñidos con DAPI en azul. Barra de escala = 50 μm

Para realizar estudios de cuantificación tanto del daño como de la posible protección de estas células, es necesario visualizar las RGCs con marcadores específicos. Los factores de transcripción Brn3 se expresan exclusivamente en las células ganglionares, e intervienen en la diferenciación neuronal y la supervivencia. Antes del uso Brn3, para cuantificar RGCs era común el uso de Fluorogold, un marcador retrógrado que marca aproximadamente un 98% del total de RGCs. Un anticuerpo marcado contra Brn3a permite teñir el núcleo de un 92.2% de RGCs marcadas con Fluorogold (Nadal-Nicolas et al., 2009). El marcaje con anticuerpos frente a Brn3a, además de ser más fácil de realizar, es importante porque Brn3 es un marcador endógeno, y su nivel de expresión puede reflejar el estado fisiológico de las células. Por esto, Brn3a es un marcador fiable, y eficiente para marcar y cuantificar RGCs. Además, aunque no han sido utilizados en este estudio, es importante destacar la existencia de los marcadores Brn3b y Brn3c debido a que su expresión es variable en las RGCs y permite diferenciar distintos subtipos de células ganglionares. Algunas de las características de estos marcadores son que Brn3a marca un mayor porcentaje de RGCs, seguido de Brn3b y finalmente de Brn3c. También es importante la característica de que las RGCs que expresan sólo Brn3b y las que coexpresan a los tres miembros tienen los núcleos más grandes (Nadal-Nicolas et al., 2012). Además solo Brn3b está presente en las células ipRGCs (Jain et al., 2012), un subtipo de RGCs intrínsecamente fotosensible que se caracteriza por la expresión de melanopsina (Provencio et al., 2000).

Por otro lado, RBPMS es otro marcador específico para RGCs que fue descubierto años más tarde. Esta proteína de unión a RNA con múltiples sitios de splicing (RBPMS) y con función aún no bien conocida, permite que anticuerpos contra ella marquen el soma de RGCs en múltiples especies de mamíferos (Rodriguez et al., 2014). En este trabajo se han utilizado tanto marcajes frente a Brn3a como a RBPMS. Para cultivos celulares de RGCs, anticuerpos frente a β-III-tubulina son una buena forma de marcar los microtúbulos de las RGCs para así poder tanto visualizarlas, contabilizarlas y clasificarlas (Ruzafa and Vecino, 2015; Vecino et al., 2016).

Conocida la implicación de las células ganglionares en numerosas patologías oculares y debido a que su muerte conlleva a una ceguera irreversible, la neuroprotección de las RGCs ha sido la línea conductora de esta Tesis Doctoral.

1.3. Glía Retiniana: tipos y funciones

En la retina existen principalmente tres tipos de glía: células de Müller, astrocitos y microglía (Fig. 2). El estudio de la glía retiniana facilita la comprensión de la interacción glía-neurona, por lo que permiten conocer el papel de estas células tanto en retinas sanas como en patologías (Kolb, 2003).

Las células de Müller constituyen el elemento glial que predomina en la retina, pudiendo representar el 90% de la glía de la retina. Se disponen radialmente orientadas atravesando la retina desde la parte más interna, en contacto con el vítreo, hasta la capa nuclear externa. Sus cuerpos celulares se sitúan en la capa nuclear interna, y sus prolongaciones rodean todas las neuronas de la retina (Fig. 4). La morfología de las células de Müller se refleja en una multitud de funciones en relación a las neuronas. Una de las funciones especificas de estas células es que pueden actuar como elementos guiadores de la luz (Labin and Ribak, 2010), además, estas pueden adoptar características de células progenitores de la retina que se podrían servir para reparar la retina dañada (Das et al., 2006; Fischer and Reh, 2001; Ooto et al., 2004).

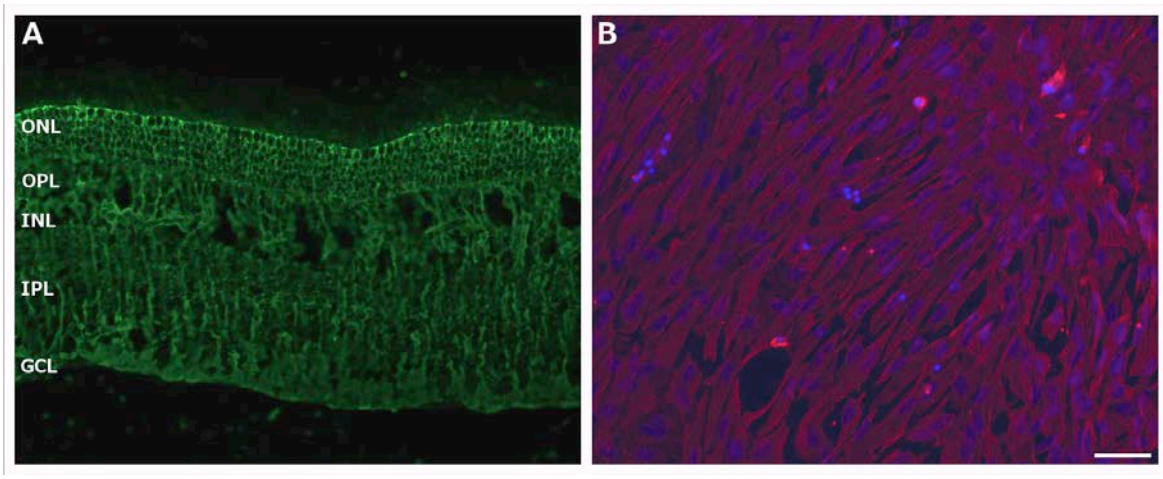

Fig. 4. Células de Müller *in vivo* e *in vitro*. (A) Células de Müller en un corte de retina de cerdo marcadas con un anticuerpo frente a glutamina sintetasa en verde. (B) Cultivo primario de células de Müller de cerdo, las células han sido marcadas con un anticuerpo frente a vimentina en rojo, y los núcleos han sido teñidos con DAPI en azul. Capa nuclear externa (ONL), capa plexiforme externa (OPL), capa nuclear interna (INL), capa plexiforme interna (IPL), y capa de células ganglionares (GCL). Barra de escala = 50 μm

Los astrocitos presentan un aspecto estrellado, con cuerpo celular aplanado y prolongaciones radiales. Se encuentran casi exclusivamente en las partes más internas de la retina, sobre la superficie de los haces de axones de las RGCs, además se encuentran en una densidad más alta cerca de la cabeza del nervio óptico y la densidad va disminuyendo progresivamente hacia la periferia de la retina. Suelen estar en contacto con los vasos sanguíneos, envolviendo a los mismos con su prolongaciones, y a su vez, también están en contacto con las neuronas (Fig. 5) (Hogan and Feeney, 1963; Karschin et al., 1986).

La macroglía retiniana, células de Müller y astrocitos, coinciden en muchas de sus funciones, la mayoría relacionadas con el contacto intimo entre estas células y las neuronas. Ambos tipos celulares envuelven los axones y somas de células ganglionares (Vecino et al., 2016). También proporcionan un soporte estructural a las neuronas, pudiendo alterar su elasticidad y rigidez mediante sus filamentos intermedios, como el GFAP en astrocitos y la vimentina en células de Müller, y con ello modifican la biomecánica celular de la retina (Bringmann et al., 2009; Lindqvist et al., 2010; Lu et al., 2011; Vecino et al., 2016).

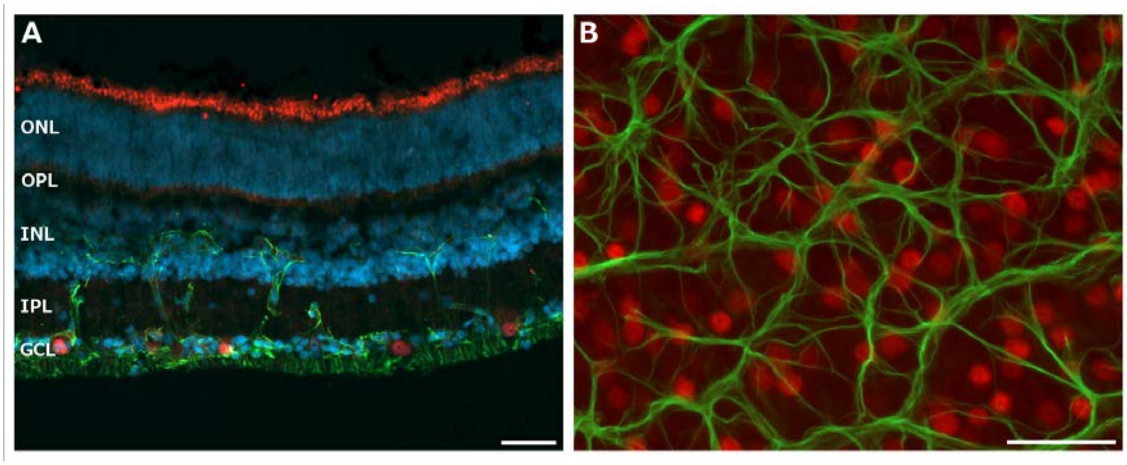

Fig. 5. Astrocitos y RGCs en la retina *in vivo*. Astrocitos marcadas con un anticuerpo frente a GFAP en verde y RGCs marcadas con un anticuerpo frente a Brn3a en rojo. (A) Corte de retina de cerdo donde los núcleos han sido teñidos con DAPI en azul. (B) Retina *in toto* de retina de ratón. Capa nuclear externa (ONL), capa plexiforme externa (OPL), capa nuclear interna (INL), capa plexiforme interna (IPL), y capa de células ganglionares (GCL). Barra de escala = 50 μm

Los cambios de volumen de estas células gliales están altamente asociados a las características viscoelásticas de la retina. También es importante destacar que la matriz extracelular que aporta la macroglía es una fuente de soporte y señalización en la retina y contribuye a la formación de la membrana limitante interna, el límite entre la retina y el humor vítreo. Los componentes de la matriz extracelular son mediadores de la activación glial, y tienen la capacidad de inducir efectos protectores y/o degenerativos sobre las RGCs. Algunos de los componentes de la matriz extracelular de la retina de mamíferos sana son la laminina, el colágeno, la fibronectina, vitronectina, tenacina, proteoglicanos, e integrinas entre otros (Vecino et al., 2016).

Tanto **astrocitos como células de Müller** tienen un papel importante en el metabolismo de la retina. Las células de la retina presentan un metabolismo especializado y adaptado a las necesidades para su mantenimiento y las demandas específicas relacionadas con el procesamiento visual. Las células gliales y las neuronas tienen complejas relaciones metabólicas entre ellas, cabe destacar el intercambio de nutrientes y metabolitos, las respuestas a señales de células vecinas o distantes, y la adaptación de la maquinaria transcripcional para suministrar los metabolitos requeridos con el fin de ajustar su actividad metabólica dependiendo de las necesidades (Hosoya and Tachikawa, 2012; Hurley et al., 2014; Ng et al., 2014; Yu et al., 2013). La relación metabólica entre diferentes poblaciones de células retinianas incluye muchas moléculas y reacciones, y

puede verse resumida en la Figura 6 (Vecino et al., 2016). Además, pueden participar en el metabolismo lipídico, sintetizando y transportando lípidos para satisfacer la necesidad de las neuronas (Mauch et al., 2001).

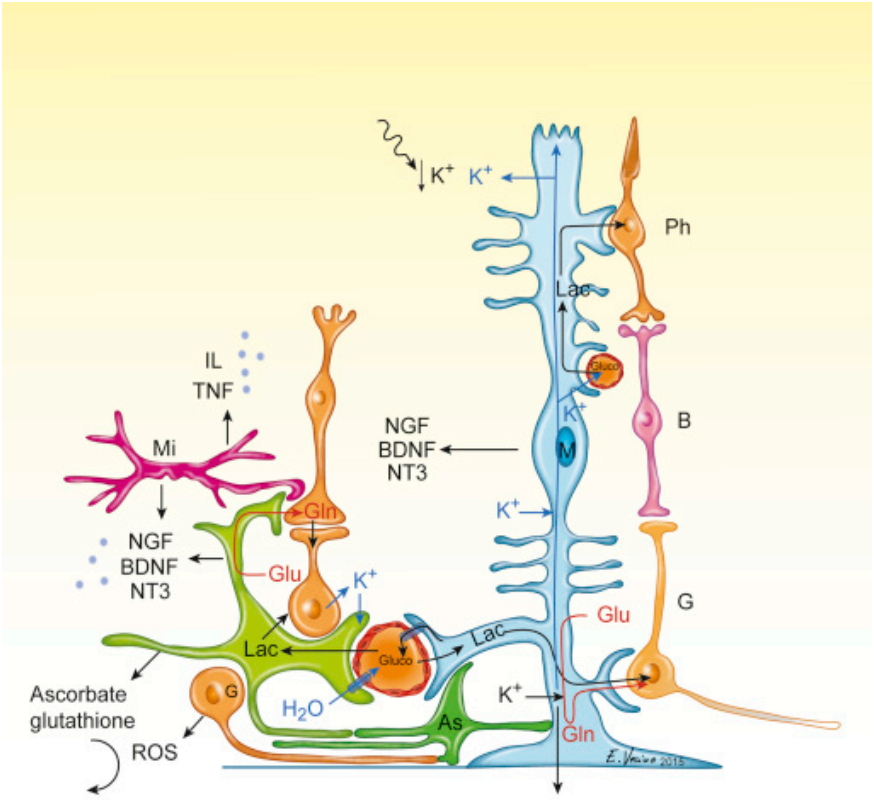

Fig. 6. Esquema que muestra las principales interacciones de las células gliales con las neuronas en el metabolismo de la glucosa, la homeostasis de K^+, el H_2O, el glutamato (Glu) y el metabolismo de glutamina (Gln), la secreción de factores tróficos e interleucinas. As (astrocitos), B (células bipolares), G (células ganglionares), M (Células de Müller), Mi (microglia), Ph (fotorreceptores) (Vecino et al., 2016).

Las células de la glía también participan en la regulación de la actividad neuronal. Los neurotransmisores liberados por neuronas pre-sinápticas pueden activar células de la glía pudiendo también retroalimentar el terminal pre-sináptico para mejorar o suprimir la liberación del neurotransmisor. A su vez, pueden estimular directamente las neuronas post-sinápticas, produciendo respuestas tanto excitatorias como inhibitorias. Esto se debe a que tanto las neuronas como las células macrogliales expresan transportadores de alta afinidad para neurotransmisores (Vecino et al., 2016). Además, estas células participan en la remodelación de los circuitos neuronales, promueven la formación de sinapsis y ayudan a mantener la función neuronal proporcionando terminales nerviosas

con sustratos energéticos y precursores de neurotransmisores (Pfrieger and Barres, 1996).

Es importante destacar que en respuesta a una multitud de trastornos en la retina entre los que se incluyen traumatismos, daño isquémico, infección, neuroinflamación y/o neurodegeneración, la glía se vuelve reactiva y se origina la gliosis, donde se altera la morfología de la retina, se produce una hipertrofia de las células de Müller y los astrocitos con un engrosamiento y ampliación de sus prolongaciones laterales, pudiéndose producir alteraciones dramáticas en la expresión génica (Hernandez et al., 2000; Pekny and Nilsson, 2005). El concepto de gliosis reactiva aun no está claramente definido, es una reacción compleja en la que están implicados muchos elementos y de la que se está empezando a comprender su contribución a la patogénesis de enfermedades y a la recuperación de lesiones (Barres, 2008; Burda and Sofroniew, 2014; Pekny and Pekna, 2014; Zamanian et al., 2012).

Debido a la multitud de funciones que presentan estos dos tipos celulares se ha estudiado si existe cierta heterogeneidad dentro de las dos poblaciones de células. En astrocitos, aunque no haya diferencias morfológicas entre ellos, se ha observado que pueden presentar diferentes comportamientos fisiológicos, lo que prueba la existencia de diferentes subpoblaciones (Matyash and Kettenmann, 2010). Respecto a las células de Müller, se observó una expresión génica heterogénea (Roesch et al., 2008) además de observarse diversidad fenotípica en relación a la expresión de diferentes marcadores (Luna et al., 2010; Vecino et al., 2016), lo que demuestra cierta heterogeneidad, aunque más conocimientos son necesarios para entender esta diversidad funcional.

Las células de la microglía son macrófagos con capacidad fagocítica residentes del CNS, por lo que forman parte del sistema inmune. Las microglía desempeña un papel muy importante en la defensa contra microorganismos invasores, pero también en la regulación inmunológica y en la reparación tisular. Estas células se activan debido a una infección, trauma o neurodegeneración, lo que conlleva la proliferación local, la adquisición de un fenotipo ameboide, la capacidad de fagocitosis mejorada, la secreción de citoquinas, quimiocinas y neurotoxinas, y también la capacidad de migración de las zonas interna de la retina, donde suelen estar en estado fisiológico, hacia el espacio sub-retinal (Fig. 7) (Kettenmann et al., 2011; Ling and Wong, 1993; Omri et al., 2011; Streit et al., 1988; Wieghofer et al., 2014). Durante la neurodegeneración, las células

microgliales activadas participan en la fagocitosis de los desechos celulares y facilitan los procesos regenerativos (Chen et al., 2002). Aunque estando en estado inactivo, también se encargan de mantener la homeostasis en la retina sana secretando citoquinas e interaccionando con otras células gliales y neuronas. Po otro lado, la activación crónica de la microglía está asociada con diversas enfermedades neurodegenerativas incluyendo distrofias retinianas (Langmann, 2007). La microglía también participa en actividades relacionadas con la actividad sináptica pudiendo liberar factores que influyen tanto en la neurotransmisión como en la plasticidad sináptica (Bilimoria and Stevens, 2014; Schafer et al., 2013), además modifica el número de sinapsis en diferentes circunstancias (Miyamoto et al., 2013), y también participa en el pruning sináptico reduciendo y remodelando el exceso de contactos neuronales sinápticos para obtener circuitos neuronales funcionales mediante su actividad fagocítica (Bilimoria and Stevens, 2014).

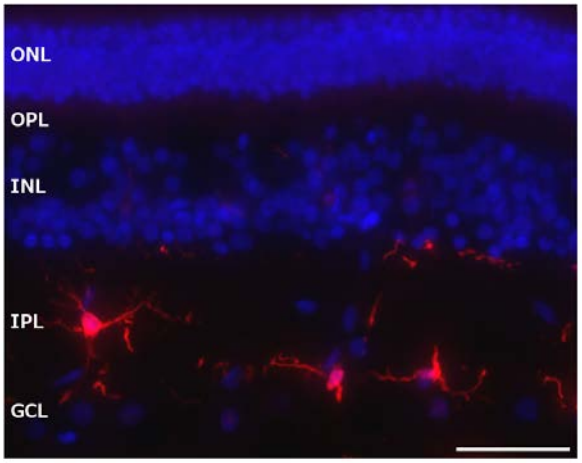

Fig. 7. Microglía en la retina *in vivo*. Corte de retina de cerdo donde la microglía ha sido marcada con un anticuerpo frente a Iba 1 en rojo, y los núcleos fueron teñidos con DAPI en azul. Capa nuclear externa (ONL), capa plexiforme externa (OPL), capa nuclear interna (INL), capa plexiforme interna (IPL), y capa de células ganglionares (GCL). Barra de escala = 50 μm

Finalmente, es necesario mencionar la importancia de células gliales para mantener la supervivencia de las neuronas, se sabe que tanto células de Müller, como astrocitos y microglía sintetizan factores neurotróficos que pueden mediar directa o indirectamente el desarrollo y supervivencia de las neuronas (Garcia et al., 2003a; Vecino et al., 1998a; Vecino et al., 1998b).

1.4. Relación Glía-RGC en condiciones patológicas

El estudio de la interacción de la glía con las células ganglionares proporciona información de gran interés para el estudio de enfermedades relacionadas con la pérdida de las RGCs. La mayoría de las funciones de la glía tienen como objetivo el mantenimiento de la homeostasis de la retina y en relación con las diferentes patologías, las funciones relacionadas con la protección de las neuronas cobran una gran importancia.

Es también de gran interés el hecho de que ante un daño en la retina, la glía responde volviéndose reactiva. Esto nos puede servir de marcador de daño previo a la muerte de neuronas, lo que nos permitiría ampliar el rango de acción para el tratamiento de una enfermedad neurodegenerativa. Ante un daño en la retina, las células de Müller se activan, y en las primeras fases de retinopatía diabética, por ejemplo, esta activación puede producir neuroprotección contra la neurotoxicidad inducida por altas concentraciones de glucosa (Matteucci et al., 2014). Bajo condiciones de enfermedad o traumatismo, también los astrocitos se activan y se vuelven reactivos (Pekny et al., 2014; Yang et al., 2014), experimentan una serie de cambios como proliferación, migración, hipertrofia, expresión de GFAP y secreción de señales proinflamatorias, entre otras, con el fin abordar el daño junto con otras células gliales (Nahirnyj et al., 2013). Pero como consecuencia de la activación de los astrocitos, las RGCs no solo reciben señales positivas, sino que también pueden recibir señales negativas debido al deterioro astrocítico, pudiéndose alterar la homeostasis de las RGCs y desencadenar la muerte de estas. Por otro lado, en retinas sanas, las células de la microglía se localizan en la parte interna de la retina, sin embargo, frente a un daño como puede ser una degeneración causada por la edad, la distribución de microglía cambia drásticamente, estas células se activan y migran a ubicaciones sub-retinianas (Ma et al., 2009; Ma et al., 2012). En patologías con un alto componente inflamatorio, las capacidades migratorias, secretorias y de crecimiento, así como la capacidad neuroprotectora de la microglía juega un papel muy importante en el desarrollo de la enfermedad.

Una de las patologías de mayor interés para nuestro estudio es el glaucoma, donde tiene lugar una muerte selectiva de RGC mediante apoptosis (Garcia-Valenzuela et al., 1995; Vecino and Sharma, 2011), provocando así una pérdida progresiva e irreversible del campo visual, produciendo finalmente ceguera (Mi et al., 2014; Quigley, 2011; Rieck,

2013). Aún queda mucho por conocer sobre la etiología y la fisiopatología del glaucoma, aunque se han encontrado varios factores de riesgo y mecanismos que influyen en la enfermedad. El factor de riesgo que se puede considerar más importante es la elevación de la presión intraocular (IOP), pero otros factores que se han asociado con la enfermedad son: la baja presión de perfusión ocular diastólica, parámetros hemodinámicos, las enfermedades sistémicas como la hipertensión sostenida o la diabetes, el grupo étnico, la edad, o la miopía (Hernandez et al., 2009a). La muerte de las RGCs en el glaucoma probablemente dependa de la suma de varios factores que causen estrés, como pueden ser la acumulación de especies reactivas de oxigeno, de glutamato, o el deterioro mitocondrial, así como respuestas celulares inadecuadas (Rieck, 2013). Debido a las limitaciones que se presentan al estudiar esta patología en individuos humanos, los modelos animales de glaucoma son herramientas muy eficientes para descubrir y caracterizar los factores etiológicos, los mecanismos patológicos y el alcance y las consecuencias de la muerte de las RGCs. Además, son necesarios para evaluar el valor terapéutico de fármacos en ensayos preclínicos (Smedowski et al., 2014). Sin embargo, existen diferencias en la anatomía y la fisiología de la retina entre especies animales, y los procedimientos utilizados para obtener tales modelos experimentales pueden variar, por lo que es necesario determinar las ventajas y limitaciones de cada modelo en particular y escoger el más adecuado para cada estudio (Smedowski et al., 2014; Vecino, 2008; Vecino and Sharma, 2011; Vecino et al., 2017).

Los astrocitos sufren cambios morfológicos relacionados con el daño producido a las RGCs (Lye-Barthel et al., 2013; Zhang et al., 2013). Además, se propone que los astrocitos serían los primeros en notar el daño en las primeras etapas del glaucoma (Dai et al., 2012). Las células de Müller también se alteran en retinas glaucomatosas, sobreexpresan glutamina sintetasa y su citoesqueleto está parcialmente desorganizado, además se induce la expresión de AQP7 (Tran et al., 2014; Vecino et al., 2016). La función de la activación de astrocitos y células de Müller aún no se conoce con exactitud, aunque una semana después de la elevación de la IOP ya se observa una gliosis astrocítica que disminuye posteriormente (Hernandez et al., 2009b). Además, existe la posibilidad de que los astrocitos detecten el aumento de la presión directamente, o a través del resto de células gliales, y reaccionan liberando señales neurotróficas que podrían ayudar a las RGCs a resistir el daño. Otra posible función de los astrocitos reactivos podría estar relacionada con la reparación del daño a la barrera

hemato-retiniana (Bush et al., 1999; Voskuhl et al., 2009). Sin embargo, cuando el daño es prolongado en el tiempo, existe un lado perjudicial de la gliosis, y es que los astrocitos reactivos pueden exacerbar el proceso glaucomatoso por la sobreexpresión de toxinas, produciendo un efecto tóxico directo sobre las RGCs.

El desarrollo del glaucoma y de otras patologías retinianas como la degeneración macular asociada a la edad, la retinopatía del prematuro, o la retinopatía diabética proliferativa, entre otras, podría estar relacionado con una reducción de la tensión de oxigeno (Grimm and Willmann, 2012), ya que la retina es sensible a la hipoxia, definida esta como un inadecuado o disminuido suministro de oxigeno en un organismo, tejido o célula (Caprara and Grimm, 2012). Por este motivo se estudiará el efecto que tiene la hipoxia en la supervivencia y en la activación de la apoptosis de las RGCs, las neuronas más sensibles de la retina y las principales afectadas en el glaucoma (Garcia-Valenzuela et al., 1995; Kergoat et al., 2006). También se estudiará la morfología de los astrocitos de la retina para evaluar si se vuelven reactivos debido a este daño, dada su importante vinculación entre los vasos sanguíneos y las neuronas, ya que pueden ser las primeras células que perciban la falta de oxigeno (Chan-Ling and Stone, 1992; Garcia et al., 1993). Aunque se cree que los astrocitos son más resistentes al daño hipóxico que las neuronas (Zhou et al., 2013) y puedan inducir su protección (Bevensee and Boron, 2008; Fletcher et al., 2010), la hipoxia también les afecta negativamente (Vangeison and Rempe, 2009), de hecho, la degeneración de los astrocitos se asocia con el fallo funcional de la barrera retinal-sanguínea en neuropatías inducidas por oxígeno (Chan-Ling and Stone, 1992; Dorrell et al., 2010). La activación de la apoptosis y el posible cambio de morfología de los astrocitos también se evaluará en el colículo superior (estructura cerebral que recibe aferencias de axones de la retina y proyecciones de la corteza visual) (Leventhal et al., 1981; Wang et al., 2010), para realizar una comparativa del efecto de la hipoxia, que se administrará de manera sistémica, en estas dos partes del sistema nervioso central. Este estudio se llevará a cabo en cerdos de varios días de edad, como parte de un estudio de hipoxia neonatal.

Previamente a este estudio, el grupo de investigación en el que se realiza esta Tesis Doctoral ha trabajado en la realización de varios estudios en los que se analiza un grado más en el daño por la ausencia de oxigeno, como es la isquemia. En ellos se han estudiado las alteraciones de las células de Müller (Vecino et al., 1998b) o la

neuroprotección de las células ganglionares (Pinar-Sueiro et al., 2013) tras periodos transitorios de isquemia en la retina.

1.5. Funciones de la glía en el tratamiento de patologías

Como se ha mencionado previamente, las células gliales no solo están implicadas en el control del ambiente extracelular, también participan suministrando metabolitos y factores de crecimiento a las neuronas. Cuando un daño afecta a la retina, las células de Müller, como principal célula glial en la retina, juegan un papel importante en la neuroprotección y la regeneración de este tejido.

Debido a que las células de Müller expresan transportadores como GLAST (transportador de L-glutamato/L-aspartato) (Derouiche and Rauen, 1995) y que además expresan enzimas como la glutamina sintetasa (Riepe and Norenburg, 1977), pueden proteger a las neuronas de los efectos excitotóxicos del glutamato (Heidinger et al., 1999; Izumi et al., 1999; Kawasaki et al., 2000). Además, debido a la presencia de agentes antioxidantes, como el glutatión, juegan un papel importante en la prevención del daño mediante especies reactivas de oxigeno en la retina (Garcia and Vecino, 2003; Pow and Crook, 1995). Es importante también destacar su capacidad fagocítica de partículas exógenas y de debris celular, ya que este es un paso importante en la reparación de un tejido después de un daño (Sarthy and Ripps, 2001). Podrían también participar en la regeneración de la retina después de un daño debido a su capacidad de desdiferenciación a células progenitoras para, a continuación, dar lugar a diferentes tipos de células neuronales (Fischer and Reh, 2001). Estas propiedades protectoras y regeneradoras de las células de Müller han sido demostradas mediante cultivo celulares. RGCs que crecieron sobre una monocapa de células de Müller, presentaban una mejor supervivencia, un aumento del tamaño del soma, y un aumento del crecimiento de neuritas (Garcia et al., 2002; Ruzafa and Vecino, 2015). Este aumento de la supervivencia debido a la presencia de las células de Müller, se ha demostrado también bajo condiciones de hipoxia (Kitano et al., 1996), y tras un daño excitotóxico debido a la presencia de glutamato (Heidinger et al., 1999; Izumi et al., 1999; Kitano et al., 1996).

Por otro lado, las células de Müller pueden ejercer su función neuroprotectora debido a su capacidad de secretar neurotrofinas y factores de crecimiento. Esta propiedad adquiere importancia debido a que no es necesario el contacto célula-célula para ejercer un efecto beneficioso a la supervivencia y neuritogénesis de las RGCs. Ha sido demostrado que la liberación de factores neurotróficos de células gliales aumenta la supervivencia a largo plazo del desarrollo RGCs en cultivo (Meyer-Franke et al., 1995). Aunque el efecto sobre el crecimiento de las neuritas de las RGCs que ejerce el crecer sobre una monocapa de células de Müller es más fuerte que el observado únicamente con la adición el medio secretado de las mismas, sugiriendo que existen posibles efectos sinérgicos de sustrato y factores difusibles (Garcia et al., 2002). Algunas de los factores de crecimiento secretados por Müller, y que ejercen un efecto positivo en la supervivencia de neuronas retinianas, son el factor neurotrófico derivado del cerebro (BDNF) (Vecino et al., 1999), el factor neurotrófico ciliar (CTNF) (Rhee and Yang, 2010; Zack, 2000), el factor de crecimiento de fibroblastos básico (bFGF) (Bringmann et al., 2009; Hollborn et al., 2004), el factor derivado del epitelio pigmentario (PEDF) (Zhou et al., 2009) o el factor neurotrófico derivado de la glía (GDNF) (Harada et al., 2003; Hauck et al., 2006), entre otros. Aunque el efecto del medio condicionado de las células de Müller parece ser multifactorial, mediante análisis de proteómica se puede seguir analizando e identificando qué otras moléculas secretadas por las células de Müller tienen funciones neuroprotectoras. Algunas de estas pueden ser la proteínas de unión al factor de crecimiento similar a la insulina 5 (IGFBP5) y el factor de crecimiento del tejido conectivo (CTGF) (Hauck et al., 2008), o la transferrina, la osteopontina (OPN o SPP1), el factor inhibidor de leucemia (LIF), y quimioquina 10 con motivo C-X-C (CXCL10) (von Toerne et al., 2014). Además, estudios previos demuestran la relación entre algunos de estos factores, como es el caso de GDNF y la OPN, ya que la estimulación de GDNF incrementa la expresión de OPN por las células de Müller, y esta OPN promueve la supervivencia de neuronas retinianas como son los fotorreceptores (Del Rio et al., 2011). En esta tesis doctoral, se analizará mediante proteómica el medio condicionado de células de Müller cultivadas en diferentes condiciones, para identificar proteínas con función neuroprotectora sobre las RGCs. La caracterización e identificación de estas moléculas es de gran interés para la elaboración de posibles estrategias terapéuticas para proteger las RGCs en enfermedades neurodegenerativas como el glaucoma o tras una lesión en la retina. Asimismo, el

estudio de la retina de organismos *knock-out* para estas proteínas ayudaría a conocer sus funciones y su implicación en el normal funcionamiento de la retina.

Con el objetivo de probar el efecto de los factores secretados, es fundamental contar con un sistema fiable, para ello, a finales de los años 90, miembros del equipo pusieron a punto tanto el cultivo de células ganglionares de la retina adulta como de co-cultivos. Comprobando así que el efecto de los factores tróficos podría probarse en estos cultivos (Garcia et al., 2002) y que las células ganglionares expresaban en cultivo los mismos factores tróficos y sus receptores a pesar de estar en cultivo (Garcia et al., 2003b). Concluyendo por tanto, que el cultivo de células ganglionares de animales adultos es un buen modelo para comprobar los efectos neuroprotectores de distintas sustancias. Además, recientemente, se ha comprobado que este sistema de cultivos son sensibles y eficientes para el estudio de moléculas de adhesión, así como de integrinas, para el estudio de la regeneración de las RGCs (Vecino et al., 2015).

Además de la identificación de proteínas del medio condicionado para el posible tratamiento de neuropatías ópticas, es importante estudiar qué proteínas son sobreexpresadas tras un daño, como puede ser el pinzamiento del nervio óptico (Qu and Jakobs, 2013), ya que la detección de las mismas podría ayudar a proporcionar un diagnostico precoz de la enfermedad, facilitando así su posible tratamiento o retraso del avance de la misma. La osteopontina puede ser también una proteína candidata como biomarcador, ya que aumenta su expresión en modelos de glaucoma y además presenta ciertas propiedades neuroprotectoras (Birke et al., 2010).

1.6. Otras formas de neuroprotección

El PRGF (plasma rico en factores de crecimiento) se extrae del plasma sanguíneo y se encuentra enriquecido en morfógenos, proteínas y factores de crecimiento. Algunas de las proteínas presentes en el PRGF son: el factor de crecimiento derivado de plaquetas (PDGF), el factor de crecimiento transformador beta (TGF-β), el factor de crecimiento endotelial vascular (VEGF), el factor de crecimiento fibroblástico (FGF), y el factor de crecimiento nervioso (NGF) entre otros (Anitua et al., 2010; Orive et al., 2009). Debido a sus propiedades proliferativas y a su capacidad de acelerar la regeneración tisular ya ha sido utilizado en diferentes especialidades medicas (Anitua et al., 2016a; Anitua et

al., 2016b; Anitua et al., 2010). Sin embargo, en estudios recientes, en modelos de Alzheimer y Parkinson se ha observado que el PRGF posee capacidades neuroprotectoras (Anitua et al., 2014; Anitua et al., 2013; Anitua et al., 2015). Se sugiere que ll PRGF pueda actuar como un factor neurotrófico que promueve la supervivencia neuronal bajo la exposición a la beta amiloide (Aβ) (Anitua et al., 2013; Anitua et al., 2015a), además, de que pueda prevenir la degeneración dopaminérgica a través de un proceso de señalización dependiente de NF-κB (factor nuclear-kB) (Anitua et al., 2015a). Estos datos sugieren que el PRGF puede proporcionar una nueva estrategia neuroprotectora en diversas enfermedades neurodegenerativas, por este motivo, se pretende estudiar el efecto del PRGF en las RGCs, así como en las células de la glía de la retina.

Conociendo la estructura de la retina, sabiendo la importancia que tiene la glía en sus funciones, y teniendo en cuenta que durante el glaucoma tienen lugar cambios tanto en la retina como en el nervio óptico, nos proponemos estudiar diferentes situaciones y modelos que nos ayuden a entender la interacción entre la glía y las células ganglionares. El objetivo final es comprender la etiología y progresión de la enfermedad, y que a su vez, nos ayude a desarrollar mecanismos de diagnóstico y tratamiento. Para analizar los primeros cambios que pueden ocurrir en la retina al inicio del daño, nos planteamos desarrollar un modelo de hipoxia, ya que como ha sido mencionado previamente, la reducción de la tensión de oxigeno puede estar relacionado con el desarrollo de glaucoma. Este modelo será realizado en cerdos neonatales, y la hipoxia será inducida de forma sistémica, lo que permitirá realizar un estudio comparativo de las neuronas y la glía entre la retina y el cerebro.

A continuación, y sabiendo que la retina es un compendio de células de Müller, a las cuales se les ha adjudicado una función neuroprotectora, nos centramos en el estudio de la interacción de las mismas con las células ganglionares. Para esto surge la necesidad de aislar estos dos tipos celulares, por lo que se realizarán cultivos primarios de células de Müller y células ganglionares de organismos adultos. Con este fin y tras poner a punto la metodología, se usarán la rata o el cerdo como modelos de experimentación según la conveniencia del estudio. En estos sistemas serán analizados el efecto de las células de Müller sobre las células ganglionares, tanto por contacto célula-célula como

mediante factores secretados. A su vez, el secretoma de las células de Müller será estudiado mediante un análisis proteómico comparativo para poder identificar nuevas moléculas que tengan capacidad neuroprotectora sobre las células ganglionares.

Este modelo de cultivo de células de la retina, podrá ser usado también para el estudio de otros compuestos a los que recientemente se les ha adjudicado propiedades neuroprotectoras, como es el PRGF. En este caso, además del análisis de su efecto sobre las células ganglionares, debido a que el PRGF es una mezcla compleja de moléculas con diversas funciones, todas las células de la glía serán analizadas tras el tratamiento con PRGF.

Tras los análisis *in vitro*, surge la necesidad de estudiar el alcance de la función *in vivo* de las moléculas neuroprotectoras que se han identificado. Por ello, se estudiará la retina de ratones *knock-out* para la osteopontina, molécula secretada por las células de Müller y de la que previamente se ha destacado su importancia. En este estudio se analizarán tanto las células ganglionares como las células de la glía para conocer el posible papel que ejerce la osteopontina en la retina.

Por último, nos centraremos en la parte diagnóstica del daño del nervio óptico que puede tener lugar en el glaucoma, estudiando posibles biomarcadores que se secreten por células de la glía, en este caso, astrocitos de la cabeza del nervio óptico de ratón, en respuesta a un daño producido por un pinzamiento del nervio óptico. Se analizará la expresión de algunos genes que se sobreexpresan en glaucoma o tras un daño inducido a las células ganglionares, entre los que se incluye el gen de la osteopontina. También se tratará de detectar la sobreexpresión de estas moléculas a nivel proteico tanto en la cabeza del nervio óptico como en el humor acuoso.

A continuación, en el ANEXO 0, se encuentran el resumen y la información para acceder a una completa revisión realizada por este grupo sobre la interacción de las neuronas y las células de la glía en la retina de mamíferos. Además, cada artículo anexado en el apartado **4. Resultados** presenta una introducción propia del tema a tratar.

ANEXO 0

Prog Retin Eye Res. 2016 Mar;51:1-40. doi: 10.1016/j.preteyeres.2015.06.003. Epub 2015 Jun 23.

Glia-Neuron Interactions in the Mammalian Retina.

Elena Vecino[1], F. David Rodriguez[2], Noelia Ruzafa[1], Xandra Pereiro[1], Sansar C. Sharma[3].

[1] Department of Cell Biology and Histology, University of the Basque Country UPV/EHU, Leioa 48940, Vizcaya, Spain.

[2] Department of Biochemistry and Molecular Biology, E-37007, University of Salamanca, Salamanca, Spain.

[3] Department of Ophthalmology, Cell Biology and Anatomy, New York Medical College, Valhalla, NY 10595, USA; IKERBASQUE, Basque Foundation for Science at Dept. Cell Biology and Histology, UPV/EHU, Spain.

Abstract

The mammalian retina provides an excellent opportunity to study glia-neuron interactions and the interactions of glia with blood vessels. Three main types of glial cells are found in the mammalian retina that serve to maintain retinal homeostasis: astrocytes, Müller cells and resident microglia. Müller cells, astrocytes and microglia not only provide structural support but they are also involved in metabolism, the phagocytosis of neuronal debris, the release of certain transmitters and trophic factors and K(+) uptake. Astrocytes are mostly located in the nerve fibre layer and they

accompany the blood vessels in the inner nuclear layer. Indeed, like Müller cells, astrocytic processes cover the blood vessels forming the retinal blood barrier and they fulfil a significant role in ion homeostasis. Among other activities, microglia can be stimulated to fulfil a macrophage function, as well as to interact with other glial cells and neurons by secreting growth factors. This review summarizes the main functional relationships between retinal glial cells and neurons, presenting a general picture of the retina recently modified based on experimental observations. The preferential involvement of the distinct glia cells in terms of the activity in the retina is discussed, for example, while Müller cells may serve as progenitors of retinal neurons, astrocytes and microglia are responsible for synaptic pruning. Since different types of glia participate together in certain activities in the retina, it is imperative to explore the order of redundancy and to explore the heterogeneity among these cells. Recent studies revealed the association of glia cell heterogeneity with specific functions. Finally, the neuroprotective effects of glia on photoreceptors and ganglion cells under normal and adverse conditions will also be explored.

2. HIPOTESIS Y OBJETIVOS/ HYPOTHESES AND OBJECTIVES

La hipótesis de trabajo de la presente Tesis Doctoral se basa en que las células de la glía pueden detectar el daño en la retina, pudiendo actuar como sensores y/o pudiendo proteger a las células ganglionares de la retina de ese daño. Por ello pensamos que estudiando las interacciones entre estos tipos celulares en distintos modelos experimentales, podremos conocer los mecanismos moleculares que desarrollen las células gliales y que estén implicados en la neuroprotección de las células ganglionares.

Teniendo en cuenta los antecedentes descritos previamente y la hipótesis planteada, en el marco de la presente Tesis Doctoral se ha desarrollado un objetivo general:

Estudiar la interacción de las células de la glía con las células ganglionares de la retina ante un daño.

Con el propósito de cumplimentar el objetivo global se han planteado los siguientes objetivos parciales:

1- Estudiar el efecto de la hipoxia en la retina en fases neonatales y comparar dichos efectos con los que acontecen en el cerebro, estudiando tanto la vulnerabilidad de las neuronas como de la glía.
2- Analizar la interacción de las células ganglionares de la retina con la glía de Müller *in vitro.*
3- Identificar las posibles moléculas implicadas en las interacciones entre dichas células, así como estudiar el papel neuroprotector de alguna molécula candidata.
4- Analizar *in vitro* el posible efecto neuroprotector del PRGF (plasma rico en factores de crecimiento) en la supervivencia de las células ganglionares de la retina, así como su efecto en las células de la glía.
5- Valorar los cambios en la retina en animales *knock-out* para osteopontina.
6- Cuantificar los cambios que tienen lugar en la cabeza del nervio óptico así como en el humor acuoso de animales sometidos al pinzamiento del nervio óptico.

The hypothesis tested in this Doctoral Thesis was based on the capacity of glial cells to detect damage in the retina, acting as sensors and protecting retinal ganglion cells. By studying the interactions between these cell types in different experimental models, we hoped to define the mechanisms or molecules that are involved in the neuroprotection of retinal ganglion cells afforded by glia.

In light of the current state-of-the-art and the hypothesis postulated, the overall objective of this Doctoral Thesis was:

To study the interaction between the glial cells and the ganglion cells in the retina after damage.

In order to address this global objective, the following approaches were proposed:

1- To study the effect of hypoxia in the retina of neonates and to compare such effects with those in the brain, focusing on the vulnerability of neurons and glia.
2- To analyze the interaction of retinal ganglion cells with Müller glia *in vitro*.
3- To identify molecules potentially involved in the interactions between these two cell types, and to study the neuroprotective role of certain candidate molecules.
4- To analyze the possible neuroprotective effect of PRGF (plasma rich in growth factors) *in vitro*, and its influence on the survival of retinal ganglion cells, as well as its effect on glial cells.
5- To evaluate the changes in the retina in mice carrying a null mutation for osteopontin.
6- To quantify the changes that take place in the optic nerve head and aqueous humor of animals subjected to optic nerve crush.

3. MATERIAL Y MÉTODOS

Todas las técnicas que se describen a continuación están explicadas con mayor detalle en los artículos correspondientes en el apartado 4. Resultados.

3.1. Animales

Este estudio fue realizado de acuerdo con la Resolución ARVO (Association for Research in Vision and Ophthalmology) para el uso de animales en experimentación. Los ojos de cerdo adultos se obtuvieron de un matadero local, y se transportaron al laboratorio en medio DMEM CO_2 independiente (CO_2-independent Dulbecco's modified Eagle's medium; Life Technologies, Carlsbad, CA, USA) más 0,1% de gentamicina (Life Technologies, Carlsbad, CA, USA) (ANEXO 3, 4). Los cerdos neonatales se obtuvieron de granjas locales autorizadas por la Agencia Reguladora del País Vasco para suministrar animales de investigación, todos los animales fueron transportados con un certificado de su estado de salud, siendo todos ellos libres de cualquier enfermedad. Los animales fueron sacrificados por sobredosis de cloruro potásico (0.35 mg/kg) (ANEXO 1).

Se usaron ratas adultas Sprague-Dawley (200-250g) procedentes del animalario de la Facultad de Medicina de la Universidad del País Vasco (ANEXO 2, 3).

Los ratones controles C57BL/6J y knock-out (B6.129S6(Cg)-Spp1tm1Blh/J) de 3 y 20 meses de edad (ANEXO 5, 6).

Los animales tuvieron acceso libre a alimentos y agua, con un ciclo de luz-oscuridad 12 horas y con una temperatura estable de 21°C. Las ratas fueron sacrificadas por exposición a CO_2 y los ratones por dislocación cervical.

3.2. Extracción del tejido

Los ojos fueron enucleados y mantenidos en medio DMEM CO_2 independiente para su uso en cultivos.

Para realizar un marcaje de toda la retina (*in toto* o whole mount), se retiró la cornea, cristalino y vítreo, y la retina junto a la esclera se fijó en paraformaldehido (PFA) 4% en tampón fosfato 0,1 M (PB, pH 7,4) durante una noche. La copa se lavó con tampón fosfato salino (PBS, pH 7,4) y la retina se separó cuidadosamente del resto del ojo (ANEXO 1, 5).

Para la realización de cortes en criostato, los ojos fueron fijados durante una noche en PFA 4% tras realizar un agujero en la cornea. Además, el colículo superior se extrajo del cerebro y se fijó inmediatamente durante una noche en PFA al 4%. Ambos tejidos fueron crioprotegidos durante una noche a 4°C en 30% de sacarosa en 0,1 M PB. Las muestras fueron integradas en medio OCT, y se realizaron cortes de un espesor 14μm, que fueron almacenadas a -20°C (ANEXO 1, 4, 5).

3.3. Cultivos organotípicos o explantes de retina

En condiciones asépticas, las retinas se extrajeron cuidadosamente de los ojos, y se lavaron en medio DMEM CO_2 independiente. Con un troquel de 8 mm de diámetro se cortaron los explantes de retina de cerdo, cercanos al nervio óptico y evitando grandes vasos sanguíneos. Los explantes se transfirieron a insertos de cultivo celular (0,45 μm de poro, 12 mm de diámetro, Merck Millipore, Darmstadt, Alemania) con la capa de fotorreceptores pegada a la membrana. Los explantes se cultivaron en medio Neurobasal A (Life Technologies, Carlsbad, CA, USA) con 1% de L-glutamina y 0,1% de gentamicina, y se mantuvieron a 37ºC en una atmósfera húmeda y al 5% de CO_2. El medio de cultivo se cambió cada 2 días, manteniendo siempre humedecido el explante. Los explantes se fijaron a día 1 y 3 con PFA al 4% durante una noche, se crioprotegieron mediante una disolución de sacarosa al 30% y fueron embebidos en OCT para la realización de cortes de criostato de un espesor 14μm (ANEXO 4).

3.4. Cultivos de células de la retina: RGCs, células de Müller y co-cultivos

Para la realización de los cultivos celulares, las retinas fueron extraídas en condiciones de asepsia. Se realizaron 3 tipos de cultivos: de RGCs usando medio Neurobasal-A suplementado con B27 (Life Technologies, Carlsbad, CA, EUA); de Müller utilizando DMEM (Life Technologies, Carlsbad, CA, EE.UU.) con 10 o 20% de suero bovino fetal (FBS, Life Technologies, Carlsbad, CA, EE.UU.); y co-cultivos de RGCs y células Müller, utilizando Neurobasal-A medio con 10% de FBS y suplementado con B27. A todos los medios se les añadió 1% de L-glutamina (2 mM) y gentamicina al 0,1% (50 mg/ml).

Dependiendo del animal, se usaron retinas enteras de rata o se cortaron trozos de retina de cerdo con un troquel de 8mm de diámetro. Estos fragmentos de retina fueron digeridos enzimáticamente con papaína y 10% de DNasa I (kit de disociación

Worthington Papain Dissociation, Worthington Biochemical Lakewood, NJ, USA). La digestión para los cultivos de RGCs es de 90 minutos y para los de células de Müller y co-cultivos es de 30 minutos. La actividad enzimática de la papaína se detuvo mediante la adición de medio y el tejido fue desagregado mediante una suave trituración usando puntas de pipeta de diámetro decreciente. Las células disociadas se recogieron mediante centrifugación a 300g durante 5 minutos y fueron resuspendidas en su correspondiente medio. En el caso de las RGCS en medio NBA suplementado con B27 y en el caso de los cultivos de células de Müller en DMEM con distintas concentraciones de FBS dependiendo del experimento.

Para la realización del cultivo de RGCs, se realizó además un gradiente siguiendo el protocolo del kit Worthington. Todas las células resuspendidas se sembraron en placas de 24 pocillos con cubreobjetos de vidrio de 13 mm previamente revestidos con poli-L-lisina (Sigma, P4832, 100 μg/ml) y laminina (Sigma, L2020, 10 μg/ml). Las células se mantuvieron en un incubador humidificado a 37°C con una atmósfera de CO2 al 5%. En los cultivos de células Müller y co-cultivo, a día 1 de cultivo se cambió todo el medio. Para mantener los células, la mitad del medio se cambia cada 3 días. Las células se fijaron con metanol -20ºC durante 10 minutos a día 6 para RGCs o 7 para células de Müller y co-cultivo (ANEXO 2, 3, 4).

3.5. Inmunohistoquímica e inmunocitoquímica

Para la retinas *in toto*, estas se colocaron en una placa Petri de pequeño tamaño, se lavaron con PBS y se bloquearon incubándose en una disolución de PBS-TX-100-BSA (0,25% de Triton-X 100 y 1% de albúmina de suero bovino en PBS) durante una noche a 4ºC en agitación. A continuación, las retinas se incubaron con los anticuerpos primarios diluidos en PBS-TX-100-BSA, durante un día en agitación a 4ºC. Posteriormente, las retinas se lavaron tres veces en PBS durante 15 minutos y se incubaron con los anticuerpos secundarios diluidos en PBS-BSA (1%) durante 5 horas a temperatura ambiente en agitación. Finalmente, las retinas se lavaron 3 veces durante 10 minutos en PBS, y se montaron sobre portaobjetos en PBS-Glicerol (1:1) (ANEXO 1, 5).

Para los cortes de criostato, los cortes fueron lavados dos veces en PBS-TX-100 durante 10 minutos, y se incubaron durante una noche con los anticuerpos primarios a 4ºC. Tras

lavar dos veces en PBS, fueron incubados con el correspondiente anticuerpo secundario y DAPI diluido en PBS-BSA (1%) durante 1 hora a temperatura ambiente. DAPI fue utilizado como marcador nuclear a 1:10.000. Los cortes se lavaron dos veces con PBS durante 10 minutos y se montaron con un cubreobjetos en PBS-Glicerol (1:1) (ANEXO 1, 4, 5).

Para los cultivos celulares, los cubreobjetos donde las células crecieron fueron bloqueados con tampón de bloqueo (BSA al 3% y Triton X-100 al 0,1% en PBS) durante 30 minutos a temperatura ambiente. A continuación se incubaron con los anticuerpos primarios en tampón de bloqueo durante una noche a 4ºC. Tras lavar con PBS, se incubaron con los anticuerpos secundarios y DAPI en tampón de bloqueo durante 1 hora a temperatura ambiente. Para finalizar, se lavaron con PBS y fueron montaron con Fluor Save (ANEXO 2, 3, 4).

Los anticuerpos primarios usados están descritos en la Tabla 1. Todos los anticuerpos secundarios usados fueron Alexa Fluor 568, 555 y 488 (Life Technologies, Eugene, Oregon, USA) y fueron usados a una dilución de 1:1000.

ANTICUERPO	MARCAJE	DILUCIÓN	REFERENCIA
Brn3a	RGCs	1:1.000	Santa Cruz Biotechnology
RBPMS	RGCs	1:4.000	PhosphoSolutions
βIII Tubulina	RGCs	1:2.000	Promega
GFAP	Astrocitos	1:1.000	Sigma
Glutamina Sintetasa	Células de Müller	1:10.000	Abcam
Vimentina	Células de Müller	1:10.000	Dako
Iba 1	Microglía	1:2.000	Wako
Active caspase-3	Células apoptóticas	1:1.600	Cell Signaling Technology

Tabla 1. Anticuerpos primarios. Lista de anticuerpos primarios utilizados en este estudio, donde se indica la proteína que reconoce el anticuerpo, que tipo celular marca, en que dilución se utiliza y la casa comercial donde ha sido adquirido.

3.6. Captura y análisis de imágenes

Para la captura de imágenes en este estudio, se ha usado mayoritariamente un microscopio de fluorescencia (Zeiss, Jena, Germany) con cámara Zeiss Axiocam MRM (Zeiss, Jena, Germany) (ANEXO 2-5). Aunque para determinados estudios se ha usado un microscopio confocal (Olympus FV500, Olympus, Tokyo, Japan) (ANEXO 1).

Además del recuento manual de células (ANEXO 1-4), se han usado distintos programas informáticos. Para cuantificar el número de RGCs en retinas *in toto* o el número de núcleos de células de Müller en cultivos, se ha usado el software Zen (Zeiss, Jena, Germany) (ANEXO 1, 4, 5). También han sido utilizados el programa Image J (versión 1.49) y un programa desarrollado en Matlab (R2010b), ambos para cuantificar cambios en la morfología de los astrocitos (ANEXO 1, 5).

3.7. Análisis estadístico

Los datos resultantes de las cuantificaciones se han descrito como media y error estándar de la media. Para la facilidad de comprensión de los resultados, en muchos casos, estos valores han sido normalizados con el control. Y en otras ocasiones, el resultado ha sido expresado como el porcentaje de variación entre la situación control y la condición experimental.

Los análisis estadísticos para realizar la comparativa entre las distintas condiciones experimentales se realizaron utilizando el software IBM SPSS Statistics v. 21.0. La homogeneidad de las varianzas se estudió mediante la prueba de Levene ($p < 0,05$). Para evaluar si existen diferencias significativas entre las distintas condiciones, se realizó un test T de Student. Además, el test U de Mann-Witney ha sido utilizado para verificar las diferencias entre los distintos grupos. Para ambas pruebas, el valor mínimo para establecer diferencias significativas se definió como $p < 0.05$ (ANEXO 1-6).

3.8. Otras técnicas: Inducción de hipoxia a un cerdo neonatal

Para la realización de este modelo de hipoxia neonatal en cerdos, tras la analgesia y la anestesia, los animales fueron estabilizaron durante 30 minutos. A continuación, la hipoxia fue inducida disminuyendo los niveles de oxígeno a 12-14% durante 120 minutos. A este periodo le sigue un periodo de normoxia de 240 minutos. Los cerdos control no fueron sometidos a la reducción de las concentraciones de oxígeno (ANEXO 1).

3.9. Otras técnicas: Análisis proteómico

Para el análisis proteómico del medio condicionado de las células de Müller, el medio fue recogido y filtrado a través de un filtro de tamaño de poro de 0.2 μm (Fisher

Scientific, Hampton, NH, USA). Fue alicuotado y posteriormente almacenado a -80ºC hasta realizar el análisis.

Los medios condicionados de distintas condiciones se enviaron en hielo seco hasta Munich, Helmontz Centre, donde fueron analizados realizando un análisis LC-MS/MS en un espectrómetro de masas QExactive HF (Thermo Fisher Scientific Inc., Waltham, MA, USA). Los espectros adquiridos de las diferentes muestras fueron analizadas usando el software Progenesis QI para proteómica (Versión 2.0, Nonlinear Dynamics, Waters, Newcastle upon Tyne, U.K.) (ANEXO 3).

3.10. Otras técnicas: Extracción de PRGF

Se recogieron muestras de sangre humana y de cerdo en tubos con un 3.8% de citrato sódico. Las muestras se centrifugaron a 460g durante 8 minutos a temperatura ambiente. Tras la centrifugación se seleccionó la fracción de plasma que contenía plaquetas, que se incubaron con cloruro cálcico (BTI Biotechnology Institute) durante 1 hora a 34°C. Los sobrenadantes liberados se recogieron tras una centrifugación a 460g durante 15 minutos, estos se filtraron filtro de tamaño de poro de 0.2 μm (Fisher Scientific, Hampton, NH, USA) y se almacenaron a -80ºC hasta su uso (ANEXO 4).

4. RESULTADOS/RESULTS

ANEXO 1

PLoS One. 2017 Apr 13;12(4):e0175301. doi: 10.1371/journal.pone.0175301. eCollection 2017

Effect of Hypoxia on the Retina and Superior Colliculus of Neonatal Pigs

Noelia Ruzafa[1], Carmen Rey-Santano[2], Victoria Mielgo[2], Xandra Pereiro[1], Elena Vecino[1]

[1]Department of Cell Biology and Histology, University of Basque Country UPV/EHU, Leioa, Vizcaya, Spain.

[2]Research Unit for Experimental Neonatal Respiratory Physiology, Cruces University Hospital, Barakaldo, Vizcaya, Spain.

Abstract

Purpose: To evaluate the effect of hypoxia on the neonatal pig retina and brain, we analysed the retinal ganglion cells (RGCs) and neurons in the superior colliculus, as well as the response of astrocytes in both these central nervous system (CNS) structures.

Methods: Newborn pigs were exposed to 120 minutes of hypoxia, induced by decreasing the inspiratory oxygen fraction (FiO_2: 10–15%), followed by a reoxygenation period of 240 minutes (FiO_2: 21–35%). RGCs were quantified using Brn3a, a specific nuclear marker for these cells, and apoptosis was assessed through the appearance of active caspase-3. A morphometric analysis of the cytoskeleton of astrocytes (identified with GFAP) was performed in both the retina and superior colliculus.

Results: Hypoxia produced no significant change in the RGCs, although, it did induce a 37.63% increase in the number of active caspase-3 positive cells in the superior colliculus. This increase was particularly evident in the superficial layers of the superior colliculus, where 56.93% of the cells were positive for active caspase-3. In addition,

hypoxia induced changes in the morphology of the astrocytes in the superior colliculus but not in the retina.

Conclusions: Hypoxia in the neonatal pig does not affect the retina but it does affects more central structures in the brain, increasing the number of apoptotic cells in the superior colliculus and inducing changes in astrocyte morphology. This distinct sensibility to hypoxia may pave the way to design specific approaches to combat the effects of hypoxia in specific areas of the CNS.

Key words: Hypoxia; retina; superior colliculus; retinal ganglion cell; RGC; astrocyte; apoptosis

Introduction

Neonatal hypoxic-ischemic brain injury is a prominent cause of neurological disability in neonates (Cowan, 2000; Cowan et al., 2003). Since it is not possible to conduct controlled studies in children, it is necessary to perform experimental studies in suitable animal species to obtain information that is likely to be applicable to humans. In this respect, pigs have for long been used as an experimental model given that many of their anatomical and physiological characteristics closely resemble those of humans, more so than other non-primate species (Anzenbacher et al., 1998; Rey-Santano et al., 2014; Roth et al., 2013).

The retina pertains to the central nervous system (CNS) and it is one of the most metabolically active tissues in the body (Ames, 1992). Its high-energy demand is due to the highly sensitive and efficient system that converts light energy into neuronal signals, the reason why the retina consumes oxygen more rapidly than other tissues (Eshaq et al., 2014; Kimble et al., 1980). Thus, in times of increased energy demand, oxygen becomes one of the most limited metabolites in the retina (Anderson and Saltzman, 1964). For this reason, the retina is susceptible to alterations in oxygen tension and specifically, the retina is sensitive to hypoxia, a condition defined as an inadequate supply of oxygen for an organism, tissue or cell (Caprara and Grimm, 2012). At the cellular level, functional studies suggest that retinal ganglion cells (RGCs), the neurons that relay visual signals to the brain, may be the most sensitive cells in the retina to

experimental transient ischemia or systemic hypoxia (Kergoat et al., 2006). Indeed, a reduction in oxygen tension could be associated with the development of retinal pathologies, such as retinal vessel occlusion, proliferative diabetic retinopathy, retinopathy of prematurity, glaucoma, age-related macular degeneration or high altitude retinopathy (Grimm and Willmann, 2012). Death of RGCs is a hallmark of retinal diseases in which hypoxia and/or ischemia are assumed to play an etiological role (Kaur et al., 2009; Kaur et al., 2013; Liu et al., 2012; Rovere et al., 2015).

While the brain represents 2% of our body weight, it consumes 20% of the body's oxygen demand. Moreover, the immature foetal and neonatal brains are particularly vulnerable to severe alterations in oxygen tension and they may develop neurovascular malformations when oxygen levels are low (Hallak et al., 2000; Ma et al., 2014). However, in mammalian neonates certain physiological responses and adaptations exist to respond to a limited oxygen supply (Singer, 1999). The superior colliculus is a multilayered structure in the mammalian midbrain, and it is the structure in the brain where among inputs from retinal axons and the visual cortex converge (Leventhal et al., 1981; Sparks, 1986; Wang et al., 2010; Zhao et al., 2014). As hypoxia triggers apoptosis (Chen et al., 2007), it is often best to study this phenomenon by counting the number of recently activated apoptotic cells. Moreover, RGCs are sensitive to hypoxic conditions and the death of these cells provokes a gradual loss of vision that will ultimately lead to blindness. As such, we evaluated the apoptosis induced by hypoxia by examining the distribution of cells with active caspase-3 in the superior colliculus and retina, the activation of which is a marker of this form of cell death.

Glial cells play crucial roles in regulating neuronal development and neuronal activity, and astrocytes in particular are susceptible to reductions in oxygen tension (Salmaso et al., 2014). Given their importance in linking vascular and neuronal function, astrocytes are fundamental in the induction of neuronal deficits, and hypoxia is known to induce astrocyte-dependent protection of neurons (Bevensee and Boron, 2008; Fletcher et al., 2010). They are the first cells exposed to the damage from hypoxic or ischemic insults (Chan-Ling and Stone, 1992; Garcia et al., 1993). Moreover, hypoxia also affects the ability of astrocytes to sustain neuronal viability and it induces specific molecular responses in astrocytes (Vangeison and Rempe, 2009). Indeed, the degeneration of astrocytes is associated with the functional failure of the blood retinal barrier in oxygen-

related neuropathies (Chan-Ling and Stone, 1992; Dorrell et al., 2010). For these reasons, we assessed the morphological changes to the cytoskeleton of astrocytes in the retina and superior colliculus. It is important to note that within the retina, another macroglial cell type is present in addition to astrocytes that are not present in the brain, the Müller glia. These cells are specialized in maintaining the homeostatic and metabolic support of retinal neurons, as well as fulfilling other functions (Vecino et al., 2016). In addition, there is some metabolic heterogeneity and distinct vulnerability to hypoxia within different tissues (Arduini et al., 2014) that could be responsible for producing a distinct response to hypoxia of the tissues of interest here.

Given that hypoxia has a negative effect on neuronal metabolism and that it may be detrimental to the function of neurons, and since astrocytes have the capacity to sustain normal neuronal activity and to regulate the development of the vasculature, here we evaluated whether low oxygen conditions induce changes in neurons and astrocytes in the retina and superior colliculus.

Materials and Methods

Animal preparation

This study was carried out in strict accordance with the recommendations for the Experimental Research Committee of the Cruces University Hospital, which is registered in the Official Register of Breeders, Suppliers and Users of animals for experimental and other scientific purposes in the Basque Country (Spain). All the experimental protocols met with the European (2010/63/UE) and Spanish (RD53/2013) guidelines for the protection of experimental animals and they were approved by the Ethics Committee for Animal Welfare of the Cruces University Hospital. On the same day as the experiment, animals were obtained from a local farm authorized by the Basque Country Regulatory Agency to supply animals for research. All animals were free of any disease and they were transported with a certificate of health.

The protocol to produce hypoxia used in the present study has been described extensively elsewhere (Alvarez et al., 2008). Neonatal pigs (*Sus scrofa*, n = 8) aged 2-4 days old (1.7± 0.2 kg) were sedated with an intramuscular injection of ketamine (15

mg/kg) and diazepam (2 mg/kg). Before performing the surgical procedure, anaesthesia and analgesia were induced by intravenously administering fentanyl (5 μg/kg) and propofol (1.2 mg/kg), and this state was maintained by continuous intravenous infusion of fentanyl (titrated as necessary: 5-20 μg/kg/h), propofol (titrated as necessary: 2-3 mg/kg/h) and midazolam (titrated as necessary: 0.5-2 mg/Kg/h). In addition, the animals used as controls were paralysed by continuous intravenous infusion of vecuronium bromide (3 mg/kg/h). In all cases, an ear vein was catheterized to deliver the anaesthesia and analgesia. A tracheotomy was performed, and a tracheal tube (4.0 mm ID) was inserted and connected to a ventilator. Animals were then positive pressure ventilated and changing ventilator parameters were performed to maintain adequate blood gas values of arterial oxygen pressure (PaO_2) 80-110 mmHg, adequate arterial pressure of carbon dioxide ($PaCO_2$) 35–45 mmHg and a pH 7.30–7.45.

An arterial catheter was inserted into the femoral artery to monitor the mean arterial blood pressure (MABP) and heart rate (HR), and to obtain arterial blood samples for blood gas analysis: PaO_2, $PaCO_2$, pH, Base Excess (EB), oxygen saturation and lactic acid (GEM Premier 4000, Instrumentation Laboratory). Animals were also monitored continuously by three-lead electrocardiogram during the experimental procedure.

Hypoxia

The hypoxia model is based on a swine model of neonatal asphyxia (Cheung et al., 2011). Two experimental groups were established, control (n = 4) and hypoxic (n = 4) pigs. In the hypoxic group, the animals were stabilized for 30 minutes and hypoxia was then induced by decreasing oxygen levels to 12-14% for 120 minutes, followed by 240 minutes of normoxia. Hypoxia was induced by reducing the fraction of inspired oxygen (FiO_2, the fraction or percentage of oxygen in the space being measured) to 0.1 - 0.15 while increasing the concentration of inhaled nitrogen gas. Control pigs were not subjected to reduced oxygen concentrations. Following hypoxia, the FiO_2 levels were increased to 21-35% in order to maintain normoxia for 240 minutes. At the end of the experiments (4 hours after the onset of hypoxic injury), the animals were sacrificed with an intravenous overdose of potassium chloride (0.35 mg/kg).

Tissue collection

Neonates eyes were enucleated, and the cornea, crystalline lens and vitreous humour were removed. Each eyecup containing the retina was fixed overnight by immersion in 4% paraformaldehyde (PFA) in 0.1 M phosphate buffer (PB, pH 7.4) and after then washing in phosphate buffered saline (PBS, pH 7.4), the retina was carefully separated from the rest of the eye. In addition, the superior colliculus was extracted from the brain and immediately fixed overnight in 4% PFA. Control and hypoxic tissues were cryoprotected for 24 hours at 4 °C in 30% sucrose diluted in 0.1 M PB, and the tissue was then embedded in OCT medium to obtain cryosections (14 μm thick) that were stored at −20 °C.

Immunohistochemistry

Whole mount retinas were immunostained as described previously (Vecino et al., 2002), with some minor modifications. The retinas were washed with PBS and non-specific antibody binding was blocked by incubating them overnight at 4 ºC in a solution of PBS-TX-100-BSA (0.25% Triton-X 100 and 1% bovine serum albumin in PBS), with shaking. The retinas were then incubated (for one day with shaking at 4 ºC) with the primary antibodies diluted 1:1,000 in PBS-TX-100-BSA: an anti-Brn-3a goat polyclonal antiserum (Santa Cruz Biotechnology, Santa Cruz, USA) to detect RGC nuclei; and an anti-GFAP mouse monoclonal antibody (Sigma, Steinheim, Germany) to detect the cytoskeleton of astrocytes. Subsequently, the retinas were washed thrice in PBS for 15 minutes and antibody binding was detected (5 hours at room temperature with shaking) with secondary antibodies diluted 1:1,000 in PBS-BSA (1%): an Alexa Fluor 568 conjugated donkey anti-goat antibody (Invitrogen, Eugene, Oregon, USA) and an Alexa Fluor 488 conjugated rabbit anti-mouse antibody (Invitrogen, Eugene, Oregon, USA). Finally, the retinas were washed 3 times for 10 minutes in PBS, flat mounted onto slides in PBS-Glycerol (1:1) and coverslipped.

Cryostat sections of the retina and superior colliculus were immunostained as described previously (Garcia et al., 2002). After washing the sections twice in PBS-TX-100 for 10 minutes, they were incubated overnight with the primary rabbit anti-active (cleavage) caspase-3 (Asp175) antibody (1:1,600, Cell Signaling Technology #9661, Danvers, Massachusetts, USA) and an anti-GFAP mouse monoclonal antibody (1:1,000, Sigma,

Steinheim, Germany). After washing twice in PBS, antibody binding was detected for 1 hour with an Alexa Fluor 555 conjugated goat anti-rabbit antibody (1:1,000, Invitrogen, Eugene, Oregon, USA) and an Alexa Fluor 488 conjugated goat anti-mouse antibody (1:1,000, Invitrogen, Eugene, Oregon, USA) diluted in PBS-BSA (1%). The sections were washed twice with PBS for 10 minutes and mounted with a coverslip in PBS-Glycerol (1:1).

RGC quantification

To analyse the RGCs and astrocytes in the retina, confocal microscopy images of whole mount retinas were obtained at a resolution of 2048 x 2048 pixel with a 20X objective (Olympus FV500, Olympus, Tokyo, Japan). A Z-stack was obtained of five images with a 4 μm separation and a total of 8 whole mount retinas were studied (4 control and 4 hypoxic). Four different areas of the retina were analysed, the peripheral and central areas of the dorsal and ventral retina (S1 Figure). Thus, a total of 16 images from each retina were captured (four pictures of each analysed area). Since the porcine optic nerve is located ventrally, the dorsal area is larger than the ventral area, we selected the peripheral area 15 mm from the optic nerve in the dorsal domain and 6 mm from the optic nerve in the ventral domain. The central area refers to tissue 2 mm from the optic nerve in both the dorsal and ventral directions. These criteria were applied to the 8 retinas studied and thus, the total retinal area analysed was 8 mm^2 per retina (2 mm^2 per area). The method to quantify RGCs was slightly modified from that used previously (Pinar-Sueiro et al., 2013), employing AxioVision 4.7.2.0.Software. The number of Brn3a labelled RGC nuclei in each retinal area of the experimental and control eyes was counted, and compared in the dorsal and ventral peripheral and central retina.

Quantification of active Caspase-3 positive cells

The cells with active caspase-3 were quantified in the retina and superior colliculus using a fluorescent microscope (Zeiss, Jena, Germany) and the Zeiss Zen software, analysing 5 sections from the same central and peripheral areas of each retina, and 20 sections from the same rostro-caudal level of each superior colliculus from 4 control and 4 hypoxic animals. Five images from each section were acquired at 20X on a Zeiss Axiocam MRM (Zeiss, Jena, Germany) and the active caspase-3 cells were counted double blind by two experimented researchers, as described previously (Hernandez et

al., 2009). In the retina, the active caspase-3 positive cells in the ganglion cell layer (GCL) were counted and the linear distance of each micrograph was measured (Zen, Zeiss, Jena, Germany). Thus, the number of labelled cells were expressed per linear millimetre of the RGC layer (cells/mm). In the superior colliculus, the number of active caspase-3 cells was counted in the superficial layers and in the total surface of the superior colliculus, including the superficial layers, calculating the average number of active caspase-3 positive cells per mm^2 of the superior colliculus (cells/mm^2).

Astrocyte morphometry

To analyse the cytoskeletal morphology of astrocytes in the retina, images were taken of whole mount retinas using the same microscope and criteria as those used for RGC quantification. The astrocytes in the pig retina are organized mainly like those in the human retina, running parallel to the RGC axons. A semi-automatic method to measure astrocyte organization was used to measure the morphological changes in astrocytes. The aim was to quantify the differences in the astrocyte network between the control and hypoxic retinas based on the local orientation of the astrocytic processes. An *ad hoc* programme was developed in Matlab R2010b (MathWorks, Inc) to quantify the morphological changes to astrocytes. This programme estimates the local orientation of the GFAP-positive lines in an image, taking advantage of the SURF extraction algorithm (Bay et al., 2008) and its capacity to define local pixel orientation based on their neighbouring relationships. Following local characterization, a histogram of this orientation is extracted that allows the frequency of each direction to be measured (1-degree bins). This involves measuring the randomness of the histogram using Shannon's Entropy equation (Shannon and Weaver, 1949), a well-known function to measure the predictability of a variable. The higher the entropy the less predictable and consequently, the more disorganized the system. With this information, the degree of disorganization of control astrocytes and hypoxic astrocytes can be compared. The average entropy from the histogram of the images was calculated and a statistical analysis was performed to evaluate our hypothesis that the entropy is greater in hypoxic retinal astrocytes.

To analyse the astrocytes in the superior colliculus, a Zeiss Axiocam MRM fluorescent microscope (Zeiss, Jena, Germany) and the Zeiss Zen software was used, obtaining 20 images (20X) at the same rostro-caudal level of the superior colliculus of the 4 control

and 4 hypoxic animals. Since the astrocyte organization in the superior colliculus does not follow a well-established parallel pattern, the method used to analyse the astrocytes in this structure differed to that used in the retina. The morphology of the astrocyte cytoskeleton was analyzed using ImageJ (version 1.49), the image processing program developed at the National Institutes of Health (NIH). Using the "threshold color" tool, the region formed by colored pixels (labeled with the antibody against GFAP) was selected, and this area of the cytoskeleton of selected astrocytes was measured. Given the entire image area, we could calculate the proportion of the area occupied by astrocyte´s cytoskeleton in the control and hypoxic superior colliculus.

Statistical analysis

RGC density, the number of active caspase-3 positive cells and the morphological data from the astrocyte's cytoskeleton were described as the mean and standard error of mean, and these parameters were compared between control and hypoxic tissues. Statistical analyses were carried out using IBM SPSS Statistics software v. 21.0 and the homogeneity of the variances was assayed with Levene´s test ($p < 0.05$). To assess whether there were significant differences in the number of RGCs, the number of active caspase-3 positive cells and in astrocyte morphology between control and hypoxia conditions, a Student T-test was used. In addition, a Mann-Witney U test was used to verify the differences between the control and hypoxic groups. For both tests, the minimum value of significance was defined as $p<0.05$.

Results

Gas exchange

At baseline, all animals displayed adequate gas exchange, whereby the fraction of inspired oxygen (FiO_2) was 30 ±2%, the PaO_2 was 108 ±16 mmHg, $PaCO_2$ was 42 ±6 mmHg, pH was 7.34 ±0.08, EB (base excess) was -2 ±3 mmol/l and lactic acid was 2 ±1 mmol/l. In the hypoxic animals, the decrease in oxygen levels produced a FiO_2 of 12 ±2%, and a significant impairment of gas exchange, with a PaO_2 of 31 ±8 mmHg, $PaCO_2$ of 45 ±8 mmHg, pH of 6.84 ±0.05, EB of -24 ±2mmol/l and lactic acid of 17 ±2mmol/l. Moreover, the MABP (mean arterial blood pressure) decreased significantly

after hypoxia (32 ±5 vs. 78 ±12 mmHg), while the HR (heart rate) remained unchanged relative to the basal values (184 ±36 vs. 196 ±33 bpm). These parameters partially reverted during the re-oxygenation period to a FiO_2 of 33 ±1%, a PaO_2 of 92 ±17 mmHg, a $PaCO_2$ of 45 ±5 mmHg, a pH of 7.22 ±0.12, an EB of -8 ±6 mmol/l and lactic acid of 4 ±4 mmol/l. However, there was no change in either the MABP (36 ±9 mmHg) or HR (193 ±26 bpm). In the control animals that were not subjected to hypoxia, these parameters remained at the basal values throughout the experiment. Finally, the hemoglobin levels (7.0 ±0.7 g/dl) remained constant throughout the experiment and all pigs remained alive throughout.

RGC density

The number of RGCs in the control and hypoxic retinas was analysed in the four selected areas (dorsal periphery, dorsal centre, ventral periphery, ventral centre: S1 Figure, Fig 1A-D).

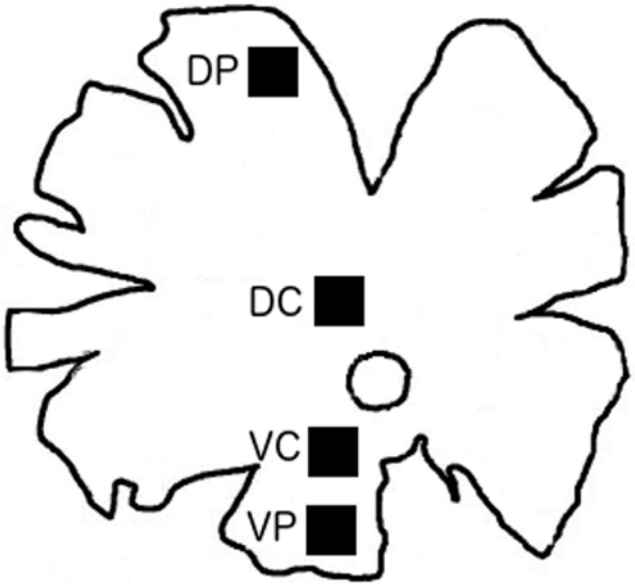

S1 Figure. Scheme of areas of RGC density. Schematic drawing of a pig retina where the four different areas of the retina analysed are represented as black squares: DP, dorsal periphery; DC, dorsal centre; VC, ventral centre; VC, central periphery.

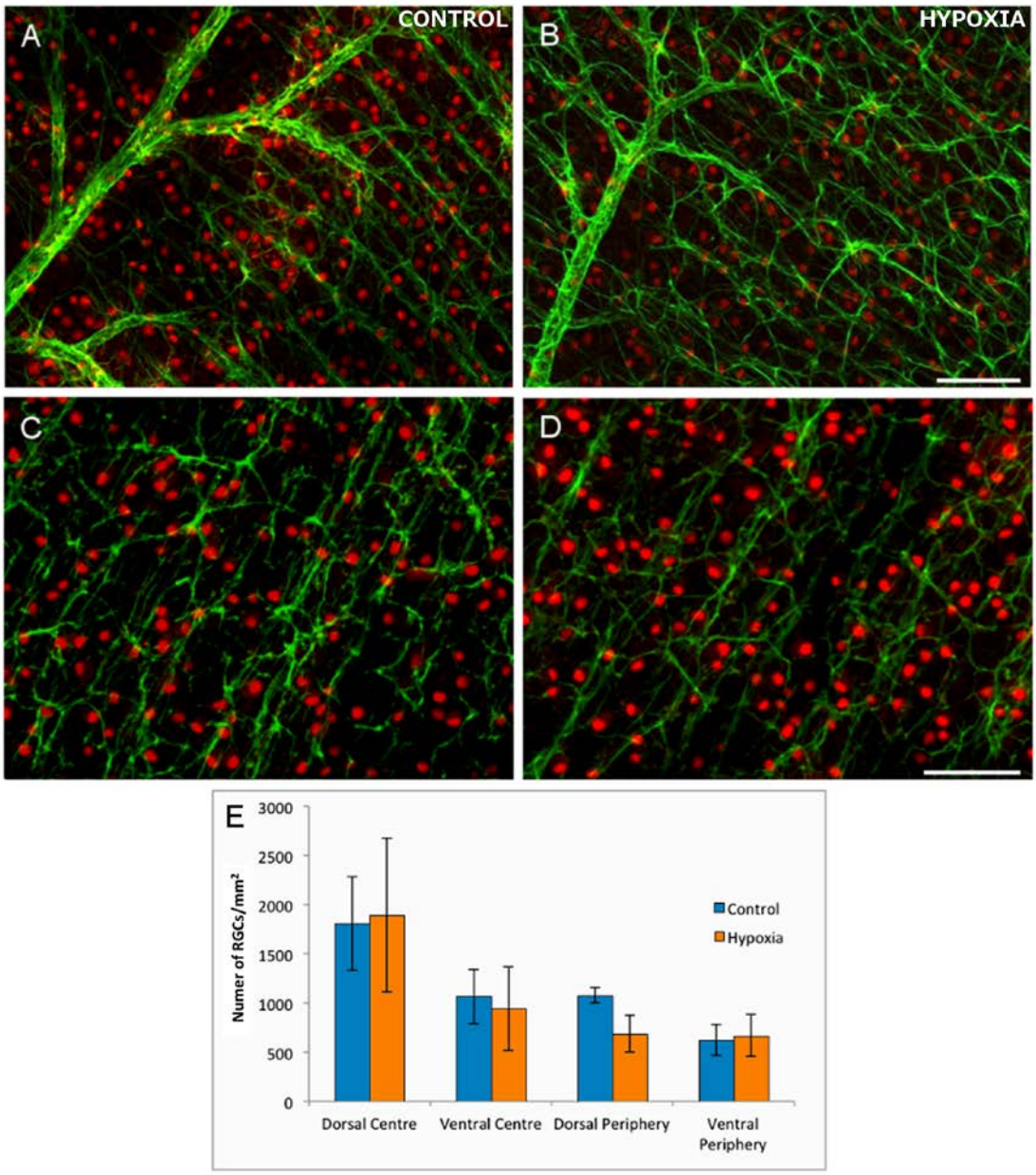

Fig 1. The analysis of flat mount retinas and RGCs. The cytoskeleton of astrocytes (green) are labelled with antibodies against GFAP and the nuclei of the RGCs (red dots) with antibodies against Brn3a in control (A, C) and hypoxic (B, D) retinas. Note the mild disorganization of the cytoskeleton in astrocytes and the reduction in the number of RGCs in hypoxic animals, although they are not significantly different from the controls. (E) Histogram representing the density of RGCs/mm^2 in the four areas of the control and hypoxic retina analysed. Standard errors of the mean are represented as error bars. Scale bar = 100 μm.

There were no significant differences in RGC number in the retinas from control and hypoxic animals in any of the four areas. While there was a mild tendency towards a loss of RGCs in the dorsal periphery of the hypoxic retinas, although this did not reach significance (Fig 1E and Table 1).

Domain	Control retina	Hypoxic retina
Dorso-peripheral	1079 ±75	686±19
Dorso-central	1808±48	1893±78
Ventral-peripheral	625±16	670±21
Ventral-central	1064±27	943±42

Table 1. Average RGC density. RGCs/mm^2 ± standard error of the mean in the distinct areas of Control and Hypoxic retinas.

Caspase-3 activation

Numerous active caspase-3 positive cells were found in the inner nuclear layer (INL) and ganglion cell layer (GCL) of the retina, both in control and hypoxic animals. Indeed, hypoxia did not produce a significant change in the number of positive active caspase-3 cells in the GCL, with 34 (±3) active caspase-3 positive cells/mm in control retinas and 38 (±4) cells/mm in hypoxic retinas (Fig. 2). By contrast there was a 37.6% increase in the number of active caspase-3 positive cells after hypoxia in the superior colliculus, rising from 279 (±13) cells/mm^2 in the control animals to 384 (±30) cells/mm^2 after hypoxia ($p = 0.013$, Fig. 3). This increase was even stronger if only the superficial layers of the superior colliculus were taken into account, where the number of apoptotic cells increased by 56.93% with respect to the controls: 610 (±7) active caspase-3 positive cells/mm^2 in the controls as opposed to 957 (±2) cells/mm^2 in the hypoxic animals, ($p = 0.002$).

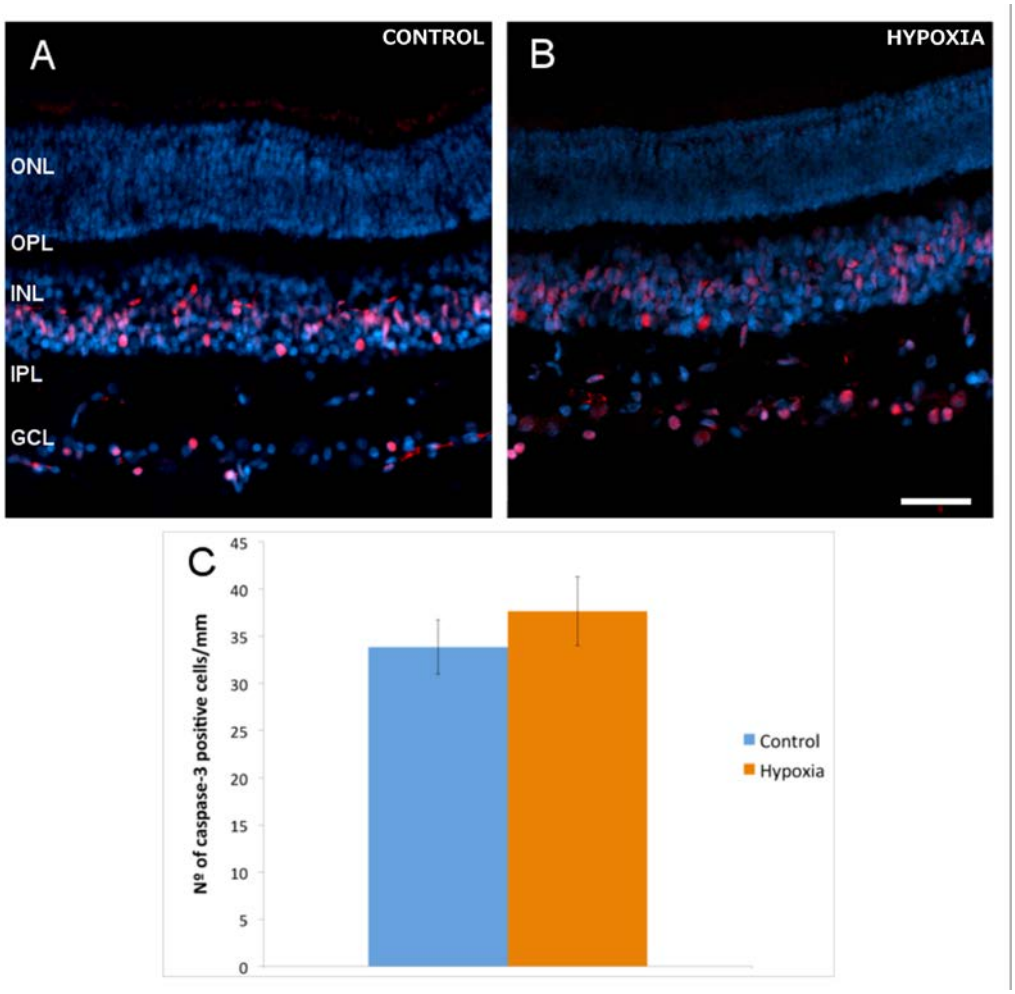

Fig 2. Active caspase-3-positive cells in retinal sections. The nuclei of neurons were labelled with DAPI (blue) and the apoptotic cells with an antibody against active caspase-3 (red) in control (A) and hypoxic (B) retinas. (C) Histogram of the average number of active caspase-3 positive cells per mm of the RGC layer in control and hypoxic retinas. The standard error of the mean is represented as an error bar: ONL, outer nuclear layer; OPL, outer plexiform layer; INL, inner nuclear layer; IPL, inner nuclear layer; GCL, ganglion cell layer. Scale bar = 50 μm.

Astrocyte morphology in the retina

When we analysed the cytoskeletal morphology of astrocytes in the control and hypoxic neonatal pig retina, retinal astrocytes appeared to be more disorganised following hypoxia, with an increase in the lateral extension of processes (Fig. 1). Using the algorithm described above, we quantified the disorganisation of the astrocyte networks in the retina, which was translated into different histograms of the orientations depending on the characteristics of the input (Fig. 4).

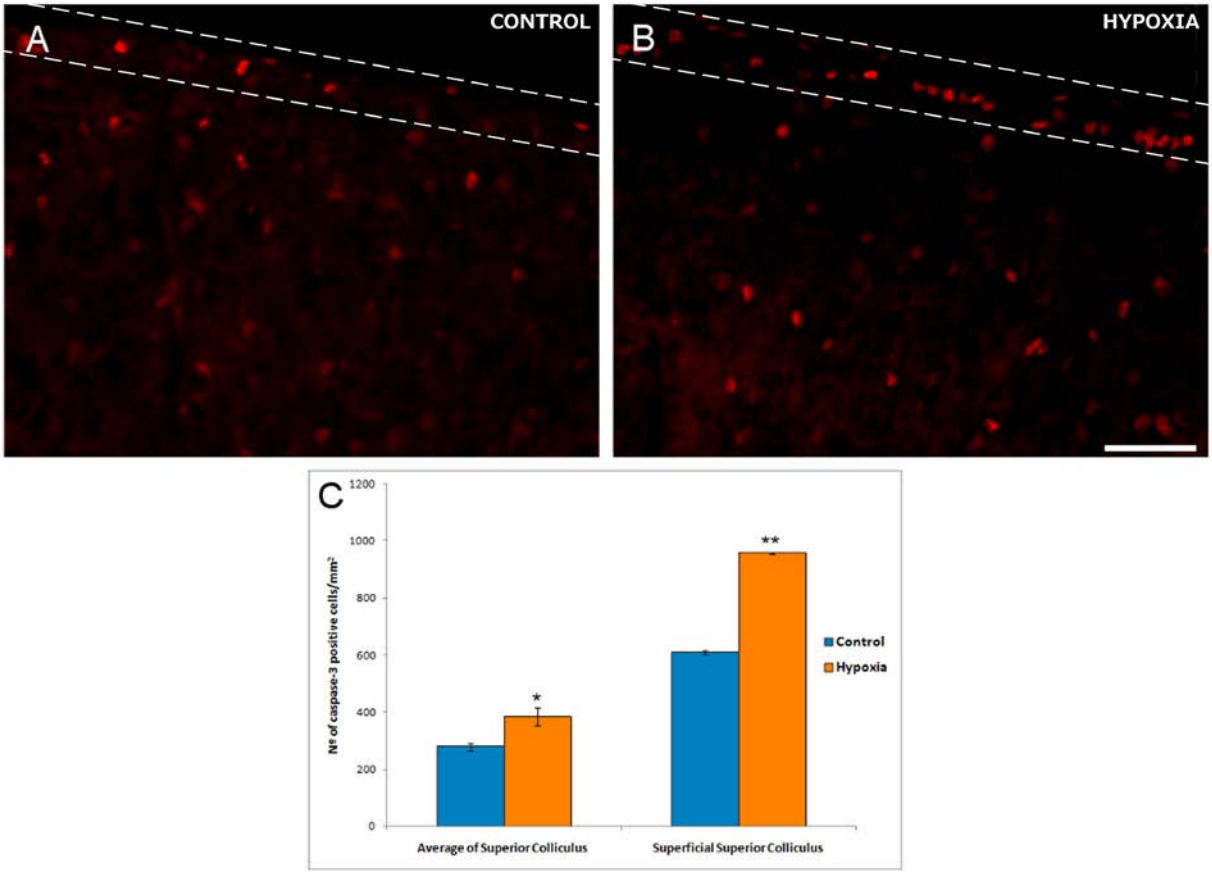

Fig 3. Active caspase-3-positive cells in sections of the superior colliculus. Images of the superior colliculus from control (A) and hypoxic (B) animals. Note that the superficial layers are defined by the dashed lines. Apoptotic cells are labelled with antibodies against active caspase-3 (red). Note the large number of active caspase-3 positive cells in the superficial layers of the superior colliculus. (C) Significant differences in the density of active caspase-3 positive cells between control and hypoxic pigs are shown in the histograms and the standard error of the mean is represented as an error bar: *p< 0.05, **p<0.01. Scale bar = 50 μm.

As such, some hypoxic retinas displayed a higher degree of randomness in the histograms, whereas control retinas seemed to have a greater difference in the frequency between the main orientation angles and other angles (Fig. 4: parallel axon processes in red and non-parallel ones in green). The *ad hoc* routine to quantify the differences in the retinal astrocyte networks in function of the local orientation of their processes highlighted the differences in the distribution of retinal astrocyte processes. However, no significant differences between control and hypoxic retinas were found in the area analysed. While these results indicate there was no significant difference between these populations (p >95%), there does appear to be a difference in the degree of organisation (a difference of approximately 93%, p = 0.069).

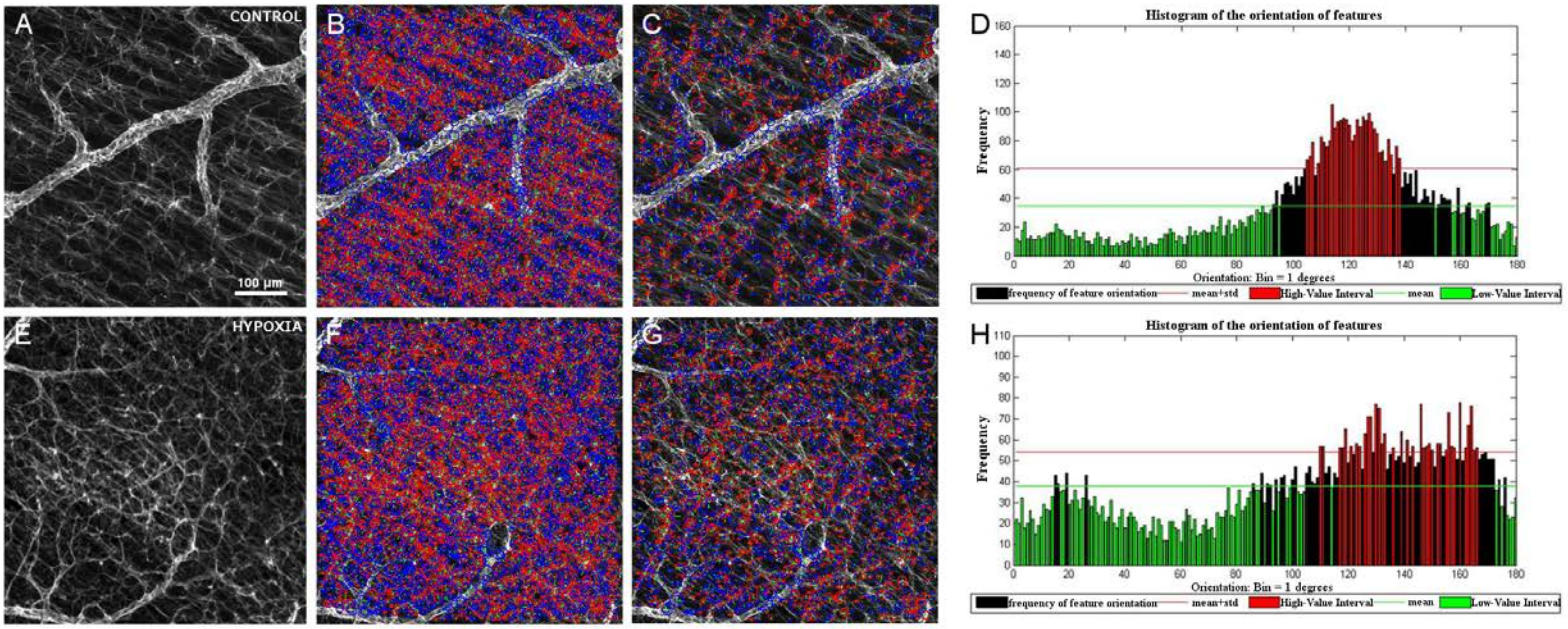

Fig 4. Astrocytes in the retina. Surf detection in GFAP labelled images of the control (A-D) and hypoxic (E-H)retina. GFAP immunohistochemistry (green) of the retina from control (A) and hypoxic animals (E) showing the relationship in the orientation of the astrocytes relative to the RGC axons (B, F). The relationship between the orientation of processes after removing the features corresponding to the main orientation (C, G). Histograms (D, H) quantifying the disorganization of the astrocytic processes using the Surf feature orientation for the input image: the higher the bar, the greater the number of features orientated in the direction indicated in the abscissa. The red bars indicate the highest number of events that take place at the angle indicated in abscises. Note that in the hypoxic histogram there are more red bars at different angles than in the control retinas. After analysing all the images, no significant differences between control and hypoxic retinas were found.

Astrocyte morphology in the superior colliculus

Activation and hypertrophy of astrocytes was evident in the hypoxic superior colliculus (Fig. 5), implying the emergence of gliosis. Thus, we cannot rule out that hypoxia induces changes in the number of astrocytes in the superior colliculus. Moreover, the disposition of astrocytes in the superior colliculus meant that we could not use the same method as that employed in the retina to measure the changes in the patterning of their processes. When the area occupied by the astrocyte cytoskeleton was quantified, the mean proportion of the area occupied by the astrocyte's cytoskeleton in the control superior colliculus was 4.07% (± 0.50), while in the hypoxic superior colliculus it was 17.75% (± 2.41). Moreover, hypoxia induced an increase in astrocyte density of 13.78%, representing a 4.36-fold increment ($p = 0.0037$).

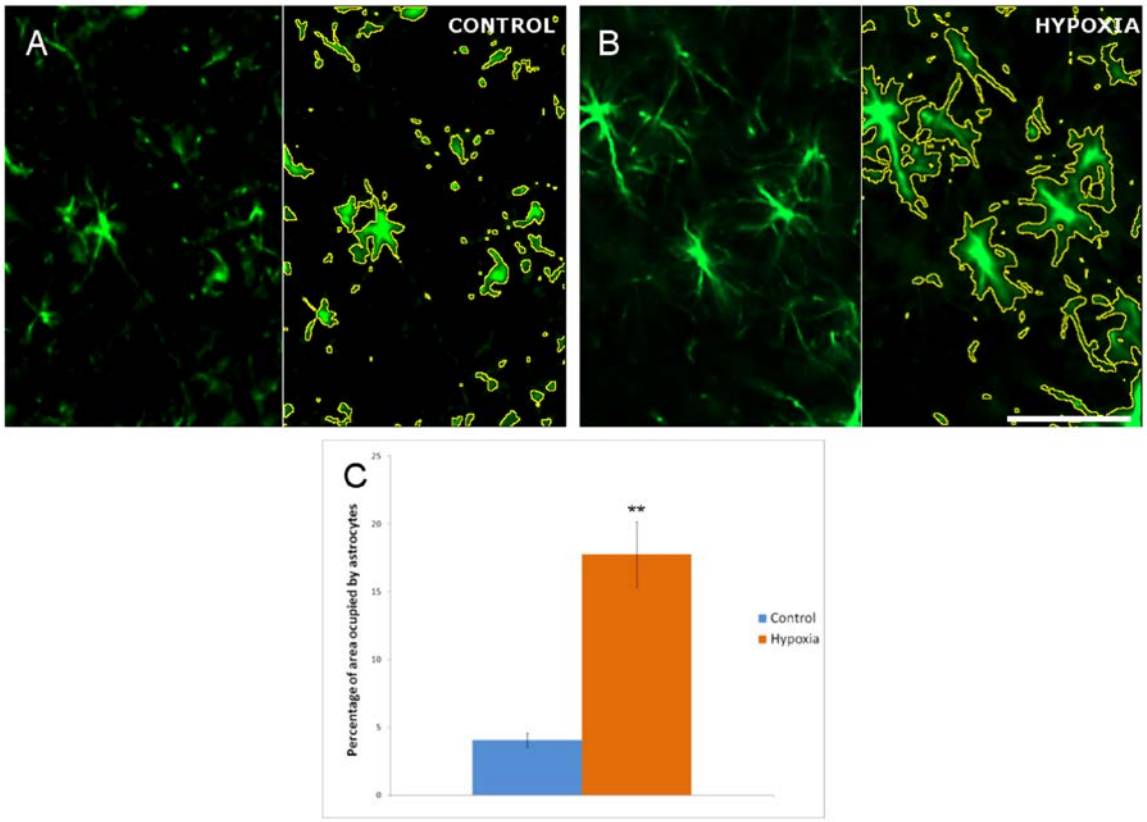

Fig 5. Analysis of astrocytes in the superior colliculus. Images of the control (A) and hypoxic (B) superior colliculus in which the cytoskeleton of the astrocytes is labelled with antibodies against GFAP (green). In A and B the pictures are split by a vertical line where in the right part each astrocyte is defined by a yellow line that represents the area of the cytoskeleton measured by the ImageJ program to quantify the cytoskeleton of the astrocytes. (C) Histogram showing the proportion of the cell occupied by GFAP, the standard errors of the mean are represented as an error bar. Significant differences were found between the control and hypoxic superior colliculus: **p<0.01. Scale bar = 50 μm.

Discussion

Experimental studies in suitable animal models commonly provide insights into human neonatal situations. In the present study we have used the pig as an animal model because beside other primates, the porcine retina is the most similar to the human retina among the large mammals (Prince and Ruskell, 1960; Vecino et al., 2015; Vecino and Sharma, 2011). Neonatal pigs have been used previously to study brain alterations and to test different drugs (Lafuente et al., 2011; Mielgo et al., 2017; Rey-Santano et al., 2014), and here we have used hypoxic conditions followed by a short recovery to detect early damage, and to compare the effects of hypoxia on the retina and brain.

We found that hypoxia produces significant neuronal apoptosis in the superior colliculus but not in the retina. Moreover, we found significant gliosis of the astrocytes in the superior colliculus but not in the retina. However, in the retina some changes in RGC density in the peripheral retina were found, although they were not significant. The changes described probably reflect the earliest events that result from the hypoxic insult and we cannot rule out that longer recovery times will produce more significant damage in the retina.

Limiting oxygen in the retina contributes to RGC neurodegeneration, which results in a loss of vision and ultimately, blindness. Cell viability can be dramatically compromised by hypoxic stress (Chen et al., 2007; Nakayama et al., 2011) and we found that the dorsal-periphery of the retina was the area where the RGCs are more vulnerable to hypoxia, even though significant differences were not found. This is consistent with the early events that take place in glaucoma, a neurodegenerative disease caused by elevated intraocular pressure (IOP) that possible causes mild hypoxia (Halpern et al., 2002; Quigley, 1999) and where peripheral RGCs are more sensitive to damage, in accordance with others studies in pigs (Laquis et al., 1998; Ruiz-Ederra et al., 2005a; Ruiz-Ederra et al., 2005b), rats (Laquis et al., 1998; Urcola et al., 2006) and mice (Reichstein et al., 2007).

Although several mechanisms of cell death are activated by oxygen depletion in neural tissues (Chen et al., 2007; Melamed, 2002), changes in apoptotic RGCs were not found and the basal number of active caspase-3 positive cells in the ganglion cell layer was similar in control and hypoxic retinas. By contrast, the proportion of active caspase-3 positive cells after hypoxia increases in the superior colliculus as a whole, and this increases further in the superficial layers of the superior colliculus with respect to the control. Cell death has been described as a natural event in the superior colliculus during development and postnatally (Arees and Astrom, 1977; Giordano et al., 1980). Moreover, hypoxic insult in the developing brain triggers the same apoptotic pathway as that activated during development (Pozo Devoto et al., 2013). The induction of apoptosis following hypoxia is evident just a few hours after insult (Pozo Devoto et al., 2006) in brain areas like the cortex and hippocampus of neonatal pigs (Alvarez et al., 2008; Lafuente et al., 2011). Furthermore, the intensity of cell death in the superficial layers of the superior colliculus could reflect the elevated cell density in these layers

(Vanegas, 1984) relative to the rest of the superior colliculus. Thus, in hypoxic conditions, the cells will have more limited access to oxygen in these superficial layers, which could induce them to more readily undergo apoptosis.

Hypoxia induces astrocyte activation in many neurological disorders (Kang and Hebert, 2011; Sun and Jakobs, 2012; Wilhelmsson et al., 2006). Reactive astrocytes divide and become hypertrophic, producing long, thick processes (Kang et al., 2014), as well as overexpressing GFAP (Garcia and Vecino, 2003; Hol and Pekny, 2015). In the superior colliculus, signs of astrocyte activation and reactive gliosis were noted, such as an increase in the surface area occupied by GFAP, although no changes in the orientation of the astrocyte's prolongations were found in the retinas.

The distinct susceptibility to hypoxia between the retina and the superior colliculus could be explained by the heterogeneity in metabolic and molecular regulation between different areas of the CNS (Greisen, 2005) that produce a distinct vulnerability to oxygen depletion, as well as a different degree of neuroprotection (Alonso-Alconada et al., 2015; Arduini et al., 2014). The more severe vulnerability of brain neurons to limited oxygen may be due to the brain tissue failing to up-regulate glycolysis sufficiently in order to compensate for the loss of respiratory ATP. By contrast, the retina has the capacity to metabolize the glucose converted to lactate from glycolysis more efficiently thanks to the Müller glia, only present in the retina (Winkler et al., 2000). In addition, the stronger resistance to hypoxia in the retina could be due also to the presence of Müller glia cells, which are not present in the brain. Although they share many characteristics with astrocytes, Müller glia have specific functions related to the homeostatic and metabolic support of retinal neurons (Reichenbach and Bringmann, 2013; Vecino et al., 2016). Müller cells resist hypoxia and low glucose conditions by activating anaerobic glycolysis and by oxidizing alternative substrates in order to obtain energy in the form of ATP, as well as providing neurons with lactate (Winkler et al., 2000). Furthermore, surfactant protein A (SP-A) is found in Müller cells, RGCs and astrocytes in the retina, and it is up-regulated during hypoxia. Since SP-A influences neovascularisation, its expression may represent a protective response against systemic inflammation and it may participate in the maintenance of the blood retinal homeostatic barrier (Bhatti et al., 2015). Finally, in transient ischemia we described an increase in brain derived neurotrophic factor (BDNF) in RGCs after ischaemic insult, as well as

changes in the neurotrophic p75 receptor in Müller cells (Vecino et al., 1998; Vecino et al., 2016). These changes may reflect the neuroprotection in the retina that makes it more resistant to hypoxia in neonates.

The lack of morphological changes in the retina after hypoxia only reflect early events, suggesting that the brain is more vulnerable to hypoxia at these early time points. However, after longer reperfusion times, retinal cells might also be sensitive to such insult. Moreover, given the limited sample size in this study some changes could remain unnoticed, with only major differences becoming evident, such as those in the superior colliculus that appears to be more sensitive to hypoxia. Consequently, a therapeutic window appears to exists in which a neuroprotective action protects the retinal neurons even though the brain has suffered damage.

The results of the present study highlight the differences in the reaction of neurons and astrocytes in different parts of the CNS. As heterogeneous responses to hypoxia were detected in different brain regions, interesting opportunities may be open to design therapeutic and preventative treatments specific to certain areas and structures in the nervous system.

References

Alonso-Alconada, D., Broad, K.D., Bainbridge, A., Chandrasekaran, M., Faulkner, S.D., Kerenyi, A., Hassell, J., Rocha-Ferreira, E., Hristova, M., Fleiss, B., Bennett, K., Kelen, D., Cady, E., Gressens, P., Golay, X., Robertson, N.J., 2015. Brain cell death is reduced with cooling by 3.5 degrees C to 5 degrees C but increased with cooling by 8.5 degrees C in a piglet asphyxia model. Stroke; a journal of cerebral circulation 46, 275-278.

Alvarez, F.J., Lafuente, H., Rey-Santano, M.C., Mielgo, V.E., Gastiasoro, E., Rueda, M., Pertwee, R.G., Castillo, A.I., Romero, J., Martinez-Orgado, J., 2008. Neuroprotective effects of the nonpsychoactive cannabinoid cannabidiol in hypoxic-ischemic newborn piglets. Pediatric research 64, 653-658.

Ames, A., 3rd, 1992. Energy requirements of CNS cells as related to their function and to their vulnerability to ischemia: a commentary based on studies on retina. Canadian journal of physiology and pharmacology 70 Suppl, S158-164.

Anderson, B., Jr., Saltzman, H.A., 1964. Retinal Oxygen Utilization Measured by Hyperbaric Blackout. Archives of ophthalmology 72, 792-795.

Anzenbacher, P., Soucek, P., Anzenbacherova, E., Gut, I., Hruby, K., Svoboda, Z., Kvetina, J., 1998. Presence and activity of cytochrome P450 isoforms in minipig

liver microsomes. Comparison with human liver samples. Drug metabolism and disposition: the biological fate of chemicals 26, 56-59.

Arduini, A., Escobar, J., Vento, M., Escrig, R., Quintas, G., Sastre, J., Saugstad, O.D., Solberg, R., 2014. Metabolic adaptation and neuroprotection differ in the retina and choroid in a piglet model of acute postnatal hypoxia. Pediatric research 76, 127-134.

Arees, E.A., Astrom, K.E., 1977. Cell death in the optic tectum of the developing rat. Anatomy and embryology 151, 29-34.

Bay, H., Ess, A., Tuytelaars, T., Van Gool, L., 2008. Speeded-Up Robust Features (SURF). Computer Vision and Image Understanding 110, 13.

Bevensee, M.O., Boron, W.F., 2008. Effects of acute hypoxia on intracellular-pH regulation in astrocytes cultured from rat hippocampus. Brain research 1193, 143-152.

Bhatti, F., Ball, G., Hobbs, R., Linens, A., Munzar, S., Akram, R., Barber, A.J., Anderson, M., Elliott, M., Edwards, M., 2015. Pulmonary surfactant protein a is expressed in mouse retina by Muller cells and impacts neovascularization in oxygen-induced retinopathy. Investigative ophthalmology & visual science 56, 232-242.

Caprara, C., Grimm, C., 2012. From oxygen to erythropoietin: relevance of hypoxia for retinal development, health and disease. Progress in retinal and eye research 31, 89-119.

Chan-Ling, T., Stone, J., 1992. Degeneration of astrocytes in feline retinopathy of prematurity causes failure of the blood-retinal barrier. Investigative ophthalmology & visual science 33, 2148-2159.

Chen, Y.N., Yamada, H., Mao, W., Matsuyama, S., Aihara, M., Araie, M., 2007. Hypoxia-induced retinal ganglion cell death and the neuroprotective effects of beta-adrenergic antagonists. Brain research 1148, 28-37.

Cheung, P.Y., Gill, R.S., Bigam, D.L., 2011. A swine model of neonatal asphyxia. Journal of visualized experiments : JoVE.

Cowan, F., 2000. Outcome after intrapartum asphyxia in term infants. Seminars in neonatology : SN 5, 127-140.

Cowan, F., Rutherford, M., Groenendaal, F., Eken, P., Mercuri, E., Bydder, G.M., Meiners, L.C., Dubowitz, L.M., de Vries, L.S., 2003. Origin and timing of brain lesions in term infants with neonatal encephalopathy. Lancet 361, 736-742.

Dorrell, M.I., Aguilar, E., Jacobson, R., Trauger, S.A., Friedlander, J., Siuzdak, G., Friedlander, M., 2010. Maintaining retinal astrocytes normalizes revascularization and prevents vascular pathology associated with oxygen-induced retinopathy. Glia 58, 43-54.

Eshaq, R.S., Wright, W.S., Harris, N.R., 2014. Oxygen delivery, consumption, and conversion to reactive oxygen species in experimental models of diabetic retinopathy. Redox biology 2, 661-666.

Fletcher, E.L., Downie, L.E., Hatzopoulos, K., Vessey, K.A., Ward, M.M., Chow, C.L., Pianta, M.J., Vingrys, A.J., Kalloniatis, M., Wilkinson-Berka, J.L., 2010. The significance of neuronal and glial cell changes in the rat retina during oxygen-induced retinopathy. Documenta ophthalmologica. Advances in ophthalmology 120, 67-86.

Garcia, J.H., Yoshida, Y., Chen, H., Li, Y., Zhang, Z.G., Lian, J., Chen, S., Chopp, M., 1993. Progression from ischemic injury to infarct following middle cerebral artery occlusion in the rat. The American journal of pathology 142, 623-635.

Garcia, M., Forster, V., Hicks, D., Vecino, E., 2002. Effects of muller glia on cell survival and neuritogenesis in adult porcine retina in vitro. Investigative ophthalmology & visual science 43, 3735-3743.

Garcia, M., Vecino, E., 2003. Role of Muller glia in neuroprotection and regeneration in the retina. Histology and histopathology 18, 1205-1218.

Giordano, D.L., Murray, M., Cunningham, T.J., 1980. Naturally occurring neuron death in the optic layers of superior colliculus of the postnatal rat. Journal of neurocytology 9, 603-614.

Greisen, G., 2005. Autoregulation of cerebral blood flow in newborn babies. Early human development 81, 423-428.

Grimm, C., Willmann, G., 2012. Hypoxia in the eye: a two-sided coin. High altitude medicine & biology 13, 169-175.

Hallak, M., Hotra, J.W., Kupsky, W.J., 2000. Magnesium sulfate protection of fetal rat brain from severe maternal hypoxia. Obstetrics and gynecology 96, 124-128.

Halpern, M.T., Covert, D.W., Robin, A.L., 2002. Projected impact of travoprost versus both timolol and latanoprost on visual field deficit progression and costs among black glaucoma subjects. Transactions of the American Ophthalmological Society 100, 109-117; discussion 117-108.

Hernandez, M., Rodriguez, F.D., Sharma, S.C., Vecino, E., 2009. Immunohistochemical changes in rat retinas at various time periods of elevated intraocular pressure. Molecular vision 15, 2696-2709.

Hol, E.M., Pekny, M., 2015. Glial fibrillary acidic protein (GFAP) and the astrocyte intermediate filament system in diseases of the central nervous system. Current opinion in cell biology 32, 121-130.

Kang, K., Lee, S.W., Han, J.E., Choi, J.W., Song, M.R., 2014. The complex morphology of reactive astrocytes controlled by fibroblast growth factor signaling. Glia 62, 1328-1344.

Kang, W., Hebert, J.M., 2011. Signaling pathways in reactive astrocytes, a genetic perspective. Molecular neurobiology 43, 147-154.

Kaur, C., Sivakumar, V., Foulds, W.S., Luu, C.D., Ling, E.A., 2009. Cellular and vascular changes in the retina of neonatal rats after an acute exposure to hypoxia. Investigative ophthalmology & visual science 50, 5364-5374.

Kaur, C., Sivakumar, V., Robinson, R., Foulds, W.S., Luu, C.D., Ling, E.A., 2013. Neuroprotective effect of melatonin against hypoxia-induced retinal ganglion cell death in neonatal rats. Journal of pineal research 54, 190-206.

Kergoat, H., Herard, M.E., Lemay, M., 2006. RGC sensitivity to mild systemic hypoxia. Investigative ophthalmology & visual science 47, 5423-5427.

Kimble, E.A., Svoboda, R.A., Ostroy, S.E., 1980. Oxygen consumption and ATP changes of the vertebrate photoreceptor. Experimental eye research 31, 271-288.

Lafuente, H., Alvarez, F.J., Pazos, M.R., Alvarez, A., Rey-Santano, M.C., Mielgo, V., Murgia-Esteve, X., Hilario, E., Martinez-Orgado, J., 2011. Cannabidiol reduces brain damage and improves functional recovery after acute hypoxia-ischemia in newborn pigs. Pediatric research 70, 272-277.

Laquis, S., Chaudhary, P., Sharma, S.C., 1998. The patterns of retinal ganglion cell death in hypertensive eyes. Brain research 784, 100-104.

Leventhal, A.G., Rodieck, R.W., Dreher, B., 1981. Retinal ganglion cell classes in the Old World monkey: morphology and central projections. Science 213, 1139-1142.

Liu, Y., Leo, L.F., McGregor, C., Grivitishvili, A., Barnstable, C.J., Tombran-Tink, J., 2012. Pigment epithelium-derived factor (PEDF) peptide eye drops reduce inflammation, cell death and vascular leakage in diabetic retinopathy in Ins2(Akita) mice. Molecular medicine 18, 1387-1401.

Ma, Q., Xiong, F., Zhang, L., 2014. Gestational hypoxia and epigenetic programming of brain development disorders. Drug discovery today.

Melamed, S., 2002. Neuroprotective properties of a synthetic docosanoid, unoprostone isopropyl: clinical benefits in the treatment of glaucoma. Drugs under experimental and clinical research 28, 63-73.

Mielgo, V.E., Valls, I.S.A., Lopez-de-Heredia, J.M., Rabe, H., Rey-Santano, C., 2017. Hemodynamic and metabolic effects of a new pediatric dobutamine formulation in hypoxic newborn pigs. Pediatric research.

Nakayama, M., Aihara, M., Chen, Y.N., Araie, M., Tomita-Yokotani, K., Iwashina, T., 2011. Neuroprotective effects of flavonoids on hypoxia-, glutamate-, and oxidative stress-induced retinal ganglion cell death. Molecular vision 17, 1784-1793.

Pinar-Sueiro, S., Zorrilla Hurtado, J.A., Veiga-Crespo, P., Sharma, S.C., Vecino, E., 2013. Neuroprotective effects of topical CB1 agonist WIN 55212-2 on retinal ganglion cells after acute rise in intraocular pressure induced ischemia in rat. Experimental eye research 110, 55-58.

Pozo Devoto, V.M., Bogetti, M.E., Fiszer de Plazas, S., 2013. Developmental and hypoxia-induced cell death share common ultrastructural and biochemical apoptotic features in the central nervous system. Neuroscience 252, 190-200.

Pozo Devoto, V.M., Chavez, J.C., Fiszer de Plazas, S., 2006. Acute hypoxia and programmed cell death in developing CNS: Differential vulnerability of chick optic tectum layers. Neuroscience 142, 645-653.

Prince, J.H., Ruskell, G.L., 1960. The use of domestic animals for experimental ophthalmology. American journal of ophthalmology 49, 1202-1207.

Quigley, H.A., 1999. Neuronal death in glaucoma. Progress in retinal and eye research 18, 39-57.

Reichenbach, A., Bringmann, A., 2013. New functions of Muller cells. Glia 61, 651-678.

Reichstein, D., Ren, L., Filippopoulos, T., Mittag, T., Danias, J., 2007. Apoptotic retinal ganglion cell death in the DBA/2 mouse model of glaucoma. Experimental eye research 84, 13-21.

Rey-Santano, C., Mielgo, V., Valls, I.S.A., Encinas, E., Lukas, J.C., Vozmediano, V., Suarez, E., 2014. Evaluation of fentanyl disposition and effects in newborn piglets as an experimental model for human neonates. PloS one 9, e90728.

Roth, W.J., Kissinger, C.B., McCain, R.R., Cooper, B.R., Marchant-Forde, J.N., Vreeman, R.C., Hannou, S., Knipp, G.T., 2013. Assessment of juvenile pigs to serve as human pediatric surrogates for preclinical formulation pharmacokinetic testing. The AAPS journal 15, 763-774.

Rovere, G., Nadal-Nicolas, F.M., Agudo-Barriuso, M., Sobrado-Calvo, P., Nieto-Lopez, L., Nucci, C., Villegas-Perez, M.P., Vidal-Sanz, M., 2015. Comparison of Retinal Nerve Fiber Layer Thinning and Retinal Ganglion Cell Loss After Optic Nerve Transection in Adult Albino Rats. Investigative ophthalmology & visual science 56, 4487-4498.

Ruiz-Ederra, J., Garcia, M., Hernandez, M., Urcola, H., Hernandez-Barbachano, E., Araiz, J., Vecino, E., 2005a. The pig eye as a novel model of glaucoma. Experimental eye research 81, 561-569.

Ruiz-Ederra, J., Garcia, M., Martin, F., Urcola, H., Hernandez, M., Araiz, J., Duran, J., Vecino, E., 2005b. [Comparison of three methods of inducing chronic elevation of intraocular pressure in the pig (experimental glaucoma)]. Archivos de la Sociedad Espanola de Oftalmologia 80, 571-579.

Salmaso, N., Jablonska, B., Scafidi, J., Vaccarino, F.M., Gallo, V., 2014. Neurobiology of premature brain injury. Nature neuroscience 17, 341-346.

Shannon, C.E., Weaver, W., 1949. The Mathematical Theory of Communication. The University of Illinois Press.

Singer, D., 1999. Neonatal tolerance to hypoxia: a comparative-physiological approach. Comparative biochemistry and physiology. Part A, Molecular & integrative physiology 123, 221-234.

Sparks, D.L., 1986. Translation of sensory signals into commands for control of saccadic eye movements: role of primate superior colliculus. Physiological reviews 66, 118-171.

Sun, D., Jakobs, T.C., 2012. Structural remodeling of astrocytes in the injured CNS. The Neuroscientist : a review journal bringing neurobiology, neurology and psychiatry 18, 567-588.

Urcola, J.H., Hernandez, M., Vecino, E., 2006. Three experimental glaucoma models in rats: comparison of the effects of intraocular pressure elevation on retinal ganglion cell size and death. Experimental eye research 83, 429-437.

Vanegas, H., 1984. Comparative neurology of the optic tectum. Plenum Press, New York.

Vangeison, G., Rempe, D.A., 2009. The Janus-faced effects of hypoxia on astrocyte function. The Neuroscientist : a review journal bringing neurobiology, neurology and psychiatry 15, 579-588.

Vecino, E., Caminos, E., Ugarte, M., Martin-Zanca, D., Osborne, N.N., 1998. Immunohistochemical distribution of neurotrophins and their receptors in the rat retina and the effects of ischemia and reperfusion. General pharmacology 30, 305-314.

Vecino, E., Galdós, M., Bayón, A., Rodríguez, F.D., Micó, C., Sharma, S.C., 2015. Elevated Intraocular Pressure induces Ultrastructural Changes in the Trabecular Meshwork. Journal of Cytology & Histology S3:007.

Vecino, E., Garcia-Crespo, D., Garcia, M., Martinez-Millan, L., Sharma, S.C., Carrascal, E., 2002. Rat retinal ganglion cells co-express brain derived neurotrophic factor (BDNF) and its receptor TrkB. Vision research 42, 151-157.

Vecino, E., Rodriguez, F.D., Ruzafa, N., Pereiro, X., Sharma, S.C., 2016. Glia-neuron interactions in the mammalian retina. Progress in retinal and eye research 51, 1-40.

Vecino, E., Sharma, S., 2011. Glaucoma Animal Models, in: Rumelt, S. (Ed.), Glaucoma - Basic and Clinical Concepts. In Tech, pp. 319-334.

Wang, L., Sarnaik, R., Rangarajan, K., Liu, X., Cang, J., 2010. Visual receptive field properties of neurons in the superficial superior colliculus of the mouse. The Journal of neuroscience : the official journal of the Society for Neuroscience 30, 16573-16584.

Wilhelmsson, U., Bushong, E.A., Price, D.L., Smarr, B.L., Phung, V., Terada, M., Ellisman, M.H., Pekny, M., 2006. Redefining the concept of reactive astrocytes as cells that remain within their unique domains upon reaction to injury. Proceedings of the National Academy of Sciences of the United States of America 103, 17513-17518.

Winkler, B.S., Arnold, M.J., Brassell, M.A., Puro, D.G., 2000. Energy metabolism in human retinal Muller cells. Investigative ophthalmology & visual science 41, 3183-3190.

Zhao, X., Liu, M., Cang, J., 2014. Visual cortex modulates the magnitude but not the selectivity of looming-evoked responses in the superior colliculus of awake mice. Neuron 84, 202-213.

ANEXO 2

ARCHIVOS DE LA SOCIEDAD ESPAÑOLA DE OFTALMOLOGÍA

Arch Soc Esp Oftalmol. 2015 Nov;90(11):522-6. doi: 10.1016/j.oftal.2015.03.009. Epub 2015 May 23

Effect of Müller cells on the Survival and Neuritogenesis in Retinal Ganglion Cells.

Noelia Ruzafa, Elena Vecino

Department of Cell Biology and Histology, University of Basque Country UPV/EHU, Leioa, Vizcaya, Spain.

Abstract:

Objetive: Retinal ganglion cells (RGCs) are the first affected cells in neuropathies like glaucoma, for that reason it is very important to explore new methods to neuroprotect these neurons. Müller cells are glial cells that provide to neurons trophic factors and scaffold. The purpose of this study was to analyze the effect of Müller cells in survival and neurite formation in RGCs.

Method: Rat Müller cells were grown until a confluent culture on which rat RGCs were added, pure culture of rat RGCs were used as controls. RGCs were labeled with βIII-tubulin and Müller cells with glutamine synthetase antibodies, in addition, nuclei were stained with DAPI. The number of RGCs and number and neurite length were measured.

Results: No differences in the number of RGCs between control and cells grown on the substrate of Müller cells were found. The proportion of RGCs with neurites increased when they grew on Müller; RGC with 1-3 neurites goes from 19% to 43%. The length

of neurites also increased in RGCs growing on Müller cells, the number of RGCs with neurites from 50 to 200μm increases from 21% to 41% and with neurites with more than 200μm goes from 6% to 20%.

Conclusions: Müller cells support the survival of RGCs and induced an increase in the number and length of neurites of RGCs.

Key words: Müller cells, retinal ganglion cells, survival, neuritogenesis.

Introduction

The central nervous system of mammals has a limited capacity for repair after a disease or lesion in the retina, as in the case of glaucoma (Glovinsky et al., 1991; Wygnanski et al., 1995), axonal degeneration (Newman and Reichenbach, 1996), ischemia (Joo et al., 1999; Selles-Navarro et al., 1996) or diabetes (Lieth et al., 2000; Zhang et al., 2000), which cause the death of retinal ganglion cells (RGCs) which can produce irreversible blindness (Garcia et al., 2002; Newman and Reichenbach, 1996). RGCs cannot regenerate efficiently after severe damage and instead die due to apoptosis (Garcia-Valenzuela et al., 1995; Quigley et al., 1995). However, it has been demonstrated that in appropriate environments RGCs can recover their regenerative capacities (Berry et al., 2008). Accordingly, initial regeneration strategies should focus on maintaining RGC survival and subsequent promotion of axonal elongation and functional reinstatement.

RGCs are in close contact with glial cells, of which there are 3 types in the retina: Müller cells, astrocytes and microglia (Newman and Reichenbach, 1996). Müller cells extended throughout the thickness of the retinal, providing structural stability and maintaining close contact with the majority of retina neurons (Bringmann and Reichenbach, 2001). They also provide trophic factors to neurons as well as the maintenance of neurotransmitters and ionic homeostasis (Bringmann et al., 2006; Reichenbach and Bringmann, 2013). These supporting cells have the ability to promote cell survival and repair, but in contrast can also facilitate tissue degeneration in their reactive form (Bringmann et al., 2006; Fleisch et al., 2011). The present research focused on studying Müller cells in vitro as regards the survival and formation of neurites in RGC.

Materials and methods

Culture cells were obtained from adult female sprague-dawley rats. The retina were dissected and tissue enzymatic dissemination was carried out using tripsin (0.25% tripsin-EDTA, Life Technologies, Carlsbad, AC, USA) during 30min for Müller cells, and papain (Worthington Papain Dissociation kit, Worthington Biochemical Lakewood, NJ, USA) during 90min for RGC. Tissue was homogenized and centrifuged for cell purification and concentration. The RGC culture was prepared following the protocol of the Worthington Papain Dissociation kit (Worthington Biochemical Lakewood, NJ, USA). After purification, the cells were seeded in plates with 24 cups over covers coated with poly-l-lysine (10μg/ml Sigma–Aldrich, St. Louis, MO, USA) and laminine (10μg/ml Sigma–Aldrich, St. Louis, MO, USA). Two types of cultures were compared: on the one hand RGC cultured during 5 days over covers treated with poly-l-lysine and laminine, which were used as controls, and on the other hand co-cultures in which Müller cells were cultured to confluence, normally acquired in cultured day 10, at which point the RGC were added and cultured 5 additional days. The cultures were maintained with a supplement of Neurobasal A (Life Technologies, Carlsbad, AC, USA). At least 3 replicas of each culture type work made, and this procedure was tripled.

After 5 days of RGC culture, cells were fixed with methanol and washed with PBS (saline phosphate tamponade, pH 7.0). After blocking nonspecific antigenes with blocking tamponade (3% BSA and 0.1% Triton X-100 in PBS) the following antibodies were added: rat anti-βIII-tubuline (Promega Madison, WI, USA) as specific RGC marker at a dilution of 1:2000 and rabbits anti-glutamine synthetase (Abcam, Cambridge, England) as specific marker for Müller cells at a dilution of 1:10,000. After washing again, the following secondary antibodies were added: anti-rat Alexa Fluor 488 and anti-rabbit Alexa Fluor 555 (Life Technologies, Carlsbad, AC, USA), both at a dilution of 1:1000 and DAPI nuclear marker (Life Technologies, Carlsbad, AC, USA) at a dilution of 1:10,000.

Images were taking using an epifluorescence microscope (Zeiss, Jena, Germany). Ten photographs with a 10× lens were randomly taken for each cover. All the cells of every photograph were counted in accordance with the following classification: cells without

neurites, cells with 1–3 neurites and cells with more than 3 neurites. Cells with neurites were classified in: neurites below 50µM, between 50 and 200µM or above 200µM. Finally, the results were statistically analyzed using the T for student test.

Results

Fig. 1 illustrates the difference between RGCs growing in control over covers coated with poly-l-lysine and laminine (Fig. 1A) and those growing over a single layer of Müller cells (Fig. 1B). RGCs in the control group are generally spherical or with short neurites but, on the contrary, when they grow over Müller cells, RGCs exhibit higher number of neurites which in addition are longer.

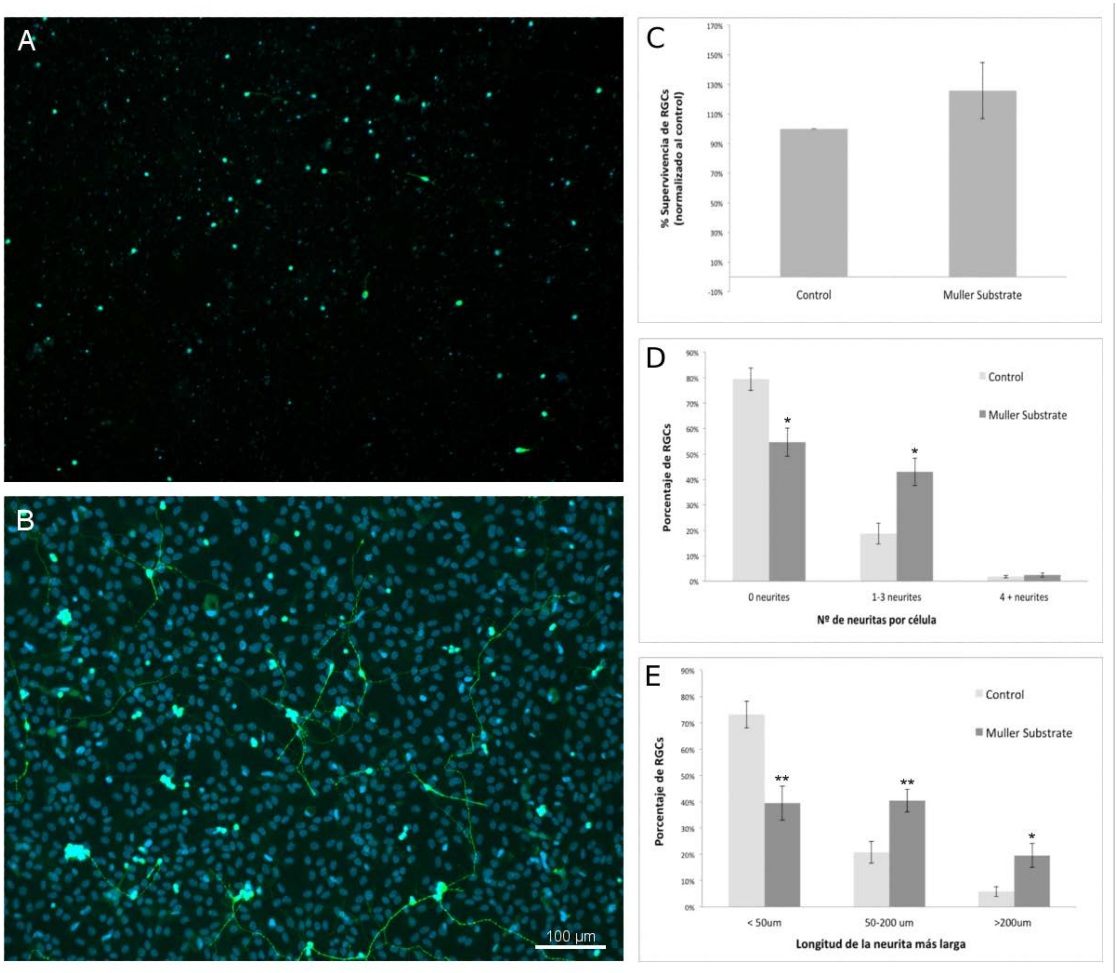

Fig. 1. Fotografía de un cultivo de RGC (A) y RGC sobre una monocapa de células de Müller (B) donde se marcan las RGCcon _III-tubulina en verde y los núcleos se ti˜nen con DAPI. Gráficas en las que se representa la supervivencia de RGC (C) encontrol frente a las células crecidas sobre un sustrato de células

de Müller, y el porcentaje de RGC respecto al número deneuritas por célula (D) y la longitud de la neurita más larga (E) (* $p < 0,05$, ** $p < 0,01$).

For analyzing cell survival, RGC growing in culture controls were counted, the mean value was standardized and taken as 100% and subsequently compared with the number of RGCs grown over Müller cell substrate. No significant differences were found between both groups in what concerns RGC survival (Fig. 1C).

The number of neurites of every RGC was counted and classified in RGC without neurites, with between 1 and 3 neurites or with over 4 neurites. The results revealed a significant increase of RGCs between 1 and 3 neurites, which went from 19% in cultures without Müller cells to 43% in co-cultures ($p=0.018$) (Fig. 1D). In what concerns neurite length, it also increased in RGCs growing over Müller cells. Accordingly, the number of RGCs having neurites between 50 and 200μm increased from 21% to 41% ($p=0.003$) and the number of cells with neurites over 200μm went from 6% to 20% ($p=0.022$) (Fig. 1E).

Discussion

Müller cells, the main type of glial cells in the retina, account for homeostatic and metabolic support of retinal neurons (Reichenbach and Bringmann, 2013). Previous studies by the same group of authors has demonstrated a neuroprotective and regenerative role played by Müller cells vis-à-vis RGC through the release of trophic factors and antioxidant agents (Garcia and Vecino, 2003). The present study has observed that, even though a significant increase of survival in 5 days of RGC rat cultures growing over a conferent monolayer of Müller cells was not observed, neuritogenesis did increase because an increase was observed in the number of cells with neurites, as well as in the length of said neurites, which was already observed in pigs (Garcia et al., 2003) and mice (de Melo Reis et al., 2008).

Together with the development of RGCs, their survival depends on factors secreted by Müller cells (Raju and Bennett, 1986). Müller cell cultures secrete nerve growth factor (NGF) and other neurotrophic molecules such as the brain-derived neurotrophic factor (BDNF) or the pigment epithelium derived factor (PEDF) among others, that supports

RGC survival and neuritogenesis (de Melo Reis et al., 2008; Hauck et al., 2014). In addition, it was observed that soluble mediators derived from the activity of Müller cells are able to attenuate the damage induced by hypoxia and RGC loss (Unterlauft et al., 2012), thus confirming the neuroprotective role thereof. In addition, it was observed that the activated glia promotes the growth of neurites besides granting additional properties (Lorber et al., 2009).

To conclude, trophic factors secreted by Müller cells enhance the formation and elongation of rat RGC in vitro neurites, which endows the latter with neuroprotective properties.

References

Berry, M., Ahmed, Z., Lorber, B., Douglas, M., Logan, A., 2008. Regeneration of axons in the visual system. Restor. Neurol. Neurosci. 26, 147-174.

Bringmann, A., Pannicke, T., Grosche, J., Francke, M., Wiedemann, P., Skatchkov, S.N., Osborne, N.N., Reichenbach, A., 2006. Muller cells in the healthy and diseased retina. Prog. Retin. Eye Res. 25, 397-424.

Bringmann, A., Reichenbach, A., 2001. Role of Muller cells in retinal degenerations. Front. Biosci. 6, E72-92.

de Melo Reis, R.A., Cabral-da-Silva, M., de Mello, F.G., Taylor, J.S., 2008. Muller glia factors induce survival and neuritogenesis of peripheral and central neurons. Brain Res. 1205, 1-11.

Fleisch, V.C., Fraser, B., Allison, W.T., 2011. Investigating regeneration and functional integration of CNS neurons: lessons from zebrafish genetics and other fish species. Biochim. Biophys. Acta 1812, 364-380.

Garcia, M., Forster, V., Hicks, D., Vecino, E., 2002. Effects of muller glia on cell survival and neuritogenesis in adult porcine retina in vitro. Invest. Ophthalmol. Vis. Sci. 43, 3735-3743.

Garcia, M., Ruiz Ederra, J., Hernandez-Barbachano, E., Urcola, J.A., Bilbao, J., Araiz, J., Duran, J.A., Vecino, E., 2003. Retinal ganglion cell neuroprotection in culture. Arch Soc Esp Oftalmol 78, 151-157.

Garcia, M., Vecino, E., 2003. Role of Muller glia in neuroprotection and regeneration in the retina. Histol. Histopathol. 18, 1205-1218.

Garcia-Valenzuela, E., Shareef, S., Walsh, J., Sharma, S.C., 1995. Programmed cell death of retinal ganglion cells during experimental glaucoma. Exp. Eye Res. 61, 33-44.

Glovinsky, Y., Quigley, H.A., Dunkelberger, G.R., 1991. Retinal ganglion cell loss is size dependent in experimental glaucoma. Invest. Ophthalmol. Vis. Sci. 32, 484-491.

Hauck, S.M., von Toerne, C., Ueffing, M., 2014. The neuroprotective potential of retinal Muller glial cells. Adv. Exp. Med. Biol. 801, 381-387.

Joo, C.K., Choi, J.S., Ko, H.W., Park, K.Y., Sohn, S., Chun, M.H., Oh, Y.J., Gwag, B.J., 1999. Necrosis and apoptosis after retinal ischemia: involvement of NMDA-mediated excitotoxicity and p53. Investigative ophthalmology & visual science 40, 713-720.

Lieth, E., Gardner, T.W., Barber, A.J., Antonetti, D.A., Penn State Retina Research, G., 2000. Retinal neurodegeneration: early pathology in diabetes. Clin. Experiment. Ophthalmol. 28, 3-8.

Lorber, B., Berry, M., Douglas, M.R., Nakazawa, T., Logan, A., 2009. Activated retinal glia promote neurite outgrowth of retinal ganglion cells via apolipoprotein E. J. Neurosci. Res. 87, 2645-2652.

Newman, E., Reichenbach, A., 1996. The Muller cell: a functional element of the retina. Trends Neurosci. 19, 307-312.

Quigley, H.A., Nickells, R.W., Kerrigan, L.A., Pease, M.E., Thibault, D.J., Zack, D.J., 1995. Retinal ganglion cell death in experimental glaucoma and after axotomy occurs by apoptosis. Invest. Ophthalmol. Vis. Sci. 36, 774-786.

Raju, T.R., Bennett, M.R., 1986. Retinal ganglion cell survival requirements: a major but transient dependence on Muller glia during development. Brain Res. 383, 165-176.

Reichenbach, A., Bringmann, A., 2013. New functions of Muller cells. Glia 61, 651-678.

Selles-Navarro, I., Villegas-Perez, M.P., Salvador-Silva, M., Ruiz-Gomez, J.M., Vidal-Sanz, M., 1996. Retinal ganglion cell death after different transient periods of pressure-induced ischemia and survival intervals. A quantitative in vivo study. Invest. Ophthalmol. Vis. Sci. 37, 2002-2014.

Unterlauft, J.D., Eichler, W., Kuhne, K., Yang, X.M., Yafai, Y., Wiedemann, P., Reichenbach, A., Claudepierre, T., 2012. Pigment epithelium-derived factor released by Muller glial cells exerts neuroprotective effects on retinal ganglion cells. Neurochem. Res. 37, 1524-1533.

Wygnanski, T., Desatnik, H., Quigley, H.A., Glovinsky, Y., 1995. Comparison of ganglion cell loss and cone loss in experimental glaucoma. Am. J. Ophthalmol. 120, 184-189.

Zhang, L., Ino-ue, M., Dong, K., Yamamoto, M., 2000. Retrograde axonal transport impairment of large- and medium-sized retinal ganglion cells in diabetic rat. Curr. Eye Res. 20, 131-136.

ANEXO 3

A Proteomics Approach to Identify Candidate Proteins Secreted by Müller Glia that Protect Ganglion Cells in the Retina

Noelia Ruzafa[1], Xandra Pereiro[1], Stefanie M. Hauck[2], Elena Vecino[1].

[1]Department of Cell Biology and Histology, University of Basque Country UPV/EHU, Leioa, Vizcaya, Spain.

[22]Protein Science Research Unit, Helmholtz Zentrum München, German Research Center for Environmental Health, Munich, Germany.

Abstract

The Müller retinal glial cells, like other types of glial cells, can enhance the survival and activity of neurons, especially of retinal ganglion cells (RGCs), which are the neurons affected in diseases such as glaucoma, diabetes and retinal ischemia. It has been demonstrated that Müller glia release neurotrophic factors that support RGC survival, yet many of these factors remain to be elucidated. To define these neurotrophic factors, we adopted a quantitative proteomic approach aimed at identifying neuroprotective proteins. Firstly, we isolated conditioned medium from porcine Müller cells cultured *in vitro* under three different conditions and we tested this conditioned media for its capacity to promote the survival of primary adult RGCs in culture. Mass spectrometry was used to identify and quantify proteins in the conditioned medium, and after a proteomics analysis, osteopontin (SPP1), clusterin (CLU) and basigin (BSG) were selected as candidate neuroprotective factors. SPP1 and BSG significantly enhanced RGC survival *in vitro*, indicating that the survival-promoting activity of the Müller cell secretome is multifactorial, and that SPP1 and BSG contribute to this activity. Thus, the strategy adopted identified proteins secreted by Müller glia that are potentially novel

neuroprotectants, and it may also serve to identify other bioactive proteins or molecular markers.

Introduction

The vascularized mammalian retina contains three types of glial cells: microglia, astrocytes, and Müller cells (for a review see Vecino et al., 2016). Müller cells are the main glial cells in the retina and they provide structural stability to the retina, constituting an anatomical link between all retinal neurons. In particular, Müller cell extensions surround the cell bodies and dendrites of retinal ganglion cells (RGCs: Newman and Reichenbach, 1996). Among the many functions of Müller cells, they are involved in maintaining extracellular homeostasis (Bringmann et al., 2006; Newman et al., 1984; Reichenbach et al., 1993), in the metabolism of glucose (Poitry-Yamate et al., 1995), neurotransmitter recycling (Barnett and Pow, 2000; Derouiche and Rauen, 1995), organizing the developing retina (Willbold et al., 1997), and in the response to retinal damage or disease. Indeed, Müller cells are responsible for the gliotic phenotype (Reichenbach and Bringmann, 2013) and in addition, they provide neurotrophic factors that can directly or indirectly affect the survival of neurons in the retina (Garcia et al., 2002; Hauck et al., 2003; Reichenbach and Bringmann, 2013; Vecino et al., 2016; von Toerne et al., 2014).

Müller cells can protect against the excitotoxic effects of glutamate, and they can enhance the survival and neuritogenesis of RGCs in culture under normal conditions, as well as during starvation (Garcia et al., 2002; Heidinger et al., 1999; Izumi et al., 1999; Kawasaki et al., 2000; Ruzafa and Vecino, 2015; Skytt et al., 2016). This support is preferentially activated by anatomical interactions, although it has been demonstrated that Müller cell conditioned medium significantly enhances the survival of cultured adult porcine RGCs (Garcia et al., 2002; Skytt et al., 2016). Indeed, the neuroprotection afforded by Muller cell condition media exceeds that observed in the retina itself (Reis et al., 2002). Müller cell trophic factors may regulate different aspects of neuronal circuits, such as synaptogenesis, differentiation and the protection of neurons in the retina (de Melo Reis et al., 2008), leading to attempts to characterize the Müller cell secretome by combining high-resolution proteomics tools and *in vitro* models of Müller

cells. However, it must be noted that the proteome of Müller cells may change in primary culture due to their adaptation to the milieu (Hauck et al., 2003). Since the neurotrophic activity in the Müller cell secretome is multifactorial (Hauck et al., 2008), identifying molecules from this source that promote the survival of RGCs could be particularly beneficial to treat degenerative retinal conditions in which RGC death provokes irreversible blindness.

In addition to well-known growth factors, several factors have been identified in the retina as potential neuroprotective molecules that significantly augment photoreceptor survival (Hauck et al., 2008), including insulin-like growth factor-binding proteins IGFBP5 and connective tissue growth factor (CTGF). Osteopontin (SPP1) was also identified and its neurotrophic activity was demonstrated on primary porcine photoreceptors, as well as on Pde6brd1 mouse mutant retinal explants (Del Rio et al., 2011). Moreover, the C-X-C motif chemokine 10 (CXCL10) was also proposed to have neuroprotective properties (von Toerne et al., 2014) and it was validated using models of photoreceptor degeneration (von Toerne et al., 2014), along with established neurotophic factors like leukemia inhibitory factor (LIF: Joly et al., 2008) and the iron-stress protective receptor transferrin (Picard et al., 2010).

As most studies have tested the effect of neurotrophic factors on photoreceptors, the objective of our study was to identify candidate proteins that enhance the survival of RGCs. While some Müller cell derived neurotrophic factors have been identified, a comprehensive study of the Müller cell secretome has yet to be performed. Thus, we adopted a quantitative proteomic approach to analyze the Müller cell secretome, maintaining primary cultures of adult Müller cells under three different conditions to help identify and select candidate neurotrophic proteins.

Material and Methods

Animals

All animal experimentation adhered to the ARVO Statement for the Use of Animals in Ophthalmic and Vision Research. For Müller cell cultures, adult porcine eyes were obtained from a local slaughterhouse and transported to the laboratory in cold CO_2-

independent Dulbecco's modified Eagle's medium (DMEM/−CO_2: Life Technologies, Carlsbad, CA, USA) containing 0.1% gentamicin (Life Technologies, Carlsbad, CA, USA).

Eyes for RGC cultures were obtained from adult female Sprague-Dawley rats (200-250g). Animals were housed under a 12 hour light-dark cycle with ad libitum access to food and water, and they were sacrificed humanely by exposure to CO_2.

Muller cell culture

Adult porcine eyes were dissected within 1 to 2 hours of enucleation and retinal Müller cell cultures were prepared according to a previously reported protocol (Garcia et al., 2002) with the following minor modifications. Briefly, the major blood vessels were removed and the retina was washed in DMEM/−CO_2 medium. The retinas were dissected out and cut using a 8 mm diameter dissecting trephine (Biomedical Research Instruments, Silver Spring, MD, USA). The retinal tissue was dissociated for 30 minutes at 37 °C in 0.2% activated papain (Worthington, Lakewood, NJ, USA) with 10% DNAse I (Worthington, Lakewood, NJ, USA). Papain activity was stopped by the addition of further Müller Medium and DNase I, and the tissue was disaggregated by gentle trituration using pipette tips of decreasing diameter.

Three types of Müller Media were used: 1) DMEM (Life Technologies, Carlsbad, CA, USA) with 10% fetal bovine serum (FBS, Life Technologies, Carlsbad, CA, USA); 2) DMEM with 20% FBS; 3) Neurobasal A medium (NBA: Life Technologies, Carlsbad, CA, USA) with 10% FBS and supplemented with 2% B27(Life Technologies, Carlsbad, CA, USA). In addition, 1% L-glutamine (2mM: Life Technologies, Carlsbad, CA, USA) and 0.1% gentamicin (50 mg/ml: Life Technologies, Carlsbad, CA, USA) were added to all the media.

Dissociated cells were collected by centrifugation (1200 rpm, 5 min), resuspended in Müller Medium and plated on poly-L-lysine (100 µg/ml: Sigma Aldrich, St. Louis, MO, USA) and laminin (10 µg/ml: Sigma Aldrich, St. Louis, MO, USA) coated 13 mm glass coverslips in 24 well plates. The cells were maintained in a humidified incubator at 37 °C in an atmosphere of 5% CO_2, and after 24 hours, the unattached cells were removed by changing the entire medium. To maintain the cells half of the medium was replaced every 3 days.

The conditioned medium was collected when the cultures had reached confluency (day 7), first washing the wells 3 times with NBA medium (NBA plus 1% L-glutamine and 0.1% gentamicin). Subsequently, NBA medium was added to each well and they were left for 3 hours before the medium was changed to eliminate the rest of the FBS and B27. Fresh NBA medium was added and left for 2 days before it was collected and sterilized by passing through a 0.22 µm filter. The conditioned medium was frozen in aliquots at -20 ºC. Finally, the Müller cells were fixed for 10 minutes with methanol at -20 ºC. At least 3 replicates of each culture were made, and the procedure was performed in triplicate.

RGC cultures

Retinal ganglion cell cultures were prepared as described previously (Vecino et al., 2015). Briefly, retinas were dissected and to obtain a mixed suspension of retinal cells, and they were dissociated enzymatically using the Papain Dissociation Kit (Worthington Biochemical Lakewood, NJ, USA) according to the manufacturer's instructions. Briefly, the retinal tissue was digested for 90 minutes at 37 °C in 0.2% activated papain with 10% DNAse I and the tissue was disaggregated by gentle trituration using pipette tips of decreasing diameter. After purification, the dissociated retinal cells were plated on 13 mm poly-L-lysine (100µg/ml: Sigma Aldrich, St. Louis, MO, USA) and laminin (10µg/ml: Sigma Aldrich, St. Louis, MO, USA) coated glass coverslips in 24 well plates to test the activity of conditioned medium, or coated well in 96 well plates to test the activity of candidate proteins. The cultures were maintained in Neurobasal A medium (Life Technologies, Carlsbad, AC, USA) supplemented with 2% B27, and with 1% L-glutamine (2mM: Life Technologies, Carlsbad, CA, USA) and 0.1% gentamicin (50 mg/ml: Life Technologies, Carlsbad, CA, USA). The RGCs were cultured for 6 days at 37 °C in a humidified atmosphere containing 5% CO_2 and the medium was changed every 3 days. The RGCs were fixed for 10 minutes with methanol -20 ºC on day 6.

To test the activity of the conditioned medium and that of the candidate proteins, the RGCs were cultured in: NBA/B27 medium:NBA medium (1:1, control); NBA/B27 medium:conditioned medium collected in NBA medium (1:1); or NBA/B27 medium:NBA medium plus protein (1:1). The proteins used were: PDGF-CC as a positive control (50 ng/ml: Peprotech, London, UK); osteopontin (SPP1, 200 ng/ml:

Life Technologies, Carlsbad, AC, USA); clusterin (CLU, 125 ng/ml: R&D System, Minneapolis, MN, USA), basigin (BSG, 1,000 ng/ml: Life Technologies, Carlsbad, AC, USA). All the media contained 1% L-glutamine and 0.1% gentamicin. At least 3 replicates were performed for the analysis of the conditioned medium analysis and 6 replicates when analyzing the candidate proteins, repeating each independent experiment three times.

Immunochemistry

After fixing in methanol and washing with PBS (phosphate buffered saline, pH 7.0), the cells were immunostained as described previously (Ruzafa and Vecino, 2015). After blocking the binding of non-specific antigens with blocking buffer (3% BSA and 0.1% Triton X-100 in PBS), the cells were incubated with antibodies against vimentin as a specific marker of Müller cells (mouse monoclonal antibody diluted 1:10,000: Dako, Glostrup, Denmark) and bIII-tubulin as a specific RGC marker (rabbit polyclonal antibody diluted 1:2,000: Promega, Madison, WI, USA). After washing again, these antibodies were detected with anti-mouse Alexa Fluor 488 and anti-rabbit Alexa Fluor 555 goat secondary antibodies (Life Technologies, Carlsbad, CA, USA), both at a dilution of 1:1,000, and the cells were counterstained with the nuclear marker DAPI (Life Technologies, Carlsbad, CA, USA), diluted 1:10,000.

Quantification of RGCs and statistical analysis

RGCs were analyzed on an epifluorescence microscope (Zeiss, Jena, Germany) coupled to a digital camera (Zeiss Axiocam MRM, Zeiss, Jena, Germany). At least 3 (for activity test of conditioned medium) or 6 (for activity test of candidate proteins) coverslips were analyzed for each experimental condition and from three independent experiments. The RGC density was quantified and the cells were classified as: (1) cells with no neurites; (2) cells with a longest neurite <50 μm; (3) cells with the longest neurite between 50 μm and 200 μm; and (4) cells with neurites longer than 200 μm. The total number of RGCs surviving in each condition was recorded.

The cell density was described as the mean (cells/mm^2) and standard error of mean, and this parameter was compared between the different conditioned media. The data were also normalized to the control to simplify the representation. Statistical analyses were carried out using IBM SPSS Statistics software v. 21.0 and the homogeneity of the

variances was assayed with Levene´s test ($p < 0.05$). A Student T-test and a Mann-Whitney U test were used to assess whether there were significant differences between the groups. The minimum value of significance for both tests was defined as $p<0.05$.

Mass Spectrometry

LC-MS/MS analysis of the conditioned medium was performed on a QExactive HF mass spectrometer (Thermo Fisher Scientific Inc., Waltham, MA, U.S.A.). Proteolysed samples were loaded onto a nano-trap column (300 µm inner diameter × 5 mm, packed with Acclaim PepMap100 C18, 5 µm, 100 Å: LC Packings, Sunnyvale, CA) and separated by reversed phase chromatography (PepMap, 25 cm, 75 µm ID, 2µm/100 Å pore size: LC Packings) on a nano-RSLC apparatus (Ultimate 3000, Dionex, Sunnyvale, CA). Peptides were eluted over 130 minutes with the following gradient of increasing ACN concentrations in 0.1% formic acid: 90 minutes of 5% to 26%, followed by 5 minutes from 26% to 41% ACN, followed again by 5 minutes from 41% to 85% ACN. Between each gradient the concentration of ACN in 0.1% FA was reverted to the starting conditions for 20 minutes.

A high-resolution (60,000 full-width half maximum) MS spectrum was acquired in the Orbitrap with a mass range from 300 to 1,500 Da. The 10 most abundant peptide ions were selected for fragmentation if they exceeded an intensity of at least 1xe4 counts and if they were at least doubly charged. MS/MS spectra were also recorded in the Orbitrap at a resolution of 15,000 with a maximum injection time of 50 ms. Dynamic exclusion was set to 30 sec.

Label-free analyses, database search and protein identification

The acquired spectra of the different samples were loaded and analyzed using Progenesis QI software for label-free proteomics quantification (Version 2.0, Nonlinear Dynamics, Waters, Newcastle upon Tyne, U.K.), as described previously (Hauck et al., 2010). Briefly, the profile data of the MS scans were transformed into peak lists with respective m/z values, intensities, abundances and m/z width. The MS/MS spectra were transformed similarly and then stored in peak lists comprising m/z and abundance. Using one sample as reference, the retention times of the other samples were aligned

automatically to give a maximal overlay of the 2D features. After alignment and feature exclusion, the samples were allocated to their respective experimental groups and the raw abundances of all the features were normalized.

The MS/MS spectra were exported from the Progenesis QI software as Mascot generic files (mgf) and used for peptide identification with Mascot (version 2.5). Identifications were re-imported into Progenesis QI. For quantification, all unique peptides of an identified protein were included and the total cumulative normalized abundance was calculated by summing the abundances of all the unique peptides allocated to the respective protein. Statistical analysis with a Student´s T-test was performed using normalized abundances and values of $p < 0.05$ were considered as significant for all further results. Two technical replicates were measured for each type of sample to verify the experimental reproducibility.

Heat maps

Heat maps of significantly altered proteins were generated separately for the three different sample preparation methods, using the heat map function in the Excel (Microsoft) XLStat add-in included in the OMICS module (Addinsoft). Normalized protein abundances were used for the independent clustering of samples and proteins, applying hierarchical clustering based on Euclidian distances. The matrices are colored in green for highly abundant proteins and in red for low abundant proteins.

Results

Proteomic strategy to identify proteins secreted by Müller cells that promote RGC survival

In order to identify factors secreted by Müller cells that promote the survival of RGCs, a strategy was developed that integrates biological activity within a proteomics workflow (Fig. 1). We started with the secretome of Müller cells cultured in 3 different media, each of which has a distinct effect on the survival and neuritogenesis of RGCs. As such, we established a possible means to select candidate neuroprotectant proteins from the many proteins identified by mass spectrometry.

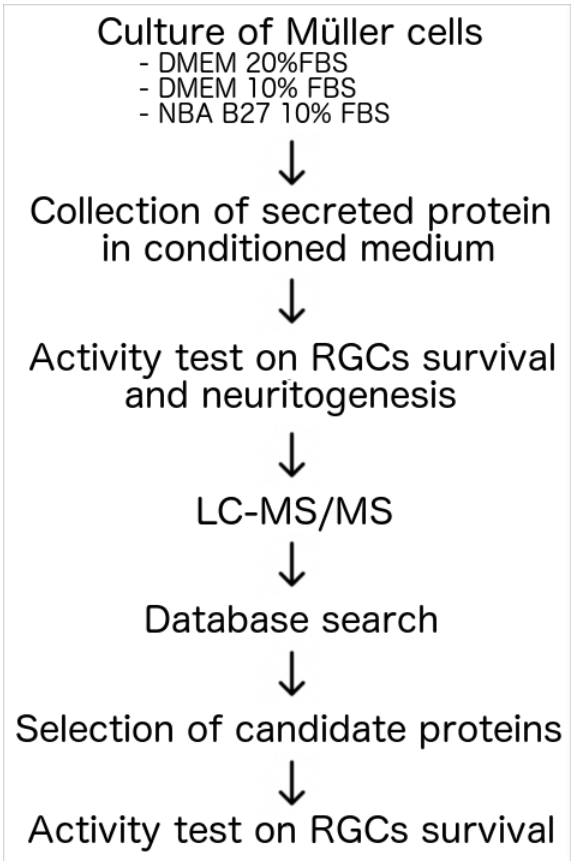

Fig 1. Proteomics work flow to identify proteins secreted by Müller cells that promote RGC survival. We start by culturing retinal Müller cells in different media and collecting the secretome of these cells. The effect of the conditioned medium on the survival and neuritogenesis of RGCs was tested in RGC cultures. The proteins in these conditioned media were analyzed by mass spectrometry (LC-MS/MS), allowing several candidate proteins to be identified. The proteins selected were analyzed thoroughly and their pro-survival activity tested in RGCs cultures.

Effect of Müller cell conditioned medium on RGC survival and neuritogenesis *in vitro*

Müller cells were cultured in 3 types of medium (DMEM + 10% FBS, DMEM + 20% FBS and NBA/B27 + 10% FBS) and after collecting the conditioned medium from these cultures, the cells were labeled with an antibody against vimentin (Fig. 2A-C). As a result, the Müller cells grown in DMEM were clearly more elongated and they were closer to each other than when maintained in NBA/B27. These differences were even more pronounced when the cells were maintained in DMEM + 20% FBS.

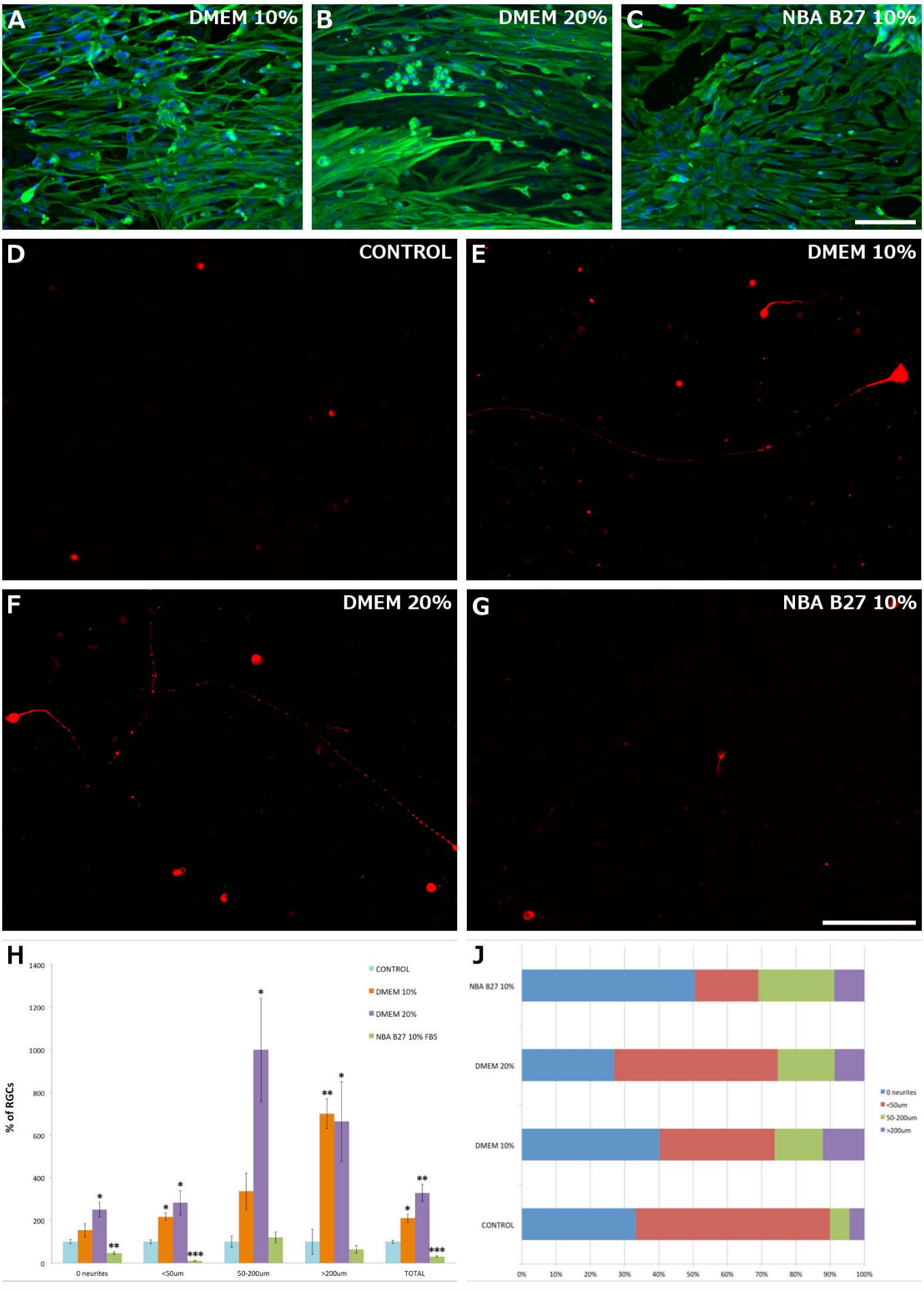
A
DMEM 10%
B
DMEM 20%
C
NBA B27 10%
D
CONTROL
E
DMEM 10%
F
DMEM 20%
G
NBA B27 10%
H
% of RGCs
CONTROL
DMEM 10%
DMEM 20%
NBA B27 10% FBS
0 neurites
<50um
50-200um
>200um
TOTAL
J
NBA B27 10%
DMEM 20%
DMEM 10%
CONTROL
0 neurites
<50um
50-200um
>200um

Fig 2. Effect of Müller cell conditioned medium on the survival and neuritogenesis of RGCs *in vitro*. Images of Müller cells cultured in DMEM + 10% FBS (A), DMEM + 20% FBS (B) and NBA/B27 + 10% FBS (C). The cells were labeled with antibodies against vimentin (green) and the nuclei are marked with DAPI (blue). Images of RGCs in control conditions (D) or cultured in conditioned media from Müller cells cultured in DMEM + 10% FBS (E), DMEM + 20% FBS (F) and NBA/B27 + 10% FBS (G). The cells were labeled with antibodies against β-III-tubulin (red). H. RGC survival in control conditions (blue) or in the presence of media conditioned by Müller cells cultured in DMEM + 10% FBS (orange), DMEM + 20% FBS (purple) and NBA/B27 + 10% FBS (green). To analyze neuritogenesis, the RGCs were classified as RGCs without neurites, with the longest neurite <50 μm, with the longest neurite between 50 μm and 200 μm, and with neurites longer than 200 μm. To analyze survival, the total number of RGCs was assessed and all the data were normalized considering the control as 100% for each condition. J. Percentage of RGCs without neurites (blue), with a longest neurite <50 μm (red), with the longest neurite between 50 μm and 200 μm (green), and with neurites longer than 200 μm (purple), for control cells and RGCs maintained in the presence of the three types of conditioned medium. The total number of RGC for each condition is considering as 100%: Scale bar = 100μm; * $p < 0.05$; ** $p < 0.01$;*** $p < 0.001$.

The RGCs were cultured in NBA/B27 medium:NBA medium (1:1, control) or in NBA/B27 medium:conditioned medium (1:1) from each of the 3 conditions of Müller cell culture. There were more RGCs and with longer neurites when the cells were maintained in the presence of medium conditioned by Müller cells grown in DMEM, whereas these parameters were similar or smaller to the control RGC cultures when RGCs were maintained in the presence of medium conditioned by Müller cells grown in NBA/B27 (Fig. 2D-G).

RGC survival and neuritogenesis was quantified (Table 1, Fig. 2H-J) and the total number of RGCs were classified according to their neurite length, normalizing the data to the controls for each condition (considered as 100%: Fig. 2H). Exposing the cultured RGCs to the conditioned media altered the number of the cells counted, increasing the total number of RGCs 3.29-fold when cultured with conditioned medium from Müller cells grown in DMEM + 20% FBS ($p< 0.01$) and 2.1-fold when cultured with medium conditioned by Müller cells that grown in DMEM + 10% FBS ($p< 0.05$: Table 1). Conversely, the number of RGCs decreased by 69.36% when they were cultured with medium conditioned by Müller cells grown in NBA/B27 + 10% FBS ($p< 0.001$). Similarly, in the presence of medium conditioned by Müller cells grown in DMEM + 20% FBS the number of RGCs with no neurites increased 2.51 times ($p< 0.05$) and it decreased by 53.66% in the presence of conditioned medium from Müller cells grown

in NBA/B27 + 10% FBS ($p < 0.01$). Similar effects were observed on the RGCs with neurites smaller than 50 μm: a 2.82-fold increase with medium conditioned by Müller cells grown in DMEM + 20% FBS ($p< 0.05$); a 2.17-fold increase in the presence of medium conditioned by Müller cells grown in DMEM + 10% FBS ($p< 0.05$); and a 90.07% decrease in conditioned medium from Müller cells grown in NBA/B27 + 10% FBS ($p< 0.001$). Moreover, the RGCs with a length of neurites between 50 μm and 200 μm increased 10-fold with medium conditioned by Müller cells grown in DMEM + 20% FBS ($p< 0.05$). Finally, the RGCs with neurites greater than 200 μm long increased 6.63-fold when RGCs were cultured with medium conditioned by Müller cells grown in DMEM + 20% FBS ($p< 0.05$) and 7-fold when the RGCs are cultured with medium conditioned by Müller cells grown in DMEM + 10% FBS ($p< 0.05$).

	0 neurites	<50μm	50-200μm	>200μm	TOTAL
CONTROL	0.206 ± 0.019	0.354 ± 0.031	0.035 ± 0.009	0.027 ± 0.016	0.622 ± 0.045
DMEM 10%	0.317 ± 0.063	0.769 ± 0.061	0.118 ± 0.029	0.193 ± 0.019	1.308 ± 0.122
DMEM 20%	0.517 ± 0.069	0.999 ± 0.199	0.351 ± 0.085	0.183 ± 0.051	2.051 ±0.252
NBA B27 10%	0.095 ± 0.012	0.035 ± 0.005	0.042 ± 0.009	0.017 ± 0.005	0.191 ± 0.020

Table 1. Average of RGC survival and neuritogenesis of RGCs *in vitro* maintained in the presence of Müller cell conditioned medium. RGCs/mm^2 (± standard error) when cultured in control conditions or when maintained in the presence of medium conditioned by Müller cells cultured in DMEM + 10% FBS, DMEM + 20% FBS, or NBA/B27 + 10% FBS. RGCs were classified as: RGCs without neurites, with a longest neurite <50 μm, with the longest neurite between 50 μm and 200 μm, and with neurites longer than 200 μm. The total number of RGCs is also shown.

The proportion of each type of RGC was calculated for each culture condition to determine whether the conditioned medium affects RGC neurite length (Fig. 2J). When RGCs were maintained in medium conditioned by Müller cells grown in DMEM + 10% FBS, the proportion of RGCs with the longest neurite greater than 200 μm increased from 4.39% (control) to 12.18% ($p< 0.001$). Similarly, the conditioned medium from Müller cells grown in DMEM + 20% FBS increase the proportion of RGCs with the longest neurite between 50 μm and 200 μm from 5.63% (control) to 16.58% ($p< 0.01$). By contrast, in the presence of the medium conditioned by Müller cells grown in NBA/B27 + 10% FBS the percentage of RGCs with the longest neurite smaller than 50 μm decreased from 56.76% (control) to 18.57% ($p< 0.001$), in conjunction with an increase in the percentage of RGCs with the longest neurite between 50 μm and 200 μm from 5.63% (control) to 22.14% ($p< 0.01$). No significant differences were found in the proportion of RGCs without neurites.

Protein identification, database search and candidate protein selection

From the secretome of the cultured Müller glial cells, 1,325 proteins were identified and quantified by LC-MS/MS analysis. Heat maps of significantly altered proteins were generated for the samples obtained with the three different types of conditioned media, and fresh NBA medium that had not been in contact with Müller cells was used as a control. The three culture conditions clearly segregated and the heat maps illustrated the fundamental differences between the distinct culture conditions (2 technical replicates were used for each sample type to verify experimental reproducibility), with highly abundant proteins in the matrices colored green and low abundance proteins red (Fig 3A).

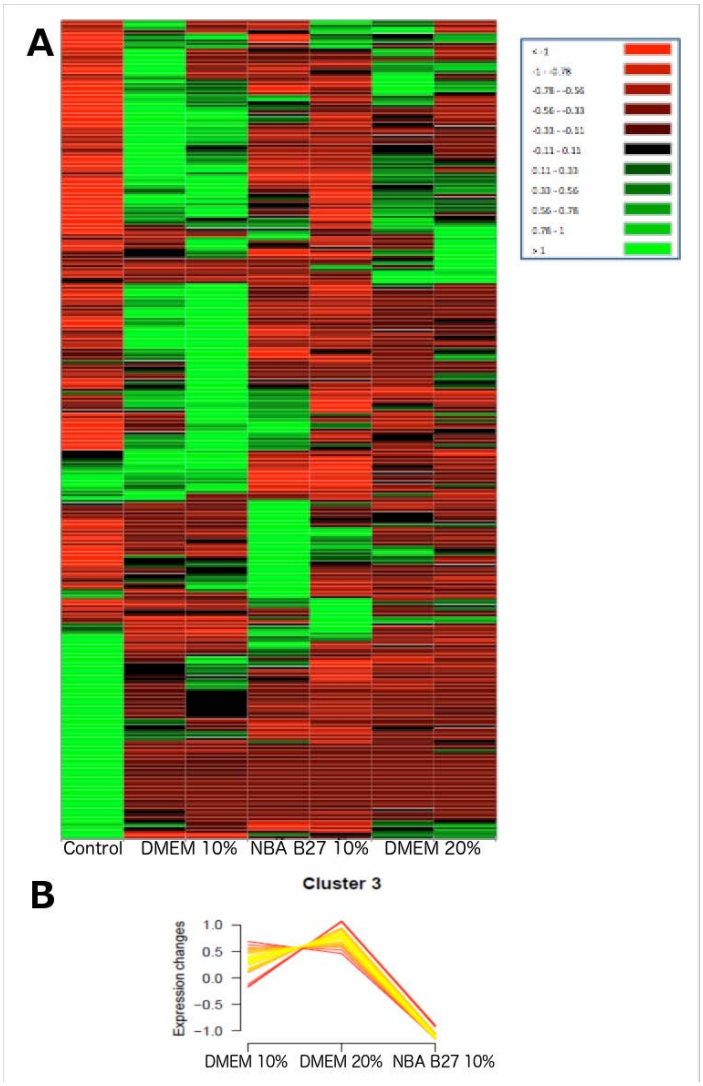

Fig 3. Protein identification, database search and selection of candidate proteins. A. Heat maps of significantly altered proteins in the three different samples of media conditioned by Müller cells cultured

in DMEM + 10% FBS, DMEM + 20% FBS and NBA/B27 + 10% FBS. Two technical replicates were assessed for each sample type (two columns for each conditions) to verify the experimental reproducibility and a column with NBA medium is shown as a negative control. The matrices are colored in green for highly abundant proteins and red for weakly abundant proteins. B. Clusters of the normalized protein abundance of the samples and proteins, applying hierarchical clustering based on Euclidian distances. Based on the Gprox analysis, all the proteins that were significantly altered ($p < 0.05$) in one of the comparisons and the proteins with similar behavior were combined into clusters. Although six clusters were generated, only cluster 3 is represented as in this cluster the proteins in the different conditioned media behaved as expected.

The proteins were quantified and the ratio between the mean normalized abundance of each sample was compared with the other two samples. Secreted proteins of interest were identified in each of the Müller cell conditioned media, such as growth factors or adhesion molecules, including: LIF (leukemia inhibitory factor), SERPINF1 (or PEDF, pigment epithelium-derived factor), PDGF (platelet derived growth factor), CTGF (connective tissue growth factor precursor), NCAM (neural cell adhesion molecule 1), BCAM (basal cell adhesion molecule) or ICAM (intercellular adhesion molecule 1 and 2). However, these proteins are present in all the samples and there were no significant differences in their abundance between them. As the three conditioned media do not have the same effect on the survival of RGCs, these proteins were therefore ruled out as candidate neuroprotective proteins.

Müller cell secreted molecules enhanced RGC survival in all the conditions in which they were cultured, yet we searched for candidate molecules with the strongest effect on RGC survival. Hence, we searched for proteins that were more abundant in the conditioned medium from Müller cells cultured in DMEM than in the conditioned medium from Müller cells cultured in NBA/B27. Due to its neuroprotective properties, we became particularly interested in osteopontin (SPP1), which is significantly more abundant in DMEM + 10% FBS than in NBA/B27 (16.0-fold, $p < 0.01$). However, although there appeared to be more osteopontin in DMEM + 20% FBS than in NBA/B27, this difference was not significant (9.1-fold, $p > 0.05$). As such, the effects of osteopontin may be concentration dependent and they may be less effective when the concentration becomes too high.

Normalized abundance was used to independently cluster the samples and proteins, and all proteins that were significantly different in one of the comparisons were included in

the analysis, with the proteins expressed similarly combined into clusters. While 6 different changes in expression were generated, cluster number 3 was that which was of most interest to us (Fig. 3B). The proteins in this cluster are those that were most abundant in the conditioned medium produced by Müller cells cultured in DMEM + 20% FBS, the medium that had the strongest effect on RGC survival. Moreover, the proportion of these proteins in the medium conditioned by Müller cells cultured in NBA/B27 + 10% FBS was lowest, this medium diminishing RGC survival (see Table 2 for a list of the 39 proteins included in this cluster and their relative abundance). After analyzing the function of this list of proteins, clusterin (CLU) and basigin (BSG) were selected as candidate proteins to evaluate their capacity to afford neuroprotection to RGCs.

Effect of candidate proteins on the survival of RGCs *in vitro*

To identify which proteins from the conditioned medium might be responsible for promoting the survival of RGCs, these cells were cultured separately in the presence of three of the candidate proteins: SPP1, CLU and BSG (Fig. 4). The effect of the isolated proteins was compared to that of conditioned medium from Müller cells cultured in DMEM + 20% FBS, and PDGF was used as a positive control promoting RGC survival. As indicated above, the conditioned medium increased the total number of RGCs 3.65-fold (from is 1.106 ± 0.168 RGCs/mm^2 in the controls to 4.041 ± 0.691 RGCs/mm^2 in the presence of the conditioned medium: $p< 0.001$) and PDGF enhanced the survival of RGCs by 47.08% (to 1.627 ± 0.248 RGCs/mm^2: $p< 0.001$). SPP1 and BSG increased the survival of RGCs by 71.31% (1.895 ± 0.128 RGCs/mm^2: $p< 0.001$) and 55.81% (1.724 ± 0.285 RGCs/mm^2: $p< 0.001$), respectively, whereas CLU did not produce a significant change in RGC survival, although a tendency towards greater RGC survival was evident (36.02% to 1.505 ± 0.313 RGCs/mm^2). The combination of SPP1 and BSG did not exert a synergistic effect, these proteins together increasing the survival of RGCs by 86.79% (2.067 ± 0.065 RGCs/mm^2: $p< 0.001$). Thus, the action of the conditioned medium on the survival of RGCs appears to be dependent on the combination of more proteins than those identified, these two proteins failing to exert the full protective effect of the conditioned medium alone.

GEN	DMEM 10%	DMEM 20%	NBA B27 10%	DEFINITION
ACO1	30	58	11	aconitase 1
ADAMTS12	29	49	22	ADAM metallopeptidase with thrombospondin type 1 motif
SNRPG	37	45	18	small nuclear ribonucleoprotein
COL23A1	45	55	0	collagen, type XXIII, alpha 1
LMP2	44	47	10	proteasome subunit, beta type, 9
ABCB11	45	50	5	ATP-binding cassette, sub-family B
SCAF11	41	53	6	SR-related CTD-associated factor 11
RAB11B	41	47	12	member RAS oncogene family
ECM1	40	51	9	extracellular matrix protein 1
CLU	36	51	12	clusterin
TGM2	47	41	12	transglutaminase 2
CLEC11A	31	47	22	C-type lectin domain family 11
CAPZA2	38	47	15	capping protein muscle Z-line, alpha 2
SDCBP	43	51	6	syndecan binding protein
KCTD12	42	42	16	potassium channel tetramerization domain containing 12
ACP2	43	45	11	Uncharacterized protein
YWHAH	41	43	16	Tyrosine 3-monooxygenase/tryptophan 5-monooxygenase activation protein
UFD1L	41	48	10	ubiquitin fusion degradation 1 like
LGALS3	40	39	21	galactoside-binding, soluble, 3
DF	42	53	5	Complement factor D
PFDN4	37	48	15	prefoldin subunit 4
PTPN6	42	56	2	Tyrosine-protein phosphatase non-receptor type 6
MOB1A	37	63	1	Uncharacterized protein
RHO	48	49	3	rhodopsin
IFITM1	45	50	5	Uncharacterized protein
ATP6V1H	37	60	2	ATPase, H+ transporting lysosomal,V1 subunit H
GIMAP4	40	50	11	GTPase, IMAP family member 4
PNP	49	44	8	purine nucleoside phosphorylase
IDE	40	47	13	insulin-degrading enzyme
IDH1	40	49	10	isocitrate dehydrogenase 1
BSG	24	76	0	basigin
PEPD	39	41	20	Uncharacterized protein
VSIG4	36	50	13	V-set and immunoglobulin domain-containing protein 4
GBE1	37	55	9	Uncharacterized protein
PITPNB	42	49	10	phosphatidylinositol transfer protein, beta
RAP1GDS1	40	57	3	GTP-GDP dissociation stimulator 1
CLIC4	35	46	19	chloride intracellular channel 4
PCSK1N	29	59	12	proprotein convertase subtilisin/kexin type 1 inhibitor
FBP1	31	61	1	fructose-1,6-bisphosphatase 1

Table 2. Proteins in cluster 3. The genes encoding the proteins that are included in cluster number 3. The proportion of the proteins in the 3 different mediums is represented in this table. In addition, the definition of each protein is indicated.

As the analysis was carried out in 96 wells plate to minimize the amount of recombinant proteins required, only a small proportion of RGCs developed neurites and thus, only RGC survival was assessed, although there appeared to be no significant difference in terms of neuritogenesis between each of the conditions tested.

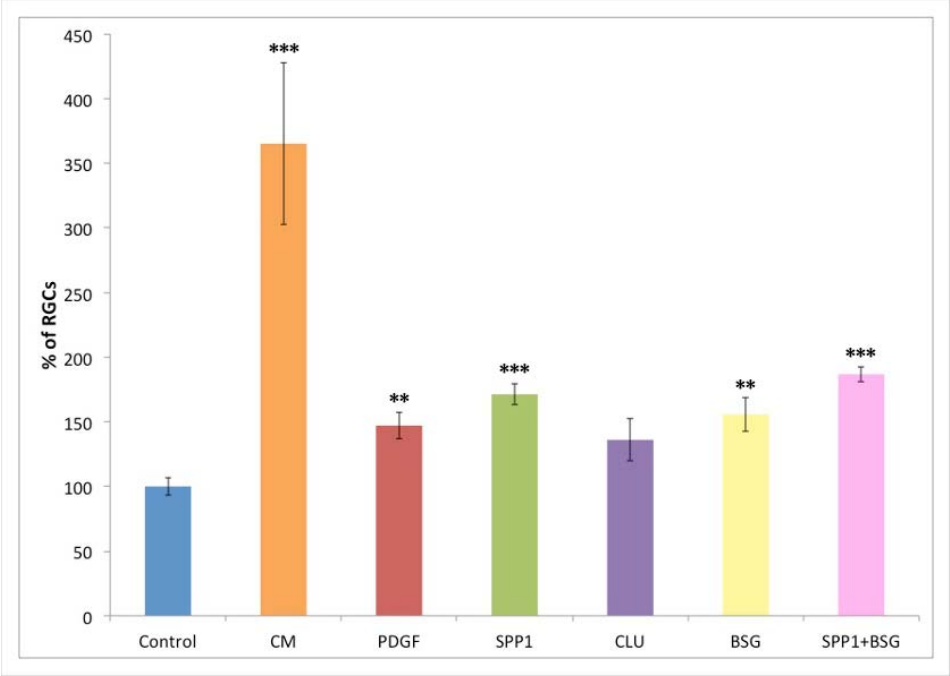

Fig 4. Effect of candidate proteins on the survival of RGCs *in vitro*. Histogram representing RGC survival after 6 days in culture in: control conditions; in the presence of the medium conditioned by Müller cells maintained in DMEM + 20% FBS (CM); in the presence of PDGF, a protein with a demonstrated positive effect on RGC survival as a positive control; and in the presence of the candidate proteins osteopontin (SPP1), clusterin (CLU) and basigin (BSG), or the combination of SPP1 and BSG. The data are normalized considering the control as 100% for each condition: ** $p < 0.01$;*** $p < 0.001$.

Discussion

Although efforts have been made to analyse extracellular fluids to identify proteins with therapeutic potential, this process is often hindered by their relatively low abundance. Conversely, the isolation and culture of primary cells is an aid to the identification of such agents (Mbeunkui et al., 2007; Sze et al., 2007). Studies on conditioned media with neuroprotective properties have been performed previously in order to identify potential

therapeutic proteins (Dreixler et al., 2014; Johnson et al., 2014; Lin et al., 2016). Here, we have adopted a similar approach by performing a proteomic analysis of the secretome of cultured adult Müller cells in order to identify proteins that enhance RGC survival.

There is evidence that the secretome of Müller cells contains neurotrophic molecules, given that factors secreted by porcine Müller cells in culture promote RGC (Garcia et al., 2002) and photoreceptors (Balse et al., 2005) survival. Müller cells synthesize known neurotrophic factors, such as brain-derived neurotrophic factor (BDNF: Vecino et al., 1999), ciliary neurotrophic factor (CTNF: Rhee and Yang, 2010; Zack, 2000), basic fibroblast growth factor (bFGF: Bringmann et al., 2009; Hollborn et al., 2004), pigment epithelium derived factor (PEDF: Zhou et al., 2009) or glial-derived neurotrophic factor (GDNF: Harada et al., 2003; Hauck et al., 2006). In addition, other neuroprotective factors have been seen to be secreted by Müller cells, such as IGFBP5, CTGF (Hauck et al., 2008), SPP1 (Del Rio et al., 2011), CXCL10 (von Toerne et al., 2014), LIF (Joly et al., 2008) and transferrin (Picard et al., 2010). However, it seems unlikely that all the proteins responsible for the neuronal survival-promoting effects of the Müller cells have been identified.

To identify proteins in the secretome of Müller cells, cultured Müller cells were used. It is known that characteristic features of Müller cells may be altered or lost after 2 weeks in culture (Guidry, 1996) and that the protein expression of Müller cells in culture for 21 days reflects trans-differentiation from a multifunctional, highly differentiated, glial cell to a dedifferentiated fibroblast-like phenotype (Hauck et al., 2003; Merl et al., 2012). In order to preserve the features of differentiated Müller cells *in vitro*, the secretome of these cells was collected on day 7 in culture. Moreover, to take advantage of the effect of the adaptation of these cells to distinct *in vitro* conditions (Hauck et al., 2003), the proteome of the Müller cells was assessed in 3 different culture conditions. Indeed, since the neuroprotective effect of the 3 different conditioned media was distinct in terms of RGC survival, this aided the identification of proteins that might be involved in this phenomenon.

The strategy employed here intended to demonstrate the importance of endogenous neurotrophic activities in the retina. As such, we monitored the secreted protein pool for its RGCs survival-promoting activity, first classifying the secretome based on RGC

protection and the promotion of neuritogenesis. The secretome of Müller cells cultured in the presence of a higher proportion in FBS (20%) better promoted RGC survival and neuritogenesis, whereas the secretome of Müller cells cultured in NBA, a medium more specific to neurons than glial cells, had the worst effect. These differences were also evident when the conditioned media were analysed by mass spectrometry, identifying and quantifying the proteins present. The distinct effects of the media on RGC survival facilitated the comparison between the proteins analysed and enabled the proteins to be classified into clusters according their relative abundance in medium with a strong, medium or weak positive effect on RGC survival. This quantitative or comparative proteomics strategy is essential to characterize a complex proteome and compare it with others (Ong and Mann, 2005; Unwin et al., 2006). Using LC-MS/MS, the relative abundance of each labelled peptide can be compared in two or more samples by analysing peptides identical in sequence but differing in mass (Kinoshita et al., 2006). As this method is semi-quantitative it can detect changes in protein abundance with high confidence (Colinge et al., 2005) and it is suitable for high-throughput, multisample proteome profiling (Kinoshita et al., 2006). Moreover, the proteomic clustering analysis provides a means of identifying and visualizing relationships in complex mixtures with many interacting elements (Jablonowski, 2017).

We selected a cluster of proteins (cluster number 3) whose relative abundance was correlated with the neuroprotective effect of the 3 conditioned media. In other words, the proteins in the cluster are more abundant in the medium that has a positive effect on RGC survival and less abundant in the media with a negative effect on the RGCs. After analysing the protein's functions in this cluster, 2 candidate proteins were selected from the 39 proteins identified: clusterin and basigin. Clusterin was chosen because it is implicated in DNA repair, cell cycle regulation and apoptotic cell death, and it also exerts a pro-survival role during cell death and confers resistance against cytotoxic agents (Shannan et al., 2006; Trougakos and Gonos, 2006; Trougakos et al., 2009). Basigin was selected because it is required for normal retinal development and function, and for normal neuron-glia interactions in the visual system (Curtin et al., 2007; Fadool and Linser, 1993; Munro et al., 2010; Ochrietor and Linser, 2004). In addition, SPP1 was selected as a candidate molecule after confirming its presence in the conditioned medium because it is a neuroprotective factor for photoreceptors (Del Rio et al., 2011), and its protective effect on RGCs has not yet been analysed. The concentrations of these

recombinant proteins used in the RGCs culture were concentrations of the proteins found in plasma (Thambisetty et al., 2012) or those used previously in culture (Belton et al., 2008; Birke et al., 2010).

The role of the selected candidate proteins in RGC survival was assessed in primary cell cultures of adult RGCs, using PDGF as a positive control as it is a potent neuroprotective factor known to enhance RGC survival (He et al., 2014; Tang et al., 2010). Indeed, we have confirmed that PDGF is present in the secretome of Müller cells and as expected, it produced a significant increase in RGC survival in culture. Although CLU appeared to enhance RGC survival, these changes were not significant with respect to the controls. Conversely, BSG significantly enhanced RGC survival, a novel neuroprotective property of this protein. The presence of SPP1 in the culture medium even further enhanced RGC survival in culture, consistent with data from *ex vivo* cultured glaucomatous retinas treated with SPP1 in which cell degeneration within the ganglion cell layer was inhibited (Birke et al., 2010). Moreover, the essential role of SPP1 in the retina has been demonstrated in the SPP1 knock-out mouse, where the lack of SPP1 induces a decrease in RGC number (Ruzafa et al., 2017).

Although the proteins exert a positive effect on RGC survival, the use of one protein or the sum of two of these does not fully replicate the neuroprotective effect exerted by the conditioned medium, which enhances RGC survival 3.65-fold *in vitro*. This indicates that the protective activity in the Müller cell conditioned medium is multifactorial, SPP1 and BSG forming only part of this activity. However, SPP1 and BSG are both proteins known to have neuroprotective properties, and thus, further studies with these recombinant proteins are needed. Moreover, this study highlights the potential of use of these proteins as possible therapeutic agents in neurodegenerative diseases in which RGCs are affected.

In conclusion, primary adult porcine Müller cells cultures represent a suitable model to study the neuroprotection of RGCs provided by Müller cells. The functional assay-driven proteomics screening approach adopted, based on the survival of RGCs, not only served to validate known neurotrophic factors but also, it identified novel proteins secreted by Müller cell as potential neuroprotectants. This strategy can be also applied to the identification of other bioactive proteins or molecular markers as it allows single molecules derived from complex protein mixtures to be characterized.

Acknowledgments

We acknowledge the support of Retos-MINECO Fondos Fender (RTC-2016-48231) and Grupos Consolidados del Gobierno Vasco (IT437-10) to E.V.

References

Balse, E., Tessier, L.H., Fuchs, C., Forster, V., Sahel, J.A., Picaud, S., 2005. Purification of mammalian cone photoreceptors by lectin panning and the enhancement of their survival in glia-conditioned medium. Invest. Ophthalmol. Vis. Sci. 46, 367-374.

Barnett, N.L., Pow, D.V., 2000. Antisense knockdown of GLAST, a glial glutamate transporter, compromises retinal function. Invest. Ophthalmol. Vis. Sci. 41, 585-591.

Belton, R.J., Jr., Chen, L., Mesquita, F.S., Nowak, R.A., 2008. Basigin-2 is a cell surface receptor for soluble basigin ligand. J. Biol. Chem. 283, 17805-17814.

Birke, M.T., Neumann, C., Birke, K., Kremers, J., Scholz, M., 2010. Changes of osteopontin in the aqueous humor of the DBA2/J glaucoma model correlated with optic nerve and RGC degenerations. Invest. Ophthalmol. Vis. Sci. 51, 5759-5767.

Bringmann, A., Iandiev, I., Pannicke, T., Wurm, A., Hollborn, M., Wiedemann, P., Osborne, N.N., Reichenbach, A., 2009. Cellular signaling and factors involved in Müller cell gliosis: Neuroprotective and detrimental effects. Prog. Retin. Eye Res. 28, 423–451.

Bringmann, A., Pannicke, T., Grosche, J., Francke, M., Wiedemann, P., Skatchkov, S.N., Osborne, N.N., Reichenbach, A., 2006. Müller cells in the healthy and diseased retina. Prog. Retin. Eye Res. 25, 397-424.

Colinge, J., Chiappe, D., Lagache, S., Moniatte, M., Bougueleret, L., 2005. Differential proteomics via probabilistic peptide identification scores. Anal. Chem. 77, 596-606.

Curtin, K.D., Wyman, R.J., Meinertzhagen, I.A., 2007. Basigin/EMMPRIN/CD147 mediates neuron-glia interactions in the optic lamina of Drosophila. Glia 55, 1542-1553.

de Melo Reis, R.A., Ventura, A.L., Schitine, C.S., de Mello, M.C., de Mello, F.G., 2008. Muller glia as an active compartment modulating nervous activity in the vertebrate retina: neurotransmitters and trophic factors. Neurochem. Res. 33, 1466-1474.

Del Rio, P., Irmler, M., Arango-Gonzalez, B., Favor, J., Bobe, C., Bartsch, U., Vecino, E., Beckers, J., Hauck, S.M., Ueffing, M., 2011. GDNF-induced osteopontin from Muller glial cells promotes photoreceptor survival in the Pde6brd1 mouse model of retinal degeneration. Glia 59, 821-832.

Derouiche, A., Rauen, T., 1995. Coincidence of L-glutamate/L-aspartate transporter (GLAST) and glutamine synthetase (GS) immunoreactions in retinal glia: evidence for coupling of GLAST and GS in transmitter clearance. J. Neurosci. Res. 42, 131-143.

Dreixler, J.C., Poston, J.N., Balyasnikova, I., Shaikh, A.R., Tupper, K.Y., Conway, S., Boddapati, V., Marcet, M.M., Lesniak, M.S., Roth, S., 2014. Delayed administration of bone marrow mesenchymal stem cell conditioned medium significantly improves outcome after retinal ischemia in rats. Invest. Ophthalmol. Vis. Sci. 55, 3785-3796.

Fadool, J.M., Linser, P.J., 1993. 5A11 antigen is a cell recognition molecule which is involved in neuronal-glial interactions in avian neural retina. Dev. Dyn. 196, 252-262.

Garcia, M., Forster, V., Hicks, D., Vecino, E., 2002. Effects of muller glia on cell survival and neuritogenesis in adult porcine retina in vitro. Invest. Ophthalmol. Vis. Sci. 43, 3735-3743.

Guidry, C., 1996. Isolation and characterization of porcine Muller cells. Myofibroblastic dedifferentiation in culture. Invest. Ophthalmol. Vis. Sci. 37, 740-752.

Harada, C., Harada, T., Quah, H.M., Maekawa, F., Yoshida, K., Ohno, S., Wada, K., Parada, L.F., Tanaka, K., 2003. Potential role of glial cell line-derived neurotrophic factor receptors in Muller glial cells during light-induced retinal degeneration. Neuroscience 122, 229-235.

Hauck, S.M., Dietter, J., Kramer, R.L., Hofmaier, F., Zipplies, J.K., Amann, B., Feuchtinger, A., Deeg, C.A., Ueffing, M., 2010. Deciphering membrane-associated molecular processes in target tissue of autoimmune uveitis by label-free quantitative mass spectrometry. Mol. Cell. Proteomics 9, 2292-2305.

Hauck, S.M., Gloeckner, C.J., Harley, M.E., Schoeffmann, S., Boldt, K., Ekstrom, P.A., Ueffing, M., 2008. Identification of paracrine neuroprotective candidate proteins by a functional assay-driven proteomics approach. Mol. Cell. Proteomics 7, 1349-1361.

Hauck, S.M., Kinkl, N., Deeg, C.A., Swiatek-de Lange, M., Schoffmann, S., Ueffing, M., 2006. GDNF family ligands trigger indirect neuroprotective signaling in retinal glial cells. Mol. Cell Biol. 26, 2746-2757.

Hauck, S.M., Suppmann, S., Ueffing, M., 2003. Proteomic profiling of primary retinal Muller glia cells reveals a shift in expression patterns upon adaptation to in vitro conditions. Glia 44, 251-263.

He, C., Zhao, C., Kumar, A., Lee, C., Chen, M., Huang, L., Wang, J., Ren, X., Jiang, Y., Chen, W., Wang, B., Gao, Z., Zhong, Z., Huang, Z., Zhang, F., Huang, B., Ding, H., Ju, R., Tang, Z., Liu, Y., Cao, Y., Li, X., Liu, X., 2014. Vasoprotective effect of PDGF-CC mediated by HMOX1 rescues retinal degeneration. Proc. Natl. Acad. Sci. U. S. A. 111, 14806-14811.

Heidinger, V., Hicks, D., Sahel, J., Dreyfus, H., 1999. Ability of retinal Muller glial cells to protect neurons against excitotoxicity in vitro depends upon maturation and neuron-glial interactions. Glia 25, 229-239.

Hollborn, M., Jahn, K., Limb, G.A., Kohen, L., Wiedemann, P., Bringmann, A., 2004. Characterization of the basic fibroblast growth factor-evoked proliferation of the human Muller cell line, MIO-M1. Graefes Arch. Clin. Exp. Ophthalmol. 242, 414-422.

Izumi, Y., Kirby, C.O., Benz, A.M., Olney, J.W., Zorumski, C.F., 1999. Muller cell swelling, glutamate uptake, and excitotoxic neurodegeneration in the isolated rat retina. Glia 25, 379-389.

Jablonowski, K., 2017. Proteomic Clustering Analysis of SH2 Domain Datasets. Methods Mol. Biol. 1555, 99-113.

Johnson, T.V., DeKorver, N.W., Levasseur, V.A., Osborne, A., Tassoni, A., Lorber, B., Heller, J.P., Villasmil, R., Bull, N.D., Martin, K.R., Tomarev, S.I., 2014. Identification of retinal ganglion cell neuroprotection conferred by platelet-derived

growth factor through analysis of the mesenchymal stem cell secretome. Brain 137, 503-519.

Joly, S., Lange, C., Thiersch, M., Samardzija, M., Grimm, C., 2008. Leukemia inhibitory factor extends the lifespan of injured photoreceptors in vivo. J. Neurosci. 28, 13765-13774.

Kawasaki, A., Otori, Y., Barnstable, C.J., 2000. Muller cell protection of rat retinal ganglion cells from glutamate and nitric oxide neurotoxicity. Invest. Ophthalmol. Vis. Sci. 41, 3444-3450.

Kinoshita, Y., Uo, T., Jayadev, S., Garden, G.A., Conrads, T.P., Veenstra, T.D., Morrison, R.S., 2006. Potential applications and limitations of proteomics in the study of neurological disease. Arch. Neurol. 63, 1692-1696.

Lin, C.H., Wang, C.H., Hsu, S.L., Liao, L.Y., Lin, T.A., Hsueh, C.M., 2016. Molecular Mechanisms Responsible for Neuron-Derived Conditioned Medium (NCM)-Mediated Protection of Ischemic Brain. PLoS One 11, e0146692.

Mbeunkui, F., Metge, B.J., Shevde, L.A., Pannell, L.K., 2007. Identification of differentially secreted biomarkers using LC-MS/MS in isogenic cell lines representing a progression of breast cancer. J. Proteome Res. 6, 2993-3002.

Merl, J., Ueffing, M., Hauck, S.M., von Toerne, C., 2012. Direct comparison of MS-based label-free and SILAC quantitative proteome profiling strategies in primary retinal Muller cells. Proteomics 12, 1902-1911.

Munro, M., Akkam, Y., Curtin, K.D., 2010. Mutational analysis of Drosophila basigin function in the visual system. Gene 449, 50-58.

Newman, E., Reichenbach, A., 1996. The Muller cell: a functional element of the retina. Trends Neurosci. 19, 307-312.

Newman, E.A., Frambach, D.A., Odette, L.L., 1984. Control of extracellular potassium levels by retinal glial cell K+ siphoning. Science 225, 1174-1175.

Ochrietor, J.D., Linser, P.J., 2004. 5A11/Basigin gene products are necessary for proper maturation and function of the retina. Dev. Neurosci. 26, 380-387.

Ong, S.E., Mann, M., 2005. Mass spectrometry-based proteomics turns quantitative. Nat. Chem. Biol. 1, 252-262.

Picard, E., Jonet, L., Sergeant, C., Vesvres, M.H., Behar-Cohen, F., Courtois, Y., Jeanny, J.C., 2010. Overexpressed or intraperitoneally injected human transferrin prevents photoreceptor degeneration in rd10 mice. Mol. Vis. 16, 2612-2625.

Poitry-Yamate, C.L., Poitry, S., Tsacopoulos, M., 1995. Lactate released by Muller glial cells is metabolized by photoreceptors from mammalian retina. J. Neurosci. 15, 5179-5191.

Reichenbach, A., Bringmann, A., 2013. New functions of Muller cells. Glia 61, 651-678.

Reichenbach, A., Stolzenburg, J.U., Eberhardt, W., Chao, T.I., Dettmer, D., Hertz, L., 1993. What do retinal muller (glial) cells do for their neuronal 'small siblings'? J. Chem. Neuroanat. 6, 201-213.

Reis, R.A., Cabral da Silva, M.C., Loureiro dos Santos, N.E., Bampton, E., Taylor, J.S., de Mello, F.G., Linden, R., 2002. Sympathetic neuronal survival induced by retinal trophic factors. J. Neurobiol. 50, 13-23.

Rhee, K.D., Yang, X.J., 2010. Function and Mechanism of CNTF/LIF Signaling in Retinogenesis. Adv. Exp. Med. Biol. 664, 647–654.

Ruzafa, N., Pereiro, X., Aspichueta, P., Araiz, J., Vecino, E., 2017. The retina of osteopontin deficient mice in aging. Mol. Neurobiol.

Ruzafa, N., Vecino, E., 2015. Effect of Muller cells on the survival and neuritogenesis in retinal ganglion cells. Archivos de la Sociedad Espanola de Oftalmologia 90, 522-526.

Shannan, B., Seifert, M., Leskov, K., Willis, J., Boothman, D., Tilgen, W., Reichrath, J., 2006. Challenge and promise: roles for clusterin in pathogenesis, progression and therapy of cancer. Cell Death Differ. 13, 12-19.

Skytt, D.M., Toft-Kehler, A.K., Braendstrup, C.T., Cejvanovic, S., Gurubaran, I.S., Bergersen, L.H., Kolko, M., 2016. Glia-Neuron Interactions in the Retina Can Be Studied in Cocultures of Muller Cells and Retinal Ganglion Cells. BioMed research international 2016, 1087647.

Sze, S.K., de Kleijn, D.P., Lai, R.C., Khia Way Tan, E., Zhao, H., Yeo, K.S., Low, T.Y., Lian, Q., Lee, C.N., Mitchell, W., El Oakley, R.M., Lim, S.K., 2007. Elucidating the secretion proteome of human embryonic stem cell-derived mesenchymal stem cells. Mol. Cell. Proteomics 6, 1680-1689.

Tang, Z., Arjunan, P., Lee, C., Li, Y., Kumar, A., Hou, X., Wang, B., Wardega, P., Zhang, F., Dong, L., Zhang, Y., Zhang, S.Z., Ding, H., Fariss, R.N., Becker, K.G., Lennartsson, J., Nagai, N., Cao, Y., Li, X., 2010. Survival effect of PDGF-CC rescues neurons from apoptosis in both brain and retina by regulating GSK3beta phosphorylation. J. Exp. Med. 207, 867-880.

Thambisetty, M., An, Y., Kinsey, A., Koka, D., Saleem, M., Guntert, A., Kraut, M., Ferrucci, L., Davatzikos, C., Lovestone, S., Resnick, S.M., 2012. Plasma clusterin concentration is associated with longitudinal brain atrophy in mild cognitive impairment. Neuroimage 59, 212-217.

Trougakos, I.P., Gonos, E.S., 2006. Regulation of clusterin/apolipoprotein J, a functional homologue to the small heat shock proteins, by oxidative stress in ageing and age-related diseases. Free Radic. Res. 40, 1324-1334.

Trougakos, I.P., Lourda, M., Antonelou, M.H., Kletsas, D., Gorgoulis, V.G., Papassideri, I.S., Zou, Y., Margaritis, L.H., Boothman, D.A., Gonos, E.S., 2009. Intracellular clusterin inhibits mitochondrial apoptosis by suppressing p53-activating stress signals and stabilizing the cytosolic Ku70-Bax protein complex. Clin. Cancer Res. 15, 48-59.

Unwin, R.D., Evans, C.A., Whetton, A.D., 2006. Relative quantification in proteomics: new approaches for biochemistry. Trends Biochem. Sci. 31, 473-484.

Vecino, E., Heller, J.P., Veiga-Crespo, P., Martin, K.R., Fawcett, J., 2015. Influence of different extracellular matrix components on the expression of integrins and regeneration of adult retinal ganglion cells. PLoS One In press.

Vecino, E., Rodriguez, F.D., Ruzafa, N., Pereiro, X., Sharma, S.C., 2016. Glia-neuron interactions in the mammalian retina. Prog. Retin. Eye Res. 51, 1-40.

Vecino, E., Ugarte, M., Nash, M.S., Osborne, N.N., 1999. NMDA induces BDNF expression in the albino rat retina in vivo. Neuroreport 10, 1103-1106.

von Toerne, C., Menzler, J., Ly, A., Senninger, N., Ueffing, M., Hauck, S.M., 2014. Identification of a novel neurotrophic factor from primary retinal Muller cells using stable isotope labeling by amino acids in cell culture (SILAC). Mol. Cell. Proteomics 13, 2371-2381.

Willbold, E., Berger, J., Reinicke, M., Wolburg, H., 1997. On the role of Muller glia cells in histogenesis: only retinal spheroids, but not tectal, telencephalic and cerebellar spheroids develop histotypical patterns. J. Hirnforsch. 38, 383-396.

Zack, D.J., 2000. Neurotrophic rescue of photoreceptors: are Müller cells the mediators of survival? Neuron 26, 285–286.

Zhou, X., Li, F., Kong, L., Chodosh, J., Cao, W., 2009. Anti-inflammatory effect of pigment epithelium-derived factor in DBA/2J mice. Mol. Vis. 15, 438-450.

ANEXO 4

The Effect of Plasma Rich in Growth Factors (PRGF) in Retinal Neurons and Glial Cells Cultures.

Noelia Ruzafa, Xandra Pereiro, Arantxa Acera, Elena Vecino.

[1]Department of Cell Biology and Histology, University of Basque Country UPV/EHU, Vizcaya, Spain.

Abtract

Plasma rich in growth factors or PRGF is a supernatant enriched in plasma and platelet-derived morphogens, proteins, and growth factors. PRGF may promote neuronal survival, stimulate tissue regeneration and inhibit inflammatory response. The retina has a limited capacity for repair after damage, and injury causes the death of retinal ganglion cells (RGCs) which might result in irreversible blindness. RGCs are in close contact with glial cells (astrocytes, Müller cells and resident microglia), which serve to maintain retinal homeostasis. In the present study, we aimed to determine whether PRGF provides neuroprotection to RGCs, proliferation of Müller cells and/or inhibition of microglia migration within the retina. Autologous and heterologous PRGF from pig blood at different concentrations as well as human PRGF was tested in pure RGC primary cell cultures, in co-cultures of RGC and Müller cells, as well as in organotipic explants form adult pig retinas. In addition, the effect of heat inactivation of the PRGF and the addition of dexametasone was also tested in organotipic explants of retina. Moreover the presence of cytokines in the PRGF was analyzed. The presence of PRGF decreases the survival of RGCs more than 90%, and between 80-90% in co-culture of RGCs and Müller cells. By contrast, PRGF induce proliferation in Müller cells. In organotypic cultures, the microglia migrates to the outer nuclear layer (ONL) as a sign of inflammation in presence of PRGF, probably due to the presence of inflammatory cytokines in the PRGF. Human PRGF elicites the microglial migration more than the pig PRGF, and the heat-inactivation of PRGF or the presence of dexamethasone can mitigate the migrating capacity. In conclusion, PRGF markedly decreases the survival

of RGCs in presence or absence of Müller cells, and PRGF induce the activation of microglia. However, PRGF promotes Müller cells proliferation. Although PRGF could be a candidate to stimulate tissue regeneration, further studies should be performed to study the negative effect of PRGF on neurons and on immune system.

Introduction

The autologous plasma rich in growth factors (PRGF) have approval to be clinically applied by the European Community and the U.S. Food and Drug Administration (Anitua et al., 2014b), and it constitutes a biological system that provides a complex pool of active mediators that may stimulate and accelerate tissue regeneration (Anitua et al., 2012b; Anitua et al., 2008). It consists in a supernatant enriched in plasma and platelet-derived morphogens, proteins, and growth factors. Recently, it has been reported an intranasal delivery system with PRGF which allowed neurodegeneration reversion and memory rescue in a transgenic mouse model of Alzheimer's disease (Anitua et al., 2014b; Anitua et al., 2013). Most interestingly, PRGF acts as neurotrophic factor promoting neuronal survival under amyloid beta (Aβ) exposure (Anitua et al., 2013; Anitua et al., 2015a). Additionally, PRGF can prevent dopaminergic degeneration via an NF-κB (nuclear factor-kB) dependent signaling process, these data suggest that PRGF provides a novel neuroprotective strategy for Parkinson's disease (Anitua et al., 2015a). The retina, as a part of the central nervous system, has a limited capacity for repair after a disease or lesion. The injury causes the death of retinal ganglion cells (RGCs), the cells responsible for the communication between the eye and the brain, which might result in irreversible blindness (Garcia et al., 2002; Newman and Reichenbach, 1996), as occur in the case of glaucoma (Glovinsky et al., 1991; Wygnanski et al., 1995), axonal degeneration (Newman and Reichenbach, 1996), ischemia (Joo et al., 1999; Selles-Navarro et al., 1996) or diabetes (Lieth et al., 2000; Zhang et al., 2000). However, it has been demonstrated that in appropriate environments, RGCs can recover their regenerative capacities (Berry et al., 2008; Ruzafa and Vecino, 2015). Thus, we wanted to study if the PRGF induces neuroprotection to the RGCs and increases the survival of these cells.

On the other hand, RGCs are in close contact with glial cells. Three main types of glial

cells are found in the mammalian retina that serve to maintain retinal homeostasis: astrocytes, Müller cells and resident microglia. These cells are involved in metabolism, in the phagocytosis of neuronal debris, in the release of certain transmitters and trophic factors, and in K^+ uptake (Vecino et al., 2016). Specifically, Müller cells extended throughout the thickness of the retinal, providing structural stability and maintaining close contact with the majority of retina neurons (Bringmann and Reichenbach, 2001). They also provide trophic factors to neurons as well as the maintenance of homeostasis, thereby they have the ability to promote cell survival and repair (Bringmann et al., 2006; Reichenbach and Bringmann, 2013). Among other activities, microglia, as the main form of active immune defence in the central nervous system, can be stimulated to fulfil a macrophage function, as well as to interact with other glial cells and neurons by secreting growth factors (Vecino et al., 2016). PRGF can also interact with the glial cells because PRGF has growth factors that are known to accelerate cell proliferation and differentiation, promote cell survival and stimulate angiogenesis (Anitua et al., 2013; Anitua et al., 2009; Jin et al., 2002; O'Kusky et al., 2000). Some of the proteins present in the PRGF are platelet-derived growth factor (PDGF), transforming growth factor beta (TGF-β), vascular endothelial growth factor (VEGF), fibroblast growth factor (FGF), epidermal growth factor (EGF), insulin-like growth factor I (IGF-I) and nerve growth factor (NGF) among others (Anitua et al., 2010; Orive et al., 2009). In addition to these growth factors, PRGF content enhanced levels of hepatocyte growth factor (HGF) and transforming growth factor β1 (TGFβ1), which participated in anti-inflammatory effect by modulating NF-kB activation (Bendinelli et al., 2010).

Based on the neuroprotective properties of the PRGF and on the hypothesis that PRGF may modulate neuronal survival, in the present study, we aimed to determine whether PRGF provides neuroprotection to RGCs. In addition, knowing the implication of PRGF in proliferation and inflammation, we wanted to analyze the proliferation of Müller cells and the inhibition of inflammatory response in microglia. The analyzed parameters were studied after damage in the retina result of *in vitro* and organotopic retina cultures.

Moreover, knowing that the use of PRGF in clinic is autologous and it is obtained from patient's own blood (Anitua et al., 2014a), and it was use human PRGF in studies with mice (Anitua et al., 2014b; Anitua et al., 2013; Anitua et al., 2015a), we checked the

effect of PRGF obtained from human and pig blood on the adult pig cultures. In addition, to suppress the inflammatory response, the PRGF was inactivated by heat, and dexamethasone was added as an anti-inflammatory drug, in order to study the inflammatory response of retinal microglia in the different conditions. Finally, the inflammatory cytokines present in the PRGF were quantified in order to characterize it.

Materia and Methods

Animals

Adult porcine eyes and blood were obtained from a local slaughterhouse and transported to the laboratory in cold CO_2-independent Dulbecco's modified Eagle's medium (DMEM/−CO_2, Life Technologies, Carlsbad, CA, USA) plus 0.1% gentamicin. Eyes were dissected within 1 to 2 hours after enucleation. All animal experimentation adhered to the ARVO Statement for the Use of Animals in Ophthalmic and Vision Research.

Human and Pig PRGF

Informed consent from all subjects was obtained prior to their participation. Human blood samples were obtained through antecubital vein puncture. Plasma rich in growth factors was obtained as described previously (Anitua et al., 2013) with some minor modifications. Briefly, human (n= 3) and pig (n= 5) blood was collected into tubes with 3.8% (wt/vol) sodium citrate. Samples were centrifuged at 460g for 8 minutes at room temperature. The plasma fraction containing platelets but not buffy coat and erythrocytes was separated. Plasma fractions were incubated with calcium chloride (BTI Biotechnology Institute) for 1 hour at 34°C in glass tubes. The released supernatants were collected after centrifugation at 460g for 15 minutes. A small amount of PRGF was incubated at 56 ºC for 60 minutes to plasma inactivation. Finally, platelet enriched plasma fractions were filtered with a filter pore size of 0.2 μm (Fisher Scientific, Hampton, NH, USA), aliquoted and stored at −80°C until use.

Cell culture

Retinal cell cultures were prepared according to a method previously reported (Garcia et al., 2002) with the following minor modifications. Three types of cultures were used: RGCs using B27-supplemented Neurobasal-A medium (Life Technologies, Carlsbad, CA, USA); Müller cells using DMEM (Life Technologies, Carlsbad, CA, USA) with 10% fetal bovine serum (FBS, Life Technologies, Carlsbad, CA, USA); and co-culture of RGCs and Müller cells, using B27-supplemented Neurobasal-A medium with 10% FBS. 1% L-glutamine (2mM) and 0.1% gentamicin (50mg/ml) was added to all media.

The retinas were dissected and pieces using a 8 mm diameter dissecting trephine (Biomedical Research Instruments, MD, USA) were used, in such a way as to avoid taking the most peripheral retina and visible blood vessels. The tissue enzymatic dissemination was carried out at 37ºC using papain (Worthington Papain Dissociation kit, Worthington Biochemical Lakewood, NJ, USA) with 10% DNAse I (Worthington Papain Dissociation kit, Worthington Biochemical Lakewood, NJ, USA) during 90 minutes for RGC and during 30 minutes for Müller cells and co-culture. Papain enzyme activity was stopped by the addition of media and the tissue was disaggregate by gentle trituration using tips of decreasing diameter. Dissociated retinal cells were collected by centrifugation at 300g 5 minutes and resuspended in media. The RGC culture was prepared following the protocol of the Worthington Papain Dissociation kit (Worthington Biochemical Lakewood, NJ, USA). All the resuspended cells were plated onto one 24 wells plate with 13 mm glass coverslips previously poly-L-lisine (Sigma, P4832, 100 µg/ml) and laminin (Sigma, L2020, 10 µg/ml) coated. Cells were maintained in a humidified incubator at 37°C with an atmosphere of 5% CO_2. In Müller cell culture and co-culture, allow cells to sit for 24 hours and remove all cells are not attached to the coverslip changing the entire medium. To maintain all the cells, replace half of the medium every 3 days. The cells were fixed with methanol -20ºC for 10 minutes after 6 days, before the Müller cells were confluents. At least 3 replicas of each culture type work made, and this procedure was tripled.

The PRGF is added from the beginning at the end of the cell culture maintained a proportion of 5% and 10%. When the PRGF is added to the Müller cells culture and to the co-culture, the FBS is removed and replaced by PRGF. The B27 it cannot be replaced for the survival of RGCs.

Organotypic Retinal Cultures

Under aseptic conditions, each pig eyeball was immersed in 70% ethanol and then washed in clean CO_2-independent DMEM medium. Neuroretinal explants were obtained as previously described (Niyadurupola et al., 2011). The eyes were dissected to exclude the lens and the vitreous. The entire retina was detached by paintbrushing and cutting the optic nerve. Five retinal explants close to the optic nerve were taken from each eye using a 8 mm diameter dissecting trephine. The explants were transferred to cell culture inserts (0.45 μm pore, 12 mm diameter; Merck Millipore, Darmstadt, Germany) with the photoreceptor layer facing the membrane. Explants were cultured in Neurobasal A with 1% L-glutamine and 0.1% gentamicin. Explants were maintained at 37 °C in a humid atmosphere of 5% CO_2 for 1 and 3 days. The culture medium level was maintained in contact with the support membrane beneath the explant and changed with freshly prepared warmed medium on the every second day.

Explants were cultured in different experimental conditions described below and at least 3 replicas of different animals was performance for each condition. The explants were cultured in presence or absence of 5 and 10% PRGF. The PRGF samples were from the same pig (autologus), from other pig or from a human donor. The pig and human PRGF were added in the active and inactive form. And dexamethasone was added at 1μM (Sigma Aldrich, St. Louis, MO, USA) to 10% human PRGF.

After fixation overnight in 4% paraformaldehide, the explants were cryoprotected overnight in 30% sucrose in 0.1 M PB (phosphate buffer, pH 7.4) at 4°C, and embedded in OCT medium. Cryosections were cut at a thickness of 14 μm and stored at −20°C.

Immunochemistry

In the cultures, the cells were fixed with methanol and washed with PBS (phosphate-buffered saline, pH 7.4) and were immunostained as previously described (Ruzafa and Vecino, 2015). After blocking nonspecific antigens with blocking buffer (3% BSA and 0.1% Triton X-100 in PBS) the following antibodies were added: anti-bIII-tubuline rabbit polyclonal antibody (Promega, Madison, WI, USA) as specific RGC marker at a dilution of 1:2000 and anti-vimentin mouse monoclonal antibody (Dako, Glostrup, Denmark) as specific marker for Müller cells at a dilution of 1:10000. After washing again, the following secondary antibodies were added: anti-rabbit Alexa Fluor 555 and

anti-mouse Alexa Fluor 488 (Life Technologies, Carlsbad, CA, USA), both at a dilution of 1:1000 and DAPI nuclear marker (Life Technologies, Carlsbad, CA, USA) at a dilution of 1:10000.

The cryostat sections of the explants to detect microglia were immunostained as previously described (Vecino et al., 2002), the sections were washed twice with PBS-TX-100 for 10 minutes and were incubated overnight with the primary antibody using anti-Iba-1 rabbit antibody (WAKO, Osaka, Japan) at dilution of 1:2000. After two washes with PBS we added goat anti-rabbit antibody Alexa Fluor 555 (Invitrogen, Eugene, Oregon, USA) at a dilution of 1:1000 in PBS-BSA (1%) for 1 hour and DAPI nuclear marker were used at a dilution of 1:10000. The sections were washed twice with PBS for 10 minutes, and mounted with a coverslip with PBS-Glycerol (1:1).

Cells Quantification

In the cell cultures, the surfaces of the whole 13 mm diameter coverslips were analyzed. At least 3 replicas of each culture condition were made and analyzed, and this procedure was tripled. Images were taken with an epifluorescence microscope (Zeiss, Jena, Germany) coupled to a digital camera (Zeiss Axiocam MRM, Zeiss, Jena, Germany) and the Zeiss Zen software (Zeiss, Jena, Germany) were used. A mosaic of the entire coverslip was performance using 359, 488 and 555nm filters with a 10X objective. Once the mosaic was defined, the coverslip surface area was calculated (132.73 mm^2). A software program measures the total nuclei of Müller cells. The program employed for Muller cells counting and for mosaic definition was Zeiss Zen program (Zeiss, Jena, Germany). The RGC density was also analyzed. The cell density was calculated as the mean of cells/mm^2, and the data were normalized to the control to simplify the representation.

For the microglia analysis at least 3 slides, with a minimum of 6 cryostat sections of explants each, were analyzed for each condition, and this procedure was tripled. The total number of microglia cells was counted and the number of microglia per linear millimetre of retina was calculated. In addition, the number of microglia in the outer nuclear layer was counted and the percentage of microglia in this layer of the retina was calculated for each condition.

Multiplex cytokine assays

To detect and quantify the cytokines present in the PRGF, it was used a multiplex enzyme-linked immunosorbent assay (ELISA) (Human Cytokine Screen, 110996HU, Q-Plex™, Quansys Bioscience, Logan, UT, USA), which measures IL-1α, IL-1β, IL-2, IL-4, IL-5, IL-6, IL-8, IL-10, IL-12p70, IL-13, IL-15, IL-17, IL-23, IFNγ, TNFα, and TNFβ. The assay was performed according to the manufacturer´s instruction. The standards were measured in duplicate and cytokine concentrations were calculated using a standard curve. All the samples were performed in four replicas and arithmetic averages were calculated.

Statistical analyses

Statistical analyses were carried out using IBM SPSS Statistics software v. 21.0. The mean and the standard error for each condition were calculated. The data of different conditions were compared using a Student T-test, and it was supplemented with Mann-Whitney U test to verify the differences between the groups. To determine if there are statistically significant differences between three or more individuals in the same condition, a nonparametric test were used, the Kruskal-Wallis H test. The minimum value for significant differences for all tests was defined as $p< 0.05$.

Results

In order to determine neuroprotective effects of PRGF, we calculated the density of RGCs in absence and in presence of PRGF (Fig 1). In control, the density of RGCs is 0.55 ± 0.11 cells/mm^2. The RGC survival analysis reveals a significant decrement in the RGCs density in presence of 5 and 10% of pig and human PRGF. When the PRGF is added to the culture, the survival of RGCs decrease more than 90% in all cases ($p < 0.001$, Fig 1C). Surprisingly, we notice that the Müller cells proliferate in the pig RGCs culture when pig PRGF is added (Fig 1D), but this growth does not happen if the PRGF is from human blood. In addition, the increase in Müller cells density is higher when the proportion of PRGF is higher. The number of Müller cells in control is 11.52 ± 3.79 cells/mm^2 and it increase 8 times at a concentration of 5% pig PRGF ($p< 0.01$) and 11 times at a 10% pig PRGF ($p< 0.001$).

The density of Müller cells in presence and in absence of pig and human PRGF was also assessed (Fig 2). For this purpose, we compared the density of Müller cell in positive control (569.69 ± 59.85 cells/mm^2), where 10% FBS is added to DMEM medium, versus DMEM media supplemented with 5% and 10% pig and human PRGF.

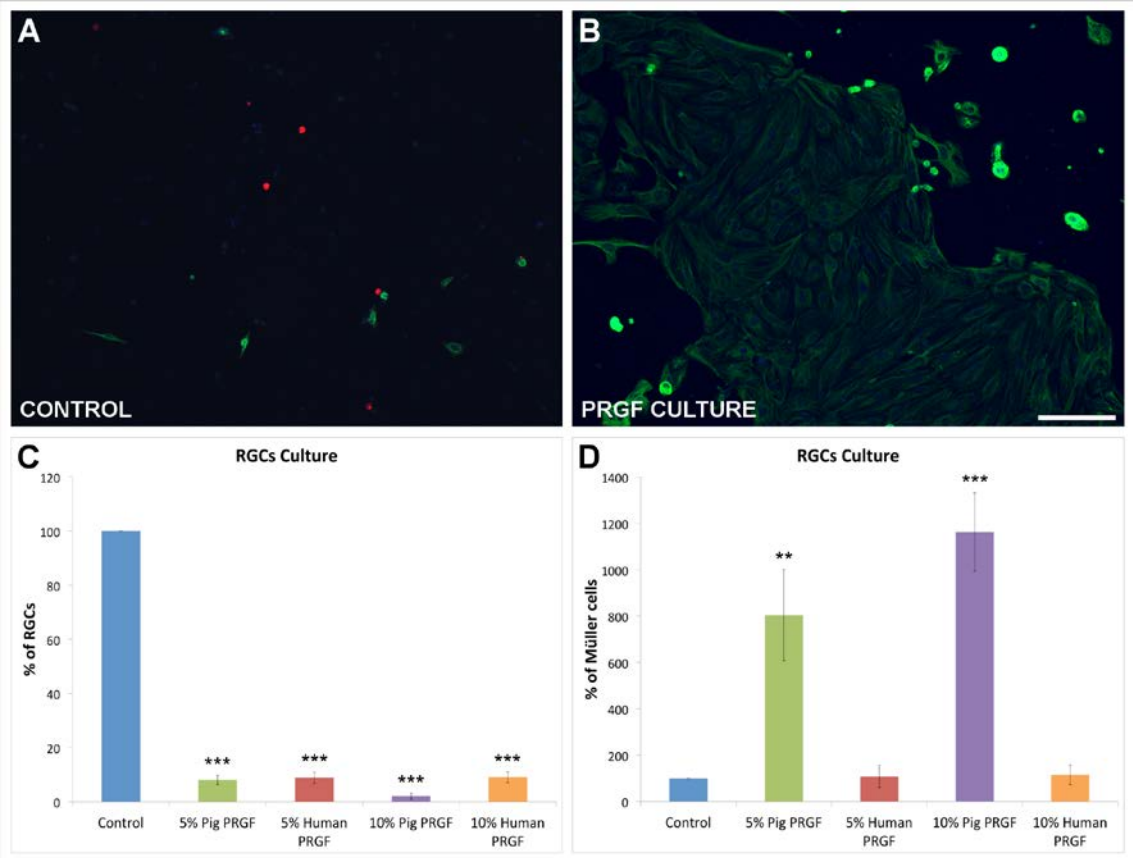

Fig 1. RGCs Culture. Images taken of adult pig RGCs culture in absence (A) or presence of PRGF (B). The RGCs were labeled with antibodies against bIII-Tubuline (red), and antibodies against vimentin (green) were used to label Müller cells. The nuclei were labelled with DAPI in blue. The percentage, with regard to the control, of RGCs (C) and Müller cells (D) were represented on histograms for each condition of PRGF: 5% pig PRGF, 5% human PRGF, 10% pig PRGF and 10% human PRGF. Scale bar = 100µm. ** $p < 0,01$; *** $p < 0,001$.

The DMEM medium without supplement (FBS or PRGF), the negative control, was suppressed due to the absence of Müller cells proliferation. We can notice that in presence of PRGF the Müller cells are less dense compared with control, although both surface are confluence (Fig 2A, B). When the 10% FBS is replaced by 5% pig PRGF, and 5% and 10% human PRGF the Müller cell density decrease 35.87% ($p< 0.05$), 70.77% ($p< 0.001$) and 60.56% ($p< 0.01$) respectively. However, in presence of 10% pig PRGF there are not significantly difference in the density of Müller cells (Fig 2C).

The density of Müller cells is high when the proportion of PRGF is higher and when the PRGF come from pig blood. Although all conditions of PRGF induce Müller cell proliferation because in absence of PRGF would not grow Müller cells.

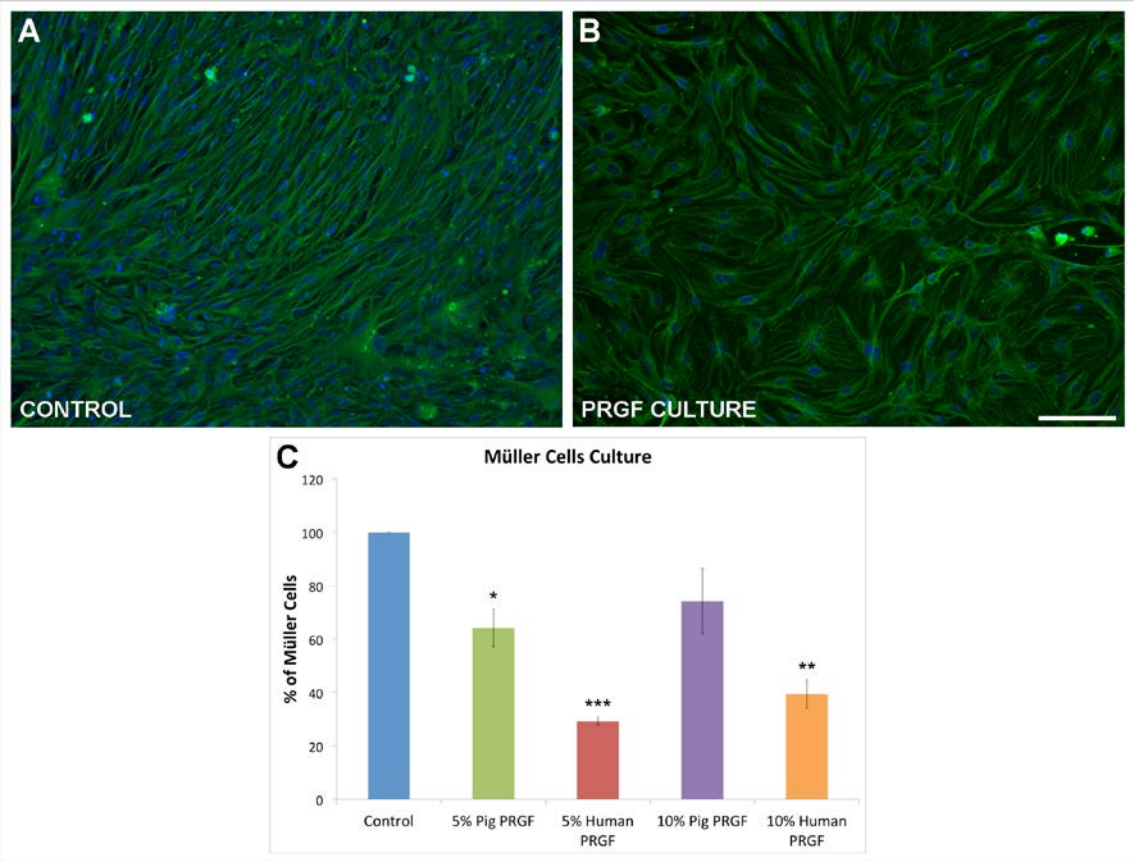

Fig 2. Müller cells Culture. Images taken of adult pig Müller cells culture in absence (A) or presence of PRGF (B). The Müller cells were labeled with antibodies against vimentin (green) and the nuclei were labelled with DAPI (blue). The percentage of Müller cells (C), with regard to the control, were represented on histograms for each condition of PRGF: 5% pig PRGF, 5% human PRGF, 10% pig PRGF and 10% human PRGF. Scale bar = 100µm. * $p < 0,05$; ** $p < 0,01$; *** $p < 0,001$.

Knowing the neuroprotective properties of Müller cells and that the PRGF increase their proliferation, we checked the effect of PRGF on the RGCs in presence of Müller cells in co-cultures (Fig 3). Interestingly, the results of RGCs and Müller cells density in co-culture are similar to the both cells type cultured separately. But in the presence of Müller cells, the RGCs have a density of 16.5% in 5% pig PRGF, 12.31% in 5% human PRGF, 10.39% in 10% pig PRGF and 17.59% in 10% human PRGF taking as reference the control condition (12.97 ± 1.33 RGCs/mm^2) ($p< 0.001$, Fig 3 C). And in absence of Müller cells (Fig 1 C), the RGCs density is 8.01%, 8.86%, 2.04% and 9.03% respectively. Even though the survival of RGCs is significantly less in presence of

PRGF respect the control, in co-culture with Müller cells, the survival of RGCs is slightly higher. By contrast, the Müller cells in co-culture have a density of 33.76% in 5% pig PRGF ($p< 0.01$), 21.22% in 5% human PRGF ($p< 0.001$), 61.23% in 10% pig PRGF ($p> 0.05$) and 9.05% in 10% human PRGF ($p< 0.001$) taking as reference the control condition (209.29 ± 28.43 Müller cells/mm^2) (Fig 3D). And in absence of RGCs (Fig 2 C), the Müller cells density is 64.12%, 29.22%, 74.21% and 39.43% respectively, that is slightly higher than in co-culture. As well as in Müller cells culture, in co-culture, in presence of 10% pig PRGF there are not significantly difference in the density of Müller cells comparing with control.

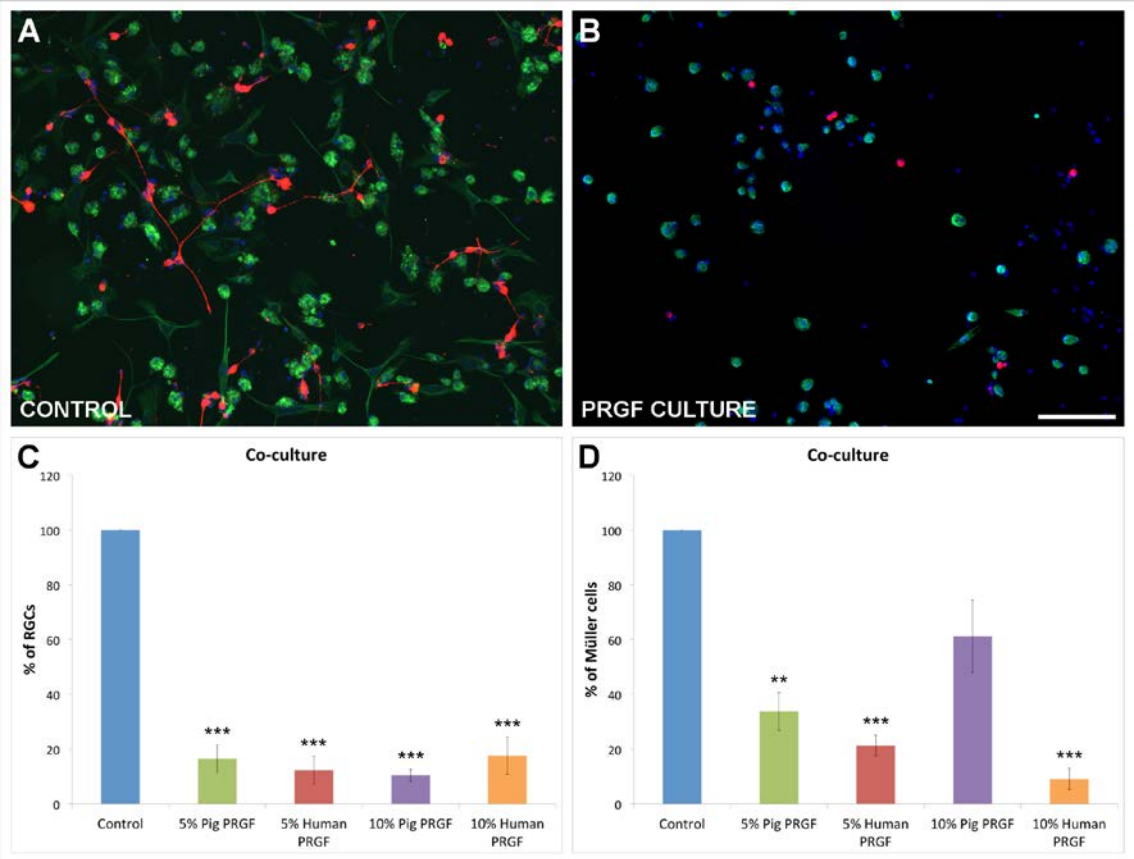

Fig 3. RGCs and Müller cells Co-culture. Images taken of adult pig co-culture of RGCs and Müller cells in absence (A) or presence of PRGF (B). The RGCs were labeled with antibodies against bIII-Tubuline (red), the Müller cells were labeled with antibodies against vimentin (green) and the nuclei were labelled with DAPI (blue). The percentage, with regard to the control, of RGCs (C) and Müller cells (D) were represented on histograms for each condition of PRGF: 5% pig PRGF, 5% human PRGF, 10% pig PRGF and 10% human PRGF. Scale bar = 100µm. ** $p <0,01$; *** $p < 0,001$.

The microglia behavior was assessed in the pig organotypic retinal cultures, and we do not found changes in microglia morphology neither in the number of microglial cells

per linear millimeter of retina (11.24 ± 0.24 cells/mm) when the retinal explants are compared in presence and absence of PRGF. The microglia in a control retina is located in the inner part of the retina (Fig 4 A), if the retina is cultured as an explant, the microglia can migrate to the outer plexiform layer (Fig 4 B), but only when the retina is cultured with PRGF, some microglial cells migrate to the outer nuclear layer (ONL) (Fig 4 C). Knowing that the migration of microglia is a sign of microglia activation, the percentage of microglia that migrate to the ONL is calculated for each condition (Fig 4 D, E). In control explants, we do not find any microglial cells in the ONL. The proportion of microglia that migrates to the ONL increase at day 3 compared to day 1 of culture. When the PRGF is autologous, the percentage of migration of microglia is lower than the percentage when the explant is cultured with PRGF from other pig. And this percentage is higher when the PRGF is from another specie, as a human PRGF.

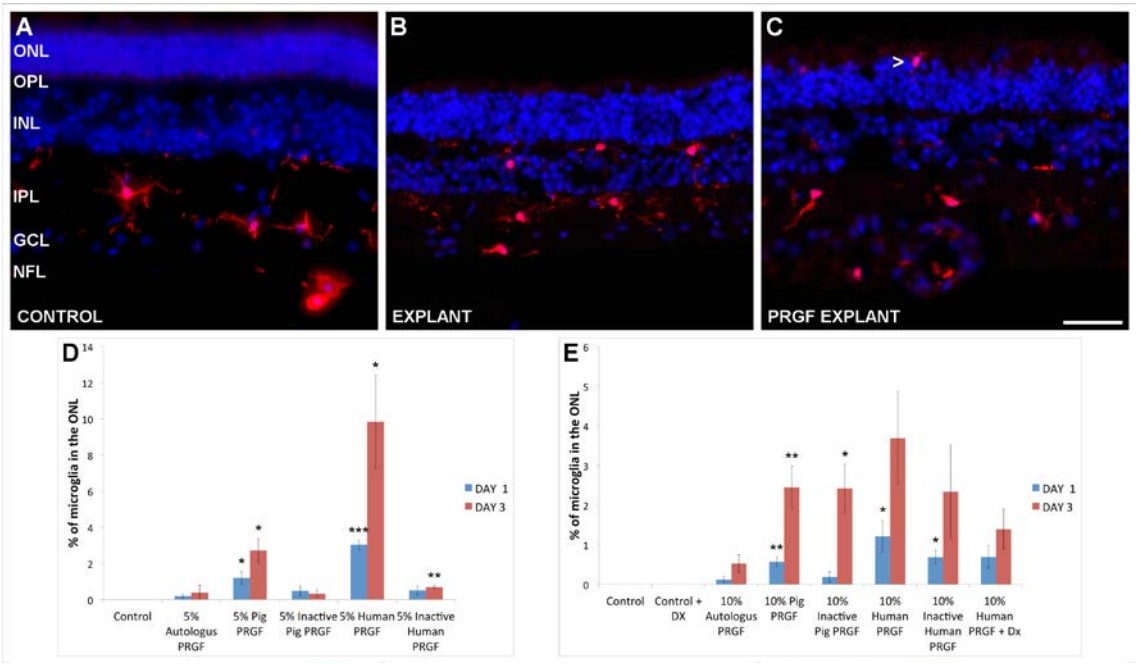

Fig 4. Microglia on Organotypic Retinal Culture. Images taken from adult pig retinas from a control eye (A), from an explant or organotypic culture in absence (B) or presence of PRGF (C). The microglial cells were labeled with antibodies against Iba1 (red) and the nuclei were labelled with DAPI (blue). The percentages of microglia that migrate to the outer nuclear layer (ONL) were represented on histograms for each condition of 5% of PRGF (D) and 10% of PRGF (E): autologous PRGF, pig PRGF, inactive pig PRGF, human PRGF, inactive human PRGF, and 10% human PRGF plus dexamethasone. ONL, outer nuclear layer; OPL, outer plexiform layer; INL, inner nuclear layer; IPL, inner nuclear layer; GCL, ganglion cell layer. Scale bar = 100µm. * $p < 0,05$; ** $p < 0,01$; *** $p < 0,001$.

The percentage of microglia in the ONL when 5% of PRGF (Fig 4 D) is added to the culture is 0,19 ± 0,09% for autologous PRGF, 1.21 ± 0.35% for pig PRGF and 3.03 ± 0.25% for human PRGF at day 1. At day 3, the percentages increase at 0,39 ± 0,39% for autologous PRGF, 2.71 ± 0.66% for pig PRGF and 9.83 ± 2.56% for human PRGF. The increments for pig ($p< 0.05$) and human ($p<0.001$ at day 1 and $p<0.05$ at day 3) PRGF are significantly different to the control at day 1 as well as a day 3. By contrast, there are no significant differences between the explants with and without autologous PRGF. The effect of PRGF on the activation of the microglia can be partially suppressed if the PRGF is inactivated by heat, and the percentages decrease at 0.47 ± 0.27% for inactive pig PRGF and 0.51 ± 0.25% for inactive human PRGF at day 1, and 0.33 ± 0.2% for inactive pig PRGF and 0.69 ± 0.08% for inactive human PRGF at day 3. The migration of microglia in the explants with 5% inactive PRGF has not significant differences with the control explants, except 5% inactive human PRGF at day 3 ($p< 0.01$), although the inactivation of 5% human PRGF reduced significantly de microglia migration in respect of the 5% human PRGF at day 3 ($p < 0.05$, Table 1).

5% PRGF	Autologous	Pig	Inactive Pig	Human	Inactive Human
Day 1	0.19 ± 0.09%	1.21 ± 0.35%	0.47 ± 0.27%	3.03 ± 0.25%	0.51 ± 0.25%
Day 3	0.39 ± 0.39%	2.71 ± 0.66%	0.33 ± 0.2%	9.83 ± 2.56%	0.69 ± 0.08%

Table 1. Percentage of microglia migration to the outer nuclear layer. Mean of the percentage ± standard error of the mean of the percentage of microglial cells that migrate to the ONL in the retinal explants cultured with different types of PRGF at 5%.

The percentage of microglia in the ONL on the retinal explant when it is added 10% of PRGF (Fig 4 E) is 0.12 ± 0.07% for autologous PRGF, 0.56 ± 0.11% for pig PRGF and 1.21 ± 0.4% for human PRGF at day 1. And the percentages increase at 0,52 ± 0,21% for autologous PRGF, 2.45 ± 0.53% for pig PRGF and 3.68 ± 1.16% for human PRGF at day 3. There are no significant differences between the control explants and the explants plus autologous PRGF. The increments for pig ($p< 0.01$) and human ($p< 0.05$) PRGF are significantly different to the control, except for 10% human PRGF at day 3. We tried partially suppress the migration of microglia adding an anti-inflammatory drug as dexamethasone, or inducing the inactivation of PRGF by heat, although this suppresion is not as marked as in the 5% PRGF. The percentages are 0.18 ± 0.12% for inactive pig PRGF and 0.68 ± 0.16% for inactive human PRGF at day 1, and 2.41 ± 0.61% for inactive pig PRGF and 2.33 ± 1.17% for inactive human PRGF at day 3. And the percentages are 0.69 ± 0.28% for 10% human PRGF plus dexamethasone at day 1

and 1.39 ± 0.5% at day 3. Although there are decreases in the percentage of microglia migration, the decrement is not significantly different compared with the 10% PRGF active or without dexamethasone. Only the 10% inactive pig PRGF decreases the microglia migration significantly and the percentage is not different to the control explants. The 10% inactive pig PRGF at day 3 ($p< 0.05$) and the 10% inactive human at day 1 ($p<0.05$) PRGF increase the microglia migration and this increase is significantly different to control situation (Table 2).

10% PRGF	Autologous	Pig	Inactive Pig	Human	Inactive Human	Human + DX
Day 1	0.12 ± 0.07%	0.56 ± 0.11%	0.18 ± 0.12%	1.21 ± 0.4%	0.68 ± 0.16%	0.69 ± 0.28%
Day 3	0.52 ± 0.21%	2.45 ± 0.53%	2.41 ± 0.61%	3.68 ± 1.16%	2.33 ± 1.17%	1.39 ± 0.5%

Table 2. Percentage of microglia migration to the outer nuclear layer. Mean of the percentage ± standard error of the mean of the percentage of microglial cells that migrate to the ONL in the retinal explants cultured with different types of PRGF at 10%.

After demonstrate that PRGF can activate the microglial cells and promote microglia migration, we proposed to analyze the presence of inflammatory cytokines in the PRGF. We have confirmed the presence of IL-1α, IL-1ß, IL-2, IL-4, IL-6, IL-8, IL-10, IL-12, IL13, IL-15, IL-17, IL-23, TNFα and TNFß in the human and porcine PRGF. These cytokines have been also quantified and the quantification is represented in Table 3.

Cytokine	**Human PRGF**	**Pig PRGF**
IL-1α	6,34 ± 2,18	8,15 ± 1,67
IL-1ß	17,03 ± 4,35	14,65 ± 4,93
IL-2	4,54 ± 0,54	4,58 ± 1,15
IL-4	0,39 ± 0,32	0,29 ± 0,28
IL-6	4,24 ± 1,08	3,61 ± 0,49
IL-8	29,59 ± 5,73	1,32 ± 0,42
IL-10	7,21 ± 1,52	4,65 ± 1,47
IL-12	5,00 ± 3,87	4,96 ± 1,11
IL-13	0,75 ± 0,75	0,37 ± 0,21
IL-15	7,09 ± 2,79	2,29 ±0,49
IL-17	1,68 ± 0,99	4,59 ± 0,21
IL-23	283,14 ± 214,27	185,47 ± 43,63
TNFα	14,42 ± 8,00	4,65 ± 4,25
TNFß	18,15 ± 14,21	18,40 ± 4,64

Table 3. Concentration of cytokines in PRGF preparations from human and porcine pig samples (pg/ml).

The human cytokines concentrations were compared with the pig cytokines concentrations, and only the IL-8 is significantly higher in the human PRGF in relation

to the pig PRGF ($p< 0.001$). The quantification of the cytokines in the inactive PRGF was also assessed, but significant differences were not found in cytokine concentration when the active PRGF is compared with the PRGF inactivated by heat, either in pig or human PRGF.

In addition to these comparisons, we appreciated some variability in the quantification of cytokines, thus, we evaluated the different cytokines concentrations between individuals. Significant differences between individuals in the human PRGF were found in the cytokines: IL-8, IL-12, IL-13, IL-15, IL-17, IL-23 and TNFα ($p< 0.05$). In the pig PRGF were also found significant differences between different individuals in the cytokines: IL-1ß, IL-10, IL-15, IL-17 and IL-23 ($p< 0.05$). The remainder of cytokines are homogeneous between individuals and significant differences between them were not found.

Discusion

The composition of PRGF, as a biological system that provides a pool of growth factors, suggests that may stimulate and accelerate tissue regeneration, hence it is a potential therapeutic agent to treat neurodegenerative diseases (Anitua et al., 2014b; Anitua et al., 2013; Anitua et al., 2015a). In this study, the role of PRGF was assessed in neurons, reducing the number of RGCs, and in glial cells, promoting the proliferation of Müller cells and the migration of the microglia.

Studies suggest that PRGF induce neuroprotection mediated by the activation of antiapoptotic PI3K/Akt signaling pathway and/or the reduction of caspase-3 levels (Anitua et al., 2014b). Our findings reveal that the PRGF drastically reduce the survival of RGCs, although the RGCs were cultured with Müller cells in co-culture. The concentrations of PRGF used were 10%, just as other studies of neurodegenerative diseases, as Alzheimer´s (Anitua et al., 2014b; Anitua et al., 2013) and Parkinson´s diseases (Anitua et al., 2015a). In the previously mentioned studies, cell proliferation and survival was augmented by PRGF treatment in primary neuronal cultures and the number of degenerating neurons was reduced in a mouse model of Alzheimer´s Disease. In addition in this model, PRGF decrease astrocyte reactivity, prevented protein

synaptic loss and stimulate global improvements in anxiety, learning, and memory behaviors (Anitua et al., 2014b; Anitua et al., 2013). By contrast, other study reveals that thrombin-activated platelet-rich plasma releases glutamate, and when this activated plasma is applied to neuronal cultures is neurotoxic (Bell et al., 2014). Though the plasma is differently activated, this result is similar to our finding, where even 5% of PRGF used to try to minimize the impact that the PRGF exerted on the RGCs, the results in the survival of RGCs was also reduced. Moreover, this may be due to some of the morphogens or growth factors PRGF could have adverse effects to the neurons, as TGF-β1, present in PRGF, that in platelet-rich plasma exerts negative effects on axon growth in rat brain-spinal cord co-culture (Takeuchi et al., 2012).

On the other hand, our results demonstrate that the PRGF induce the proliferation of Müller cells. The presence of 10% of pig PRGF is equivalent to the positive control, and substitute the 10% of serum when the Müller cells are cultured alone or in co-culture with RGCs. This fact is due to the growth factors that exist in the PRGF, as IGF-1, PDGF or FGF that are powerful stimulators of cell replication and proliferation (Anitua et al., 2009; Vahabi et al., 2015). The proliferative feature of PRGF is not only in the pig PRGF, to a lesser extent, the human PRGF can partially activate the proliferation of pig Müller cells, shown that this effect of PRGF occurs also interspecifically. It is important to mention the fact that in RGCs primary cultures, when pig PRGF is added, some of the few Müller cells that are in the culture drastically proliferate. This behavior is similar in different types of fibroblasts, because different plasma preparations, including PRGF, induce proliferative response, compared to non-stimulated cells (Anitua et al., 2011; Anitua et al., 2009; Vahabi et al., 2015) as are the Müller cells in the control RGCs medium that is absence of serum. Moreover, the biological effects of plasma, platelet-derived growth factors and/or PRGF on the proliferation have been demonstrated also in keratocytes and endothelial cells (Anitua et al., 2011; Kilian et al., 2004). In the retina, platelet-rich plasma injections induce intravitreal and preretinal proliferation composed of fibroblast-like cells, and it can be use as a model of proliferative vitreoretinopathy (Pinon et al., 1992). And it was be also demonstrated in Müller cells, because different platelet preparations were able to support proliferation significantly better than the control culture with serum-free medium of immortalized human Müller cells (MIO-M1 Müller cell line), in addition to stimulating their migration capacity (Burmeister et al., 2009). In addition to the biological effects of

PRGF on the proliferation of various cell types, the effects of PRGF on tissue regeneration have been demonstrated in dentistry, oral implantology, orthopedics, sports medicine, and treatment of skin disorders (Anitua et al., 2010).

The PRGF induce the same results on RGCs and Müller cells when they are in co-culture than when they are separately cultured. Due to PRGF promote Müller cells proliferation and knowing that Müller cells provide structural support, maintain retinal homeostasis, promote the survival of neurons and secrete neurotrophins and growth factors that offered protection to neurons (Garcia et al., 2003; Vecino et al., 2016), we expected that the survival of RGCs do not decline in co-culture, but dramatically decrease. If the percentages are compared, in co-culture, slightly increase the survival of RGCs and decrease the proliferation of Müller cells, may be due to the Müller cells are doing an extra effort to maintain the RGCs alive.

Besides that, it is suggested that PRGF could posses an inherent anti-inflammatory function mediated by via NF-kB (Anitua et al., 2014b; Anitua et al., 2015a). In addition, PRGF administration could decrease the inflammatory state of a cell culture inflammatory model induced by IL-1β and TNFα by decreasing significantly ICAM-1 and COX-2 levels in comparison with autologous serum (Anitua et al., 2016). In the inflammatory response, one of critical steps is the recruitment and migration of immune and inflammatory cells to inflammatory sites, and in the central nervous system, the microglia is the resident innate immune cells (Lull and Block, 2010; Omri et al., 2011). In the healthy retina, microglial cells are located in the inner part of retina (Ling and Wong, 1993; Omri et al., 2011; Streit et al., 1988), but these cells become activated and migrate in the subretinal space in several retinopathies associated with ocular inflammation such as diabetic retinopathy (Zeng et al., 2008), and age-related macular degeneration (Combadiere et al., 2007). In our study, we analyzed microglia in organotypic cultures or explants, a commonly used model of inflammation (Bauer et al., 2016; Carter and Dick, 2003), whereby we analyzed the effect of the presence of PRGF. In this model, the PRGF, instead of reduce the activation of microglia due to the culture, induce the activation of these cells, and they migrate to the outer part of the retina. These results are not in line with the results of some authors which stipulated that PRGF induce neuroprotection associated with a down-regulation of activated microglial cell number and a significant decrease of pro-inflammatory mediators (Anitua et al., 2015a);

because our findings reveal, in addition to a drastically reduction in the number of neurons, an activation of microglia by PRGF, though the number of microglia has not increased.

To understand why the PRGF induce the activation of microglial cells, inducing an inflammatory response, we analyzed the presence of inflammatory cytokines in the PRGF. It has been confirmed that there are some cytokines present in the PRGF itself: IL-6 (Masuki et al., 2016), IL-8 (Anitua et al., 2010), IL-4, and TNFα (Anitua et al., 2012a). However, it has been also suggested that the presence of proinflammatory cytokines is almost absent or very low from PRGF (Anitua et al., 2015b). In order to show that the cytokines present in the PRGF may be involved in eliciting an immune response in the tissue or cells to which PRGF is added, we thought necessary to analyze the presence of cytokines in the PRGF. In this study, we demonstrate the presence of inflammatory cytokines in the PRGF.

The activation of the microglia by cytokines is demonstrated due to the presence of cytokines receptor by microglial cells. Microglia cells express mRNA transcript for IL-1 receptor I and II, IL-6, IL-8, IL-10, IL-12, IL-13, IL-15 receptors and TNF receptors I and II (Lee et al., 2002). And it has been demonstrated that IL-6, IL-12 and TNFα can activate microglia (Luo and Chen, 2012). Thus, the cytokines present in the PRGF can trigger by themselves an inflammatory response, independently of activating the secretion of cytokines by the tissue with which it is in contact, because it has been also shown that PRGF induces the expression of cytokines such as IL-1β, IL-6 or IL-10 (Mozzati et al., 2010). Besides, it has been suggested that the anti-inflammatory effect of PRGF is due to the high content of IL-4 (Anitua et al., 2012a), however, the presence of this and others anti-inflammatory cytokines, as IL-10 and IL-13 (Cavaillon, 2001), is low in comparison with others cytokines with the opposite effect (Table 3).

To decrease the activation of microglial migration in the retinal explant in presence of PRGF, we use dexamethasone as a treatment against inflammation (Tsurufuji et al., 1984) in presence of 10% human PRGF (because it is a high concentration and it is originate from another specie, being the condition most likely to induce inflammation); and the heat-inactivated PRGF was also used (Anitua et al., 2014a). The dexamethasone slightly decreases the number of activated microglia but there are not significant differences between the absence of dexamethasone may be due to the high variability

between samples. In the other hand, the inactivation of PRGF can reduce, though not entirely, the microglia migration, due to the heat-inactivation maintaining the biological activity of PRGF but completely reduced complement activity and deceased significantly the presence of IgE (Anitua et al., 2014a). However, after this inactivation, all cytokines are present in the PRGF equally to the active PRGF. In addition, IgG and IgM are also present in the inactivated PRGF (Anitua et al., 2014a), and IgG increase activated microglia expressing high affinity IgG receptor (FcαRI) (Orr et al., 2005). Thus, we can observe microglia migration after inactivation of PRGF by heat.

We have also demonstrated that the proportion of microglia migration is higher when the PRGF donor is more different to the animal that donates the retina, being very low for autologous PRGF. The human PRGF induce a higher microglial activation that the pig PRGF, and this could be due to the presence of the pro-inflammatory cytokine IL-8, which is more abundant in the human PRGF. Moreover, the presence of other receptors in the microglial cells, as toll like receptors (TLR), that respond to self and nonself activators (Shastri et al., 2013), could be implicated in the higher activation of microglia when the PRGF is not autologous or it is from other specie.

In conclusion, PRGF do not induce neuroproteccion to the RGCs, the survival of RGCs markedly decreases in presence or absence of Müller cells. In addition, PRGF can induce the activation of microglia in the retina being an inflammatory sign, may be due to the presence of inflammatory cytokines. On the other hand, PRGF promote Müller cells proliferation. Human PRGF is not as effective as pig PRGF inducing pig Müller cells proliferation, may be due to because it active a higher proportion of microglia. Although PRGF could be a good candidate to stimulate and accelerate tissue regeneration due to their proliferative properties, more studies are necessary to clarify their negative effect on neurons and on immune system, because autologous platelet injection are being used as a treatment for recurrent retinal detachment secondary to optic nerve coloboma (Nadal et al., 2012). Furthermore, the use of platelets is common during macular hole surgery, but is associated to complication including focal macular epithelial pigmentary hypertrophy, retinal folds emanating from the macula, development of epiretinal membrane, in addition, progression of cataracts and raised intraocular pressure may occur (Cheung et al., 2005; Minihan et al., 1997; Nugent and Lee, 2015). Even thought PRGF have been used in different medical and surgical

specialties with success and extensive data indicate that platelet-rich plasma induce tissue regeneration, many studies are not rigorous or controlled, the data is limited, and other studies yield contrary results (Kuffler, 2015). Although the differences in levels of the factors of PRGF and other blood-derived products may explain the variability in the obtained results between different studies (Vahabi et al., 2015), as we found significant differences in cytokines concentrations between individuals. For all these reasons further animal and clinical studies should be performed to study all the properties of the PRGF.

Acknowledgments

We acknowledge the support of Retos-MINECO Fondos Fender (RTC-2016-48231) and Grupos Consolidados del Gobierno Vasco (IT437-10) to E.V.

References

Anitua, E., Alkhraisat, M.H., Orive, G., 2012a. Perspectives and challenges in regenerative medicine using plasma rich in growth factors. J. Control. Release 157, 29-38.

Anitua, E., Muruzabal, F., De la Fuente, M., Merayo-Lloves, J., Orive, G., 2014a. Effects of heat-treatment on plasma rich in growth factors-derived autologous eye drop. Exp. Eye Res. 119, 27-34.

Anitua, E., Muruzabal, F., de la Fuente, M., Riestra, A., Merayo-Lloves, J., Orive, G., 2016. PRGF exerts more potent proliferative and anti-inflammatory effects than autologous serum on a cell culture inflammatory model. Exp. Eye Res. 151, 115-121.

Anitua, E., Pascual, C., Antequera, D., Bolos, M., Padilla, S., Orive, G., Carro, E., 2014b. Plasma rich in growth factors (PRGF-Endoret) reduces neuropathologic hallmarks and improves cognitive functions in an Alzheimer's disease mouse model. Neurobiol. Aging 35, 1582-1595.

Anitua, E., Pascual, C., Perez-Gonzalez, R., Antequera, D., Padilla, S., Orive, G., Carro, E., 2013. Intranasal delivery of plasma and platelet growth factors using PRGF-Endoret system enhances neurogenesis in a mouse model of Alzheimer's disease. PLoS One 8, e73118.

Anitua, E., Pascual, C., Perez-Gonzalez, R., Orive, G., Carro, E., 2015a. Intranasal PRGF-Endoret enhances neuronal survival and attenuates NF-kappaB-dependent inflammation process in a mouse model of Parkinson's disease. J. Control. Release 203, 170-180.

Anitua, E., Prado, R., Orive, G., 2012b. Bilateral sinus elevation evaluating plasma rich in growth factors technology: a report of five cases. Clin. Implant Dent. Relat. Res. 14, 51-60.

Anitua, E., Sanchez, M., Merayo-Lloves, J., De la Fuente, M., Muruzabal, F., Orive, G., 2011. Plasma rich in growth factors (PRGF-Endoret) stimulates proliferation and migration of primary keratocytes and conjunctival fibroblasts and inhibits and reverts TGF-beta1-Induced myodifferentiation. Invest. Ophthalmol. Vis. Sci. 52, 6066-6073.

Anitua, E., Sanchez, M., Orive, G., 2010. Potential of endogenous regenerative technology for in situ regenerative medicine. Advanced drug delivery reviews 62, 741-752.

Anitua, E., Sanchez, M., Orive, G., Andia, I., 2008. Delivering growth factors for therapeutics. Trends Pharmacol. Sci. 29, 37-41.

Anitua, E., Sanchez, M., Zalduendo, M.M., de la Fuente, M., Prado, R., Orive, G., Andia, I., 2009. Fibroblastic response to treatment with different preparations rich in growth factors. Cell Prolif. 42, 162-170.

Anitua, E., Zalduendo, M.M., Prado, R., Alkhraisat, M.H., Orive, G., 2015b. Morphogen and proinflammatory cytokine release kinetics from PRGF-Endoret fibrin scaffolds: evaluation of the effect of leukocyte inclusion. Journal of biomedical materials research. Part A 103, 1011-1020.

Bauer, P.M., Zalis, M.C., Abdshill, H., Deierborg, T., Johansson, F., Englund-Johansson, U., 2016. Inflamed In Vitro Retina: Cytotoxic Neuroinflammation and Galectin-3 Expression. PLoS One 11, e0161723.

Bell, J.D., Thomas, T.C., Lass, E., Ai, J., Wan, H., Lifshitz, J., Baker, A.J., Macdonald, R.L., 2014. Platelet-mediated changes to neuronal glutamate receptor expression at sites of microthrombosis following experimental subarachnoid hemorrhage. J. Neurosurg. 121, 1424-1431.

Bendinelli, P., Matteucci, E., Dogliotti, G., Corsi, M.M., Banfi, G., Maroni, P., Desiderio, M.A., 2010. Molecular basis of anti-inflammatory action of platelet-rich plasma on human chondrocytes: mechanisms of NF-kappaB inhibition via HGF. J. Cell. Physiol. 225, 757-766.

Berry, M., Ahmed, Z., Lorber, B., Douglas, M., Logan, A., 2008. Regeneration of axons in the visual system. Restor. Neurol. Neurosci. 26, 147-174.

Bringmann, A., Pannicke, T., Grosche, J., Francke, M., Wiedemann, P., Skatchkov, S.N., Osborne, N.N., Reichenbach, A., 2006. Müller cells in the healthy and diseased retina. Prog. Retin. Eye Res. 25, 397-424.

Bringmann, A., Reichenbach, A., 2001. Role of Muller cells in retinal degenerations. Front. Biosci. 6, E72-92.

Burmeister, S.L., Hartwig, D., Limb, G.A., Kremling, C., Hoerauf, H., Muller, M., Geerling, G., 2009. Effect of various platelet preparations on retinal muller cells. Invest. Ophthalmol. Vis. Sci. 50, 4881-4886.

Carter, D.A., Dick, A.D., 2003. Lipopolysaccharide/interferon-gamma and not transforming growth factor beta inhibits retinal microglial migration from retinal explant. Br. J. Ophthalmol. 87, 481-487.

Cavaillon, J.M., 2001. Pro- versus anti-inflammatory cytokines: myth or reality. Cell. Mol. Biol. (Noisy-le-grand) 47, 695-702.

Cheung, C.M., Munshi, V., Mughal, S., Mann, J., Hero, M., 2005. Anatomical success rate of macular hole surgery with autologous platelet without internal-limiting membrane peeling. Eye (Lond.) 19, 1191-1193.

Combadiere, C., Feumi, C., Raoul, W., Keller, N., Rodero, M., Pezard, A., Lavalette, S., Houssier, M., Jonet, L., Picard, E., Debre, P., Sirinyan, M., Deterre, P., Ferroukhi, T., Cohen, S.Y., Chauvaud, D., Jeanny, J.C., Chemtob, S., Behar-Cohen, F., Sennlaub, F., 2007. CX3CR1-dependent subretinal microglia cell accumulation is associated with cardinal features of age-related macular degeneration. J. Clin. Invest. 117, 2920-2928.

Garcia, M., Forster, V., Hicks, D., Vecino, E., 2002. Effects of muller glia on cell survival and neuritogenesis in adult porcine retina in vitro. Invest. Ophthalmol. Vis. Sci. 43, 3735–3743.

Garcia, M., Forster, V., Hicks, D., Vecino, E., 2003. In vivo expression of neurotrophins and neurotrophin receptors is conserved in adult porcine retina in vitro. Invest. Ophthalmol. Vis. Sci. 44, 4532-4541.

Glovinsky, Y., Quigley, H.A., Dunkelberger, G.R., 1991. Retinal ganglion cell loss is size dependent in experimental glaucoma. Invest. Ophthalmol. Vis. Sci. 32, 484-491.

Jin, K., Zhu, Y., Sun, Y., Mao, X.O., Xie, L., Greenberg, D.A., 2002. Vascular endothelial growth factor (VEGF) stimulates neurogenesis in vitro and in vivo. Proc. Natl. Acad. Sci. U. S. A. 99, 11946-11950.

Joo, C.K., Choi, J.S., Ko, H.W., Park, K.Y., Sohn, S., Chun, M.H., Oh, Y.J., Gwag, B.J., 1999. Necrosis and apoptosis after retinal ischemia: involvement of NMDA-mediated excitotoxicity and p53. Invest. Ophthalmol. Vis. Sci. 40, 713-720.

Kilian, O., Flesch, I., Wenisch, S., Taborski, B., Jork, A., Schnettler, R., Jonuleit, T., 2004. Effects of platelet growth factors on human mesenchymal stem cells and human endothelial cells in vitro. Eur. J. Med. Res. 9, 337-344.

Kuffler, D.P., 2015. Platelet-Rich Plasma Promotes Axon Regeneration, Wound Healing, and Pain Reduction: Fact or Fiction. Mol. Neurobiol. 52, 990-1014.

Lee, Y.B., Nagai, A., Kim, S.U., 2002. Cytokines, chemokines, and cytokine receptors in human microglia. J. Neurosci. Res. 69, 94-103.

Lieth, E., Gardner, T.W., Barber, A.J., Antonetti, D.A., Penn State Retina Research, G., 2000. Retinal neurodegeneration: early pathology in diabetes. Clin Exp Ophthalmol 28, 3-8.

Ling, E.A., Wong, W.C., 1993. The origin and nature of ramified and amoeboid microglia: a historical review and current concepts. Glia 7, 9-18.

Lull, M.E., Block, M.L., 2010. Microglial activation and chronic neurodegeneration. Neurotherapeutics 7, 354-365.

Luo, X.G., Chen, S.D., 2012. The changing phenotype of microglia from homeostasis to disease. Translational neurodegeneration 1, 9.

Masuki, H., Okudera, T., Watanebe, T., Suzuki, M., Nishiyama, K., Okudera, H., Nakata, K., Uematsu, K., Su, C.Y., Kawase, T., 2016. Growth factor and pro-inflammatory cytokine contents in platelet-rich plasma (PRP), plasma rich in growth factors (PRGF), advanced platelet-rich fibrin (A-PRF), and concentrated growth factors (CGF). International journal of implant dentistry 2, 19.

Minihan, M., Goggin, M., Cleary, P.E., 1997. Surgical management of macular holes: results using gas tamponade alone, or in combination with autologous platelet concentrate, or transforming growth factor beta 2. Br. J. Ophthalmol. 81, 1073-1079.

Mozzati, M., Martinasso, G., Pol, R., Polastri, C., Cristiano, A., Muzio, G., Canuto, R., 2010. The impact of plasma rich in growth factors on clinical and biological factors involved in healing processes after third molar extraction. Journal of biomedical materials research. Part A 95, 741-746.

Nadal, J., Lopez-Fortuny, M., Sauvageot, P., Perez-Formigo, D., 2012. Treatment of recurrent retinal detachment secondary to optic nerve coloboma with injection of autologous platelet concentrate. J. AAPOS 16, 100-101.

Newman, E., Reichenbach, A., 1996. The Muller cell: a functional element of the retina. Trends Neurosci. 19, 307-312.

Niyadurupola, N., Sidaway, P., Osborne, A., Broadway, D.C., Sanderson, J., 2011. The development of human organotypic retinal cultures (HORCs) to study retinal neurodegeneration. Br. J. Ophthalmol. 95, 720-726.

Nugent, R.B., Lee, G.A., 2015. Ophthalmic use of blood-derived products. Surv. Ophthalmol. 60, 406-434.

O'Kusky, J.R., Ye, P., D'Ercole, A.J., 2000. Insulin-like growth factor-I promotes neurogenesis and synaptogenesis in the hippocampal dentate gyrus during postnatal development. J. Neurosci. 20, 8435-8442.

Omri, S., Behar-Cohen, F., de Kozak, Y., Sennlaub, F., Verissimo, L.M., Jonet, L., Savoldelli, M., Omri, B., Crisanti, P., 2011. Microglia/macrophages migrate through retinal epithelium barrier by a transcellular route in diabetic retinopathy: role of PKCzeta in the Goto Kakizaki rat model. Am. J. Pathol. 179, 942-953.

Orive, G., Anitua, E., Pedraz, J.L., Emerich, D.F., 2009. Biomaterials for promoting brain protection, repair and regeneration. Nat. Rev. Neurosci. 10, 682-692.

Orr, C.F., Rowe, D.B., Mizuno, Y., Mori, H., Halliday, G.M., 2005. A possible role for humoral immunity in the pathogenesis of Parkinson's disease. Brain 128, 2665-2674.

Pinon, R.M., Pastor, J.C., Saornil, M.A., Goldaracena, M.B., Layana, A.G., Gayoso, M.J., Guisasola, J., 1992. Intravitreal and subretinal proliferation induced by platelet-rich plasma injection in rabbits. Curr. Eye Res. 11, 1047-1055.

Reichenbach, A., Bringmann, A., 2013. New functions of Muller cells. Glia 61, 651-678.

Ruzafa, N., Vecino, E., 2015. Effect of Muller cells on the survival and neuritogenesis in retinal ganglion cells. Archivos de la Sociedad Espanola de Oftalmologia 90, 522-526.

Selles-Navarro, I., Villegas-Perez, M.P., Salvador-Silva, M., Ruiz-Gomez, J.M., Vidal-Sanz, M., 1996. Retinal ganglion cell death after different transient periods of pressure-induced ischemia and survival intervals. A quantitative in vivo study. Invest. Ophthalmol. Vis. Sci. 37, 2002-2014.

Shastri, A., Bonifati, D.M., Kishore, U., 2013. Innate immunity and neuroinflammation. Mediators Inflamm. 2013, 342931.

Streit, W.J., Graeber, M.B., Kreutzberg, G.W., 1988. Functional plasticity of microglia: a review. Glia 1, 301-307.

Takeuchi, M., Kamei, N., Shinomiya, R., Sunagawa, T., Suzuki, O., Kamoda, H., Ohtori, S., Ochi, M., 2012. Human platelet-rich plasma promotes axon growth in brain-spinal cord coculture. Neuroreport 23, 712-716.

Tsurufuji, S., Kurihara, A., Ojima, F., 1984. Mechanisms of anti-inflammatory action of dexamethasone: blockade by hydrocortisone mesylate and actinomycin D of the inhibitory effect of dexamethasone on leukocyte infiltration in inflammatory sites. J. Pharmacol. Exp. Ther. 229, 237-243.

Vahabi, S., Vaziri, S., Torshabi, M., Rezaei Esfahrood, Z., 2015. Effects of Plasma Rich in Growth Factors and Platelet-Rich Fibrin on Proliferation and Viability of Human Gingival Fibroblasts. J Dent (Tehran) 12, 504-512.

Vecino, E., Garcia-Crespo, D., Garcia, M., Martinez-Millan, L., Sharma, S.C., Carrascal, E., 2002. Rat retinal ganglion cells co-express brain derived neurotrophic factor (BDNF) and its receptor TrkB. Vision Res. 42, 151-157.

Vecino, E., Rodriguez, F.D., Ruzafa, N., Pereiro, X., Sharma, S.C., 2016. Glia-neuron interactions in the mammalian retina. Prog. Retin. Eye Res. 51, 1-40.

Wygnanski, T., Desatnik, H., Quigley, H.A., Glovinsky, Y., 1995. Comparison of ganglion cell loss and cone loss in experimental glaucoma. Am. J. Ophthalmol. 120, 184-189.

Zeng, H.Y., Green, W.R., Tso, M.O., 2008. Microglial activation in human diabetic retinopathy. Arch. Ophthalmol. 126, 227-232.

Zhang, L., Ino-ue, M., Dong, K., Yamamoto, M., 2000. Retrograde axonal transport impairment of large- and medium-sized retinal ganglion cells in diabetic rat. Curr. Eye Res. 20, 131-136.

ANEXO 5

Mol Neurobiol. 2017 (in press)

Analysis of the Retina in Osteopontin-Deficient Mice in Aging.

Noelia Ruzafa[1], Xandra Pereiro[1], Patricia Aspichueta[2], Javier Araiz[3], Elena Vecino[1]

[1]Department of Cell Biology and Histology, University of Basque Country, Experimental Ophtalmo-Biology Group (www.ehu.es/GOBE) UPV/EHU, Vizcaya, Spain.

[2]Department of Physiology, University of the Basque Country UPV/EHU, Spain; Biocruces Research Institute, Spain.

[3] Department of Ophthalmology, University of the Basque Country UPV/EHU, Vizcaya, Spain

Abstract

Osteopontin (OPN) is a secreted glycosylated phosphoprotein that influences cell survival, inflammation, migration and homeostasis after injury. As the role of OPN in the retina remains unclear, this study issue was addressed by aimed to studying how the absence of OPN in knock-out mice affects the retina and the influence of age on these effects. The study focused on retinal ganglion cells (RGCs) and glial cells (astrocytes, Müller cells and resident microglia) in 3- and 20-month-old mice. The number of RGCs in the retina were quantified and the area occupied by astrocytes was measured. In addition, the morphology of Müller cells and microglia was examined in retinal sections. The deficiency in OPN reduces RGC density by 25.09% at 3 months of age and by 60.37% at 20 months of age. The astrocyte area was also reduced by 51.01% in 3 month old mice and by 57.84% at 20 months of age, although Müller glia and microglia did not seem to be affected by the lack of OPN. This study demonstrates the

influence of OPN on astrocytes and RGCs, whereby the absence of OPN in the retina diminishes the area occupied by astrocytes and produces a secondary reduction in the number of RGCs. Accordingly, OPN could be a target to develop therapies to combat neurodegenerative diseases and astrocytes may represent a key mediator of such effects.

Key Words

Retina, osteopontin, retinal ganglion cells, glia, astrocytes, Müller cells, microglia

Introduction

Osteopontin (OPN) is a secreted glycosylated phosphoprotein encoded by the *spp1* gene (Neumann et al., 2014; Wang and Denhardt, 2008) that has an arginine-glycine-aspartic acid cell binding sequence (Giachelli et al., 1998; Marsh et al., 2007). OPN is a cytokine that binds to integrins and CD44 variants on the cell surface (Denhardt et al., 2001), integrins fulfilling many different functions in cells that influence: cell survival and apoptosis, inflammation, microcalcification, cell attachment and migration, intracellular signaling, chemotaxis (Maetzler et al., 2007; Scatena et al., 2007), the maintenance of homeostasis after an injury (Maetzler et al., 2010), and the modulation of neuronal regeneration following injury (Scatena et al., 2007). OPN can be found in the nervous system, in the developing and adult rodent brain, and neurons in the olfactory bulb, retina, striatum and brainstem produce OPN (Boeshore et al., 2004; Ichikawa et al., 2000; Rittling et al., 1998). Moreover, while OPN may be only weakly expressed under physiological conditions, it may augment during inflammation and in neurodegenerative diseases (Hashimoto et al., 2007; Neumann et al., 2014; Scatena et al., 2007; Wang and Denhardt, 2008).

In the retina, OPN is expressed by retinal ganglion cells (RGCs) (Chidlow et al., 2008), the neurons that relay visual signals to the brain (Ju et al., 2000). RGCs are also the retinal cells most vulnerable to ischemic and excitotoxic insults (Osborne et al., 2004), which upregulate OPN expression (Chidlow et al., 2008) to possibly afford protection against death, as occurs in experimental glaucoma (Birke et al., 2010; Chowdhury et al., 2011). The retinal glia, astrocytes, microglia and Müller cells, maintain homeostasis within the retina, where they provide structural support and influence metabolism,

phagocytosis of neuronal debris, immune responses and other activities (Vecino et al., 2016). Reactive astrocytes express OPN following different types of brain insult (Chabas et al., 2001; Choi et al., 2003; Jin et al., 2006) and it has also been associated with the microglia that fulfill macrophagic functions (Vecino et al., 2016). As occurs in astrocytes, OPN is upregulated in activated microglia after CNS damage (Chang et al., 2016; Choi et al., 2007; Ellison et al., 1998; Hashimoto et al., 2003; Kim et al., 2002; Shin et al., 2005), suggesting that it may play a key role in the pathogenesis of neuroinflammation (Choi et al., 2003). OPN binds to the integrin αvβ3 receptor, which means it may act as a chemoattractant in recruiting astrocytes and microglia during the formation of the glial scar following ischemic injury (Choi et al., 2007; Choi et al., 2003; Ellison et al., 1999; Ellison et al., 1998; Wang et al., 1998). Indeed, OPN may be involved in glial activation, cell repair, glial and macrophage migration, and matrix remodeling by reactive astrocytes (Choi et al., 2003; Ellison et al., 1999; Ellison et al., 1998; Wang et al., 1998). On this basis, the effect of OPN on retinal astrocytes and microglia is worthy of study. Moreover, OPN is found in the secretome of Müller cells (Del Rio et al., 2011; von Toerne et al., 2014) and as a result, their morphology has been studied to understand how OPN affects these retinal glial cells.

Aging is the main risk factor for neurodegenerative diseases and OPN has age-dependent neuroprotective effects (Albertsson et al., 2014). Several modifications occurs in the normal retina with aging, which include RGC loss, stronger GFAP (glial fibrillary acidic protein) expression by astrocytes, an increase in cytoplasmic organelles (Bonnel et al., 2003; Curcio and Drucker, 1993; Ramirez et al., 2001) and the acquisition of an activated phenotype by microglial cells (von Bernhardi et al., 2015). Thus, it is important to compare how the absence of OPN affects the retina in young (3-month-old) and old (20-month-old) mice.

The aim of this study was to investigate the effect of OPN deficiency in the retina using an OPN knock-out mouse, focusing on RGCs, astrocytes, microglia and Müller cells. In addition, as the influencing of aging on OPN function is unclear, the effects of this deficiency were studied in animals of different ages.

Materials and Methods

Animals

Female knock-out (B6.129S6(Cg)-*Spp1*^{tm1Blh}/J) and C57BL/6J mice aged 3 months (n = 3 wild type and n = 3 knock out) and 20 months old (n = 4 wild type and n = 4 knock out) were used in these experiments (The Jackson Laboratory, Bar Harbor, Maine, USA). The animals had free access to food and water, and they were kept at a constant temperature of 21 °C on a 12 hour light–dark cycle. All procedures were carried out in adherence to the ARVO Statement for the Use of Animals in Ophthalmic and Vision Research.

Tissue collection

Animals were sacrificed by cervical dislocation and their eyes were enucleated. The cornea, crystalline lens and the vitreous were removed, and the retina was carefully extracted. The retina was immediately fixed for 5 hours in 4% paraformaldehyde (PFA) prepared in 0.1 M phosphate buffer (pH 7.4) and then extended on filter paper (Millipore, Madrid, Spain). To obtain sections, the eyes were extracted and immediately fixed overnight in 4% PFA. They were then cryoprotected for 24 hours in 30% sucrose in 0.1 M phosphate buffer at 4 °C and embedded in OCT (optimal cutting temperature) medium. Cryosections (14 μm thick) were obtained and stored at −20 °C.

Immunochemistry

Whole mount retinas were immunostained as described previously (Pinar-Sueiro et al., 2013), with some minor modifications. The flat fixed retinas were washed in phosphate buffered saline (PBS, pH 7.4) and they were blocked by incubating them overnight with shaking at 4 ºC in a solution of PBS-TX-100-BSA (0.25% Triton-X 100 and 1% bovine serum albumin in PBS). The retinas were then incubated for one day at 4 ºC with the primary antibodies diluted in PBS-TX-100-BSA: an anti-RBPMS (RNA-binding protein with multiple splicing) guinea pig antibody (1:4,000 PhosphoSolutions, Aurora, USA) to detect RGCs; and an anti-GFAP mouse antibody (1:1,000 Sigma, Steinheim, Germany) to detect astrocytes. Subsequently, the retinas were washed three times in PBS for 15 minutes and antibody binding was detected over 5 hours at room temperature with shaking using secondary antibodies diluted 1:1,000 in PBS-BSA (1%):

an Alexa Fluor 555 conjugated goat anti-guinea pig antibody (Invitrogen, Eugene, Oregon, USA) and an Alexa Fluor 488 conjugated goat anti-mouse antibody (Invitrogen). Finally, the retinas were washed 3 times for 10 minutes in PBS, flat mounted onto slides in PBS:Glycerol (1:1) and coverslipped.

Microglia and Müller cells were immunostained in cryostat sections of the eye, as described previously (Vecino et al., 2002). The sections were washed twice with PBS-TX-100 for 10 minutes, and they were then incubated overnight with a primary rabbit anti-Iba1 antibody (1:2,000; Wako, Osaka, Japan) to detect microglia, and a rabbit antibody against glutamine synthetase (1:10,000; Abcam, Cambridge, United Kingdom) to detect Müller cells. The RGCs were also labeled with the anti-RBPMS guinea pig antibody. After two washes with PBS, antibody binding was detected for 1 hour with Alexa Fluor 555 or 488 goat anti-rabbit or anti-guinea pig secondary antibodies (Invitrogen) diluted 1:1,000 in PBS-BSA (1%). The sections were washed twice with PBS for 10 minutes and mounted with a coverslip with PBS:Glycerol (1:1).

Image capture

Images were acquired with a digital camera (Zeiss Axiocam MRM, Zeiss, Jena, Germany) coupled to an epifluorescence microscope (Zeiss) using the Zen software (Zeiss). For whole-mount retinas, a mosaic of the entire retina was generated using the 555 and 488 filters with a 10X objective. The area of the mosaic was defined in overlapping micrographs of a defined area of the retina obtained automatically and once the mosaic was defined, the contour of the retina was measured and the retinal surface area was calculated.

RGC quantification

The number of RGCs was counted semi-automatically using Zen software (Zeiss) and the RGC density (mean ± standard error) was compared between the wild type and OPN knock-out retinas using a Student's T-test. In addition, a Mann-Whitney U test was used to verify the differences between groups. These statistical analyses were carried out using IBM SPSS Statistics software v. 21.0. For both tests, the minimum value of significant differences was defined as $p<0.05$.

Astrocyte morphology

The morphology of astrocytes was analyzed using the ImageJ image processing and analysis software developed at the National Institutes of Health (NIH, version 1.49). The region formed by the colored pixels (labeled with the antibody against GFAP) was selected using the "threshold color" tool, and the surface area of the selected astrocytes was measured. We calculated the proportion of the retinal surface occupied by astrocytes and we compared this in the most central part of the retina (1mm diameter) of control and OPN knock-out mice, taking the optic nerve as the center yet disregarding this structure. At the optic nerve the morphology of the astrocyte's branches impedes their quantification due to their complexity.

Statistical analyses were again carried out using IBM SPSS Statistics software v. 21.0. The average of the percentages and the standard errors were calculated and compared for the wild type and OPN knock-out retinas using a Student T-test, and it was supplemented with Mann-Whitney U test to verify the differences between the groups. The minimum value for significant differences for both tests was defined as $p<0.05$.

Results

The RGCs and astrocytes in the retina of 3- and 20-month-old wild type and OPN knock-out mice were analyzed by labeling them with an antibody against RBPMS or GFAP, respectively (Fig. 1). There were some regions in the retina of the OPN knock-out mice where the cell density was very low, particularly in the peripheral areas, 2.5 mm from the optic nerve. In these regions, the low density of RGCs and astrocytes were further exaggerated with age.

The number of RGCs labeled with RBPMS in the entire retina and the area of each retina was evaluated and their density calculated (RGCs/mm^2). In 3-month-old wild type mice, the average RGC density (2607.15 ± 38.36 RGCs/mm^2) was greater than in the OPN knock-out mice (1953.37 ± 29.75 RGCs/mm^2), as was also evident in 20-month-old animals (wild type 2101.86 ± 84.73 RGCs/mm^2; OPN knock-out mice 832.77 ± 114.28 RGCs/mm^2). Thus, the OPN deficiency triggered a mean reduction in RGC density of 25.09% at 3 months of age ($p < 0.001$), which was further reduced to 60.37% at 20 months of age ($p < 0.001$, Fig. 2).

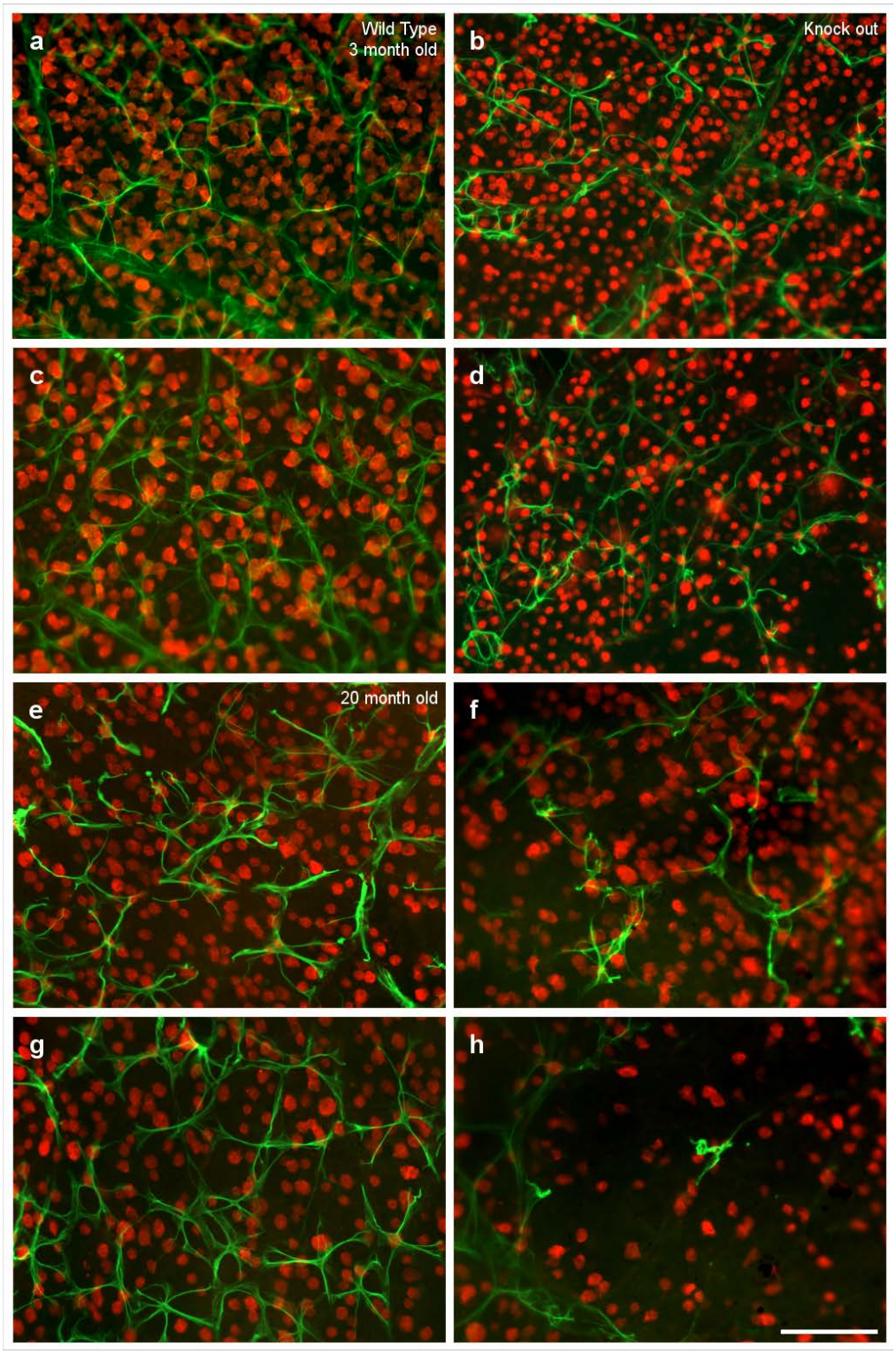

Fig 1. Flat mount retinas. Images of whole mount retinas from wild type (a, c, e, g) and OPN knock-out (b, d, f, h) mice of two different ages: 3 (a, b, c, d) and 20 months of age (e, f, g, h). The retinas were labeled with an antibody against GFAP (green) to identify astrocytes and an antibody against RBPMS (red) to label RGCs. The pictures were taken at a distance of 1 mm (a, b, e, f) and 2.5 mm (c, d, g, h) from the optic nerve. Scale bar = 100 μm.

In the retinas of wild type mice, astrocytes form a network that covers the whole surface of the retina, surrounding the vessels, and they are connected through their stellar morphology. By contrast, OPN knock-out mice seem to have fewer astrocytes and there are larger gaps between them, with less linear extensions than in the controls. The smaller number of astrocytes, with shorter branches and fewer processes, was suggestive of astroglial atrophy. This effect is more severe in 20-month-old mice than in 3-month-old mice, with larger areas lacking astrocytes and some cells that have lost their stellate morphology (Fig. 1e-h). It is important to note that there are more areas without astrocytes and a lower density of RGCs in the peripheral regions of the retina in OPN knock-out mice (Fig. 1d, h), relative to the regions closer to the optic nerve (Fig. 1b, f). These differences were found in both 3-month-old and 20-month-old mice.

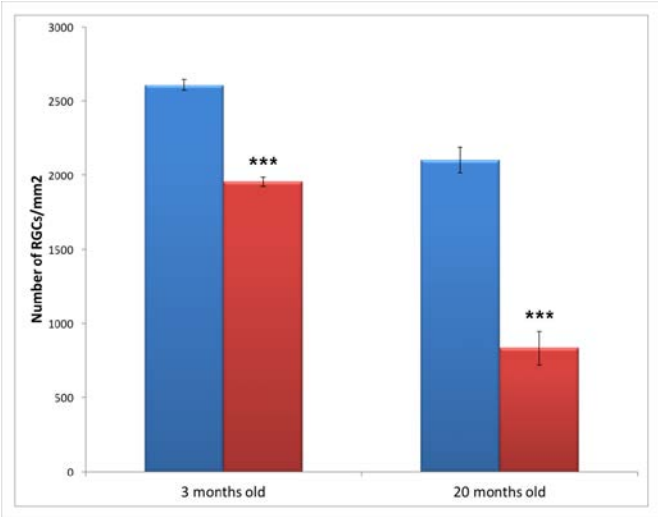

Fig 2. Retinal ganglion cell analysis. Histogram representing the number of RGCs (RGCs/mm^2) in wild type (blue) and OPN knock-out (red) mice at two different ages: 3- and 20-months-old: *** $p < 0.001$

When the area occupied by astrocytes was quantified, the average area occupied by astrocytes in 3-month-old wild type mice (33.05% ± 0.95) was greater than in the OPN knock-out mice (16.19% ± 3.47). Thus, the absence of OPN induces a 51.01% reduction in astrocyte density ($p < 0.01$). In 20-month-old mice the proportion of the wild type retina occupied by astrocytes (21.67% ± 1.02) was still 57.84% higher than in the OPN knock-out mice (9.14% ± 1.95), confirming that the absence of OPN reduces the astrocyte density in the retina ($p < 0.01$, Fig. 3). Furthermore, the number of RGCs and the area covered by astrocytes in the 3-month-old OPN knock-out mice was very similar to the same parameters in the 20-month-old wild type mice, with no significant differences between these two ages.

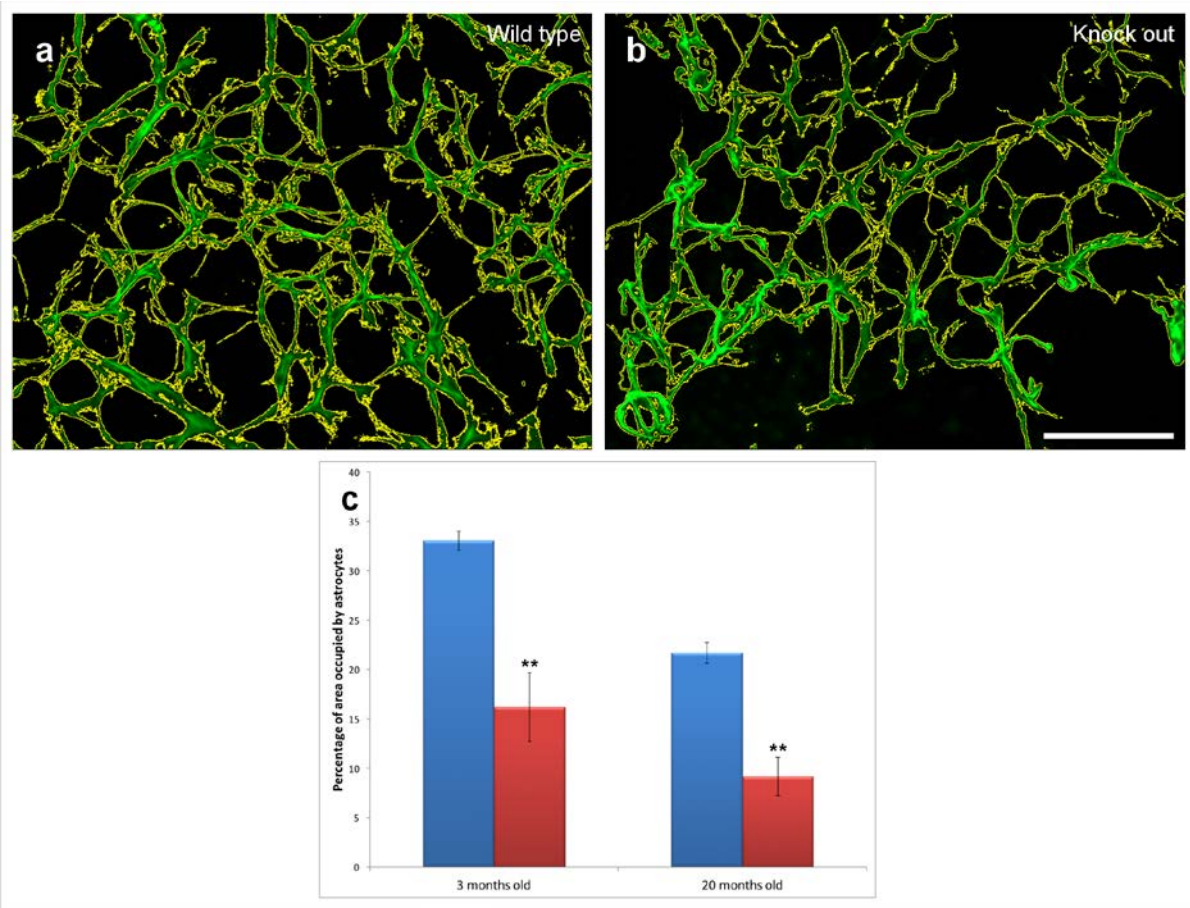

Fig 3. Astrocyte analysis. Measurement of the area occupied by the astrocytes labeled with an antibody against GFAP (green). The area defined by the yellow line was measured automatically. The astrocytes were compared between wild type (a) and OPN knock-out (b) mice. Astrocyte density was measured as the area occupied by astrocytes, and it was represented graphically in wild type (blue) and OPN knock-out (red) mice at 3 and 20 months of age (c). Scale bar = 100 μm: ** $p < 0.01$

Interestingly, no signs of microglia activation were detected in the OPN knock-out retinas at 3 or 20 months of age (Fig. 4). The morphology of the microglia is similar in the presence and absence of OPN, and these cells do not seem to adopt an amoeboid aspect and they do not undergo morphological changes, such as a thickening and retraction of branches. Moreover, microglial cells are located at the inner part of the retina in all cases, meaning that they are not active as migration to the sub-retinal space is a sign of activation.

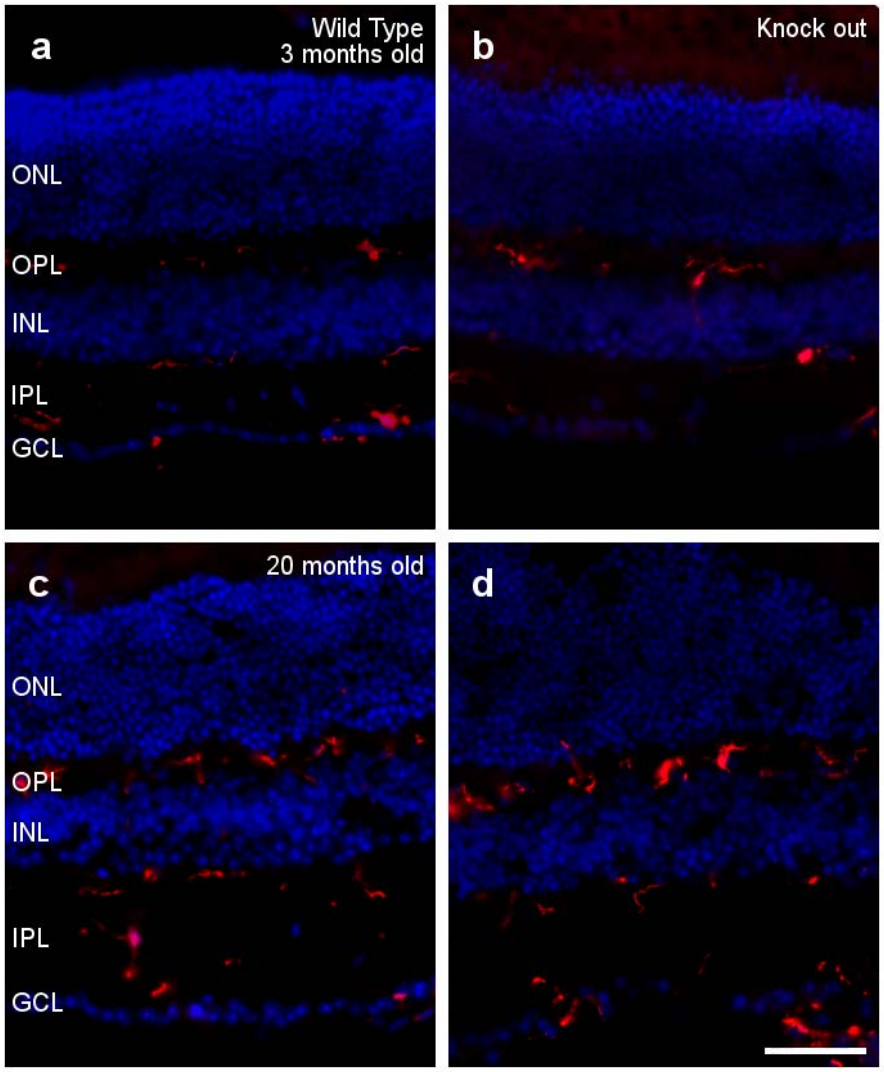

Fig. 4. Microglial analysis. Retinal sections from 3- (a, b) and 20-month-old (c, d) wild type (a, c) and OPN knock-out (b, d) mice, in which the nuclei are labelled with DAPI (blue) and the microglia are labelled with an antibody against Iba1 (red): ONL, outer nuclear layer; OPL, outer plexiform layer; INL, inner nuclear layer; IPL, inner nuclear layer; GCL, ganglion cell layer. Scale bar = 50 μm

Finally, we did not detect differences between the Müller cell structure in wild type and OPN knock-out mice at 3 and 20 months of age (Fig. 5). In both cases, the Müller cells, labeled by the antibody against glutamine synthetase, cross the retina in a radial orientation and their processes surrounded the cell bodies of retinal neurons. Although the morphology of the retina may be altered in 20-month-old mice, the Müller cells continue to surround the soma of the RGCs (see Fig. 5) and the photoreceptors (ONL in Fig. 5).

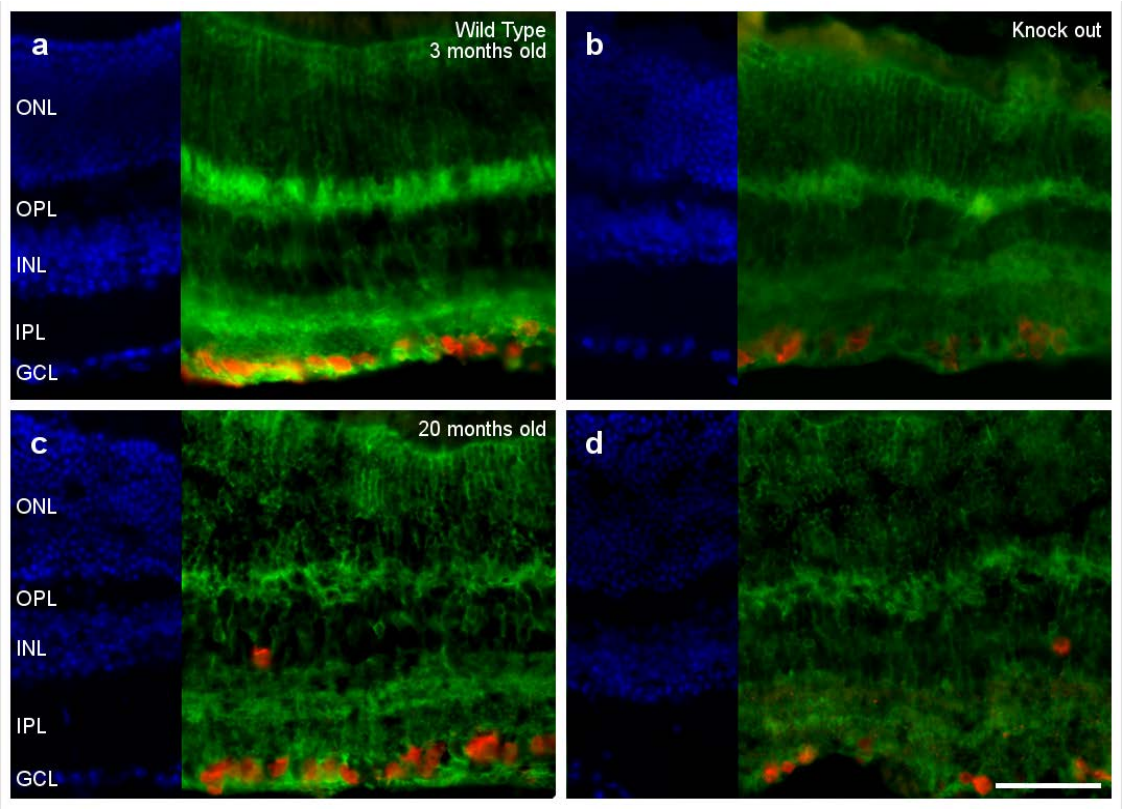

Fig. 5. Müller cell analysis. Retinal sections from 3- (a, b) and 20-month-old (c, d) wild type (a, c) and OPN knock-out (b, d) mice, in which the nuclei are labelled with DAPI (blue), Müller cells with an antibody against glutamine synthetase (green) and the RGCs are labelled with antibody against RBPMS (red): ONL, outer nuclear layer; OPL, outer plexiform layer; INL, inner nuclear layer; IPL, inner nuclear layer; GCL, ganglion cell layer. Scale bar = 50 μm

Discussion

Since OPN is involved in many important homeostatic processes (Maetzler et al., 2010; Maetzler et al., 2007; Scatena et al., 2007), the OPN knock-out mouse model offers the possibility of studying how OPN affects the retina. In aging, the expression of OPN in the CNS gradually decreases (Albertsson et al., 2014), whereas OPN expression is induced or upregulated in response to damage (Choi et al., 2007; Choi et al., 2003; Iczkiewicz et al., 2007; Wang et al., 1998). This induction of OPN expression is evident in glial cells like astrocytes and microglia (Choi et al., 2007; Choi et al., 2003; Iczkiewicz et al., 2007), and the absence of OPN could alter nervous tissue. In the retina of OPN knock-out mice, the RGC density is reduced, as is the surface occupied by astrocytes.

The spinal cord of these OPN deficient mice has a percentage of white matter significantly different to that of wild type mice (Hashimoto et al., 2007) and the mechanical withdrawal threshold increases significantly in OPN knock-out mice (Marsh et al., 2007). In addition, when the nervous system of these mutant mice is injured, it suffers more damage due to the lack of OPN (Hashimoto et al., 2007; Maetzler et al., 2007; van Velthoven et al., 2011; Wright et al., 2014). The decrease in the number of RGCs in the OPN knock-out mice may reflect the more limited neuroprotection in these animals (Meller et al., 2005). OPN has positive effects on survival, proliferation, migration and neural stem cell differentiation (Rabenstein et al., 2015), and nasal administration of OPN decreases neuronal cell death and brain edema after insult (Topkoru et al., 2013). In the retina, the neuroprotective effect of OPN has been demonstrated in porcine photoreceptor cells, significantly reducing the proportion of apoptotic cells (Del Rio et al., 2011). Moreover, the neuroprotective effect of OPN has been seen in RGCs after ischemic-like damage (Chidlow et al., 2008), and it can stimulate axon growth in RGCs (Ries et al., 2007). Conversely, OPN is also significantly correlated with the progressive degree of optic nerve degeneration and RGC loss in a mouse glaucoma model. In fact, OPN treatment inhibited cell degeneration within the ganglion cell layer in cultured glaucomatous eyes (Birke et al., 2010). Thus, not all RGCs appear to have the same needs, and some RGCs can survive for almost the entire life of the OPN knock-out mice. However, at least one subpopulation of RGCs appears to need OPN to survive and thus, these cells could be rescued by OPN.

The neuroprotective properties of OPN might be associated with an integrin-linked kinase and CD44 signaling. Integrin receptors trigger Akt and FAK activation, which stimulates the phosphoinositide 3-kinase pathway that is in turn directly associated with cleaved-caspase-3 inhibition and anti-apoptotic cell death (Topkoru et al., 2013). This has been demonstrated in the developing brain using an integrin antagonist that attenuates the neuroprotective effect of OPN (Chen et al., 2011). In addition, OPN treatment of cortical neuron cultures causes an increase in Akt and p42/p44 mitogen-activated protein kinase phosphorylation, again consistent with OPN induced neuroprotection (Meller et al., 2005). OPN can also upregulate the phospho-Akt, cyclin D1 and phospho-Rb content of cells, subsequently enhancing the proliferation of neural progenitors in the presence of fibroblast growth factor 2 (Kalluri and Dempsey, 2012).

Moreover, OPN can also protect against toxicity by decreasing glial cell activation (Broom et al., 2015).

OPN is also necessary for a subpopulation of astrocytes, as we find that astrocytes are absent from some areas of the retina in the OPN knock-out mice. The reduction in the surface area occupied by astrocytes could be a consequence of OPN's role in cell adhesion, migration and survival, and also its influence on the metabolic activity of astrocytes (Neumann et al., 2014). The influence of OPN on the survival of astrocytes has been demonstrated in glioblastoma, with OPN secreted by stromal astrocytes conferring them resistance to radiation (Friedmann-Morvinski et al., 2016). In addition, only astrocytes that express OPN survive after ischemic injury in the brain, because OPN is involved in calcium precipitation and it allows astrocytes to participate in the phagocytosis of calcium deposits (Park et al., 2012). Therefore, the lack of OPN could make some subpopulations of astrocytes more sensitive to cell death than others. This astrocyte heterogeneity has also been demonstrated in relation to other issues (Chaboub and Deneen, 2012; Vecino et al., 2016) and these cells could be implicated in different pathways of neuroprotection.

We also found that the distribution of astrocytes and the RGC density in the 3-month-old OPN knock-out mice is similar to that found in 20-month-old wild type mice. This could indicate that the absence of OPN induces premature ageing in the retina. In aged rats, there is an increase in GFAP protein, although astrocytes are less numerous and have distorted morphologies, with shorter and fragmented branches (Cerbai et al., 2012). Indeed, the astrocytes in the aging rat retina are very similar in appearance to those found in the OPN knock-out mouse retina (Diniz et al., 2010; Rodriguez-Arellano et al., 2016). The lack of astrocytes and RGCs is more evident in the peripheral areas of the retina than in the central areas. This is consistent with descriptions that the peripheral retina is more sensitive to damage such as experimental glaucoma, where more RGC death has been described (Quigley, 2011; Ruiz-Ederra et al., 2005; Urcola et al., 2006). Since the loss of astrocytes is very dramatic in peripheral areas of younger animals (3-month-old animals) and it is maintained along the animal's life (20-month-old animals), the reduction in the number of RGCs take place progressively during the animal's life, indicating that RGC cell death could be secondary to the astrocyte death.

Although there are signs of degeneration in the OPN knock-out retinas, there were no signs of activation in microglial cells, such as migration to the sub-retinal space from the inner parts of the retina (Omri et al., 2011) or a change in their morphology to amoeboid microglia (Lull and Block, 2010). This is consistent with what is seen in the brain, where no sign of microglia activation has been found in OPN deficient mice (Maetzler et al., 2007). Although the number of microglial cells increases in aged retinas (Karlstetter et al., 2015), as evident in 20-month-old retinas, there are no differences between knock-out and wild type retinas. Microglia undergo morphological changes with age, with gradually larger cell bodies, as well as progressively shorter and thicker cell processes (von Bernhardi et al., 2015). However, the microglia in the OPN knock-out retinas do not show signs of aging relative to the wild type retinas. OPN could be synthesized de novo by activated microglia in response to retinal neurodegeneration (Chidlow et al., 2008) and OPN can activate amoeboid transformation, phagocytosis and the motility of the microglia (Ellert-Miklaszewska et al., 2016). Thus, the lack of OPN could prevent the shift of microglia to an amoeboid phenotype and there acquisition of migratory capacity.

A characteristic pattern of OPN may be found in Müller cells of control retinas (Deeg et al., 2011) and through its presence in the secretome of Müller cells (von Toerne et al., 2014). Thus, Müller cells can express and secrete OPN in response to GDNF (glial cell-derived neurotrophic factor) and this OPN exerts a direct effect on the survival of photoreceptors, possibly stimulating Müller cells to overexpress other cytokines with neuroprotective activity (Del Rio et al., 2011). The neuroprotective effects of OPN may be in part mediated by preventing cytotoxic Müller cell swelling, as well as by the release of VEGF (vascular endothelial growth factor) and adenosine from Müller cells (Wahl et al., 2013). There are no apparent changes in the Müller cells of the retina in OPN knock-out and thus, OPN may not be necessary for the survival of Müller cells, although it could affect their response to cell damage.

In OPN knock-out mice, there is a decrease in RGC density and a reduction of the surface area occupied by astrocytes. Peripheral areas of the retina seem to be more sensitive to damage than central areas and these changes become more prominent with age. Moreover, the density of RGCs and astrocytes in the retina of 3-month-old OPN knock-out mice is very similar to that in the 20-month-old wild type mice. These results suggest that the lack of OPN may induce premature ageing. However, microglia and

Müller cells seem not to be affected by the lack of OPN, at least not when only aging is considered and the retina suffers no damage. Thus, OPN could be a candidate molecule to develop treatments to combat neurodegenerative disease and astrocytes may represent a specific target of interest in such circumstances.

Acknowledgments

We acknowledge the support of Retos-MINECO Fondos Fender (RTC-2016-48231) and Grupos Consolidados del Gobierno Vasco (IT437-10) to E.V.

References

Albertsson, A.M., Zhang, X., Leavenworth, J., Bi, D., Nair, S., Qiao, L., Hagberg, H., Mallard, C., Cantor, H., Wang, X., 2014. The effect of osteopontin and osteopontin-derived peptides on preterm brain injury. J. Neuroinflammation 11, 197.

Birke, M.T., Neumann, C., Birke, K., Kremers, J., Scholz, M., 2010. Changes of osteopontin in the aqueous humor of the DBA2/J glaucoma model correlated with optic nerve and RGC degenerations. Invest. Ophthalmol. Vis. Sci. 51, 5759-5767.

Boeshore, K.L., Schreiber, R.C., Vaccariello, S.A., Sachs, H.H., Salazar, R., Lee, J., Ratan, R.R., Leahy, P., Zigmond, R.E., 2004. Novel changes in gene expression following axotomy of a sympathetic ganglion: a microarray analysis. J. Neurobiol. 59, 216-235.

Bonnel, S., Mohand-Said, S., Sahel, J.A., 2003. The aging of the retina. Exp. Gerontol. 38, 825-831.

Broom, L., Jenner, P., Rose, S., 2015. Increased neurotrophic factor levels in ventral mesencephalic cultures do not explain the protective effect of osteopontin and the synthetic 15-mer RGD domain against MPP+ toxicity. Exp. Neurol. 263, 1-7.

Cerbai, F., Lana, D., Nosi, D., Petkova-Kirova, P., Zecchi, S., Brothers, H.M., Wenk, G.L., Giovannini, M.G., 2012. The neuron-astrocyte-microglia triad in normal brain ageing and in a model of neuroinflammation in the rat hippocampus. PLoS One 7, e45250.

Chabas, D., Baranzini, S.E., Mitchell, D., Bernard, C.C., Rittling, S.R., Denhardt, D.T., Sobel, R.A., Lock, C., Karpuj, M., Pedotti, R., Heller, R., Oksenberg, J.R., Steinman, L., 2001. The influence of the proinflammatory cytokine, osteopontin, on autoimmune demyelinating disease. Science 294, 1731-1735.

Chaboub, L.S., Deneen, B., 2012. Developmental origins of astrocyte heterogeneity: the final frontier of CNS development. Dev. Neurosci. 34, 379-388.

Chang, S.W., Kim, H.I., Kim, G.H., Park, S.J., Kim, I.B., 2016. Increased Expression of Osteopontin in Retinal Degeneration Induced by Blue Light-Emitting Diode Exposure in Mice. Front. Mol. Neurosci. 9, 58.

Chen, W., Ma, Q., Suzuki, H., Hartman, R., Tang, J., Zhang, J.H., 2011. Osteopontin reduced hypoxia-ischemia neonatal brain injury by suppression of apoptosis in a rat pup model. Stroke 42, 764-769.

Chidlow, G., Wood, J.P., Manavis, J., Osborne, N.N., Casson, R.J., 2008. Expression of osteopontin in the rat retina: effects of excitotoxic and ischemic injuries. Invest. Ophthalmol. Vis. Sci. 49, 762-771.

Choi, J.S., Kim, H.Y., Cha, J.H., Choi, J.Y., Lee, M.Y., 2007. Transient microglial and prolonged astroglial upregulation of osteopontin following transient forebrain ischemia in rats. Brain Res. 1151, 195-202.

Choi, J.S., Park, H.J., Cha, J.H., Chung, J.W., Chun, M.H., Lee, M.Y., 2003. Induction and temporal changes of osteopontin mRNA and protein in the brain following systemic lipopolysaccharide injection. J. Neuroimmunol. 141, 65-73.

Chowdhury, U.R., Jea, S.Y., Oh, D.J., Rhee, D.J., Fautsch, M.P., 2011. Expression profile of the matricellular protein osteopontin in primary open-angle glaucoma and the normal human eye. Invest. Ophthalmol. Vis. Sci. 52, 6443-6451.

Curcio, C.A., Drucker, D.N., 1993. Retinal ganglion cells in Alzheimer's disease and aging. Ann. Neurol. 33, 248-257.

Deeg, C.A., Eberhardt, C., Hofmaier, F., Amann, B., Hauck, S.M., 2011. Osteopontin and fibronectin levels are decreased in vitreous of autoimmune uveitis and retinal expression of both proteins indicates ECM re-modeling. PLoS One 6, e27674.

Del Rio, P., Irmler, M., Arango-Gonzalez, B., Favor, J., Bobe, C., Bartsch, U., Vecino, E., Beckers, J., Hauck, S.M., Ueffing, M., 2011. GDNF-induced osteopontin from Muller glial cells promotes photoreceptor survival in the Pde6brd1 mouse model of retinal degeneration. Glia 59, 821-832.

Denhardt, D.T., Noda, M., O'Regan, A.W., Pavlin, D., Berman, J.S., 2001. Osteopontin as a means to cope with environmental insults: regulation of inflammation, tissue remodeling, and cell survival. J. Clin. Invest. 107, 1055-1061.

Diniz, D.G., Foro, C.A., Rego, C.M., Gloria, D.A., de Oliveira, F.R., Paes, J.M., de Sousa, A.A., Tokuhashi, T.P., Trindade, L.S., Turiel, M.C., Vasconcelos, E.G., Torres, J.B., Cunnigham, C., Perry, V.H., Vasconcelos, P.F., Diniz, C.W., 2010. Environmental impoverishment and aging alter object recognition, spatial learning, and dentate gyrus astrocytes. Eur. J. Neurosci. 32, 509-519.

Ellert-Miklaszewska, A., Wisniewski, P., Kijewska, M., Gajdanowicz, P., Pszczolkowska, D., Przanowski, P., Dabrowski, M., Maleszewska, M., Kaminska, B., 2016. Tumour-processed osteopontin and lactadherin drive the protumorigenic reprogramming of microglia and glioma progression. Oncogene.

Ellison, J.A., Barone, F.C., Feuerstein, G.Z., 1999. Matrix remodeling after stroke. De novo expression of matrix proteins and integrin receptors. Ann. N. Y. Acad. Sci. 890, 204-222.

Ellison, J.A., Velier, J.J., Spera, P., Jonak, Z.L., Wang, X., Barone, F.C., Feuerstein, G.Z., 1998. Osteopontin and its integrin receptor alpha(v)beta3 are upregulated during formation of the glial scar after focal stroke. Stroke 29, 1698-1706; discussion 1707.

Friedmann-Morvinski, D., Bhargava, V., Gupta, S., Verma, I.M., Subramaniam, S., 2016. Identification of therapeutic targets for glioblastoma by network analysis. Oncogene 35, 608-620.

Giachelli, C.M., Lombardi, D., Johnson, R.J., Murry, C.E., Almeida, M., 1998. Evidence for a role of osteopontin in macrophage infiltration in response to pathological stimuli in vivo. Am. J. Pathol. 152, 353-358.

Hashimoto, M., Koda, M., Ino, H., Murakami, M., Yamazaki, M., Moriya, H., 2003. Upregulation of osteopontin expression in rat spinal cord microglia after traumatic injury. J. Neurotrauma 20, 287-296.

Hashimoto, M., Sun, D., Rittling, S.R., Denhardt, D.T., Young, W., 2007. Osteopontin-deficient mice exhibit less inflammation, greater tissue damage, and impaired locomotor recovery from spinal cord injury compared with wild-type controls. J. Neurosci. 27, 3603-3611.

Ichikawa, H., Itota, T., Nishitani, Y., Torii, Y., Inoue, K., Sugimoto, T., 2000. Osteopontin-immunoreactive primary sensory neurons in the rat spinal and trigeminal nervous systems. Brain Res. 863, 276-281.

Iczkiewicz, J., Rose, S., Jenner, P., 2007. Osteopontin expression in activated glial cells following mechanical- or toxin-induced nigral dopaminergic cell loss. Exp. Neurol. 207, 95-106.

Jin, J.K., Na, Y.J., Moon, C., Kim, H., Ahn, M., Kim, Y.S., Shin, T., 2006. Increased expression of osteopontin in the brain with scrapie infection. Brain Res. 1072, 227-233.

Ju, W.K., Kim, K.Y., Cha, J.H., Kim, I.B., Lee, M.Y., Oh, S.J., Chung, J.W., Chun, M.H., 2000. Ganglion cells of the rat retina show osteopontin-like immunoreactivity. Brain Res. 852, 217-220.

Kalluri, H.S., Dempsey, R.J., 2012. Osteopontin increases the proliferation of neural progenitor cells. Int. J. Dev. Neurosci. 30, 359-362.

Karlstetter, M., Scholz, R., Rutar, M., Wong, W.T., Provis, J.M., Langmann, T., 2015. Retinal microglia: just bystander or target for therapy? Prog. Retin. Eye Res. 45, 30-57.

Kim, S.Y., Choi, Y.S., Choi, J.S., Cha, J.H., Kim, O.N., Lee, S.B., Chung, J.W., Chun, M.H., Lee, M.Y., 2002. Osteopontin in kainic acid-induced microglial reactions in the rat brain. Mol. Cells 13, 429-435.

Lull, M.E., Block, M.L., 2010. Microglial activation and chronic neurodegeneration. Neurotherapeutics 7, 354-365.

Maetzler, W., Berg, D., Funke, C., Sandmann, F., Stunitz, H., Maetzler, C., Nitsch, C., 2010. Progressive secondary neurodegeneration and microcalcification co-occur in osteopontin-deficient mice. Am. J. Pathol. 177, 829-839.

Maetzler, W., Berg, D., Schalamberidze, N., Melms, A., Schott, K., Mueller, J.C., Liaw, L., Gasser, T., Nitsch, C., 2007. Osteopontin is elevated in Parkinson's disease and its absence leads to reduced neurodegeneration in the MPTP model. Neurobiol. Dis. 25, 473-482.

Marsh, B.C., Kerr, N.C., Isles, N., Denhardt, D.T., Wynick, D., 2007. Osteopontin expression and function within the dorsal root ganglion. Neuroreport 18, 153-157.

Meller, R., Stevens, S.L., Minami, M., Cameron, J.A., King, S., Rosenzweig, H., Doyle, K., Lessov, N.S., Simon, R.P., Stenzel-Poore, M.P., 2005. Neuroprotection by osteopontin in stroke. J. Cereb. Blood Flow Metab. 25, 217-225.

Neumann, C., Garreis, F., Paulsen, F., Hammer, C.M., Birke, M.T., Scholz, M., 2014. Osteopontin is induced by TGF-beta2 and regulates metabolic cell activity in cultured human optic nerve head astrocytes. PLoS One 9, e92762.

Omri, S., Behar-Cohen, F., de Kozak, Y., Sennlaub, F., Verissimo, L.M., Jonet, L., Savoldelli, M., Omri, B., Crisanti, P., 2011. Microglia/macrophages migrate through retinal epithelium barrier by a transcellular route in diabetic retinopathy: role of PKCzeta in the Goto Kakizaki rat model. Am. J. Pathol. 179, 942-953.

Osborne, N.N., Casson, R.J., Wood, J.P., Chidlow, G., Graham, M., Melena, J., 2004. Retinal ischemia: mechanisms of damage and potential therapeutic strategies. Prog. Retin. Eye Res. 23, 91-147.

Park, J.M., Shin, Y.J., Kim, H.L., Cho, J.M., Lee, M.Y., 2012. Sustained expression of osteopontin is closely associated with calcium deposits in the rat hippocampus after transient forebrain ischemia. J. Histochem. Cytochem. 60, 550-559.

Pinar-Sueiro, S., Zorrilla Hurtado, J.A., Veiga-Crespo, P., Sharma, S.C., Vecino, E., 2013. Neuroprotective effects of topical CB1 agonist WIN 55212-2 on retinal ganglion cells after acute rise in intraocular pressure induced ischemia in rat. Exp. Eye Res. 110, 55-58.

Quigley, H.A., 2011. Glaucoma. Lancet 377, 1367-1377.

Rabenstein, M., Hucklenbroich, J., Willuweit, A., Ladwig, A., Fink, G.R., Schroeter, M., Langen, K.J., Rueger, M.A., 2015. Osteopontin mediates survival, proliferation and migration of neural stem cells through the chemokine receptor CXCR4. Stem Cell. Res. Ther. 6, 99.

Ramirez, J.M., Ramirez, A.I., Salazar, J.J., de Hoz, R., Trivino, A., 2001. Changes of astrocytes in retinal ageing and age-related macular degeneration. Exp. Eye Res. 73, 601-615.

Ries, A., Goldberg, J.L., Grimpe, B., 2007. A novel biological function for CD44 in axon growth of retinal ganglion cells identified by a bioinformatics approach. J. Neurochem. 103, 1491-1505.

Rittling, S.R., Matsumoto, H.N., McKee, M.D., Nanci, A., An, X.R., Novick, K.E., Kowalski, A.J., Noda, M., Denhardt, D.T., 1998. Mice lacking osteopontin show normal development and bone structure but display altered osteoclast formation in vitro. J. Bone Miner. Res. 13, 1101-1111.

Rodriguez-Arellano, J.J., Parpura, V., Zorec, R., Verkhratsky, A., 2016. Astrocytes in physiological aging and Alzheimer's disease. Neuroscience 323, 170-182.

Ruiz-Ederra, J., Garcia, M., Hernandez, M., Urcola, H., Hernandez-Barbachano, E., Araiz, J., Vecino, E., 2005. The pig eye as a novel model of glaucoma. Exp. Eye Res. 81, 561-569.

Scatena, M., Liaw, L., Giachelli, C.M., 2007. Osteopontin: a multifunctional molecule regulating chronic inflammation and vascular disease. Arterioscler. Thromb. Vasc. Biol. 27, 2302-2309.

Shin, T., Ahn, M., Kim, H., Moon, C., Kang, T.Y., Lee, J.M., Sim, K.B., Hyun, J.W., 2005. Temporal expression of osteopontin and CD44 in rat brains with experimental cryolesions. Brain Res. 1041, 95-101.

Topkoru, B.C., Altay, O., Duris, K., Krafft, P.R., Yan, J., Zhang, J.H., 2013. Nasal administration of recombinant osteopontin attenuates early brain injury after subarachnoid hemorrhage. Stroke 44, 3189-3194.

Urcola, J.H., Hernandez, M., Vecino, E., 2006. Three experimental glaucoma models in rats: comparison of the effects of intraocular pressure elevation on retinal ganglion cell size and death. Exp. Eye Res. 83, 429-437.

van Velthoven, C.T., Heijnen, C.J., van Bel, F., Kavelaars, A., 2011. Osteopontin enhances endogenous repair after neonatal hypoxic-ischemic brain injury. Stroke 42, 2294-2301.

Vecino, E., Garcia-Crespo, D., Garcia, M., Martinez-Millan, L., Sharma, S.C., Carrascal, E., 2002. Rat retinal ganglion cells co-express brain derived neurotrophic factor (BDNF) and its receptor TrkB. Vision Res. 42, 151-157.

Vecino, E., Rodriguez, F.D., Ruzafa, N., Pereiro, X., Sharma, S.C., 2016. Glia-neuron interactions in the mammalian retina. Prog. Retin. Eye Res. 51, 1-40.

von Bernhardi, R., Eugenin-von Bernhardi, L., Eugenin, J., 2015. Microglial cell dysregulation in brain aging and neurodegeneration. Front. Aging Neurosci. 7, 124.

von Toerne, C., Menzler, J., Ly, A., Senninger, N., Ueffing, M., Hauck, S.M., 2014. Identification of a novel neurotrophic factor from primary retinal Muller cells using stable isotope labeling by amino acids in cell culture (SILAC). Mol. Cell. Proteomics 13, 2371-2381.

Wahl, V., Vogler, S., Grosche, A., Pannicke, T., Ueffing, M., Wiedemann, P., Reichenbach, A., Hauck, S.M., Bringmann, A., 2013. Osteopontin inhibits osmotic swelling of retinal glial (Muller) cells by inducing release of VEGF. Neuroscience 246, 59-72.

Wang, K.X., Denhardt, D.T., 2008. Osteopontin: role in immune regulation and stress responses. Cytokine Growth Factor Rev. 19, 333-345.

Wang, X., Louden, C., Yue, T.L., Ellison, J.A., Barone, F.C., Solleveld, H.A., Feuerstein, G.Z., 1998. Delayed expression of osteopontin after focal stroke in the rat. J. Neurosci. 18, 2075-2083.

Wright, M.C., Mi, R., Connor, E., Reed, N., Vyas, A., Alspalter, M., Coppola, G., Geschwind, D.H., Brushart, T.M., Hoke, A., 2014. Novel roles for osteopontin and clusterin in peripheral motor and sensory axon regeneration. J. Neurosci. 34, 1689-1700.

ANEXO 6

Detection and Quantification of Molecular Markers of Damage in the Optic Nerve

Noelia Ruzafa[1], Tatjana C. Jakobs[2], Elena Vecino[1]

[1]Department of Cell Biology and Histology, University of Basque Country UPV/EHU, Vizcaya, Spain.

[2]Department of Ophthalmology, Harvard Medical School, Massachusetts Eye and Ear Infirmary, Boston, MA, USA.

Introduction

Gliosis is a reactive change of glial cells in response to damage to central nervous system, that is a complex process that involves changes in gene expression and morphological remodeling. The mouse optic nerve is a suitable model for studying the molecular mechanisms of reactive gliosis. In the optic nerve, astrocytes, microglia (Bosco et al., 2011) and oligodendrocytes interact with retinal ganglion cell (RGC) axons and each other. The optic nerve head (ONH) has been shown to be the initial site of insult to RGC axons in glaucoma (Burgoyne et al., 2005; Howell et al., 2007; Jakobs et al., 2005; Quigley et al., 1981), and gene expression changes in that region have been investigated in models of ocular hypertension and glaucoma (Howell et al., 2011; Johnson et al., 2007).

In previous studies, gliosis was triggered at the mouse optic nerve head by optic nerve crush and the expression profiles of 14,000 genes from 1 day to 3 months were analysed. The transcriptome showed profound changes, the optic nerve crush is followed by a strong and immediate response of genes involved in immune response and inflammation, and in the regulation of cell proliferation. The changed were greatest

shortly after injury, but they returning nearly to resting levels by 3 months (Qu and Jakobs, 2013).

Some of the genes that are up-regulated after damage could be used as molecular biomarkers of the damage. Biomarkers have gained immense scientific and clinical interest to solve important question in glaucoma that remain unsolved, with countless molecules that have been candidate as potential biomarkers (Agnifili et al., 2015). In our study, the genes selected as candidate biomarker were osteopontin (SPP1 or OPN), lipocalin 2 (LCN2) and leukemia inhibitor factor (LIF) due to they are up-regulated after optic nerve crush, in glaucoma or after other damage to the RGCs (Birke et al., 2010; Johnson et al., 2011; Khalyfa et al., 2007; Parmar et al., 2016; Qu and Jakobs, 2013), in addition to have potential neuroprotective properties (Agca and Grimm, 2014; Meller et al., 2005; Samardzija et al., 2012; Topkoru et al., 2013; von Toerne et al., 2014; Xing et al., 2014).

The purpose of this study was to show that the astrocytes, and not microglia or oligodendrocytes, are the cells responsible to up-regulate molecular markers like *spp1*, *lif* and *lcn2* after optic nerve crush. For that purpose we isolated, the astrocytes from the optic nerve head after crushing the optic nerve following the described protocol (Choi et al., 2015). Moreover the quantification of the up-regulated molecules was performed at the protein level from the optic nerve head as well as in the aqueous humour after optic nerve crush compared to control condition.

Material and Methods

Animals

All animals were treated in accordance with the ARVO Statement for the Use of Animals in Ophthalmic and Vision Research, and all procedures were approved by the Institutional Animal Care and Use Committee at Schepens Eye Research Institute. The mice used in this study were wild-type C57BL/6 (Charles River Laboratories, Wilmington, MA). Mice were housed under a 12 hours light/dark cycle with free access to food and water.

Optic nerve crush and tissue collection

This procedure was obtained as described previously (Qu and Jakobs, 2013). Briefly, mice were anesthetized by intraperitoneal injection of ketamine and xylazine (100 mg/kg and 20 mg/kg body weight). A drop of 0.5% proparacaine was applied to the eye for local anesthesia. A small incision was made in the conjunctiva at the superior pole of the eye. Through this incision, a blunt dissection of the conjunctiva was made with forceps towards the back of the eye to expose the retrobulbar optic nerve. The optic nerve was crushed with jeweler's forceps for 10 seconds at 1mm behind the globe under direct visual control, avoiding the vascular supply to the eye. After the surgery, bacitracin ointment was applied to avoid infection and the animal recovered on a warming pad. Only the optic nerve of the left eye was crushed, the right eye served as negative control. Mice were euthanized with carbon dioxide followed by cervical dislocation at day 1, 4 and 8 after the crush. The skull and the brain were removed, and the eye together with the optic nerve was carefully dissected out without imposing any mechanical stress or damage to the tissue

Isolation and collection of single astrocytes from the optic nerve head

The isolation and collection of single cells was made as previously described (Choi et al., 2015). Two optic nerve heads were used for cell dissociation. The optic nerve heads were transferred into the papain solution (9µl papain suspension (35 mg protein per ml) (Worthington Cat No. 3126, Lakewood, NJ) and 2.5µl L-cystein solution (10 mg/ml in HBSS) (Sigma Aldrich, St. Louis, MO) to 500µl HBSS (Ca^{2+}/Mg^{2+} free Hank's balanced salt solution, Lonza, Walkersville, MD) and incubated for 20 min. Digested optic nerve heads were centrifuged at 2000rpm for 5 min at room temperature to remove the papain solution. The optic nerve heads were resuspended in 200µl HBSS with 10% normal horse serum (Jackson Immuno Research, West Grove, PA) and mechanically dissociated by gentle trituration 3-5 times using a heat-polished Pasteur pipette (the diameter at the tip should be approximately 300µm). The cell suspension and undissociated tissue were centrifuged at 2000 rpm for 5 minutes at room temperature and resuspended in 200µl HBSS containing 10% horse serum and 60U/ml DNase (Sigma Aldrich). Lastly, the undissociated tissue is triturated with a series of heat-polished Pasteur pipettes with progressively smaller openings (~300µm to 100µm) until it is completely dissociated. The resulting cell suspension is kept on ice and used within

an hour. About 50µl of the cell suspension are pipetted into one of the rings on a Gold Seal slide (Gold Seal Products 8, Portsmouth, NH). Then individual, isolated cells are visualized and aspirated into the micropipette. The cell is transferred into a thin-wall PCR tube that contained 5 µl of washing buffer (1× PBS containing 2% BSA). The tube is centrifuged briefly and immediately put on dry ice until further use.

Single-cell RT-PCR of isolated astrocytes

The single cells were transferred into a thin-wall reaction tube containing a mix of 3 pmol of each primer and reaction buffer for reverse transcription and first round PCR. The primer mix contained primers for *gfap* (as a control that the selected cell was an astrocyte), *cd45* (as a negative control to rule out contamination by microglia), and *gapdh* (glyceraldehyde 3-phosphate dehydrogenase as a positive control, due to is a housekeeping gene and it is expressed in all cells). Reverse transcription and first round PCR was done in a single vial reaction with the Access RT-PCR kit (Promega). The cells were lysed in the buffer/primer mix for 1 min at 65°C, 2U AMV-RT and 2U Tfl polymerase were added, then 45 min at 48°C were allowed for reverse transcription followed by 19 cycles of 1 min at 94°C, 1 min 60°C, and 2 min 68°C. Second round PCR was done separately for every target using 1/60 of the first round reaction, 7.5 pmol of each primer, and 0.25 U AmpliTaq Gold polymerase (Applied Biosystems). After a 32 cycles of amplification the PCR products were analyzed on 2% agarose gels.

QPCR of RNA extract from isolated astrocytes and from optic nerve head after optic nerve crush and in control

The Arcturus Pico Pure RNA isolation kit (Applied Biosystems) was used to extract total RNA from isolated astrocytes and from 2 optic nerve heads for each condition. The RNA was transcribed and amplified using an Ovation qPCR system kit (NuGen, San Carlos, CA). qPCR was performed using an StepOnePlus qPCR thermocycler (Applied Biosystems). Parameters for qPCR were: 10 min at 95°C, followed by 40 cycles of 15 sec at 95°C and 1 min at 60°C. The primers used in qPCR were chosen from the validated primers in PrimerBank (http://pga.mgh.harvard.edu/primerbank). *Oaz1* was used as endogenous control in all the QPCR reactions.

ELISA of protein extract from optic nerve head and aqueous humour after optic nerve crush and in control

The samples used for ELISA were the protein extracts of 2 optic nerve heads for each condition, obtained after sonication in a hypotonic buffer for cell lysis. And the aqueous humour carefully extracted from 3 eyes for each condition. ELISA 96-well Maxisorp plates (Nunc, Life Technologies, Carlsbad, CA, USA) were coated with 5µg/ml human recombinant SPP1, LIF or LCN2 proteins (Life Technologies) in PBS overnight at 4°C. As a negative control, wells were also coated with 5µg/ml BSA. After washing the plate with PBS, the plate was blocked in blocking buffer (PBS with 1% BSA) at room temperature for 2 hours. After washes, rabbit anti-Spp1, Lif and Lcn2 antibodies (1:500 in PBS 1% BSA, Life Technologies) was added and incubated at room temperature for 2 hours. After washes, horseradish peroxidase-conjugated goat anti-rabbit IgG (1:500 in PBS 1% BSA, Life Technologies) was added and incubated at room temperature for 2 hour. After extensive washes, the plate was incubated with TMB (3,3´,5,5´-tertamethylbenzidine) at room temperature for 20 minutes after which stop solution (2M H_2SO_4) was added and the absorbance was measured at 450nm using ELISA plate reader.

Results

After preparation of optic nerve head cell suspension, single astrocytes were collected (Fig 1 A-B). The single-cell gen expression analysis by reverse transcription PCR confirmed that the collected cells were astrocytes due to they expressed *gfap*. We discarded that the cells were microglia because they did not express *cd45* (Fig 1 C).

To confirm that the candidate genes (*spp1*, *lif* and *lcn2*) are up-regulated after damage in the optic nerve, and to quantify this up-regulation, a quantitative PCR was performed. However, the results of the QPCR were null due to limited amount of RNA in the sample.

In order to establish a quantification of the up-regulation after optic nerve crush, a QPCR of the entire optic nerve head was carried out. The results of the QPCR from the ONH 1 day after crush injury compared to the ONH from the uninjured contralateral eye for *spp1* were shown in the Fig 2.

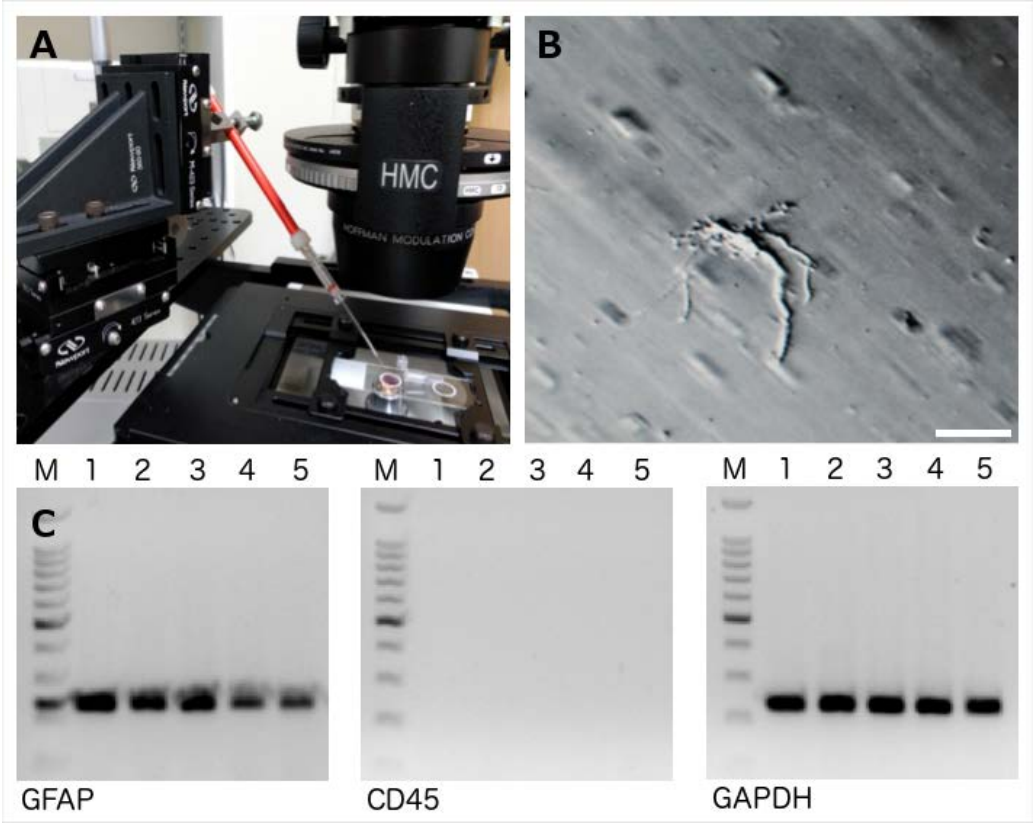

Fig 1. Isolation of astrocytes from the optic nerve head. A. Picture of experimental setup on a Zeiss Axiovert 200 microscope equipped with a micromanipulator, with a gold seal slide with two rings to hold the cell suspension and the washing buffer. (B) Picture of a dissociated cell showing the morphology of optic nerve head astrocytes with elongated cell bodies and long primary processes. (C) Agarose gels showing results of single-cell RT-PCR. Presence of astrocyte marker (*gfap*) and absence of microglia marker (*cd4*5) confirmed the identity of the cells as astrocytes. *Gapdh* was used as a positive control. M-molecular weight pattern. 1-5- numbers of different preparations of isolated astrocytes. Scale bars: 40µm.

The RNA started to be quantifiable at 0.001 (vertical exe) that correspond to the amplification cycle of PCR number 10 for the endogenous control gene *oza1* for control and crush ONH (Fig 2 A). This means that there is no variation of expression of the *oaz1* gen after optic nerve crush. However, for the gen *spp1*, the gene start to be quantifiable in the cycle number 18 for control and cycle number 14 in crush ONH, entailing that after crush, the amount of RNA is higher and it is detectable in smaller cycles. The three lines of each experimental replicate are also overlapped, indicating reliable results.

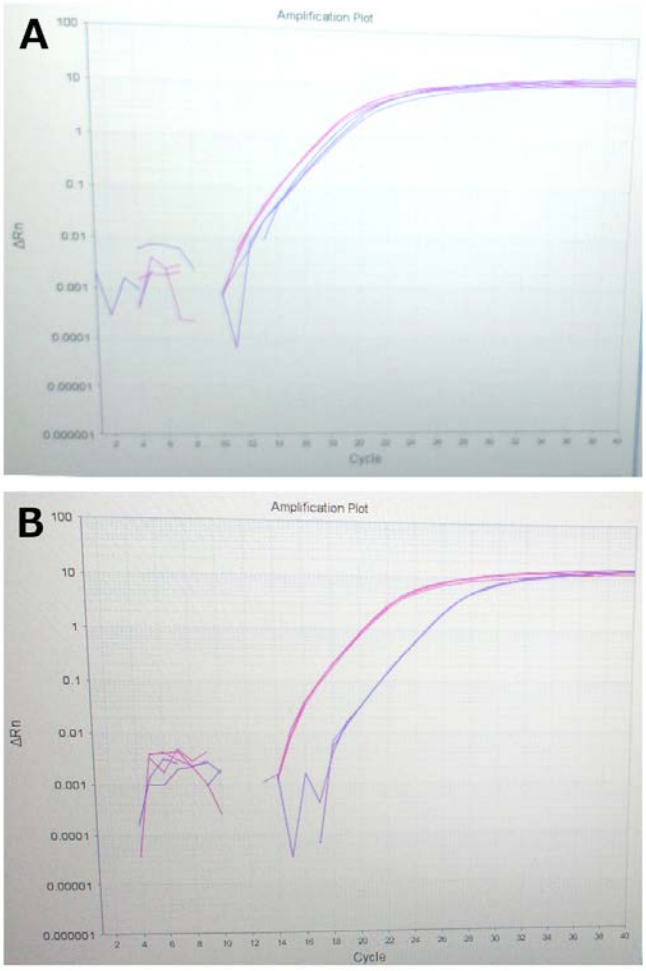

Fig 2. Quantitative PCR from optic nerve head 1 day after optic nerve crush. Amplification curves for the expression of the *oaz1* gene (A), as endogenous control, and *spp1* gene (B) in the optic nerve head from control (purple) versus crushed (pink) optic nerves. 3 experimental replicas were performed for each condition and for each gen, each line represent one experimental replicate.

In addition to *spp1*, we tested the expression levels of the genes *cd44* (receptor of SPP1), *lcn2* and *lif* in four biological replicates for each condition. The fold change of up-regulation for each gen was calculated and the data was represented in the Table 1.

For *spp1*, this data indicate a 9.16±0.68–fold up-regulation in the ONH at day 1 after optic nerve crush, and this increment is significant higher than in control (p value = 2,04E-05).

Although it is evident a high up-regulation of the other genes after the optic nerve crush, the expression fold change is highly variable, and there are not significant differences with respect to the control.

	spp1	*cd44*	*lcn2*	*lif*
	8.78	89.77	12.53	1.71
	7.49	43.48	2613.01	62.74
	9.64	2.01	6780.62	24.85
	10.71	562.94	15.38	11.72
Mean	9.16	174.55	2355.38	25.26
Standard Error	0.68	130.69	1597.22	13.36

Table 1. Data of the biological replicates of the QPCR for the four candidate genes. The represented number is the expression fold change. These data have as reference the endogenous gen *oaz1* for each biological replica, which represent 1. These values represent the number of times that is up-regulated the gene after crush with respect to the control. The mean and the standard error of the mean for each gen are indicated.

After RNA quantification, we wanted to check if the amount of these proteins is also up-regulated after a optic nerve crush to serve a molecular biomarker of damage. For this purpose, after develop the technique, ELISA for SPP1, LCN2 and LIF proteins were performed in the whole ONH, 1, 4 and 8 days after optic nerve crush (Table 2).

	SPP1	LCN2	LIF
Control 1d	0.017	0.000	0.038
Crush 1d	0.017	0.021	0.021
Control 4d	0.051	0.011	0.010
Crush 4d	0.012	0.022	0.013
Control 8d	0.014	0.008	-
Crush 8d	0.007	0.008	-

Table 2. Values of absorbance results of the ELISA for SPP1, LCN2 and LIF proteins in the optic nerve head. The samples were collected at day 1, 4 and 8 after optic nerve crush, the uninjured contralateral eye represent the control.

SPP1 and LIF proteins did not changed after crush the optic nerve. However, LCN2 protein tended to be up-regulated at day 1 and 4 after optic nerve crush, therefore it could be a candidate biomarker. After the extrapolation of the absorbance values with the standard curve of LCN2, we calculated that 1 day after crush, the LCN2 concentration is 1ng/µg of total protein.

On the other hand, we are particularly interested in checking if this protein could migrate from the optic nerve head to the aqueous humour to be a biomarker easily measured. For that reason, we collected some samples of aqueous humour of these mice to quantify LCN2 by ELISA. The results are in the Table 3.

	LCN2
Control 1d	0.013
Crush 1d	0.096
Control 4d	0.031
Crush 4d	0.011

Table 3. Values of absorbance results of the ELISA for LCN2 protein in the aqueous humour. The samples were collected at day 1 and 4 after optic nerve crush, the uninjured contralateral eye represent the control.

LCN2 appeared up-regulated in the aqueous humour 1 day after optic nerve crush, but it reverted at day 4. Although this result shows that LCN2 could be a good molecular biomarker of damage, more biological replicas are needed to demonstrate and quantify this fact.

Discussion

Biomarkers in disease detection and management have become important tools in modern clinical medicine, including retinal diseases. The proteins that we selected could be good candidates as biomarkers due to they are up-regulated after damage (Birke et al., 2010; Johnson et al., 2011; Khalyfa et al., 2007; Parmar et al., 2016; Qu and Jakobs, 2013).

Since the amount of RNA form single astrocytes isolated was not enough to quantify the increment of the selected molecules, we had to use the complete optic nerve head to demonstrate the protein upregulation of the markers, thus we can not conclude that are astrocytes but not other glial cells the responsible for the increment of the markers. However we were able of isolate single astrocytes from the mice optic nerve head.

In addition, the QPCR results of the ONH were variable and not consistent. This may be due to the variability of these molecules in control condition that are very low or absent, and under the experimental condition, they vary very much their expression. But we

could confirm that the RNA of these genes are up-regulated after optic nerve crush, although we cannot demonstrate the exactly quantification. However, the data for *spp1* were homogeneous, and we could demonstrate that the osteopontin RNA increase 9 fold in the ONH the first day after optic nerve crush.

The proteins of our candidate biomarkers were also quantified. Interestingly, only LCN2 seems to be up-regulated, and it reverted at day 8 after optic nerve crush, confirming that this up-regulation is reversible, as it has been demonstrated before (Qu and Jakobs, 2013). In addition, more studies are necessary to confirm the concentration of LCN2 after optic nerve crush, because it seems to be too high for a cytokine as it is the LCN2.

The main objective was to be able to detect glaucoma in its initial stages, when the damage to the optic nerve head begins. In addition, the method to detect and quantify the molecules has to be safe, easy and low-invasive, and it could be possible with a simple analysis of the aqueous humour. Thus we quantified the protein LCN2 in the aqueous humour, and there is evidence that could be detected at day 1 after optic nerve crush, shown damage in the optic nerve head. However, the damage should be maintained to perform a long-term monitoring, event that could be feasible in glaucoma.

Although the experiments would have to be repeated to demonstrate these facts, the results are looking promising and it is a good starting point to continue the search for biomarkers of diseases involving damage to the optic nerve head.

References

Agca, C., Grimm, C., 2014. Leukemia inhibitory factor signaling in degenerating retinas. Adv. Exp. Med. Biol. 801, 389-394.

Agnifili, L., Pieragostino, D., Mastropasqua, A., Fasanella, V., Brescia, L., Tosi, G.M., Sacchetta, P., Mastropasqua, L., 2015. Molecular biomarkers in primary open-angle glaucoma: from noninvasive to invasive. Prog. Brain Res. 221, 1-32.

Birke, M.T., Neumann, C., Birke, K., Kremers, J., Scholz, M., 2010. Changes of osteopontin in the aqueous humor of the DBA2/J glaucoma model correlated with optic nerve and RGC degenerations. Invest. Ophthalmol. Vis. Sci. 51, 5759-5767.

Bosco, A., Steele, M.R., Vetter, M.L., 2011. Early microglia activation in a mouse model of chronic glaucoma. J. Comp. Neurol. 519, 599-620.

Burgoyne, C.F., Downs, J.C., Bellezza, A.J., Suh, J.K., Hart, R.T., 2005. The optic nerve head as a biomechanical structure: a new paradigm for understanding the

role of IOP-related stress and strain in the pathophysiology of glaucomatous optic nerve head damage. Prog. Retin. Eye Res. 24, 39-73.

Choi, H.J., Sun, D., Jakobs, T.C., 2015. Isolation of intact astrocytes from the optic nerve head of adult mice. Exp. Eye Res. 137, 103-110.

Howell, G.R., Libby, R.T., Jakobs, T.C., Smith, R.S., Phalan, F.C., Barter, J.W., Barbay, J.M., Marchant, J.K., Mahesh, N., Porciatti, V., Whitmore, A.V., Masland, R.H., John, S.W., 2007. Axons of retinal ganglion cells are insulted in the optic nerve early in DBA/2J glaucoma. J. Cell Biol. 179, 1523-1537.

Howell, G.R., Macalinao, D.G., Sousa, G.L., Walden, M., Soto, I., Kneeland, S.C., Barbay, J.M., King, B.L., Marchant, J.K., Hibbs, M., Stevens, B., Barres, B.A., Clark, A.F., Libby, R.T., John, S.W., 2011. Molecular clustering identifies complement and endothelin induction as early events in a mouse model of glaucoma. J. Clin. Invest. 121, 1429-1444.

Jakobs, T.C., Libby, R.T., Ben, Y., John, S.W., Masland, R.H., 2005. Retinal ganglion cell degeneration is topological but not cell type specific in DBA/2J mice. J. Cell Biol. 171, 313-325.

Johnson, E.C., Doser, T.A., Cepurna, W.O., Dyck, J.A., Jia, L., Guo, Y., Lambert, W.S., Morrison, J.C., 2011. Cell proliferation and interleukin-6-type cytokine signaling are implicated by gene expression responses in early optic nerve head injury in rat glaucoma. Invest. Ophthalmol. Vis. Sci. 52, 504-518.

Johnson, E.C., Jia, L., Cepurna, W.O., Doser, T.A., Morrison, J.C., 2007. Global changes in optic nerve head gene expression after exposure to elevated intraocular pressure in a rat glaucoma model. Invest. Ophthalmol. Vis. Sci. 48, 3161-3177.

Khalyfa, A., Chlon, T., Qiang, H., Agarwal, N., Cooper, N.G., 2007. Microarray reveals complement components are regulated in the serum-deprived rat retinal ganglion cell line. Mol. Vis. 13, 293-308.

Meller, R., Stevens, S.L., Minami, M., Cameron, J.A., King, S., Rosenzweig, H., Doyle, K., Lessov, N.S., Simon, R.P., Stenzel-Poore, M.P., 2005. Neuroprotection by osteopontin in stroke. J. Cereb. Blood Flow Metab. 25, 217-225.

Parmar, T., Parmar, V.M., Arai, E., Sahu, B., Perusek, L., Maeda, A., 2016. Acute Stress Responses Are Early Molecular Events of Retinal Degeneration in Abca4-/-Rdh8-/- Mice After Light Exposure. Invest. Ophthalmol. Vis. Sci. 57, 3257-3267.

Qu, J., Jakobs, T.C., 2013. The Time Course of Gene Expression during Reactive Gliosis in the Optic Nerve. PLoS One 8, e67094.

Quigley, H.A., Addicks, E.M., Green, W.R., Maumenee, A.E., 1981. Optic nerve damage in human glaucoma. II. The site of injury and susceptibility to damage. Arch. Ophthalmol. 99, 635-649.

Samardzija, M., Wariwoda, H., Imsand, C., Huber, P., Heynen, S.R., Gubler, A., Grimm, C., 2012. Activation of survival pathways in the degenerating retina of rd10 mice. Exp. Eye Res. 99, 17-26.

Topkoru, B.C., Altay, O., Duris, K., Krafft, P.R., Yan, J., Zhang, J.H., 2013. Nasal administration of recombinant osteopontin attenuates early brain injury after subarachnoid hemorrhage. Stroke 44, 3189-3194.

von Toerne, C., Menzler, J., Ly, A., Senninger, N., Ueffing, M., Hauck, S.M., 2014. Identification of a novel neurotrophic factor from primary retinal Muller cells using stable isotope labeling by amino acids in cell culture (SILAC). Mol. Cell. Proteomics 13, 2371-2381.

Xing, C., Wang, X., Cheng, C., Montaner, J., Mandeville, E., Leung, W., van Leyen, K., Lok, J., Wang, X., Lo, E.H., 2014. Neuronal production of lipocalin-2 as a help-me signal for glial activation. Stroke 45, 2085-2092.

5. DISCUSIÓN

Las células ganglionares de la retina son las neuronas encargadas de transmitir la información visual desde la retina al cerebro, principalmente en el núcleo geniculado lateral y en el colículo superior, a través de sus axones, que forman el nervio óptico (Wassle and Boycott, 1991). Estas células interaccionan con las células gliales presentes en la retina, como son las células de Müller, los astrocitos y la microglía (Kolb, 2003; Vecino et al., 2016). El estudio de esta interacción entre la glía y las RGCs nos permite conocer su papel tanto en retinas sanas como en patológicas.

Como ha sido previamente mencionado, la patología de mayor interés para nuestro estudio es el glaucoma, donde se produce una muerte selectiva de las RGCs, lo que conduce a una ceguera irreversible (Garcia-Valenzuela et al., 1995; Vecino and Sharma, 2011)(Mi et al., 2014; Quigley, 2011; Rieck, 2013). La hipoxia, o un inadecuado o disminuido suministro de oxigeno, podría estar relacionado con el inicio de esta patología, así como de otras patologías importantes como la degeneración macular asociada a la edad o la retinopatía diabética (Grimm and Willmann, 2012). Con el objetivo de estudiar la etiología de esta enfermedad, se ha analizado la respuesta ante una reducción en la tensión de oxigeno, como símil a los primeros estadíos de la enfermedad. Además de las RGCs, en este estudio también han sido analizados los astrocitos dada su vinculación entre los vasos sanguíneos y las neuronas, y debido a que pueden ser las primeras células que perciban la falta de oxigeno (Chan-Ling and Stone, 1992; Garcia et al., 1993). A su vez, y debido a la diferente susceptibilidad que pueden tener distintas regiones del sistema nervioso (Arduini et al., 2014), se ha realizado un estudio comparativo con las neuronas y los astrocitos del colículo superior. Sorprendentemente, la hipoxia no indujo cambios significativos en el número de RGCs en la retina ni en la activación de la apoptosis, aunque sí se produjo un aumento en el número de células positivas a caspasa-3 en el colículo superior, indicando un aumento de la muerte celular por apoptosis. Además, la hipoxia indujo cambios en la morfología de los astrocitos en el colículo superior, pero no en la retina. Estos resultados nos sugieren que las condiciones de hipoxia en las que se llevó a cabo el estudio no afectan a la retina, pero sí afectan al cerebro (Ruzafa et al., 2017b) (Anexo 1). La diferente respuesta entre estos dos tejidos puede deberse a la heterogeneidad metabólica en estas diferentes áreas del sistema nervioso central (Greisen, 2005). Además, el hecho de que la retina pueda ser más resistente a la hipoxia podría deberse a la presencia de las células Müller, que aunque comparten muchas funciones con los astrocitos, tienen

funciones especializadas relacionadas con el apoyo homeostático y metabólico de las neuronas de la retina (Reichenbach and Bringmann, 2013; Vecino et al., 2016), asimismo, podría estar relacionado con la capacidad de estas células de secretar neurotrofinas y factores de crecimiento (Vecino et al., 1998b; Vecino et al., 2016).

Debido a que las células de Müller pueden tener la capacidad de hacer que la retina sea más resistente que otras zonas del sistema nervioso central, nos propusimos estudiar con profundidad las propiedades neuroprotectoras de estas células. Para esto, nos trasladamos a modelos *in vitro*, en el que se ha demostrado que las RGCs que han crecido sobre una monocapa de células de Müller, presentaban una mayor supervivencia, un aumento del tamaño del soma, y un aumento del crecimiento de neuritas (Garcia et al., 2002; Ruzafa and Vecino, 2015) (Anexo 2). Y sabiendo que la liberación de factores neurotróficos por parte de la células de Müller puede ser responsable de estas propiedades neuroprotectoras (Meyer-Franke et al., 1995), nos centramos en analizar los factores secretados por las células de Müller con el fin de identificar factores noveles con capacidad neuroprotectora sobre las RGCs. Para esto, nos basamos en una estrategia en la que cultivamos células de Müller con distintos medios de cultivo, estas células tienen un secretoma diferente y por tanto el efecto de este sobre la supervivencia y neuritogenesis de las RGCs también es distinto. Mediante esta estrategia proteómica cuantitativa en la que comparamos las proteínas de los distintos secretomas pudimos seleccionar 3 proteínas con posible capacidad protectora, estas son la osteopontina (SPP1), la clusterina (CLU) y la basigina (BSG). Tras probar el efecto de añadir estas proteínas recombinantes en un cultivo de RGCs, demostramos que tanto BSG como SPP1 aumentan la supervivencia de los RGC (Anexo 3), con valores incluso más altos que el control positivo PDGF, que ya había sido demostrado como un potente factor neuroprotector de las RGCs (He et al., 2014; Tang et al., 2010). Sin embargo, una proteína o la suma de dos de ellas no lograron superar el efecto del medio condicionado, lo que indica que la actividad promotora de la supervivencia del medio acondicionado de células Müller es multifactorial y SPP1 y BSG son sólo una parte de esta actividad (Anexo 3). Por lo que en este estudio, además de confirmar el efecto neuroprotector de las células de Müller, ha sido desarrollado un modelo basado en los cultivos primarios adecuado para estudiar la neuroprotección de las RGCs asociada a células Müller. También hay que destacar la estrategia proteómica basada en el análisis funcional, en este caso, en el efecto sobre la supervivencia de las RGCs, lo

que ha permitido validar no sólo factores neurotróficos conocidos, sino nuevas proteínas candidatas secretadas por células de Müller. Esta estrategia es aplicable también a la búsqueda de otras moléculas bioactivas o marcadores moleculares debido a que permite la caracterización de moléculas individuales derivadas de mezclas complejas.

Por lo tanto, los modelos de cultivos celulares que se han desarrollado en esta tesis doctoral nos han permitido la realización de estudios de otras posibles sustancias con capacidad neuroprotectora, además de los factores secretados por las células de Müller. Este es el caso del PRGF, ya que inicialmente se partía de la idea de que podría ser un novel tratamiento frente a enfermedades neurodegenerativas (Anitua et al., 2014; Anitua et al., 2013; Anitua et al., 2015). Desafortunadamente, nuestros estudios en las células de la retina revelan que, además de reducir drásticamente la supervivencia de las RGCs, induce la activación del proceso inflamatorio favoreciendo la migración de la microglía. Sin embargo, posee capacidades proliferativas demostradas como un aumento del número de células de Müller (Anexo 4). El efecto negativo sobre las RGCs puede deberse a que puede ser neurotóxico al igual que el plasma rico en plaquetas activado por trombina, debido a la liberación de glutamato (Bell et al., 2014), o debido a la presencia de moléculas como TGF-β1, presente en el PRGF, que ejerce efectos negativos sobre el crecimiento axonal (Takeuchi et al., 2012). A su vez, también puede ser debido a la activación de la respuesta inflamatoria ya que hemos confirmado y cuantificado la presencia de las citoquinas IL-1α, IL-1ß, IL-2, IL-4, IL-6, IL-8, IL-10, IL-12, IL13, IL-15, IL-17, IL-23, TNFα y TNFß tanto en el PRGF humano como en el porcino (Anexo 4).

Debido a que la osteopontina ha sido una molécula de estudio por nuestro grupo debido a que promueve la supervivencia de neuronas de la retina como los fotorreceptores (Del Rio et al., 2011), y tras confirmar su efecto positivo en la superviviencia de las RGCs, surge la necesidad de caracterizar esta molécula que puede ser de gran interés para la elaboración de estrategias terapéuticas con el fin de proteger las RGCs. Por esto, el análisis de la retina de ratones *knock-out* para esta proteína nos ha ayudado a conocer sus funciones y su implicación en el normal funcionamiento de la retina (Ruzafa et al., 2017a) (Anexo 5). La deficiencia en OPN reduce la densidad de RGCs en un 25% a los 3 meses de edad y en un 60% a los 20 meses de edad, este hecho se puede deber principalmente al efecto neuroprotector de OPN, que ha sido demostrado previamente en RGCs (Birke et al., 2010; Chidlow et al., 2008). El área de astrocitos también se

redujo en un 51% en ratones de 3 meses de edad y en un 58% a los 20 meses de edad. Esta reducción de la superficie ocupada por astrocitos podría ser una consecuencia de la ausencia del papel que tiene la OPN en la adhesión celular, la migración, y la supervivencia, además de la influencia en la actividad metabólica, de los astrocitos (Neumann et al., 2014). Sin embargo, las células de Müller y la microglia no se vieron afectadas. La OPN podría ser una molécula candidata para desarrollar terapias para combatir enfermedades neurodegenerativas, en las que se vean afectadas neuronas como las RGCs, siendo los astrocitos la célula diana en la que actuar, ya que teniendo en cuenta la edad, la reducción de RGCs parece ser secundaria a la desaparición de los astrocitos.

Otro de nuestros principales objetivos, además de la identificación de proteínas neuroprotectoras, ha sido la de buscar marcadores moleculares relacionados con el daño en las RGCs. La osteopontina, además de su función neuroprotectora, también puede ser un indicador de daño ya que, junto a otras moléculas como la lipocalina 2 (LCN2) o el factor inhibidor de leucemia (LIF), ha sido confirmada su sobreexpresión en glaucoma, tras el pinzamiento del nervio óptico, o tras otro daño inducido a las RGCs (Birke et al., 2010; Khalyfa et al., 2007; Qu and Jakobs, 2013). Tras analizar la cabeza del nervio óptico de ratones que han sido sometidos a un pinzamiento del nervio óptico, hemos comprobado que el gen de la osteopontina se sobreexpresa más de 9 veces. Sin embargo, esta cuantificación en otros genes no ha sido consistente debido a que estas moléculas en control están prácticamente ausentes, y tras un daño, la sobreexpresión es muy variable. Respecto a la cuantificación a nivel proteico, solo LCN2 parece aumentar a día 1 y 4 tras el pinzamiento del nervio óptico en la cabeza de este nervio. Pero para poder servir de marcador molecular, se analizó su sobreexpresión en el humor acuoso, y se vio que podía mantenerse un día tras el daño, pero revertía a día 4 (Anexo 6). Estos resultados parecen prometedores y pueden ser un buen punto de partida para la búsqueda de marcadores moleculares secretados por las células de la glía, en este caso probablemente secretados por astrocitos, de daño sobre las RGCs, aunque se necesitan más estudios para comprobar estos resultados.

En conclusión, las células de la glía están integradas con las neuronas que forman la retina, permitiendo un correcto funcionamiento de este tejido. Por lo tanto, es crucial que cuando se exploran los cambios dentro de la retina, exista un enfoque integrado

entre las interacciones de la glía con las neuronas, con el fin de comprender plenamente la retina sana o sometida a una enfermedad o lesión. Esta tesis doctoral ha demostrado la estrecha relación entre la glía y las células ganglionares, ya que ante un daño, no solo las células ganglionares se ven afectadas, sino que las células de la glía también responden a este estimulo. Por lo tanto, la glía retiniana puede servir de sensor frente a un daño en la retina cambiando su morfología o secretando marcadores moleculares, y a su vez, podemos aprovechar su capacidad neuroportectora para desarrollar estrategias terapeuticas contra enfermedades neurodegenerativas en las que se vean afectadas las células ganglionares de la retina, como ocurre en el glaucoma.

6. CONCLUSIONES/ CONCLUSIONS

Tras la realización de esta Tesis Doctoral, se han llegado a las siguientes conclusiones:

1- En animales neonatales, en los momentos iniciales tras un daño hipóxico, la retina se afecta en menor grado que al cerebro. Estas diferencias son posiblemente debidas a la presencia de las células de Müller en la retina.
2- Las células de Müller tienen un efecto neuroprotector sobre las células ganglionares de la retina *in vitro*. Esta función se ejerce tanto por contacto como mediante factores secretados.
3- Del análisis proteómico de los factores secretados por las células de Müller, han sido seleccionadas tres proteínas: osteopontina, basigina y clusterina, de las cuales, se ha confirmado el efecto neuroprotector de osteopontina y basigina. No descartamos que además de estas, existan otras proteínas no seleccionadas que puedan tener un efecto sinérgico y neuroprotector.
4- El PRGF (plasma rico en factores de crecimiento) produce la muerte de las células ganglionares de la retina *in vitro*, descartando su posible papel neuroprotector. Además, activa mecanismos de inflamación, observados por la migración de la microglía, posiblemente debido a la presencia de citoquinas inflamatorias en el PRGF. A su vez, induce la proliferación de células de Müller.
5- La ausencia de osteopontina en animales *knock-out* causa la muerte de células ganglionares de la retina así como una disminución del área ocupada por astrocitos, por lo que podría ser una proteína candidata con función neuroprotectora en la retina.
6- La osteopontina puede ser utilizada como un biomarcador de daño ya que sus niveles de RNA aumentan más de 9 veces en la cabeza del nervio óptico después del pinzamiento del nervio óptico. Sin embargo, más estudios son requeridos para cuantificar la sobreexpresión de los niveles de proteína, tanto de osteopontina como de lipocalina 2, en la cabeza del nervio óptico y en el humor acuoso.

Following the completion of this Doctoral Thesis, the following conclusions can be drawn:

1- In the initial moments after hypoxic damage in neonatal animals the retina is affected to a lesser extent than the brain, a difference that is possibly due to the presence of Müller cells in the retina.
2- Müller cells have a neuroprotective effect on retinal ganglion cells *in vitro*. This function is exerted by cell-cell contact and by secreted factors.
3- Through a proteomic analysis of the factors secreted by Müller cells, three proteins that may exert a neuroprotective effect were identified: osteopontin, basigin and clusterin. The neuroprotection afforded by osteopontin and basigin has been confirmed, yet we do not rule out the possibility that there are other proteins in addition to these that may have a synergistic neuroprotective effect.
4- PRGF (plasma rich in growth factors) causes the death of retinal ganglion cells *in vitro*, ruling out a possible neuroprotective role. Indeed, it activates inflammation, as witnessed through the migration of the microglia, possibly due to the presence of inflammatory cytokines. Moreover, PRGF induces the proliferation of Müller cells.
5- The absence of osteopontin in *knock-out* animals causes the death of retinal ganglion cells, as well as a decrease in the area occupied by astrocytes. Hence, osteopontin could be a protein that provides neuroprotection in the retina.
6- Osteopontin can be used as a biomarker of damage since after optic nerve crush, there is a more than 9-fold increase in its RNA transcripts at the optic nerve head. However, further studies are required to quantify the upregulation of proteins levels of osteopontin, and also of lipocalin 2, in the optic nerve head and in the aqueous humor.

7. REFERENCIAS

Agca, C., Grimm, C., 2014. Leukemia inhibitory factor signaling in degenerating retinas. Adv. Exp. Med. Biol. 801, 389-394.

Agnifili, L., Pieragostino, D., Mastropasqua, A., Fasanella, V., Brescia, L., Tosi, G.M., Sacchetta, P., Mastropasqua, L., 2015. Molecular biomarkers in primary open-angle glaucoma: from noninvasive to invasive. Prog. Brain Res. 221, 1-32.

Amthor, F.R., Oyster, C.W., Takahashi, E.S., 1984. Morphology of on-off direction-selective ganglion cells in the rabbit retina. Brain Res. 298, 187-190.

Anitua, E., Muruzabal, F., de la Fuente, M., Merayo, J., Duran, J., Orive, G., 2016a. Plasma Rich in Growth Factors for the Treatment of Ocular Surface Diseases. Curr. Eye Res. 41, 875-882.

Anitua, E., Muruzabal, F., de la Fuente, M., Riestra, A., Merayo-Lloves, J., Orive, G., 2016b. PRGF exerts more potent proliferative and anti-inflammatory effects than autologous serum on a cell culture inflammatory model. Exp. Eye Res. 151, 115-121.

Anitua, E., Pascual, C., Antequera, D., Bolos, M., Padilla, S., Orive, G., Carro, E., 2014. Plasma rich in growth factors (PRGF-Endoret) reduces neuropathologic hallmarks and improves cognitive functions in an Alzheimer's disease mouse model. Neurobiol. Aging 35, 1582-1595.

Anitua, E., Pascual, C., Perez-Gonzalez, R., Antequera, D., Padilla, S., Orive, G., Carro, E., 2013. Intranasal delivery of plasma and platelet growth factors using PRGF-Endoret system enhances neurogenesis in a mouse model of Alzheimer's disease. PLoS One 8, e73118.

Anitua, E., Pascual, C., Perez-Gonzalez, R., Orive, G., Carro, E., 2015. Intranasal PRGF-Endoret enhances neuronal survival and attenuates NF-kappaB-dependent inflammation process in a mouse model of Parkinson's disease. J. Control. Release 203, 170-180.

Anitua, E., Sanchez, M., Orive, G., 2010. Potential of endogenous regenerative technology for in situ regenerative medicine. Advanced drug delivery reviews 62, 741-752.

Arduini, A., Escobar, J., Vento, M., Escrig, R., Quintas, G., Sastre, J., Saugstad, O.D., Solberg, R., 2014. Metabolic adaptation and neuroprotection differ in the retina and choroid in a piglet model of acute postnatal hypoxia. Pediatr. Res.

Barres, B.A., 2008. The mystery and magic of glia: a perspective on their roles in health and disease. Neuron 60, 430-440.

Beauchemin, M.L., 1974. The fine structure of the pig's retina. Albrecht Von Graefes Arch. Klin. Exp. Ophthalmol. 190, 27-45.

Bell, J.D., Thomas, T.C., Lass, E., Ai, J., Wan, H., Lifshitz, J., Baker, A.J., Macdonald, R.L., 2014. Platelet-mediated changes to neuronal glutamate receptor expression at sites of microthrombosis following experimental subarachnoid hemorrhage. J. Neurosurg. 121, 1424-1431.

Bevensee, M.O., Boron, W.F., 2008. Effects of acute hypoxia on intracellular-pH regulation in astrocytes cultured from rat hippocampus. Brain Res. 1193, 143-152.

Bilimoria, P.M., Stevens, B., 2014. Microglia function during brain development: New insights from animal models. Brain Res.

Birke, M.T., Neumann, C., Birke, K., Kremers, J., Scholz, M., 2010. Changes of osteopontin in the aqueous humor of the DBA2/J glaucoma model correlated with optic nerve and RGC degenerations. Invest. Ophthalmol. Vis. Sci. 51, 5759-5767.

Bosco, A., Steele, M.R., Vetter, M.L., 2011. Early microglia activation in a mouse model of chronic glaucoma. J. Comp. Neurol. 519, 599-620.

Boycott, B.B., Wassle, H., 1974. The morphological types of ganglion cells of the domestic cat's retina. J. Physiol. 240, 397-419.

Bringmann, A., Iandiev, I., Pannicke, T., Wurm, A., Hollborn, M., Wiedemann, P., Osborne, N.N., Reichenbach, A., 2009. Cellular signaling and factors involved in Müller cell gliosis: Neuroprotective and detrimental effects. Prog. Retin. Eye Res. 28, 423–451.

Burda, J.E., Sofroniew, M.V., 2014. Reactive gliosis and the multicellular response to CNS damage and disease. Neuron 81, 229-248.

Burgoyne, C.F., Downs, J.C., Bellezza, A.J., Suh, J.K., Hart, R.T., 2005. The optic nerve head as a biomechanical structure: a new paradigm for understanding the role of IOP-related stress and strain in the pathophysiology of glaucomatous optic nerve head damage. Prog. Retin. Eye Res. 24, 39-73.

Bush, T.G., Puvanachandra, N., Horner, C.H., Polito, A., Ostenfeld, T., Svendsen, C.N., Mucke, L., Johnson, M.H., Sofroniew, M.V., 1999. Leukocyte infiltration, neuronal degeneration, and neurite outgrowth after ablation of scar-forming, reactive astrocytes in adult transgenic mice. Neuron 23, 297-308.

Caprara, C., Grimm, C., 2012. From oxygen to erythropoietin: relevance of hypoxia for retinal development, health and disease. Prog. Retin. Eye Res. 31, 89-119.

Chan-Ling, T., Stone, J., 1992. Degeneration of astrocytes in feline retinopathy of prematurity causes failure of the blood-retinal barrier. Invest. Ophthalmol. Vis. Sci. 33, 2148-2159.

Chen, L., Yang, P., Kijlstra, A., 2002. Distribution, markers, and functions of retinal microglia. Ocul. Immunol. Inflamm. 10, 27-39.

Chidlow, G., Wood, J.P., Manavis, J., Osborne, N.N., Casson, R.J., 2008. Expression of osteopontin in the rat retina: effects of excitotoxic and ischemic injuries. Invest. Ophthalmol. Vis. Sci. 49, 762-771.

Choi, H.J., Sun, D., Jakobs, T.C., 2015. Isolation of intact astrocytes from the optic nerve head of adult mice. Exp. Eye Res. 137, 103-110.

Dai, C., Khaw, P.T., Yin, Z.Q., Li, D., Raisman, G., Li, Y., 2012. Structural basis of glaucoma: the fortified astrocytes of the optic nerve head are the target of raised intraocular pressure. Glia 60, 13-28.

Das, A.V., Mallya, K.B., Zhao, X., Ahmad, F., Bhattacharya, S., Thoreson, W.B., Hegde, G.V., Ahmad, I., 2006. Neural stem cell properties of Muller glia in the mammalian retina: regulation by Notch and Wnt signaling. Dev. Biol. 299, 283-302.

De Schaepdrijver, L., Lauwers, H., Simoens, P., de Geest, J.P., 1990. Development of the retina in the porcine fetus. A light microscopic study. Anat. Histol. Embryol. 19, 222-235.

Del Rio, P., Irmler, M., Arango-Gonzalez, B., Favor, J., Bobe, C., Bartsch, U., Vecino, E., Beckers, J., Hauck, S.M., Ueffing, M., 2011. GDNF-induced osteopontin from Muller glial cells promotes photoreceptor survival in the Pde6brd1 mouse model of retinal degeneration. Glia 59, 821-832.

Derouiche, A., Rauen, T., 1995. Coincidence of L-glutamate/L-aspartate transporter (GLAST) and glutamine synthetase (GS) immunoreactions in retinal glia: evidence for coupling of GLAST and GS in transmitter clearance. J. Neurosci. Res. 42, 131-143.

Dorrell, M.I., Aguilar, E., Jacobson, R., Trauger, S.A., Friedlander, J., Siuzdak, G., Friedlander, M., 2010. Maintaining retinal astrocytes normalizes revascularization and prevents vascular pathology associated with oxygen-induced retinopathy. Glia 58, 43-54.

Drager, U.C., Olsen, J.F., 1981. Ganglion cell distribution in the retina of the mouse. Invest. Ophthalmol. Vis. Sci. 20, 285-293.

Dreher, B., Sefton, A.J., Ni, S.Y., Nisbett, G., 1985. The morphology, number, distribution and central projections of Class I retinal ganglion cells in albino and hooded rats. Brain. Behav. Evol. 26, 10-48.

Feigenspan, A., Bormann, J., Wassle, H., 1993. Organotypic slice culture of the mammalian retina. Vis. Neurosci. 10, 203-217.

Fischer, A.J., Reh, T.A., 2001. Muller glia are a potential source of neural regeneration in the postnatal chicken retina. Nat. Neurosci. 4, 247-252.

Fletcher, E.L., Downie, L.E., Hatzopoulos, K., Vessey, K.A., Ward, M.M., Chow, C.L., Pianta, M.J., Vingrys, A.J., Kalloniatis, M., Wilkinson-Berka, J.L., 2010. The significance of neuronal and glial cell changes in the rat retina during oxygen-induced retinopathy. Doc. Ophthalmol. 120, 67-86.

Fukuda, Y., 1977. A three-group classification of rat retinal ganglion cells: histological and physiological studies. Brain Res. 119, 327-334.

Galdos, M., Bayon, A., Rodriguez, F.D., Mico, C., Sharma, S.C., Vecino, E., 2012. Morphology of retinal vessels in the optic disk in a Gottingen minipig experimental glaucoma model. Vet. Ophthalmol. 15 Suppl 1, 36-46.

Garca, M., Ruiz-Ederra, J., Hernandez-Barbachano, H., Vecino, E., 2005. Topography of pig retinal ganglion cells. J. Comp. Neurol. 486, 361-372.

Garcia, J.H., Yoshida, Y., Chen, H., Li, Y., Zhang, Z.G., Lian, J., Chen, S., Chopp, M., 1993. Progression from ischemic injury to infarct following middle cerebral artery occlusion in the rat. Am. J. Pathol. 142, 623-635.

Garcia, M., Forster, V., Hicks, D., Vecino, E., 2002. Effects of muller glia on cell survival and neuritogenesis in adult porcine retina in vitro. Invest. Ophthalmol. Vis. Sci. 43, 3735-3743.

Garcia, M., Forster, V., Hicks, D., Vecino, E., 2003a. In vivo expression of neurotrophins and neurotrophin receptors is conserved in adult porcine retina in vitro. Invest. Ophthalmol. Vis. Sci. 44, 4532-4541.

Garcia, M., Ruiz Ederra, J., Hernandez-Barbachano, E., Urcola, J.A., Bilbao, J., Araiz, J., Duran, J.A., Vecino, E., 2003b. Retinal ganglion cell neuroprotection in culture. Arch Soc Esp Oftalmol 78, 151-157.

Garcia, M., Vecino, E., 2003. Role of Muller glia in neuroprotection and regeneration in the retina. Histol. Histopathol. 18, 1205-1218.

Garcia-Valenzuela, E., Shareef, S., Walsh, J., Sharma, S.C., 1995. Programmed cell death of retinal ganglion cells during experimental glaucoma. Exp. Eye Res. 61, 33-44.

Greisen, G., 2005. Autoregulation of cerebral blood flow in newborn babies. Early Hum. Dev. 81, 423-428.

Grigsby, J.G., Cardona, S.M., Pouw, C.E., Muniz, A., Mendiola, A.S., Tsin, A.T., Allen, D.M., Cardona, A.E., 2014. The role of microglia in diabetic retinopathy. J. Ophthalmol. 2014, 705783.

Grimm, C., Willmann, G., 2012. Hypoxia in the eye: a two-sided coin. High. Alt. Med. Biol. 13, 169-175.

Harada, C., Harada, T., Quah, H.M., Maekawa, F., Yoshida, K., Ohno, S., Wada, K., Parada, L.F., Tanaka, K., 2003. Potential role of glial cell line-derived neurotrophic factor receptors in Muller glial cells during light-induced retinal degeneration. Neuroscience 122, 229-235.

Hauck, S.M., Gloeckner, C.J., Harley, M.E., Schoeffmann, S., Boldt, K., Ekstrom, P.A., Ueffing, M., 2008. Identification of paracrine neuroprotective candidate proteins by a functional assay-driven proteomics approach. Mol. Cell. Proteomics 7, 1349-1361.

Hauck, S.M., Kinkl, N., Deeg, C.A., Swiatek-de Lange, M., Schoffmann, S., Ueffing, M., 2006. GDNF family ligands trigger indirect neuroprotective signaling in retinal glial cells. Mol. Cell Biol. 26, 2746-2757.

He, C., Zhao, C., Kumar, A., Lee, C., Chen, M., Huang, L., Wang, J., Ren, X., Jiang, Y., Chen, W., Wang, B., Gao, Z., Zhong, Z., Huang, Z., Zhang, F., Huang, B., Ding, H., Ju, R., Tang, Z., Liu, Y., Cao, Y., Li, X., Liu, X., 2014. Vasoprotective effect of PDGF-CC mediated by HMOX1 rescues retinal degeneration. Proc. Natl. Acad. Sci. U. S. A. 111, 14806-14811.

Heidinger, V., Hicks, D., Sahel, J., Dreyfus, H., 1999. Ability of retinal Muller glial cells to protect neurons against excitotoxicity in vitro depends upon maturation and neuron-glial interactions. Glia 25, 229-239.

Hernandez, M., Rodriguez, F.D., Sharma, S.C., Vecino, E., 2009a. Immunohistochemical changes in rat retinas at various time periods of elevated intraocular pressure. Mol. Vis. 15, 2696-2709.

Hernandez, M., Rodriguez, F.D., Sharma, S.C., Vecino, E., 2009b. Immunohistochemical changes in rat retinas at various time periods of elevated intraocular pressure. Mol. Vis. 15, 2696-2709.

Hernandez, M.R., Pena, J.D., Selvidge, J.A., Salvador-Silva, M., Yang, P., 2000. Hydrostatic pressure stimulates synthesis of elastin in cultured optic nerve head astrocytes. Glia 32, 122-136.

Hogan, M.J., Feeney, L., 1963. The Ultrastructure of the Retinal Vessels. Iii. Vascular-Glial Relationships. J. Ultrastruct. Res. 49, 47-64.

Hollborn, M., Jahn, K., Limb, G.A., Kohen, L., Wiedemann, P., Bringmann, A., 2004. Characterization of the basic fibroblast growth factor-evoked proliferation of the human Muller cell line, MIO-M1. Graefes Arch. Clin. Exp. Ophthalmol. 242, 414-422.

Hosoya, K., Tachikawa, M., 2012. The inner blood-retinal barrier: molecular structure and transport biology. Adv. Exp. Med. Biol. 763, 85-104.

Howell, G.R., Libby, R.T., Jakobs, T.C., Smith, R.S., Phalan, F.C., Barter, J.W., Barbay, J.M., Marchant, J.K., Mahesh, N., Porciatti, V., Whitmore, A.V., Masland, R.H., John, S.W., 2007. Axons of retinal ganglion cells are insulted in the optic nerve early in DBA/2J glaucoma. J. Cell Biol. 179, 1523-1537.

Howell, G.R., Macalinao, D.G., Sousa, G.L., Walden, M., Soto, I., Kneeland, S.C., Barbay, J.M., King, B.L., Marchant, J.K., Hibbs, M., Stevens, B., Barres, B.A., Clark, A.F., Libby, R.T., John, S.W., 2011. Molecular clustering identifies complement and endothelin induction as early events in a mouse model of glaucoma. J. Clin. Invest. 121, 1429-1444.

Hurley, J.B., Chertov, A.O., Lindsay, K., Giamarco, M., Cleghorn, W., Du, J., Brockerhoff, S., 2014. Vertebrate photoreceptors: functional molecular bases, Energy Metabolism in the Vertebrate Retina.

Izumi, Y., Kirby, C.O., Benz, A.M., Olney, J.W., Zorumski, C.F., 1999. Muller cell swelling, glutamate uptake, and excitotoxic neurodegeneration in the isolated rat retina. Glia 25, 379-389.

Jain, V., Ravindran, E., Dhingra, N.K., 2012. Differential expression of Brn3 transcription factors in intrinsically photosensitive retinal ganglion cells in mouse. J. Comp. Neurol. 520, 742-755.

Jakobs, T.C., Libby, R.T., Ben, Y., John, S.W., Masland, R.H., 2005. Retinal ganglion cell degeneration is topological but not cell type specific in DBA/2J mice. J. Cell Biol. 171, 313-325.

Jeon, C.J., Strettoi, E., Masland, R.H., 1998. The major cell populations of the mouse retina. J. Neurosci. 18, 8936-8946.

Johnson, E.C., Doser, T.A., Cepurna, W.O., Dyck, J.A., Jia, L., Guo, Y., Lambert, W.S., Morrison, J.C., 2011. Cell proliferation and interleukin-6-type cytokine signaling are implicated by gene expression responses in early optic nerve head injury in rat glaucoma. Invest. Ophthalmol. Vis. Sci. 52, 504-518.

Johnson, E.C., Jia, L., Cepurna, W.O., Doser, T.A., Morrison, J.C., 2007. Global changes in optic nerve head gene expression after exposure to elevated intraocular pressure in a rat glaucoma model. Invest. Ophthalmol. Vis. Sci. 48, 3161-3177.

Karschin, A., Wassle, H., Schnitzer, J., 1986. Shape and distribution of astrocytes in the cat retina. Invest. Ophthalmol. Vis. Sci. 27, 828-831.

Kawasaki, A., Otori, Y., Barnstable, C.J., 2000. Muller cell protection of rat retinal ganglion cells from glutamate and nitric oxide neurotoxicity. Invest. Ophthalmol. Vis. Sci. 41, 3444-3450.

Kergoat, H., Herard, M.E., Lemay, M., 2006. RGC sensitivity to mild systemic hypoxia. Invest. Ophthalmol. Vis. Sci. 47, 5423-5427.

Kettenmann, H., Hanisch, U.K., Noda, M., Verkhratsky, A., 2011. Physiology of microglia. Physiol. Rev. 91, 461-553.

Khalyfa, A., Chlon, T., Qiang, H., Agarwal, N., Cooper, N.G., 2007. Microarray reveals complement components are regulated in the serum-deprived rat retinal ganglion cell line. Mol. Vis. 13, 293-308.

Kitano, S., Morgan, J., Caprioli, J., 1996. Hypoxic and excitotoxic damage to cultured rat retinal ganglion cells. Exp. Eye Res. 63, 105-112.

Kolb, H., 2003. How the Retina Works: Much of the construction of an image takes place in the retina itself through the use of specialized neural circuits. Am. Sci. 91, 28-35.

Komaromy, A.M., Brooks, D.E., Kallberg, M.E., Dawson, W.W., Szel, A., Lukats, A., Samuelson, D.A., Sapp, H.L., Jr., Gelatt, K.N., Sherwood, M.B., 2003. Long-term effect of retinal ganglion cell axotomy on the histomorphometry of other cells in the porcine retina. J. Glaucoma 12, 307-315.

Labin, A.M., Ribak, E.N., 2010. Retinal glial cells enhance human vision acuity. Phys. Rev. Lett. 104, 158102.

Langmann, T., 2007. Microglia activation in retinal degeneration. J. Leukocyte Biol. 81, 1345-1351.

Leventhal, A.G., Rodieck, R.W., Dreher, B., 1981. Retinal ganglion cell classes in the Old World monkey: morphology and central projections. Science 213, 1139-1142.

Li, Z.Y., Wong, F., Chang, J.H., Possin, D.E., Hao, Y., Petters, R.M., Milam, A.H., 1998. Rhodopsin transgenic pigs as a model for human retinitis pigmentosa. Invest. Ophthalmol. Vis. Sci. 39, 808-819.

Lindqvist, N., Liu, Q., Zajadacz, J., Franze, K., Reichenbach, A., 2010. Retinal glial (Müller) cells: sensing and responding to tissue stretch. Invest. Ophthalmol. Vis. Sci. 51, 1683–1690. .

Ling, E.A., Wong, W.C., 1993. The origin and nature of ramified and amoeboid microglia: a historical review and current concepts. Glia 7, 9-18.

Lu, Y.B., Iandiev, I., Hollborn, M., Korber, N., Ulbricht, E., Hirrlinger, P.G., Pannicke, T., Wei, E.Q., Bringmann, A., Wolburg, H., Wilhelmsson, U., Pekny, M., Wiedemann, P., Reichenbach, A., Kas, J.A., 2011. Reactive glial cells: increased stiffness correlates with increased intermediate filament expression. FASEB J. 25, 624-631.

Luna, G., Lewis, G.P., Banna, C.D., Skalli, O., Fisher, S.K., 2010. Expression profiles of nestin and synemin in reactive astrocytes and Muller cells following retinal

injury: a comparison with glial fibrillar acidic protein and vimentin. Mol. Vis. 16, 2511-2523.

Luo, X., Heidinger, V., Picaud, S., Lambrou, G., Dreyfus, H., Sahel, J., Hicks, D., 2001. Selective excitotoxic degeneration of adult pig retinal ganglion cells in vitro. Invest. Ophthalmol. Vis. Sci. 42, 1096-1106.

Lye-Barthel, M., Sun, D., Jakobs, T.C., 2013. Morphology of astrocytes in a glaucomatous optic nerve. Invest. Ophthalmol. Vis. Sci. 54, 909-917.

Ma, W., Zhao, L., Fontainhas, A.M., Fariss, R.N., Wong, W.T., 2009. Microglia in the mouse retina alter the structure and function of retinal pigmented epithelial cells: a potential cellular interaction relevant to AMD. PLoS One 4, e7945.

Ma, W., Zhao, L., Wong, W.T., 2012. Microglia in the outer retina and their relevance to pathogenesis of age-related macular degeneration. Adv. Exp. Med. Biol. 723, 37-42.

Mann, I., 1964. The development of the human eye, New York.

Masland, R.H., 2001. Neuronal diversity in the retina. Curr. Opin. Neurobiol. 11, 431-436.

Matteucci, A., Gaddini, L., Villa, M., Varano, M., Parravano, M.C., Monteleone, V., Cavallo, F., Leo, L., Mallozzi, C., Malchiodi-Albedi, F., Pricci, F., 2014. Neuroprotection by rat Müller glia against high glucose-induced neurodegeneration through a mechanism involving ERK1/2 activation. Exp. Eye Res. 125, 20-29.

Matyash, V., Kettenmann, H., 2010. Heterogeneity in astrocyte morphology and physiology. Brain Res. Rev. 63, 2-10.

Mauch, D.H., Nagler, K., Schumacher, S., Goritz, C., Muller, E.C., Otto, A., Pfrieger, F.W., 2001. CNS synaptogenesis promoted by glia-derived cholesterol. Science 294, 1354-1357.

Meller, R., Stevens, S.L., Minami, M., Cameron, J.A., King, S., Rosenzweig, H., Doyle, K., Lessov, N.S., Simon, R.P., Stenzel-Poore, M.P., 2005. Neuroprotection by osteopontin in stroke. J. Cereb. Blood Flow Metab. 25, 217-225.

Mey, J., Thanos, S., 1993. Intravitreal injections of neurotrophic factors support the survival of axotomized retinal ganglion cells in adult rats in vivo. Brain Res. 602, 304-317.

Meyer-Franke, A., Kaplan, M.R., Pfrieger, F.W., Barres, B.A., 1995. Characterization of the signaling interactions that promote the survival and growth of developing retinal ganglion cells in culture. Neuron 15, 805-819.

Mi, X.S., Yuan, T.F., So, K.F., 2014. The current research status of normal tension glaucoma. Clin. Interv. Aging 9, 1563-1571.

Miyamoto, A., Wake, H., Moorhouse, A.J., Nabekura, J., 2013. Microglia and synapse interactions: fine tuning neural circuits and candidate molecules. Front. Cell. Neurosci. 7, 70.

Morgan, J.E., 1994. Selective cell death in glaucoma: does it really occur? Br. J. Ophthalmol. 78, 875-879; discussion 879-880.

Nadal-Nicolas, F.M., Jimenez-Lopez, M., Salinas-Navarro, M., Sobrado-Calvo, P., Alburquerque-Bejar, J.J., Vidal-Sanz, M., Agudo-Barriuso, M., 2012. Whole number, distribution and co-expression of brn3 transcription factors in retinal ganglion cells of adult albino and pigmented rats. PLoS One 7, e49830.

Nadal-Nicolas, F.M., Jimenez-Lopez, M., Sobrado-Calvo, P., Nieto-Lopez, L., Canovas-Martinez, I., Salinas-Navarro, M., Vidal-Sanz, M., Agudo, M., 2009. Brn3a as a marker of retinal ganglion cells: qualitative and quantitative time course studies in naive and optic nerve-injured retinas. Invest. Ophthalmol. Vis. Sci. 50, 3860-3868.

Nahirnyj, A., Livne-Bar, I., Guo, X., Sivak, J.M., 2013. ROS detoxification and proinflammatory cytokines are linked by p38 MAPK signaling in a model of mature astrocyte activation. PLoS One 8, e83049.

Nelson, R., Connaughton, V., 1995. Bipolar Cell Pathways in the Vertebrate Retina, in: Kolb, H., Fernandez, E., Nelson, R. (Eds.), Webvision: The Organization of the Retina and Visual System, Salt Lake City (UT).

Neumann, C., Garreis, F., Paulsen, F., Hammer, C.M., Birke, M.T., Scholz, M., 2014. Osteopontin is induced by TGF-beta2 and regulates metabolic cell activity in cultured human optic nerve head astrocytes. PLoS One 9, e92762.

Ng, S.K., Wood, J.P., Chidlow, G., Han, G., Kittipassorn, T., Peet, D.J., Casson, R.J., 2014. Cancer-like metabolism of the mammalian retina. Clin. Experiment. Ophthalmol.

Omri, S., Behar-Cohen, F., de Kozak, Y., Sennlaub, F., Verissimo, L.M., Jonet, L., Savoldelli, M., Omri, B., Crisanti, P., 2011. Microglia/macrophages migrate through retinal epithelium barrier by a transcellular route in diabetic retinopathy: role of PKCzeta in the Goto Kakizaki rat model. Am. J. Pathol. 179, 942-953.

Ooto, S., Akagi, T., Kageyama, R., Akita, J., Mandai, M., Honda, Y., Takahashi, M., 2004. Potential for neural regeneration after neurotoxic injury in the adult mammalian retina. Proc. Natl. Acad. Sci. U. S. A. 101, 13654-13659.

Orive, G., Anitua, E., Pedraz, J.L., Emerich, D.F., 2009. Biomaterials for promoting brain protection, repair and regeneration. Nat. Rev. Neurosci. 10, 682-692.

Parmar, T., Parmar, V.M., Arai, E., Sahu, B., Perusek, L., Maeda, A., 2016. Acute Stress Responses Are Early Molecular Events of Retinal Degeneration in Abca4-/-Rdh8-/- Mice After Light Exposure. Invest. Ophthalmol. Vis. Sci. 57, 3257-3267.

Peichl, L., Wassle, H., 1983. The structural correlate of the receptive field centre of alpha ganglion cells in the cat retina. J. Physiol. 341, 309-324.

Pekny, M., Nilsson, M., 2005. Astrocyte activation and reactive gliosis. Glia 50, 427-434.

Pekny, M., Pekna, M., 2014. Astrocyte reactivity and reactive astrogliosis: costs and benefits. Physiol. Rev. 94, 1077-1098.

Pekny, M., Wilhelmsson, U., Pekna, M., 2014. The dual role of astrocyte activation and reactive gliosis. Neurosci. Lett. 565, 30-38.

Pfrieger, F.W., Barres, B.A., 1996. New views on synapse-glia interactions. Curr. Opin. Neurobiol. 6, 615-621.

Pinar-Sueiro, S., Zorrilla Hurtado, J.A., Veiga-Crespo, P., Sharma, S.C., Vecino, E., 2013. Neuroprotective effects of topical CB1 agonist WIN 55212-2 on retinal ganglion cells after acute rise in intraocular pressure induced ischemia in rat. Exp. Eye Res. 110, 55-58.

Polyak, K., 1941. The Retina. University of Chicago Press, Chicago.

Pow, D.V., Crook, D.K., 1995. Immunocytochemical evidence for the presence of high levels of reduced glutathione in radial glial cells and horizontal cells in the rabbit retina. Neurosci. Lett. 193, 25-28.

Prince, J.H., Ruskell, G.L., 1960. The use of domestic animals for experimental ophthalmology. Am. J. Ophthalmol. 49, 1202-1207.

Provencio, I., Rodriguez, I.R., Jiang, G., Hayes, W.P., Moreira, E.F., Rollag, M.D., 2000. A novel human opsin in the inner retina. J. Neurosci. 20, 600-605.

Qu, J., Jakobs, T.C., 2013. The Time Course of Gene Expression during Reactive Gliosis in the Optic Nerve. PLoS One 8, e67094.

Quigley, H.A., 2011. Glaucoma. Lancet 377, 1367-1377.

Quigley, H.A., Addicks, E.M., Green, W.R., Maumenee, A.E., 1981. Optic nerve damage in human glaucoma. II. The site of injury and susceptibility to damage. Arch. Ophthalmol. 99, 635-649.

Reese, B.E., Cowey, A., 1986. Large retinal ganglion cells in the rat: their distribution and laterality of projection. Exp. Brain Res. 61, 375-385.

Reichenbach, A., Bringmann, A., 2013. New functions of Muller cells. Glia 61, 651-678.

Rhee, K.D., Yang, X.J., 2010. Function and Mechanism of CNTF/LIF Signaling in Retinogenesis. Adv. Exp. Med. Biol. 664, 647–654.

Rieck, J., 2013. The pathogenesis of glaucoma in the interplay with the immune system. Invest. Ophthalmol. Vis. Sci. 54, 2393-2409.

Riepe, R.E., Norenburg, M.D., 1977. Muller cell localisation of glutamine synthetase in rat retina. Nature 268, 654-655.

Rodieck, R.W., 1973. The vertebrate retina: principles of structure and function. , San Francisco.

Rodriguez, A.R., de Sevilla Muller, L.P., Brecha, N.C., 2014. The RNA binding protein RBPMS is a selective marker of ganglion cells in the mammalian retina. J. Comp. Neurol. 522, 1411-1443.

Roesch, K., Jadhav, A.P., Trimarchi, J.M., Stadler, M.B., Roska, B., Sun, B.B., Cepko, C.L., 2008. The transcriptome of retinal Muller glial cells. J. Comp. Neurol. 509, 225-238.

Ruiz-Ederra, J., Garcia, M., Hicks, D., Vecino, E., 2004. Comparative study of the three neurofilament subunits within pig and human retinal ganglion cells. Mol. Vis. 10, 83-92.

Ruiz-Ederra, J., Garcia, M., Martin, F., Urcola, H., Hernandez, M., Araiz, J., Duran, J., Vecino, E., 2005. [Comparison of three methods of inducing chronic elevation of intraocular pressure in the pig (experimental glaucoma)]. Archivos de la Sociedad Espanola de Oftalmologia 80, 571-579.

Ruiz-Ederra, J., Hitchcock, P.F., Vecino, E., 2003. Two classes of astrocytes in the adult human and pig retina in terms of their expression of high affinity NGF receptor (TrkA). Neurosci. Lett. 337, 127-130.

Ruzafa, N., Pereiro, X., Aspichueta, P., Araiz, J., Vecino, E., 2017a. The retina of osteopontin deficient mice in aging. Mol. Neurobiol.

Ruzafa, N., Rey-Santano, C., Mielgo, V., Pereiro, X., Vecino, E., 2017b. Effect of hypoxia on the retina and superior colliculus of neonatal pigs. PLoS One 12, e0175301.

Ruzafa, N., Vecino, E., 2015. Effect of Muller cells on the survival and neuritogenesis in retinal ganglion cells. Archivos de la Sociedad Espanola de Oftalmologia 90, 522-526.

Salinas-Navarro, M., Jimenez-Lopez, M., Valiente-Soriano, F.J., Alarcon-Martinez, L., Aviles-Trigueros, M., Mayor, S., Holmes, T., Lund, R.D., Villegas-Perez, M.P., Vidal-Sanz, M., 2009. Retinal ganglion cell population in adult albino and pigmented mice: a computerized analysis of the entire population and its spatial distribution. Vision Res. 49, 637-647.

Samardzija, M., Wariwoda, H., Imsand, C., Huber, P., Heynen, S.R., Gubler, A., Grimm, C., 2012. Activation of survival pathways in the degenerating retina of rd10 mice. Exp. Eye Res. 99, 17-26.

Sarthy, V., Ripps, H., 2001. Role in retinal pathophysiology., in: Blakemore, C. (Ed.), The retinal Müller cell. Structure and function. Kluwer Academic/Plenum Publishers, New York, pp. 181-215.

Sassoe-Pognetto, M., Feigenspan, A., Bormann, J., Wassle, H., 1996. Synaptic organization of an organotypic slice culture of the mammalian retina. Vis. Neurosci. 13, 759-771.

Schafer, D.P., Lehrman, E.K., Stevens, B., 2013. The "quad-partite" synapse: microglia-synapse interactions in the developing and mature CNS. Glia 61, 24-36.

Seigel, G.M., 1999. The golden age of retinal cell culture. Mol. Vis. 5, 4.

Smedowski, A., Pietrucha-Dutczak, M., Kaarniranta, K., Lewin-Kowalik, J., 2014. A rat experimental model of glaucoma incorporating rapid-onset elevation of intraocular pressure. Sci. Rep. 4, 5910.

Streit, W.J., Graeber, M.B., Kreutzberg, G.W., 1988. Functional plasticity of microglia: a review. Glia 1, 301-307.

Takeuchi, M., Kamei, N., Shinomiya, R., Sunagawa, T., Suzuki, O., Kamoda, H., Ohtori, S., Ochi, M., 2012. Human platelet-rich plasma promotes axon growth in brain-spinal cord coculture. Neuroreport 23, 712-716.

Tang, Z., Arjunan, P., Lee, C., Li, Y., Kumar, A., Hou, X., Wang, B., Wardega, P., Zhang, F., Dong, L., Zhang, Y., Zhang, S.Z., Ding, H., Fariss, R.N., Becker, K.G., Lennartsson, J., Nagai, N., Cao, Y., Li, X., 2010. Survival effect of PDGF-CC rescues neurons from apoptosis in both brain and retina by regulating GSK3beta phosphorylation. J. Exp. Med. 207, 867-880.

Topkoru, B.C., Altay, O., Duris, K., Krafft, P.R., Yan, J., Zhang, J.H., 2013. Nasal administration of recombinant osteopontin attenuates early brain injury after subarachnoid hemorrhage. Stroke 44, 3189-3194.

Tran, T.L., Bek, T., la Cour, M., Nielsen, S., Prause, J.U., Hamann, S., Heegaard, S., 2014. Altered aquaporin expression in glaucoma eyes. APMIS 122, 772-780.

Tuo, J., Bojanowski, C.M., Zhou, M., Shen, D., Ross, R.J., Rosenberg, K.I., Cameron, D.J., Yin, C., Kowalak, J.A., Zhuang, Z., Zhang, K., Chan, C.C., 2007. Murine ccl2/cx3cr1 deficiency results in retinal lesions mimicking human age-related macular degeneration. Invest. Ophthalmol. Vis. Sci. 48, 3827-3836.

Urcola, J.H., Hernandez, M., Vecino, E., 2006. Three experimental glaucoma models in rats: comparison of the effects of intraocular pressure elevation on retinal ganglion cell size and death. Exp. Eye Res. 83, 429-437.

Vangeison, G., Rempe, D.A., 2009. The Janus-faced effects of hypoxia on astrocyte function. Neuroscientist 15, 579-588.

Vecino, E., 2008. Animal models in the study of the glaucoma: past, present and future. Archivos de la Sociedad Espanola de Oftalmologia 83, 517-519.

Vecino, E., Caminos, E., Becker, E., Martin-Zanca, D., Osborne, N., 1998a. Expression of Neurotrophins and their Receptors within the Glial Cells of Retina and Optic Nerve in: Castellano, B., González, B., Nieto-Sampedro, M. (Eds.), Understanding Glial Cells. Kluwer Academic Publisher, pp. 149-166.

Vecino, E., Caminos, E., Ugarte, M., Martin-Zanca, D., Osborne, N.N., 1998b. Immunohistochemical distribution of neurotrophins and their receptors in the rat retina and the effects of ischemia and reperfusion. Gen. Pharmacol. 30, 305-314.

Vecino, E., Heller, J.P., Veiga-Crespo, P., Martin, K.R., Fawcett, J.W., 2015. Influence of extracellular matrix components on the expression of integrins and regeneration of adult retinal ganglion cells. PLoS One 10, e0125250.

Vecino, E., Rodriguez, F.D., Ruzafa, N., Pereiro, X., Sharma, S.C., 2016. Glia-neuron interactions in the mammalian retina. Prog. Retin. Eye Res. 51, 1-40.

Vecino, E., Sharma, S.C., 2011. Glaucoma animal models, in: Rumelt, S. (Ed.), Glaucoma - Basic and clinical concepts, pp. 319-334.

Vecino, E., Ugarte, M., Nash, M.S., Osborne, N.N., 1999. NMDA induces BDNF expression in the albino rat retina in vivo. Neuroreport 10, 1103-1106.

Vecino, E., Urcola, H., Sharma, S.C., 2017. Ocular hypertension/glaucoma in Minipig. Episcleral Vein Cauterizatino and Microbead Occluson Methods, Methods Mol. Biol.

Veiga-Crespo, P., del Rio, P., Blindert, M., Ueffing, M., Hauck, S.M., Vecino, E., 2013. Phenotypic map of porcine retinal ganglion cells. Mol. Vis. 19, 904-916.

Veroman, S.A., 1981. [Retinal differentiation of turkey embryos of various ages in organotypical cultures]. Arkh. Anat. Gistol. Embriol. 81, 50-57.

Volgyi, B., Chheda, S., Bloomfield, S.A., 2009. Tracer coupling patterns of the ganglion cell subtypes in the mouse retina. J. Comp. Neurol. 512, 664-687.

Volland, S., Esteve-Rudd, J., Hoo, J., Yee, C., Williams, D.S., 2015. A comparison of some organizational characteristics of the mouse central retina and the human macula. PLoS One 10, e0125631.

von Toerne, C., Menzler, J., Ly, A., Senninger, N., Ueffing, M., Hauck, S.M., 2014. Identification of a novel neurotrophic factor from primary retinal Muller cells using stable isotope labeling by amino acids in cell culture (SILAC). Mol. Cell. Proteomics 13, 2371-2381.

Voskuhl, R.R., Peterson, R.S., Song, B., Ao, Y., Morales, L.B., Tiwari-Woodruff, S., Sofroniew, M.V., 2009. Reactive astrocytes form scar-like perivascular barriers to leukocytes during adaptive immune inflammation of the CNS. J. Neurosci. 29, 11511-11522.

Wang, L., Sarnaik, R., Rangarajan, K., Liu, X., Cang, J., 2010. Visual receptive field properties of neurons in the superficial superior colliculus of the mouse. J. Neurosci. 30, 16573-16584.

Wassle, H., Boycott, B.B., 1991. Functional architecture of the mammalian retina. Physiol. Rev. 71, 447-480.

Wieghofer, P., Knobeloch, K.P., Prinz, M., 2014. Genetic targeting of microglia. Wiley Periodicals, Inc.

Xing, C., Wang, X., Cheng, C., Montaner, J., Mandeville, E., Leung, W., van Leyen, K., Lok, J., Wang, X., Lo, E.H., 2014. Neuronal production of lipocalin-2 as a help-me signal for glial activation. Stroke 45, 2085-2092.

Yang, L., Xu, Y., Li, W., Yang, B., Yu, S., Zhou, H., Yang, C., Xu, F., Wang, J., Gao, Y., Huang, Y., Lu, L., Liang, X., 2014. Diacylglycerol Kinase (DGK) Inhibitor II (R59949) Could Suppress Retinal Neovascularization and Protect Retinal Astrocytes in an Oxygen-Induced Retinopathy Model. J. Mol. Neurosci.

Yu, D.Y., Cringle, S.J., Balaratnasingam, C., Morgan, W.H., Yu, P.K., Su, E.N., 2013. Retinal ganglion cells: Energetics, compartmentation, axonal transport, cytoskeletons and vulnerability. Prog. Retin. Eye Res. 36, 217-246.

Zack, D.J., 2000. Neurotrophic rescue of photoreceptors: are Müller cells the mediators of survival? Neuron 26, 285–286.

Zamanian, J.L., Xu, L., Foo, L.C., Nouri, N., Zhou, L., Giffard, R.G., Barres, B.A., 2012. Genomic analysis of reactive astrogliosis. J. Neurosci. 32, 6391-6410.

Zhang, S., Li, W., Wang, W., Zhang, S.S., Huang, P., Zhang, C., 2013. Expression and activation of STAT3 in the astrocytes of optic nerve in a rat model of transient intraocular hypertension. PLoS One 8, e55683.

Zhou, S., Wu, H., Zeng, C., Xiong, X., Tang, S., Tang, Z., Sun, X., 2013. Apolipoprotein E protects astrocytes from hypoxia and glutamate-induced apoptosis. FEBS Lett. 587, 254-258.

Zhou, X., Li, F., Kong, L., Chodosh, J., Cao, W., 2009. Anti-inflammatory effect of pigment epithelium-derived factor in DBA/2J mice. Mol. Vis. 15, 438-450.